NSF/CEE-83002

INSTITUTE FOR PHYSICAL SCIENCE AND TECHNOLOGY



# SEISMIC ANALYSIS/DESIGN OF CURVED STEEL BOX GIRDER BRIDGES

C. P. Heins, Professor
M. N. Abdel-Salam, Graduate Research Assistant

to

National Science Foundation
Washington, D. C.

February 1983



UNIVERSITY OF MARYLAND

50272-101

| REPORT DOCUMENTATION PAGE | 1. REPORT NO. NSF/CEE-83002 | 2. | 3. Recipient's Accession No. |
|---|---|---|---|

**4. Title and Subtitle**
Seismic Analysis/Design of Curved Steel Box Girder Bridges

**5. Report Date**
February 1983

**6.**

**7. Author(s)**
C.P. Heins, M.N. Abdel-Salam

**8. Performing Organization Rept. No.**

**9. Performing Organization Name and Address**
University of Maryland
Institute for Physical Science and Technology
College Park, MD 20742

**10. Project/Task/Work Unit No.**

**11. Contract(C) or Grant(G) No.**
(C)
(G) CEE8018729

**12. Sponsoring Organization Name and Address**
Directorate for Engineering (ENG)
National Science Foundation
1800 G Street, N.W.
Washington, DC 20550

**13. Type of Report & Period Covered**

**14.**

**15. Supplementary Notes**
Submitted by: Communications Program (OPRM)
National Science Foundation
Washington, DC 20550

**16. Abstract (Limit: 200 words)**

Results are presented of a study of the seismic response of curved steel box girder bridges. One, two, three, four, and five-span bridges are examined and a model is developed in which special elements are introduced to account for the curved geometry and boundary conditions. A study of bridge parameters reveals that the number of spans, the bridge weight, and the column height are the most influential parameters on the seismic response of such bridges. A modified version of the finite element program SAP IV is shown to be a useful tool for the seismic analysis of these bridges. A design criteria is proposed on the basis of the parametric analysis.

**17. Document Analysis a. Descriptors**

Bridges (structures)
Earthquakes
Earthquake resistant structures
Dynamic analysis
Mathematical models
Computer programs
Girder bridges
Superstructures

**b. Identifiers/Open-Ended Terms**

SAP IV computer program

**c. COSATI Field/Group**

| 18. Availability Statement | 19. Security Class (This Report) | 21. No. of Pages |
|---|---|---|
| NTIS | 20. Security Class (This Page) | 22. Price |

CAPITAL
SYSTEMS
GROUP, INC.

Please note:

Page 284 of this report is missing. An attempt to secure a copy of this page from the principal investigator revealed that:

-Professor Heins is deceased.
-The original manuscript has been misplaced.

It is hoped that the report can be processed as is, with note being made of the missing page.

1803 Research Boulevard
Rockville, Maryland 20850
Phone: (301) 762-1200

# SEISMIC ANALYSIS/DESIGN OF CURVED STEEL BOX GIRDER BRIDGES

C. P. Heins, Professor
M. N. Abdel-Salam, Graduate Research Assistant

to

National Science Foundation
Washington, D.C.

February 1983



1.b

## ABSTRACT

Seismic analysis and design of bridges has developed very rapidly during the last few years resulting in equivalent static methods. These methods, however, are not recommended for curved bridges. Therefore, it is the intention of this dissertation to present the results of a comprehensive study of the seismic response of curved steel box-girder bridges. One, two, three, four, and five-span bridges are analyzed. Geometry and section properties of both the super-structure and columns are based on a current bridge survey of all existing curved box-girder bridges.

El Centro earthquake ground motion acceleration record and its corresponding response spectrum are used as dynamic input and the SAP IV computer program, which is a finite element program for static and dynamic response of linear structures, was modified and used in the analysis.

The bridge is modeled using 3-D space frame elements in which special elements are introduced to account for the curved geometry and boundary conditions. Different parameters of the bridge model and the seismic loading are examined for each case. Both response history and response spectrum techniques are performed and results are compared. The simultanious application of the three components of the earthquake is also discussed. The effects of damping, non-composite section, rotational inertia, and column height are studied, and a comparison with rigid-column models and closed form solutions is made.

Parametric analysis is made to study the effects of the number of spans, span length, span ratio, curvature, column height, deck and column stiffnesses, and the weight of the superstructure on the maximum dynamic responses. Ground motion acceleration records in the three global directions are applied simultaneously to the structure. Maximum actions at the attachments and maximum stresses at the critical sections for both the superstructure and the columns are obtained. The maximum dynamic responses are correlated with static analysis of the bridge, and equivalent loads are obtained and design curves are developed.

A design criteria is proposed and several detailed examples are discussed. A comparison between computer dynamic analysis and the proposed design criteria shows good correlation.

ACKNOWLEDGEMENTS

The contents of this report represent the Ph.D. study of Dr. M. N. Abdel-Salam, which has been supported by the National Science Foundation under Grant No. PFR-80-18729, covering the period December 1980 through May 31, 1983. This grant is a cooperative US/PRC project between the University of Maryland and Tongji University.

The cooperation and encouragement of the NSF and the Hazards and Mitigation Section is gratefully acknowledged.

TABLE OF CONTENTS

# LIST OF TABLES

LIST OF TABLES (Cont'd)

LIST OF TABLES (Cont'd)

LIST OF TABLES (Cont'd)

LIST OF TABLES (Cont'd)

LIST OF TABLES (Cont'd)

LIST OF TABLES (Cont'd)

LIST OF TABLES (Cont'd)

LIST OF TABLE (Cont'd)

LIST OF TABLES (Cont'd)

LIST OF FIGURES

LIST OF FIGURES (Cont'd)

LIST OF FIGURES (Cont'd)

LIST OF FIGURES (Cont'd)

LIST OF FIGURES (Cont'd)

## NOTATIONS AND SYMBOLS

Roman Letters:

| | |
|---|---|
| $A$ | - Maximum expected acceleration at bedrock at the site, Acceleration coefficient |
| $A_m$ | - Modified acceleration coefficient |
| $c$ | - Viscous damping coefficient |
| $C, C_s$ | - Response coefficient, Seismic response coefficient, Seismic design coefficient |
| $C_n$ | - Generalized damping |
| $C_1, C_2, \ldots, C_6$ | - Constants |
| $[c]$ | - Damping matrix |
| $E$ | - Amount of earthquake energy released |
| $E_c$ | - Young's modulus for concrete |
| $E_s$ | - Young's modulus for steel |
| $f_D$ | - Damping force |
| $f_I$ | - Inertia force |
| $f_S$ | - Elastic force |
| $g$ | - Gravitational acceleration (32.2 ft/sec$^2$) |
| $h_c$ | - Column height |
| $I_c$ | - Column moment of inertia |
| $I_D$ | - Deck moment of inertia about a vertical axis |
| IC | - Importance classification |
| $k$ | - Stiffness of the system |
| $k_{cc}, k_{cm}, k_{cp}$ | - Concrete stresses ratio factors |
| $k_{sm}, k_{sp}$ | - Steel stresses ratio factors |
| $k_p, k_v$ | - Actions ratio factors |
| $k_1, k_2$ | - Constants |

| | |
|---|---|
| $K_n$ | - Generalized stiffness |
| [k] | - Stiffness matrix |
| L | - Exterior span length |
| $L_1$ | - Interior span length |
| m | - Mass of the structure |
| $m_r$ | - Modular ratio |
| M | - Magnitude of earthquake |
| $M_a$ | - Vertical moment at the abutments |
| $M_n$ | - Generalized mass |
| $M_1$ | - Vertical moment at the end support |
| [m] | - Mass matrix |
| n | - Span ratio |
| N | - Number of degrees of freedom |
| NS | - Number of spans |
| $P_a$ | - Tangential force at the abutments |
| $P_{eff}$ | - Effective support excitation loading |
| q | - Uniform horizontal load |
| R | - Radius of curvature |
| $R_m$ | - Response modification factor |
| [r] | - Influence coefficient matrix |
| $\{r_X\}, \{r_Y\}, \{r_Z\}$ | - Influence coefficient vectors in X, Y, and Z directions, respectively |
| S | - Site coefficient |
| $S_a$ | - Spectral acceleration |
| $S_c, S_s$ | - Section modulii for concrete and steel, respectively, about a vertical axis |
| $S_d$ | - Spectral relative displacement |
| $S_{dn}$ | - Spectral displacement corresponding to mode n |

| | |
|---|---|
| $S_v$ | - Spectral pseudo velocity |
| SPC | - Seismic performance category |
| T | - The fundamental period of the bridge |
| $v$ | - Relative displacement |
| $\dot{v}$ | - Relative velocity |
| $\ddot{v}$ | - Relative acceleration |
| $v_g$ | - Ground displacement |
| $\ddot{v}_g$ | - Earthquake ground-motion-acceleration |
| $\ddot{v}_{gX}, \ddot{v}_{gY}, \ddot{v}_{gZ}$ | - Ground acceleration components in X, Y, and Z directions, respectively |
| $v^t$ | - Total absolute displacement |
| $\ddot{v}^t$ | - Absolute acceleration |
| V | - Response function |
| $V_a$ | - Radial force at the abutments |
| $V_n$ | - Response function for mode n |
| $V_{nX}, V_{nY}, V_{nZ}$ | - Response functions for mode n due to ground acceleration in the X,Y, and Z directions, respectively |
| $V_p$ | - Radial force at the pier-superstructure roller connections |
| $V_1$ | - Transverse shear at the end support |
| $\{v\}$ | - Relative displacement vector |
| $\{\dot{v}\}$ | - Relative velocity vector |
| $\{\ddot{v}\}$ | - Relative acceleration vector |
| $\{v_{n_{max}}\}$ | - Maximum displacement vector corresponding to mode n |
| $\{v^t\}$ | - Total absolute displacement vector |
| $\{\ddot{v}^t\}$ | - Total absolute acceleration vector |

$w_c, w_s$ - Equivalent static loads which induce the maximum seismic normal stresses in concrete and steel, respectively, at the abutments

$w_e$ - Equivalent static load

$w_M, w_V$ - Equivalent static loads which induce the maximum seismic vertical moment and radial force, respectively, at the abutments

$W$ - Bridge weight per unit length

$W_L$ - Seismic lateral load

$W_T$ - Total dead load of the bridge

$Y_n$ - Amplitude of the $n^{th}$ mode

$Y_{nX}, Y_{nY}, Y_{nZ}$ - Amplitude of the $n^{th}$ mode due to ground acceleration in the X,Y, and Z directions, respectively

$\{Y\}$ - Generalized coordinate vector, Modal response vector

$Z$ - Generalized coordinate

Greek Letters:

$\Gamma_n$ - Earthquake participation factor for mode n

$\Gamma_{nX}, \Gamma_{nY}, \Gamma_{nZ}$ - Earthquake participation factors for mode n in X,Y, and Z directions, respectively

$\{\Gamma_n\}$ - Earthquake participation factors vector for mode n

$[\Gamma]$ - Earthquake participation factors matrix

$\Delta$ - Displacement

$\Delta t$ - Integration time step

$\theta$ - Central angle subtended by each span

$\xi$ - Damping ratio

$\xi_n$ - Damping ratio for mode n

$\sigma_c, \sigma_s$ - Maximum normal stresses in concrete and steel, respectively, at the end support

| | |
|---|---|
| $\sigma_{ca}, \sigma_{sa}$ | - Maximum normal stresses in concrete and steel, respectively, at the abutments |
| $\sigma_{cc}$ | - Maximum normal stress in concrete at the columns bases |
| $\sigma_{cm}, \sigma_{sm}$ | - Maximum normal stresses in concrete and steel, respectively, at the mid-spans cross-sections |
| $\sigma_{cp}, \sigma_{sp}$ | - Maximum normal stresses in concrete and steel, respectively, at the cross-sections over the piers |
| $\tau$ | - Shear stress |
| $\{\phi_n\}$ | - $n^{th}$ mode of vibration |
| $[\Phi]$ | - Mode shape matrix |
| $\omega$ | - Undamped natural frequency |
| $\omega_D$ | - Damped frequency |
| $\omega_n$ | - Natural frequency of mode n |

Units:

| | |
|---|---|
| cm | - Centimeter |
| ft | - Feet |
| Hz | - Hertz |
| in. | - Inch |
| k,kip | - 1000 pounds |
| km | - Kilometer |
| ksi | - $kip/in^2$ |
| min | - Minute |
| mm | - Millimeter |
| sec | - Second |

# CHAPTER I

## INTRODUCTION

Although dynamic loadings acting on bridge structures may result from any of several different source mechanisms, including wind or wave action and vehicular motions, the type of dynamic input which is of greatest importance to the structural engineer undoubtedly is that produced by earthquakes [9]. The significance of the earthquake problem stems from the terrible consequences of major earthquakes due to the destructive forces they induce in bridge structures.

With the advent of the 1964 Alaskan earthquake (magnitude 8.4), the 1971 San Fernando earthquake (magnitude 6.6) which caused approximately $6.5 million damage to bridges [31], and more recently the 1978 Santa Barbara earthquake [43], bridge structures in the USA have undergone considerable destructive forces. These earthquakes have caused the bridge professionals to reassess the design techniques that have been applied, up until that time, for seismic design.

Bridge damages due to earthquakes result from two different types of effects; a) non-vibrational effect, and b) seismically induced vibrational effects. Most of the damage observed worldwide before the San Fernando earthquake was non-vibrational, caused by permanent ground displacement which resulted in [10]:

1) Tilting, settlement and overturning of substructures.

2) Displacement of supports and anchor bolt breakage.

3) Settlement of approach fills and wingwall damage.

Bridge damages sustained during the Alaskan earthquake are examples of this type of failure, as shown in Figure 1.1 [39]. In San Fernando, however, a significant amount of damage due to vibrational effects, such as inelastic column failures, were observed in addition to the non-vibrational effects [18] as shown in Figure 1.2 .

## 1.1 Status of the Problem

As a result of the San Fernando earthquake, there has been a recognition of the need to design highway bridges that are more resistant to the damaging effects of seismic forces induced by ground vibration. This has been reflected in the present 1977 AASHTO bridge code [51], which suggests an equivalent static force method for simple structures. This method considers the relationship of the site to active faults, the seismic response of the soils at the site, and the dynamic response characteristics of the bridge. This technique, however, is not totally satisfactory because it produces accurate results for only a limited number of bridge types [34]. For complex structures, the code suggests that a response spectrum dynamic approach should be used for seismic analysis.

In 1977, the Federal Highway Administration (FHWA) sponsored a research program directed by Applied Technology Council (ATC) to reassess the AASHTO code for seismic design of bridges [50]. The work of this council, in part, is to prepare a new specification [15,49]. These new proposed guidelines, however, exclude bridges with curvature less than 500 feet. Although this code will be an improvement over the past criteria, there are major areas of research still requiring investigation. These areas include [16]:

1. "Developing a user-oriented computer program specifically for the dynamic analysis of bridges using segments of existing programs." Initial consideration should be given to linear dynamic analysis capabilities.
2. "Performing dynamic analysis of curved bridges," as it has been found that the response spectrum technique yields unreliable results for bridges having a high degree of curvature.
3. "Developing a rational method for designers to combine the effects of earthquake loading in three orthogonal directions," as bridges with curved alignments have coupling between the component directions within each mode of vibration.
4. "Conducting parametric studies for the seismic response of common types of bridges to determine the effects of geometry and constraint on overall

seismic response." Parameters should include

a) span length

b) curvature

c) column height and stiffness

d) materials

5. Development of simple design criteria for curved bridges, because computer programs for dynamic analysis may not be available to many bridge designers, nor are they amenable for direct design [34].

It is these areas of research that will encompass this study which will involve curved steel box-girder bridges [23].

## 1.2 Research Objectives

The specific objectives of this research are as follows:

a) Modifying the SAP IV computer program [3], which is a finite element program for static and dynamic response of linear structures, to be used for analyzing curved steel box-girder bridges. The bridge will be modeled using 3-D space frame elements. Structural details of both the superstructure and the columns will be considered. Induced actions and the corresponding steel and concrete stresses time history in both bridge deck and columns will be determined.

b) Comparing the response history and the response spectrum techniques in analyzing curved steel box-girder bridges. Special attention will be paid to the coupling

effects and the simultaneous application of earthquake loadings in the three global directions.

c) Parametric analysis will be made to study the effects of the bridge geometry and materials on the seismic response. The parameters include the number of spans, span length, span ratio, curvature, column height, deck and column stiffnesses, and the weight of the superstructure per unit length.

d) Based on the parametric analysis, a design criteria will be developed by correlating the maximum dynamic responses with the static analysis of the bridge to develop equivalent loads for both actions at the attachments and maximum stresses at the critical sections.

## 1.3 Summary

To accomplish the above objectives a comprehensive research program was carried out. One, two, three, four, and five span curved steel box-girder bridges were analyzed. Both geometry and structural details of the superstructure and the columns are based on a current bridge survey of all existing curved box-girder bridges. The El Centro earthquake ground motion acceleration record and its corresponding response spectrum are used as dynamic input.

The bridge is modeled using 3-D space frame elements, and different elements of the model were examined. Both response history and response spectrum methods were used and the results were compared. Three direction simultaneous application of the seismic loadings was also studied.

Parametric analysis was made using the response history technique, simultaneously applying the three components of El Centro seismogram. Maximum dynamic responses at the critical sections were correlated with static analysis of the bridge and equivalent loads were developed.

A simplified design criteria was proposed based on the results of the parametric analysis, taking into account the relationship of the site to active faults.

In this research, Chapter II presents an overview of current analytical methods for seismic design of bridges. Both the equivalent static force methods and the response spectrum technique are discussed.

Chapter III summarizes the theory of seismic response of structures. Equations of motion and their solutions are derived for both single degree of freedom (SDOF) and multi degrees of freedom (MDOF) systems. Applying the theory to bridge structures is also discussed.

In Chapter IV seismic analysis of curved steel box-girder bridges is presented. Both the bridge structure and the seismic loading are discussed in detail. Modification of SAP IV computer program is also discussed and a description of input data is included. Bridge modeling and an illustrative example are also presented.

Results of the seismic analysis are given in Chapter V. Different parameters of the bridge model and the dynamic input loading are examined. A comparison between response history and response spectrum techniques is made. Other

factors influencing the seismic response are studied; including damping effects, non-composite sections, rotational inertia, and column height. A comparison with rigid-column models and closed form solutions is also made.

Chapter VI presents the results of the parametric analysis. Seismic responses at the critical sections are discussed, and the method of correlating these results with equivalent static loads is presented and design curves are developed.

In Chapter VII a simplified design criteria is proposed and several detailed design examples are discussed comparing the design criteria with the computer solution.

Chapter VIII summarizes the findings of this research and draws conclusions regarding these findings.

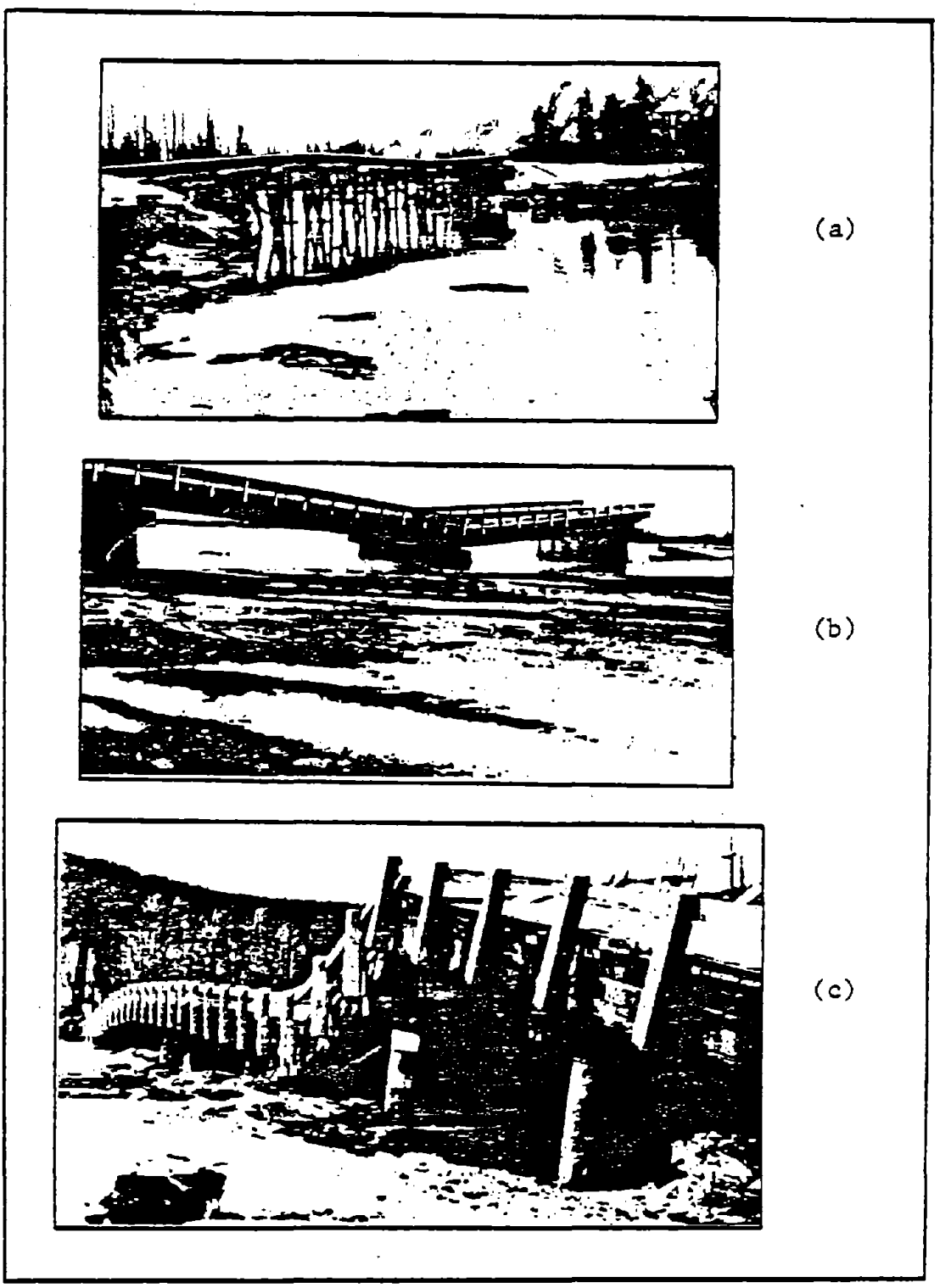


Figure 1.1 Non Vibrational Type Damage, Alaskan Earthquake 1964 [39]
(a) Buckling of Bridge Deck Due to Inward Movement of Abutments
(b) Differential Settlement of Steel-Rail-Bent Piers
(c) Bridge 605: Snow River 3, Post Earthquake View

Figure 1.2 San Fernando Column Damage - Bridge Number 53-1990R [18]

# CHAPTER II

# CURRENT BRIDGE SEISMIC DESIGN METHODOLOGY

The analytical procedures used in bridge seismic design practice can be divided into two main categories:

1. Equivalent static force methods
2. The response spectrum technique

While the first group is used for simple bridge structures and employs several simplifying assumptions, the response spectrum method requires computer facilities and is recommended for more complex types of bridges.

## 2.1 Equivalent Static Force Methods

The development of a realistic simplified equivalent static load approach for the dynamic analysis of bridges, that would suffice for the final design of simple bridges and could even be used for preliminary design of the more complex bridges, is desirable for the following reasons [31]:

1. Simple extensions of what is currently used and would be easy to implement
2. Does not require a computer
3. Quick and easy to apply

The determination of seismic response by the equivalent static force method basically involves three steps:

1. Calculating the period of the first mode of vibration in the direction under consideration.
2. Obtaining the corresponding response coefficient "C".

3. Distributing the resulting equivalent static force to the superstructure elements.

### 2.1.1 Lollipop Method

This method was widely used prior to the San Fernando Earthquake of 1971. The bridge bents were assumed to act independent of one another as single-degree-of-freedom (SDOF) oscillators with a lumped mass equivalent to the tributory deck mass as shown in Figure 2.1 . Both structure period and load distribution were generally determined using this approach. Applying this method implied the following simplifying assumptions about the dynamic behavior of a bridge:

1. Each bent vibrates in its own natural period, independent of the other bents.
2. The transverse bending and torsional stiffness of the superstructure do not contribute to the stiffness of the system.

These over-simplified assumptions made the obtained results unreliable.

### 2.1.2 Uniform Load Method

To overcome the deficiencies in the Lollipop method, an emperical approach, called the uniform load method, was devised. In this method, the continuity of the superstructure is maintained when determining the natural period of the system, and the earthquake force is distributed to all of the participating elements of the bridge. It can be summarized

as follows:

1. Apply a uniform horizontal load $q$ to the structure in the direction of vibration as shown in Figure 2.2(a), and calculate the resulting maximum displacement. Adjust $q$ to obtain a maximum displacement of 1 inch.
2. Calculate the stiffness of the structure by multiplying the adjusted uniform load by the total length, hence compute the fundamental transverse period of the bridge using the total dead load of the structure $W_T$.
3. The response coefficient $C$ can be determined from the response curves. These curves, shown in Figure 2.3, vary according to depths of alluvium to rock-like material, and depend on the maximum expected acceleration at bedrock at the site, $A$. $A$ can be obtained from the seismic risk map of the United States, shown in Figure 2.4, as follows:

| | |
|---|---|
| Zone I | $A = .09\ g$ |
| Zone II | $A = .22\ g$ |
| Zone III | $A = .50\ g$ |

where $g$ is the gravitational acceleration.

4. Determine the total earthquake force acting on the structure by combining the response coefficient with the framing factor and the total dead load. The framing factor is 1.0 for structures where single columns or piers resist the horizontal forces, and is equal to 0.8 where continuous frames resist these forces.

5. Convert this force into an equivalent uniform load, and then calculate the forces in the members.

Imbsen et al.[32] performed several case studies to evaluate the accuracy and limitations of this method. They concluded that the uniform load method can yield accurate results only for continuous, straight, non-skewed bridges, provided that the stiffness index, which is the ratio of the transverse stiffness of the entire structure to the stiffness of the superstructure alone (Figure 2.2(b)), is less or equal to 2 . For curved bridges, the results were not satisfactory.

This method is adopted by the present 1977 Standard Specifications for Highway Bridges (AASHTO) [51].

### 2.1.3 Generalized Coordinate Method

This method is based on applying the energy principles to a generalized single degree of freedom system. The shape of the vibrating structure can be assumed and represented by a shape function which can be expressed mathematically in terms of a single generalized coordinate taken as the amplitude at the point of maximum displacement. The longitudinal and transverse modes of vibration can be separated into two classes of generalized SDOF systems [34].

For longitudinal mode of vibration, the structural displacement is characterized by the behavior of a rigid deck, limiting all the columns to equal longitudinal displacements as shown in Figure 2.5(a). The transverse mode of vibration is more complex in that the transverse displacement of the

columns are not all equal but rather are functions of their positions along the superstructure as shown in Figure 2.5(b). In addition to this, the continuous superstructure will undergo bending and will thus make a contribution to the potential energy of the system.

The reliability of this method depends on the ability to predict and define the structure's mode shape. The effective application of this technique also requires that one mode dominates in each direction.

The overall procedure essentially consists of the following steps:

1. Calculate the period of vibration for the assumed mode in terms of the generalized mass and the generalized stiffness using the virtual work principle.
2. Determine the corresponding seismic response coefficient, $C_s$ . This can be obtained from the AASHTO Specifications [51] (Figure 2.3), or using the following emperical formula [49]:

$$C_s = \frac{1.2\ A\ S}{T^{2/3}} \qquad (2.1)$$

where: A = the acceleration coefficient (Figure 2.6)
S = the dimensionless coefficient for the soil profile characteristics of the site (this will be discussed in Chapter VII)
T = the fundamental period of the bridge

3. Determine the maximum generalized displacement due

to the seismic loading, using the earthquake excitation factor and the generalized mass.

4. Calculate the component forces corresponding to the maximum displacement using the assumed mode shape displacment function.

A detailed discussion of the previous steps is given in references [11] and [49], and numerical examples are discussed in references [11], [31], and [49].

Imbsen et al. [34] stated some limitations to this approach, and did not recommend it for curved bridges.

This method is adopted by the proposed guidelines for highway bridge seismic design criteria [15,49], and is called the single mode spectral method (SMSM).

### 2.1.4 Seismic Coefficient Method (SCM)

This method does not require the calculation of the structure period and is limited to simple structures located in areas with a low seismic hazard. It specifies a lateral static force equals to some fraction of the bridge weight, and is applied along the center of mass of the superstructure.

The seismic load, $W_L$ , is given by [15]:

$$W_L = C_s W_T \tag{2.2}$$

where: $W_T$ = total gravity load of the bridge

$C_s$ = the seismic design coefficient which can be determined in accordance with some emperical formulas [15].

This procedure may generally be used for preliminary design purposes.

## 2.2 The Response Spectrum Technique

The response spectrum dynamic analysis procedure is an improvement over the equivalent static force methods. For bridges having complex geometry, each mode of vibration has coupling in three global coordinate directions that makes it difficult to categorize the modes into simple longitudinal or transverse ones. In addition, several modes of vibration will in general contribute to the total response of the structure. Hence, the response spectrum technique, which is also called the multimode spectral method (MMSM), is considered to be a satisfactory approach in handling these types of structures.

### 2.2.1 Definition

The response spectrum is a graphical representation of the maximum response of all possible single-degree-of-freedom elastic systems to earthquake ground motions versus the periods or frequencies of the systems. The most usual measures of response are maximum relative displacement, maximum pseudo relative velocity, and maximum absolute acceleration.

### 2.2.2 Analysis

To apply the response spectrum technique, the frequencies and the corresponding modes of vibration for the bridge should be obtained first, using a space frame linear dynamic analysis computer program. The modal responses for a specific earthquake loading can be determined from the response spectrum plot, considering the participation factors for each mode. These modal responses, however, are maximums and generally will not occur simultaneously. It is therefore necessary to combine the various modal responses in some statistical manner in order to obtain a realistic value of the actual maximum response of the total structure at a given location. The proposed seismic design guidelines for highway bridges [15,49] relate the seismic response coefficient $C_s$ for each mode to a design response spectrum. A detailed discussion of the theory of constructing and using the response spectrum will follow in Chapter III.

### 2.2.3 Limitations of the Method

There are mainly two shortcomings that limit the applicability of the response spectrum approach. The first one is that the time domain has been removed, hence a statistical combination of modal responses, such as root mean square (RMS), has to be used in order to obtain realistic design loads. The actual combination of modal responses depends on several factors related to the type of the structure and the nature of the actual ground motion. Therefore, the use of a statistical

approach to replace the effects of the removed time domain may yield unrealistic results [34]. Imbsen et al. [33] concluded that the root mean square combination of modal contributions is in error for bridges having two modes of vibration with approximately equal periods. For such cases they suggested a "peak plus root mean square of the remaining" combination (PRMS).

The second deficiency in the response spectrum is that the duration of shaking is not accounted for by the spectrum. The major effect of duration will be on stiffness degradation and strength loss once the member begins yielding.

## 2.3 Evaluation of Bridge Seismic Analysis and Design Methods

In the last few years the area of seismic analysis and design of highway bridge structures has received extensive amount of research work. Analytical, experimental, and theoretical types of research were performed to evaluate the current state-of-the-art.

Imbsen et al. [32] performed several case studies on various highway bridges, and concluded that the uniform load method is limited to simple types of bridges, and is not recommended for curved girders. A comparison between the different static force methods [31] showed that the Lollipop method yields unreliable results, while the uniform load approach is more conservative than the generalized coordinate method. Imbsen et al. [34], however, discussed several limitations of the generalized approach and did not recommend it

for curved bridges. Case studies using the seismic coefficient method resulted in very conservative design values especially in the longitudinal direction, therefore, this method was excluded from the final seismic design guidelines for highway bridges [49].

Eighteen case studies were conducted by Imbsen et al. [33] to compare the response spectrum technique with both linear and nonlinear time history approaches. For some cases, the response spectrum results were in error because of using the root mean square combination of the modal contributions. Moreover, recent parameter studies on curved highway bridges [16] indicated that the response spectrum method yields unreliable results for bridges having high degree of curvature.

A difficult step in all the above design methods is to accurately evaluate the natural frequency of the bridge. Heins and Sahin [27] developed a simplified criteria to calculate the vertical natural frequency of steel box girder bridges. Heins and Lin [26] simulated the continuous curved bridge, restrained by equivalent springs, to evaluate the natural frequencies that were utilized, in conjunction with response spectrum curves, to obtain equivalent seismic forces.

It is to be noted that the different design methods presented herein are a combination of the highway Department for the State of California (CALTRANS) and New Zealand "force design" approaches. Those are discussed in detail in references [6], [18], and [46].

Experimental model studies had been conducted by Williams and Godden [57,58,59,60] on a series of curved bridges to study the effects of both linear and nonlinear dynamic behavior. They concluded that long curved bridges are very stiff in resisting seismic forces compared with similar straight bridges. Godden [19] performed a shaking table study on the seismic behavior of long span curved highway bridges, while Douglas [13] conducted full scale dynamic tests on straight bridges. Results of Douglas' analysis indicated that the seismic forces prescribed by the equivalent force method were too low. Kawashima and Penzien [36,37] correlated the experimental and theoretical dynamic behavior of a curved model bridge structure, emphasizing on the discontinuous behavior of expansion joints.

Extensive theoretical researches were conducted to refine the methods of analysis and design of highway bridges. Johnson and Galletly [35], and Werner et al. [55] studied the effects of traveling seismic waves on the response of highway bridges. A comparison between a uniform ground shock and a moving ground excitation showed that the second type of dynamic input results in higher responses which are more significant when the number of supports increases. A nonlinear analytical modal for simulating the dynamic behavior of expansion joints, in case of concrete bridges, was formulated by Tseng and Penzien [52,53]. The problem of soil-structure interaction of highway bridges is discussed in references [7], [39], and [48], and results are compared with equivalent seismic force methods.

## 2.4 Summary

From the above discussion, it can be concluded that both the equivalent static force methods and the response spectrum technique have some limitations and shortcomings when applied to curved bridges. Therefore, it is the intention of this dissertation to investigate the seismic analysis of curved steel box-girder bridges, and to develop possible relationship between the seismic response and equivalent force criteria.

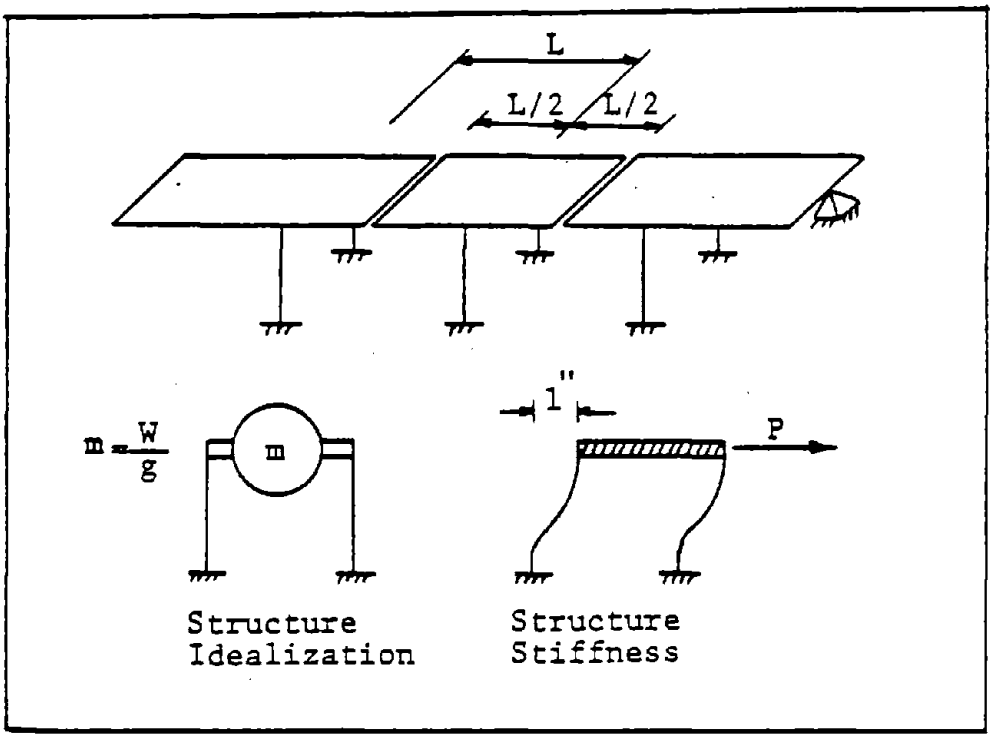


Figure 2.1 "Lollipop" Idealization [31]

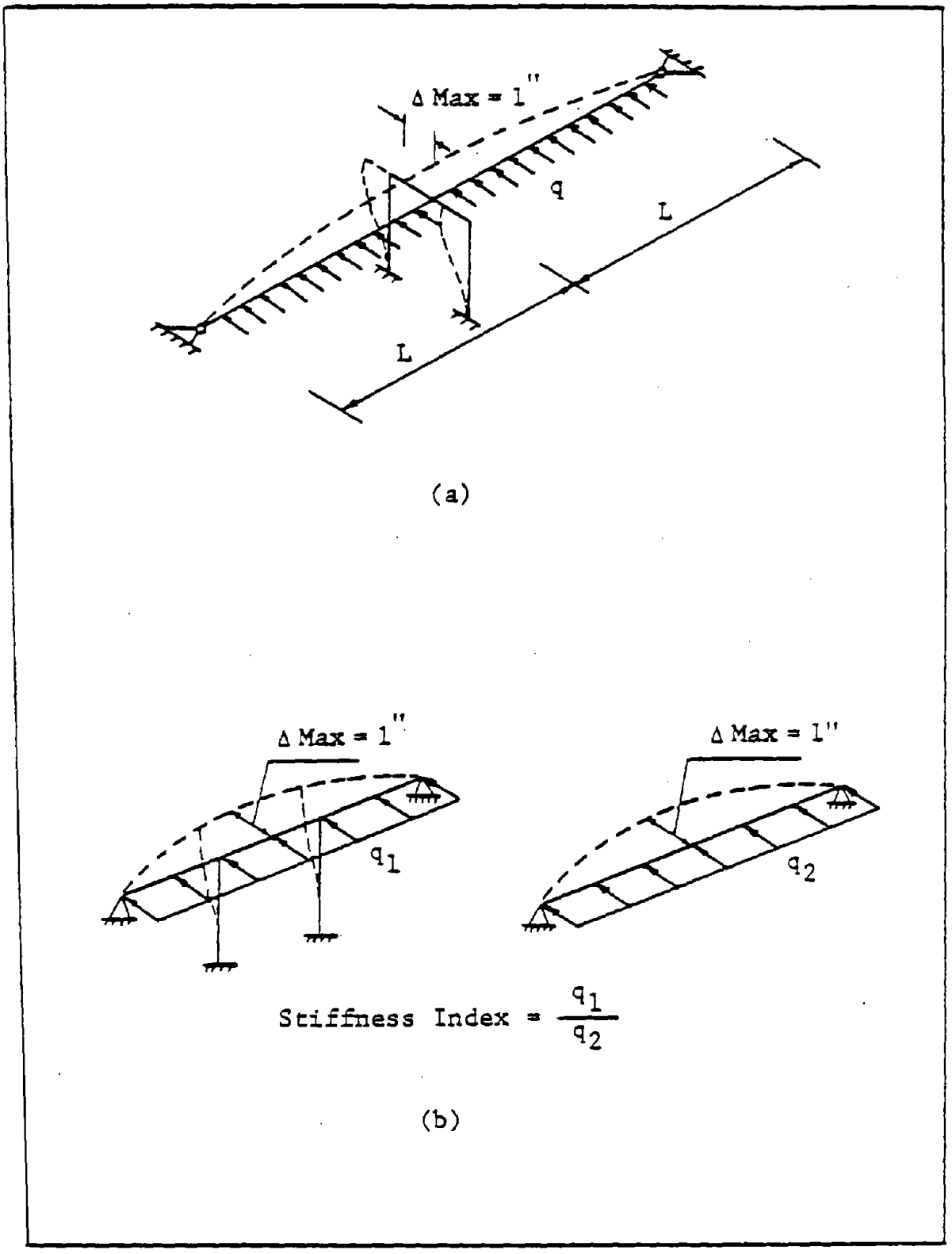


Figure 2.2 Uniform Load Method [31]: (a) Idealization
(b) Definition of Stiffness Index

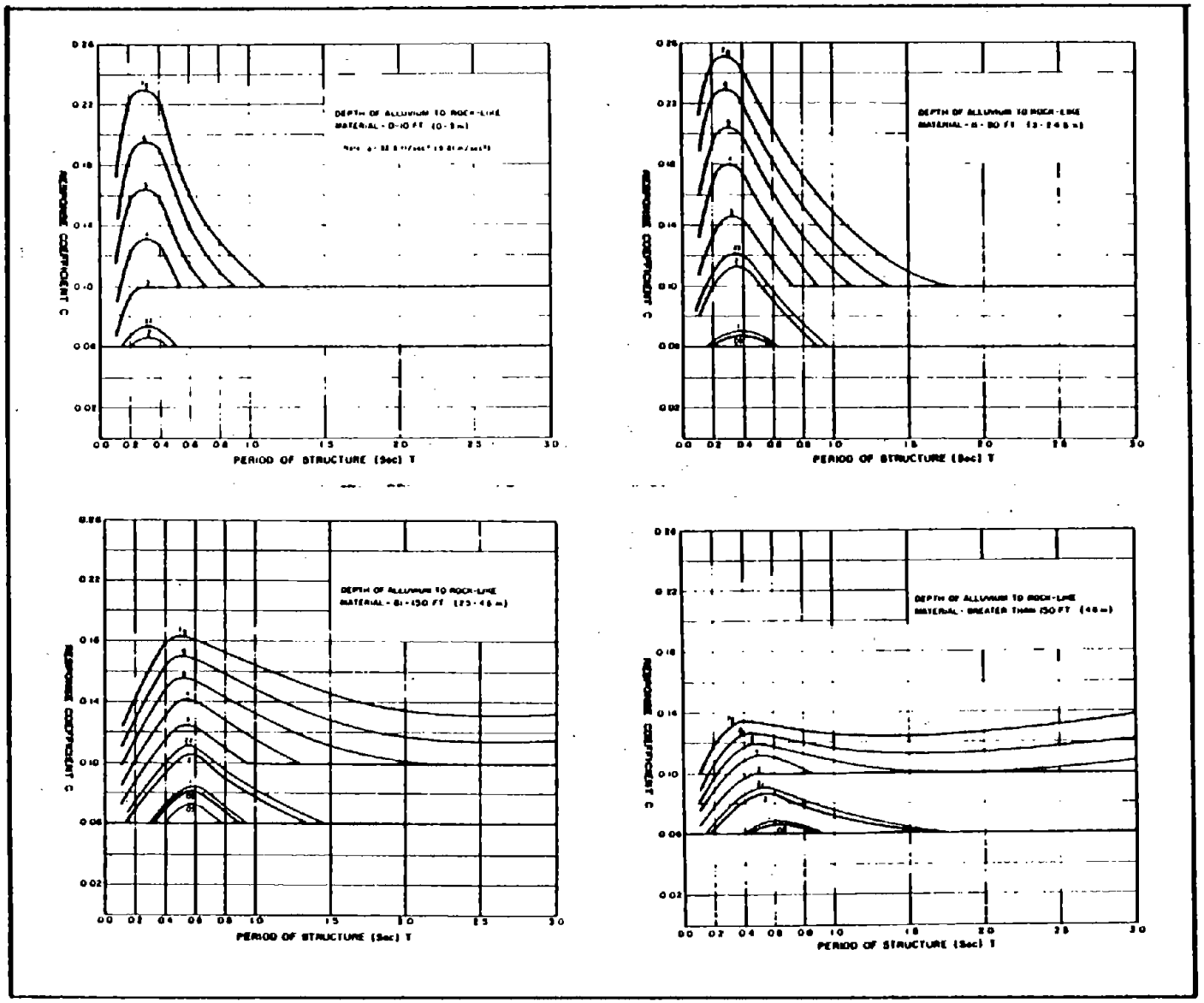


Figure 2.3 Response Curves [51]

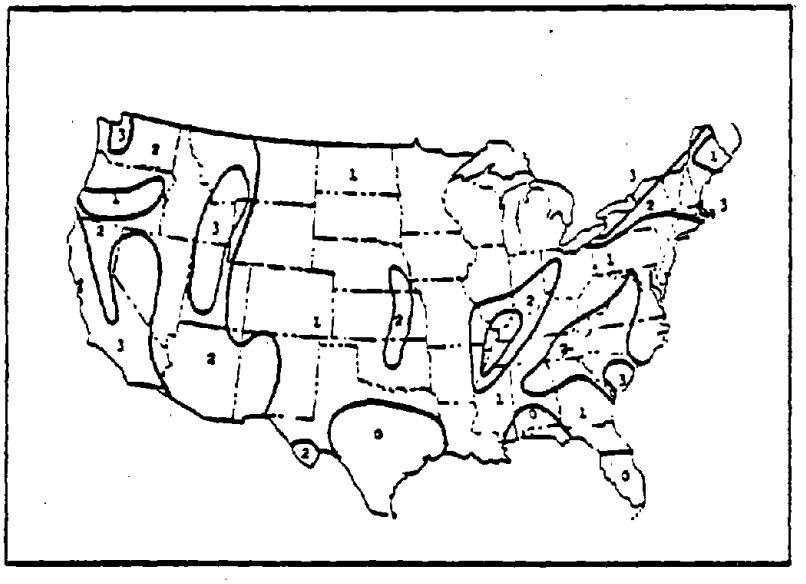

Figure 2.4 Seismic Risk Map of the United States [51]

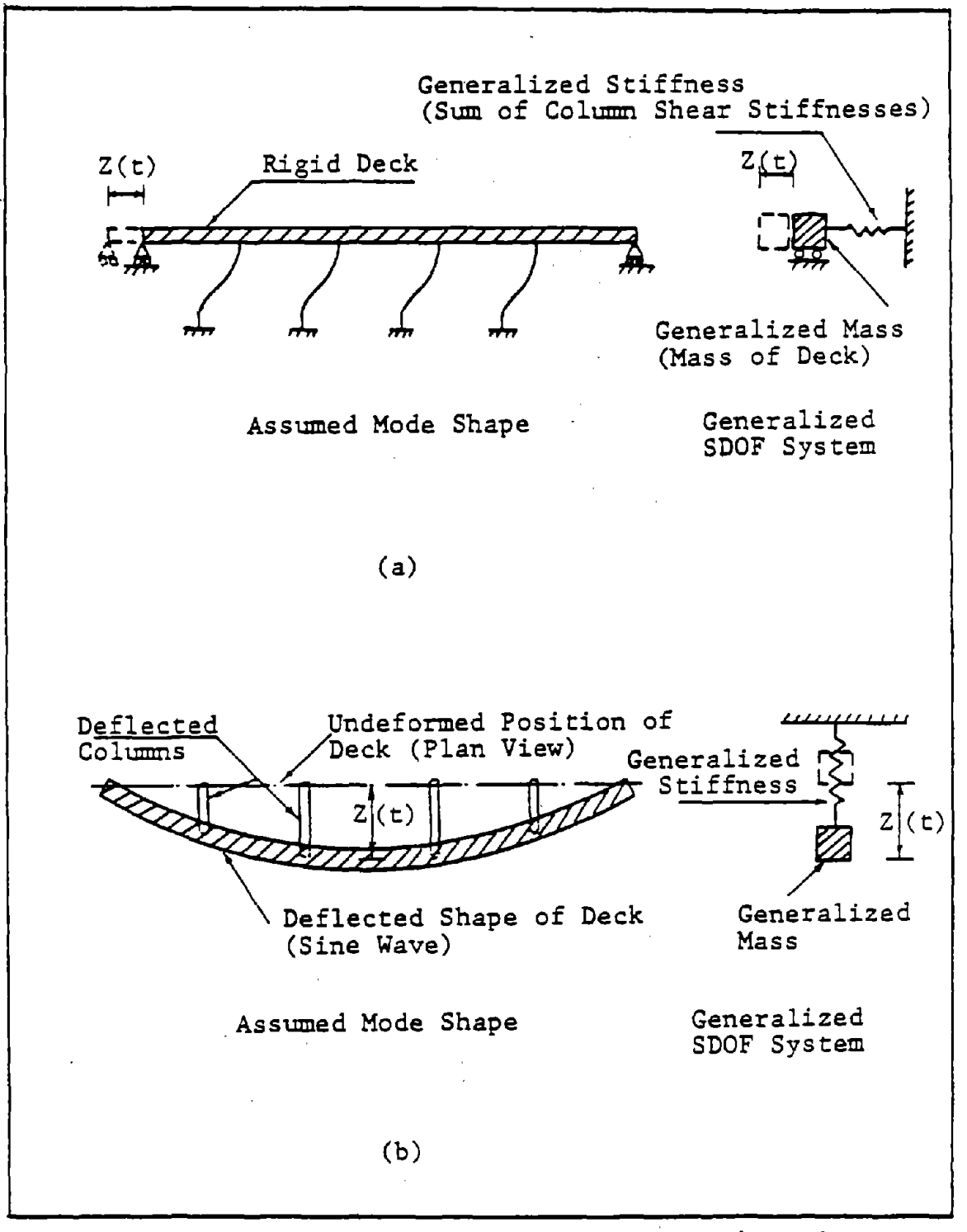


Figure 2.5 Generalized Coordinate Approach [34]
(a) Longitudinal Mode
(b) Transverse Mode (Continuous Deck)

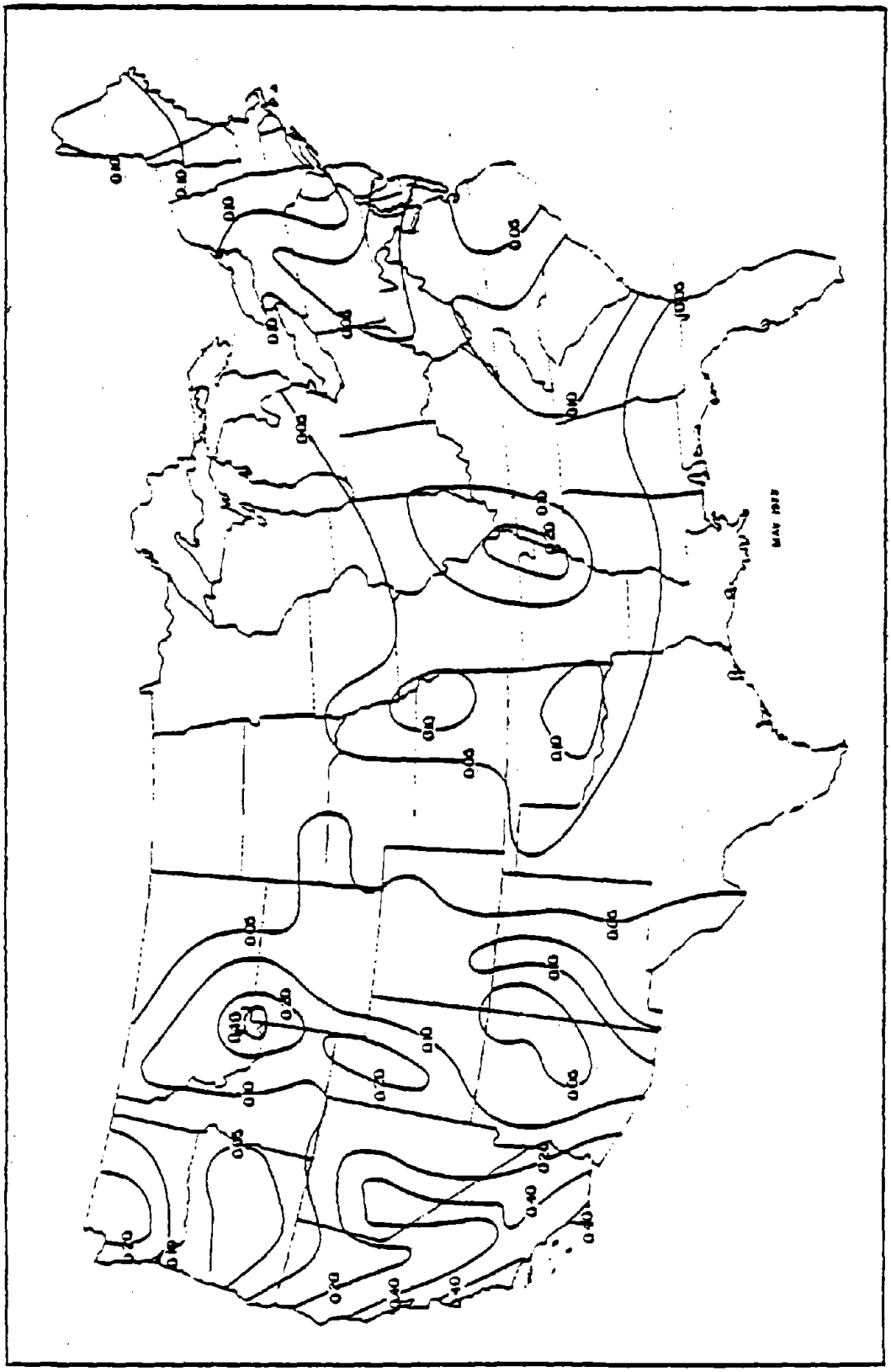

Figure 2.6 Acceleration Coefficient - Continental United States [49]

# CHAPTER III

# SEISMIC RESPONSE OF STRUCTURES

Although structural damage may result from several basically different effects of an earthquake such as foundation failure due to loss of soil strength by liquefaction, foundation displacements associated with fault break or landslide movements, or wave forces during tsunamis, the principal loading mechanism is the response to the earthquake ground motions applied at the base of the structure [56]. This Chapter summarizes the theory of structural dynamics as it applies to the calculation of such vibrating response, with emphasis on bridge structures. The problem is completely defined by the physical properties of the structural system, i.e., by its mass, stiffness, and damping characteristics, and by the ground motion acceleration time history introduced at its foundation support points. To have a better understanding of that type of dynamic input, characteristics of earthquakes will be briefly discussed.

## 3.1 Characteristics of Earthquakes

### 3.1.1 Causes of Earthquakes

Earthquakes may be classified, on the basis of cause, as [1]:

1. Tectonic ; which are related to deformation processes in the crustal rocks due to plate movements. This

is based on the plate tectonic theory which envisions the earth surface as broken into rigid plates constantly jostling one another. Most desructive earthquakes are of this type.

2. Volcanic ; which are triggered by the subterranean movement of molten rocks (magma) or gas explosions. These earthquakes are small in size, and have only local effects near volcanoes.
3. Collapse ; which can be caused by failure of rock surrounding cavities or by avalanches. These earthquakes also occur on a localized scale.
4. Explosive ; which can be caused by underground cavity formation due to nuclear and other explosions.
5. Reservoir induced seismicity ; which are localized earthquakes that can be caused by the impoundment of large reservoirs behind high dams. They can also be caused by the productional/reinjection of petroleum reservoirs.

### 3.1.2 Tectonic Earthquake Mechanism

The basic cause of tectonic earthquakes is strain induced by fault slipping which is in turn caused by plate motion. This strain is released in the form of seismic waves propagating in the earth. This mechanism can be illustrated according to the elastic rebound theory, which provides the most satisfactory explanation for that type of earthquakes.

It postulates that the two crustal blocks on both sides of the fault move in opposite directions due to plate motion, but instead of slipping along the fault, the blocks are deformed in the vicinity of the fault. As the rock is strained, elastic energy is stored in it. With the continuing deformation of the crustal structure, the strain builds up until the frictional bond that locks the fault can no longer hold at some point on the fault. The blocks will suddenly slip at this point from shear-type rupture. Once the rupture is initiated, it will propagate rapidly throughout the length of the highly strained material. The accumulated strain energy will then be released in the form of elastic seismic waves propagating in the crustal rocks and in the interior of the earth.

Two general types of elastic seismic waves are generated by earthquakes:

1. Body waves, which travel through the Earth's interior. There are two types of body waves: (i) dilatation waves (called P-waves), and (ii) shear waves (called S-waves).
2. Surface waves, which are generated at and confined to propogation paths along the surface and within the Earth's near crustal rocks. Two types of surface waves can occur: (i) Rayleigh waves (R-waves), and (ii) love waves (L-wave).

A complete discussion of these types of seismic waves, their

propagation, reflection and refraction, and attenuation can be found in references [1], [44], and [56].

### 3.1.3 Earthquake Magnitude

The amount of strain energy released at the source is a measure of the size of the earthquake. This is indicated quantitatively as the magnitude. Richter's magnitude scales are used universally . By definition, magnitude is the logarithm (base 10) of the maximum amplitude, measured in micrometers, of the earthquake record obtained by a Wood-Anderson seismograph, corrected to a distance of 100 km. This magnitude rating has been related empirically to the amount of earthquake energy released, E by the formula

$$\text{Log } E = 11.8 + 1.5\ M \qquad (3.1)$$

where M is the magnitude.

### 3.1.4 Earthquake Intensity

This is a measure of the severity of the ground motions observed at any point. It diminishes generally with distance from the source. The standard measure of intensity is the Modified Mercalli (MM) scale, which is a 12-point scale ranging from I (not felt by anyone) to XII (total destruction). This scale, however, does not provide a design criteria for earthquake-resistant structures. A better evaluation of the intensity became possible after the development of the strong-motion -recording accelerographs. The

amplitude, the frequency content, and the duration of the ground motion record can be used to describe the intensity of the earthquake. A more precise measure of the intensity of a given ground motion can be evaluated from its response spectrum, and is called the spectral intensity [45,56].

## 3.2 Earthquake Response of SDOF Systems

### 3.2.1 Equation of Motion for Lumped Mass System

A simplified model of the earthquake excitation problem is shown in Figure 3.1 , in which $m$ is the mass of the structure, $k$ is the stiffness, and $c$ is the viscous damping coefficient. The total displacement of the mass, $v^t$ van be expressed as

$$v^t = v + v_g \tag{3.2}$$

where: $v_g$ = ground displacement
$v$ = relative displacement

As shown in Figure 3.1(b), equilibrium of forces for this system may be written as

$$f_I + f_D + f_S = 0 \tag{3.3}$$

in which

$$\begin{aligned} f_I &= \text{inertia force} = m\,\ddot{v}^t \\ f_D &= \text{damping force} = c\,\dot{v} \\ f_S &= \text{elastic force} = k\,v \end{aligned} \tag{3.4}$$

Substituting Equation (3.4) into (3.3) gives

$$m\,\ddot{v}^t + c\,\dot{v} + k\,v = 0 \tag{3.5}$$

and using Equation (3.2) yields

$$m\ \ddot{v} + c\ \dot{v} + k\ v = -m\ \ddot{v}_g \equiv P_{eff} \tag{3.6}$$

in which $P_{eff}$ denotes the effective support excitation loading.

Defining the undamped natural frequency $\omega$, the damping ratio $\xi$, and the damped frequency $\omega_D$ as:

$$\omega^2 = \frac{k}{m} \tag{3.7}$$

$$\xi = \frac{c}{2m\omega} \tag{3.8}$$

$$\omega_D = \omega \sqrt{1 - \xi^2} \tag{3.9}$$

and substituting in Equation (3.6) will give

$$\ddot{v} + 2\xi\omega\ \dot{v} + \omega^2 v = -\ddot{v}_g \tag{3.10}$$

The general solution of this differential equation of motion can be expressed by means of the Duhamel Integral [9,14,47,56] as:

$$v(t) = \frac{-1}{\omega_D} \int_0^t \ddot{v}_g(\tau)\ \ EXP[-\xi\ \omega\ (t-\tau)] \sin \omega_D(t-\tau)\ d\tau \tag{3.11}$$

Once the displacement time history v(t) is obtained, then the elastic force $f_S$ can be calculated, and the columns shears and moments can be determined.

It is to be noted that in computer programs, the response v(t) is actually calculated by step-by-step integration

technique to solve the differential equation (3.10) rather than evaluating the Duhamel Integral numerically.

### 3.2.2 Response Spectrum Analysis

For a specific earthquake ground-motion-acceleration record $\ddot{v}_g(t)$, a corresponding response spectrum can be constructed. The relative displacement $v(t) = v(t,\xi,\omega)$ can be obtained from Equation (3.11). Differentiating (3.11) with respect to time will give the relative velocity $\dot{v}(t,\xi,\omega)$, and by differentiating it twice, or from Equation (3.5), we can obtain the absolute acceleration $\ddot{v}^t(t,\xi,\omega)$. The maximum absolute values of these quantities, for various damping ratios, can be evaluated for a full range of frequencies. A plot showing these relationships is called the earthquake response spectrum.

Neglecting the slight difference between the damped and undamped frequencies, and noting that the negative sign has no significance in an earthquake excitation, Equation (3.11) becomes

$$v(t,\xi,\omega) = \frac{1}{\omega} V(t,\xi,\omega) \qquad (3.12)$$

where $V(t,\xi,\omega)$ is the response function defined as

$$V(t,\xi,\omega) = \int_0^t \ddot{v}_g(\tau) \quad \text{EXP } [-\xi\ \omega\ (t-\tau)] \sin\ \omega\ (t-\tau) \quad d\tau \qquad (3.13)$$

For a specific value of damping ratio $\xi$ and natural frequency $\omega$, the response time history $v(t,\xi,\omega)$ due to

the ground motion $\ddot{v}_g(t)$ can be obtained. The maximum absolute value of $v$ is called the spectral relative displacement $S_d$

$$S_d(\xi,\omega) = \max_t |v(t,\xi,\omega)| \tag{3.14}$$

The spectral pseudo-velocity $S_v$ is defined as

$$S_v(\xi,\omega) = \max_t |V(t,\xi,\omega)| \tag{3.15}$$

and is related to the spectral displacement by the relationship

$$S_d = \frac{S_v}{\omega} \tag{3.16}$$

As indicated by Equation (3.15), $S_v$ depends not only on the ground motion history, but also on the frequency and the damping ratio. Thus for any given earthquake record, by assuming a specific value of damping in the structure it is possible to calculate values of $S_v$ for a full range of frequencies. A graph showing these spectral pseudo-velocity response values plotted as a function of frequency (or period) is called a pseudo-velocity response spectrum of the earthquake motion. Such spectrum is generally computed for several different damping ratios, and all plotted on a single graph as shown in Figure 3.2(b) for the acceleration record of Figure 3.2(a).

It is to be noted that the spectral pseudo-velocity does not actually represent the maximum velocity of the oscillator $\dot{v}$, but it provides a direct means of evaluating the true maximum relative displacement $S_d$.

The spectral acceleration $S_a$ , which is the maximum absolute value of the total acceleration $\ddot{v}^t(t,\xi,\omega)$ , can also be defined as:

$$S_a(\xi,\omega) = \omega\, S_v(\xi,\omega) = \omega^2 S_d(\xi,\omega) \qquad (3.17)$$

Plots of the spectral displacement and acceleration could be constructed in a form similar to the pseudo-velocity spectrum of Figure 3.2(b), but simple relationships existing between these three quantities make it more convient to present them all in a single plot on four-way log paper as shown in Figure 3.2(c) for the same earthquake record.

Now for a SDOF lumped mass system, the maximum elastic force in the system can be obtained, using the response spectrum, from

$$f_{S_{max}} = k\, S_d = \omega^2 m\, S_d = m\, S_a \qquad (3.18)$$

## 3.3 Multi-Degrees-Of-Freedom Systems (MDOF)

### 3.3.1 Equations of Motion

The formulation of the earthquake-response analysis of a lumped MODF system can be carried out in matrix notation in a manner entirely analogous to the previous development of the lumped SDOF equation [ 9 ]. Thus the equations of motion can be written as:

$$[m]\,\{\ddot{v}^t\} + [c]\,\{\dot{v}\} + [k]\,\{v\} = \{0\} \qquad (3.19)$$

where $[m]$ = mass matrix

$[c]$ = damping matrix

$[k]$ = stiffness matrix

$\{\ddot{v}^t\}$ = total absolute acceleration vector

$\{\dot{v}\}$ = relative velocity vector

$\{v\}$ = relative displacement vector

Formation of these matrices is discussed in references [9], [17], [31], [47], and [56].

The total displacement $\{v^t\}$ can be expressed in terms of the relative displacement $\{v\}$ and the ground displacement $v_g$. This relationship depends on the type of support displacement which has been applied, as well as the structural configuration. For purpose of discussion a simple relationship, which is used in analyzing multistory buildings, is considered, and application to bridge structures will follow in Section 3.4. This may be written as:

$$\{v^t\} = \{v\} + \{1\} v_g \qquad (3.20)$$

in which $\{1\}$ represents a column of ones. Substituting in Equation (3.19) yields

$$[m]\{\ddot{v}\} + [c]\{\dot{v}\} + [k]\{v\} = -[m]\{1\}\ddot{v}_g \qquad (3.21)$$

These coupled equations of motion can be directly solved by numerical integration schemes, which will be a large computational problem. However, a good approximation of the

actual response can be obtained by considering only the fewer lower modes of vibration [9,47,56].

### 3.3.2 Modal Analysis

To apply this technique, the natural frequencies and the mode shapes of the system should be first obtained by solving the equations of motion for a freely vibrating undamped system

$$[m]\{\ddot{v}\} + [k]\{v\} = \{0\} \qquad (3.22)$$

This equation can be transformed into an eigenvalue problem [9,41,47,56]:

$$[k]\{\phi\} = \omega^2[m]\{\phi\} \qquad (3.23)$$

This eigenvalue problem can be solved [2,9 ,40] to obtain the eigenvalues $\omega_n^2$ , which are the natural frequencies of the system, and the eigenvectors $\{\phi_n\}$ which are the modes of vibration. These eigenvectors are orthogonal with respect to both the mass and the stiffness matrices.

The displacement vector $\{v\}$ can be expressed in terms of the mode shapes as

$$\{v\} = \sum_{n=1}^{N} \{\phi_n\} Y_n = [\phi]\{Y\} \qquad (3.24)$$

where:

$[\phi]$ = mode shape matrix (NxN)

$\{Y\}$ = generalized coordinate vector (Nx1)

N = number of degress of freedom (or number of mode shapes)

Due to the orthogonality of the mode shapes, the system of N coupled simultaneous differential equations (3.21) can be transformed into a system of N decoupled equations as follows:

$$[\phi]^T [m] [\phi] \{\ddot{Y}\} + [\phi]^T [c] [\phi] \{\dot{Y}\} + [\phi]^T [k] [\phi] \{Y\} = - [\phi]^T [m] \{1\} \ddot{v}_g \qquad (3.25)$$

And assuming that the same orthogonality characteristics apply to the damping matrix [9 ,47,56], Equation (3.25) reduces to a set of N decoupled differential equations each of which represents a modal equation in the form

$$M_n \ddot{Y}_n + C_n \dot{Y}_n + K_n Y_n = -\Gamma_n \ddot{v}_g \qquad (3.26)$$

where $Y_n$ is the amplitude of the $n^{th}$ mode. The generalized mass $M_n$, the generalized damping $C_n$, the generalized stiffness $K_n$, and the earthquake participation factor $\Gamma_n$ can be obtained from

$$\begin{aligned} M_n &= \{\phi_n\}^T [m] \{\phi_n\} \\ C_n &= \{\phi_n\}^T [c] \{\phi_n\} \\ K_n &= \{\phi_n\}^T [k] \{\phi_n\} \\ \Gamma_n &= \{\phi_n\}^T [m] \{1\} \end{aligned} \qquad (3.27)$$

Equation (3.26) can be simplified by utilizing the relation between the generalized damping and stiffness and the generalized mass to yield

$$\ddot{Y}_n + 2\xi_n \omega_n \dot{Y}_n + \omega_n^2 Y_n = -\frac{\Gamma_n}{M_n} \ddot{v}_g \qquad (3.28)$$

where $\xi_n$ is the damping ratio for the $n^{th}$ mode.

Equation (3.28) shows that the equation of motion for the $n^{th}$ mode of the MDOF system is similar to equation (3.10) for SDOF systems. Thus, the response of the $n^{th}$ mode at any time may be obtained by evaluating the Duhamel Intergal expression for the given earthquake motion:

$$Y_n(t) = \frac{\Gamma_n}{M_n} \frac{1}{\omega_n} V_n(t) \qquad (3.29)$$

where $V_n(t)$ is the response function for the $n^{th}$ mode defined as

$$V_n(t) = \int_0^t \ddot{v}_g(\tau) \; EXP[-\xi_n \omega_n (t-\tau)] \sin \omega_n (t-\tau) \, d\tau \qquad (3.30)$$

The relative displacement of the structure at time t is then obtained by superposing the contribution of all modes evaluated at this time [Equation (3.24)]. Once {v} is obtained the elastic forces can be calculated, and hence all internal forces can be determined.

In computer programs, the modal response vector {Y} is actually calculated using a step-by-step integration scheme to solve the set of the decoupled differential equations (3.28).

An important advantage of the mode superposition procedure is that an approximate solution may be obtained by considering only the contribution of the fewer lower modes. This will sharply reduce the tremendous amount of computations associated with systems having large number of degrees of freedom.

There are several methods to obtain the lowest p frequencies and corresponding mode shapes for an eigenvalue problem [ 2,40 ]. One of the most efficient methods is the subspace iteration, in which the eigenvalue problem with matrices of order NxN is transformed into a smaller size eigenvalue problem with matrices of order pxp. It incorporates a sweeping technique, Rayleigh-Ritz analysis, and Jacobi method in an iterative process.

Having obtained the first p frequencies and mode shapes, Equation (3.24) reduces to

$$\{v\} = \sum_{n=1}^{p} \{\phi_n\} Y_n = [\Phi]_{Nxp} \{Y\}_{pxl} \qquad (3.31)$$

and we will have p decoupled differential equations of the form (3.28) which can be solved to obtain the modal response vector $\{Y\}_{pxl}$ . Hence the relative displacement vector $\{v\}$ and consequently the elastic forces in the system can be determined.

The p decoupled differential equations (3.28) are solved using a step-by-step integration method which employs an unconditionally stable numerical scheme such as Newmark implicit scheme or the Wilson-$\theta$ linear acceleration scheme [ 2,40 ].

### 3.3.3 Response Spectrum Technique

The entire displacement response history of any MDOF system is completely defined by Equations (3.24) or (3.31) after the modal response amplitudes have been determined

from Equation (3.29). Hence the maximum response of the system can be obtained. Alternatively, the response spectrum technique used for SDOF systems in Section 3.2.2 can be applied here.

For each individual mode of the structure, the maximum response can be obtained directly from the response spectrum taking into account the earthquake participation factor. Considering Equation (3.29), the maximum response can be determined as

$$Y_n(t)|_{max} = \frac{\Gamma_n}{M_n} \frac{1}{\omega_n} V_n(t)|_{max} = \frac{\Gamma_n}{M_n} S_{dn}(\xi_n, \omega_n) \qquad (3.32)$$

where $S_{dn}(\xi_n, \omega_n)$ is the spectral displacement corresponding to the damping and frequency of the $n^{th}$ mode. Then the distribution of maximum displacements in this mode is given by

$$\{v_{n_{max}}\} = \{\phi_n\} Y_{n_{max}} = \{\phi_n\} \frac{\Gamma_n}{M_n} S_{dn} \qquad (3.33)$$

However, the maximum total response cannot be obtained, in general, by merely adding the modal maxima because these maxima usually do not occur at the same time. A number of different formulas have been proposed to obtain a reasonable estimate of the maximum response from the spectral values. The simplest and most popular of these is the square root of the sum of the squares of the modal responses. Thus if the maximum modal displacements are given by Equation (3.33), the maximum total displacement is approximated by

$$\{^{V}max\} = \sqrt{\{^{V_1}max\}^2 + \{^{V_2}max\}^2 + \ldots} \qquad (3.34)$$

where the terms under the radical sign represent vectors of the modal displacements squared. A similar approach can be followed to obtain the maximum elastic forces in the system.

By this procedure it is possible to get a good approximation of the earthquake response of any MDOF system by working directly with the earthquake response spectrum, without the necessity of carrying out the complete response history analysis. A comparison between the two techniques will be discussed in Chapter V.

## 3.4 Application to Bridge Structures

Dynamic analysis of bridges, which are highly complicated distributed parameter systems, is generally performed using the finite element method [11,15,31,33,34,49]. The structure is discretized into finite elements and the analysis is carried out in matrix form [2,12,61]. The matrix equations for the seismic response analysis of finite element systems are identical in form to the MDOF lumped mass equations described in Section 3.3.

The bridge is modeled using 3-D space frame elements, with six degrees of freedom at each node, three translational and three rotational [47,54]. While the stiffness matrix should consider the six degrees of freedom, the structural mass is lumped at the nodes in the three translational directions. This type of idealization can yield reliable

results for bridge structures [31]. The concept of viscous damping, which proved to yield satisfactory results compared with full scale testing in case of multistory buildings, is extended to bridge structures.

### 3.4.1 Ground Motion Excitation

In practice, the seismic waves tend to excite the bridge supports in the three global directions. Moreover, due to the structure configuration the relationship between the total and relative motions will not take the simple form of Equation (3.20). Hence the ground acceleration vector can be written as

$$\{1\}\,\ddot{v}_g = \{r_X\}\,\ddot{v}_{gX} + \{r_Y\}\,\ddot{v}_{gY} + \{r_Z\}\,\ddot{v}_{gZ} \qquad (3.35)$$

in which $\ddot{v}_{gX}$, $\ddot{v}_{gY}$, $\ddot{v}_{gZ}$ are the ground acceleration components in X, Y, and Z directions, and $\{r_X\}$ is an influence coefficient vector in X-direction, which is a null vector except that these elements which correspond to the X-translational degrees of freedom are equal to one. The influence coefficient vectors $\{r_Y\}$ and $\{r_Z\}$ are analogous to $\{r_X\}$ in Y and Z directions respectively.

The modal analysis will be identical to that discussed in Section 3.3.2 except for the right hand side of Equation (3.26) which becomes

$$-\Gamma_n\,\ddot{v}_g = -(\Gamma_{nX}\,\ddot{v}_{gX} + \Gamma_{nY}\,\ddot{v}_{gY} + \Gamma_{nZ}\,\ddot{v}_{gZ}) \qquad (3.36)$$

where

$$\Gamma_{nX} = \{\phi_n\}^T [m] \{r_X\}$$

$$\Gamma_{nY} = \{\phi_n\}^T [m] \{r_Y\} \qquad (3.37)$$

$$\Gamma_{nZ} = \{\phi_n\}^T [m] \{r_Z\}$$

$\Gamma_{nX}$, $\Gamma_{nY}$, $\Gamma_{nZ}$ are the earthquake modal participation factors for mode n in X, Y, and Z directions respectively.

The vector of the modal earthquake participation factors for mode n $\{\Gamma_n\}$ can be obtained as

$$\{\Gamma_n\}_{1x3} = \{\Gamma_{nX} \quad \Gamma_{nY} \quad \Gamma_{nZ}\}$$
$$= \{\phi_n\}^T [m] [r] \qquad (3.38)$$

where [r] is the influence coefficient matrix or the rigid body matrix relating the motion at each node to the support motion, defined as

$$[r]_{Nx3} = [\{r_X\} \quad \{r_Y\} \quad \{r_Z\}] \qquad (3.39)$$

The earthquake modal participation factors matrix for the entire structure can then be obtained from

$$[\Gamma]_{Nx3} = [\Phi]^T [m] [r] \qquad (3.40)$$

The modal equation (3.28) will then reduce to

$$\ddot{Y}_n + 2 \xi_n \omega_n \dot{Y}_n + \omega_n^2 Y_n = -\left(\frac{\Gamma_{nX}}{M_n} \ddot{v}_{gX} + \frac{\Gamma_{nY}}{M_n} \ddot{v}_{gY} + \frac{\Gamma_{nZ}}{M_n} \ddot{v}_{gZ}\right) \qquad (3.41)$$

and the modal response will be

$$Y_n = Y_{nX} + Y_{nY} + Y_{nZ} \tag{3.42}$$

where $Y_{nX}$ is the amplitude of the $n^{th}$ mode due to ground acceleration in the X-direction, which can be obtained from

$$Y_{nX}(t) = \frac{\Gamma_{nX}}{M_n} \frac{1}{\omega_n} V_{nX}(t) \tag{3.43}$$

where $V_{nX}(t)$ is the response function for the $n^{th}$ mode due to ground acceleration in the X-direction, defined as

$$V_{nX}(t) = \int_0^t \ddot{v}_{gX}(\tau) \; \text{EXP}\left[-\xi_n \omega_n (t-\tau)\right] \sin \omega_n (t-\tau) \, d\tau \tag{3.44}$$

similarly for $Y_{nY}$ and $Y_{nZ}$ .

It is to be noted that step-by-step integration scheme is used in the computer programs to solve Equations (3.41)

The response spectrum analysis for bridge structures does not consider the simultaneous application of the three directional earthquake excitation. Only one component at a time may be considered, hence the analysis is identical to that discussed in Section 3.3.3 except that $\Gamma_n$ and $\ddot{v}_g$ will be replaced by $\Gamma_{ni}$ and $\ddot{v}_{gi}$, where i denotes the direction of the earthquake excitation loading.

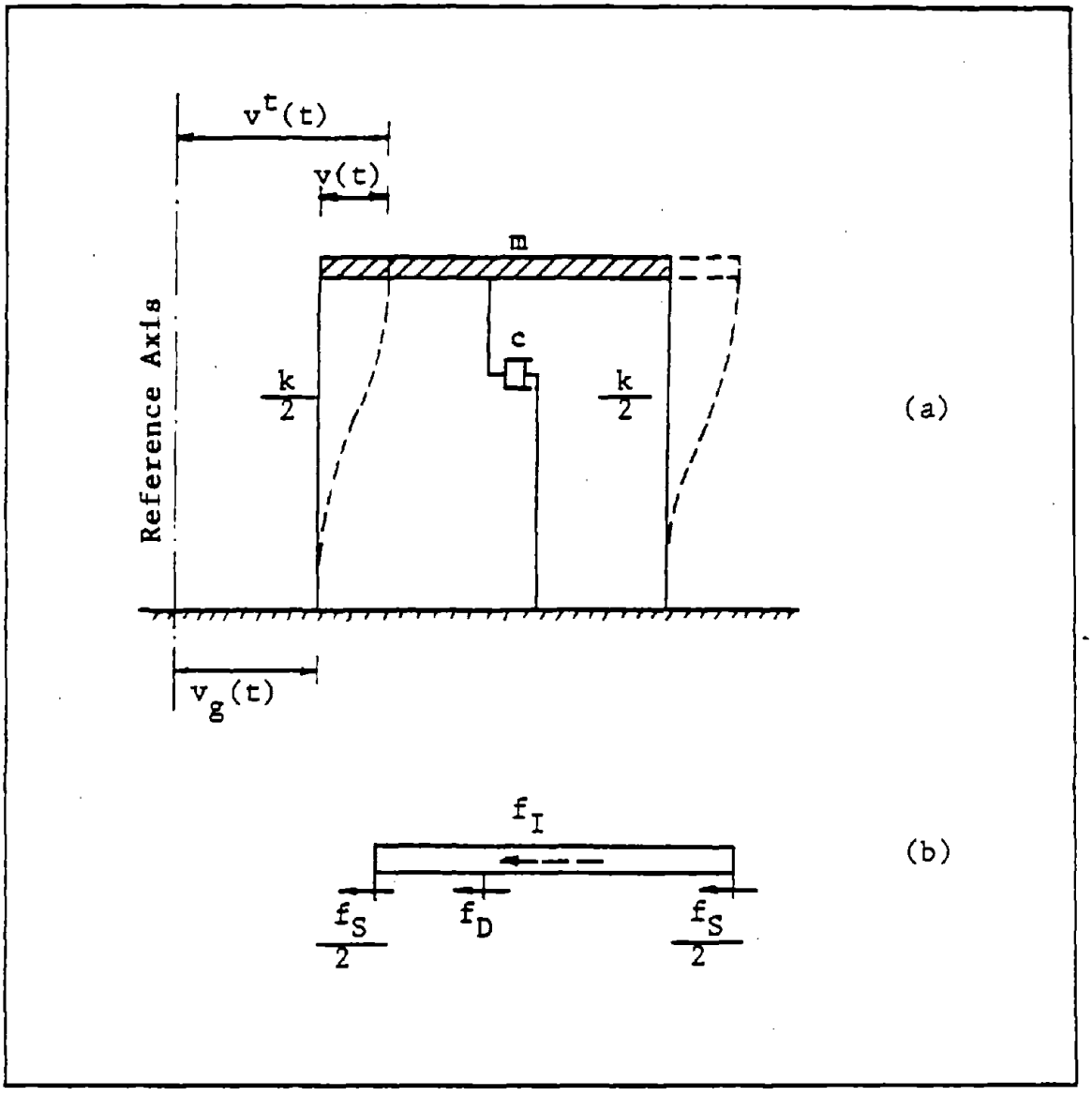


Figure 3.1 Lumped SDOF System Subjected to Support Excitation:
(a) Motion of System
(b) Equilibrium Forces

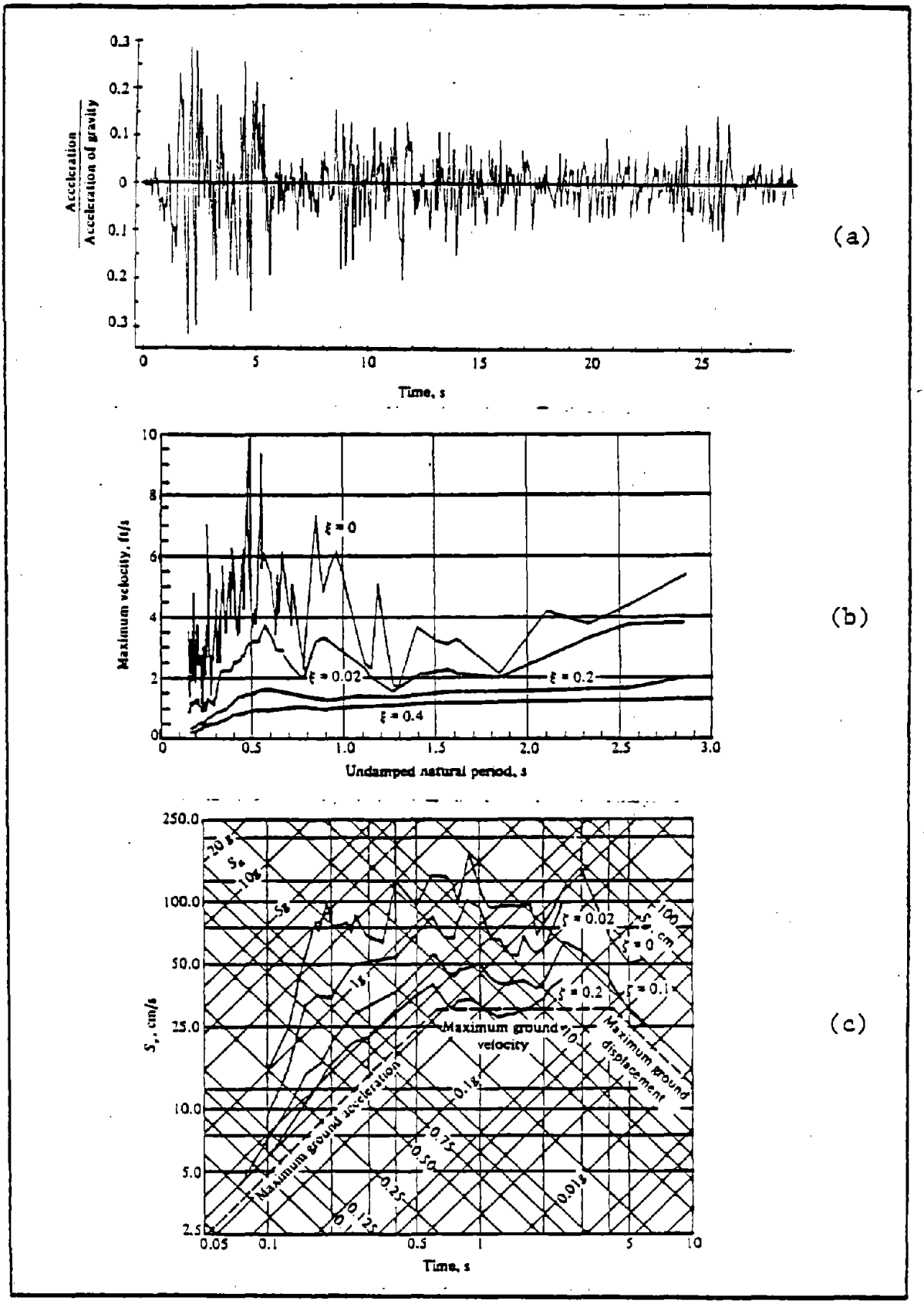


Figure 3.2 El Centro Earthquake, N-S Component [9]
(a) Acceleragram
(b) Pseudo Velocity Response Spectrum
(c) Response Spectra

# CHAPTER IV

# SEISMIC ANALYSIS OF STEEL BOX-GIRDER BRIDGES

In order to perform seismic analysis of bridges, both the bridge structure and the seismic input loading have to be defined. Geometry and structural details of both the superstructure and the columns will be presented, and the seismic loading which it applied to the structure will be discussed in detail. The finite element computer program SAP IV which is used in the analysis, and the subroutines that were developed to adjust it to the dynamic analysis of steel box girder bridges will also be discussed. Bridge modeling, taking into account the curved geometry and boundary conditions, and an illustrative example for a three span bridge are also presented.

## 4.1 Bridge Structures

The number of curved steel box-girder bridges constructed has been increasing in recent years due to more stringent route requirements and a desire for a greater sense of esthetics. Based on a survey conducted by Heins et al. [20,24,25,26] on such types of bridges, the following parameters will be considered:

1. Number of spans, NS
2. Span length, L
3. Span ratio, $n = \frac{L_1}{L}$

4. Radius of curvature, R

5. Number of girders and girder spacing

6. The structural details of the deck cross-section

7. Column geometry and stiffness

Each of the above parameters will be briefly discussed.

### 4.1.1 Number of Spans

Single, two, three, four, and five span bridges will be considered for the seismic analysis.

### 4.1.2 Span Length and Span Ratio

The span length ranges from 50 feet up to 220 feet, while the span ratio ranges between 1.0 and 1.5 .

### 4.1.3 Radius of Curvature

Both straight bridges ($R=\infty$) and curved bridges with curvature up to 1/200 ($ft^{-1}$) are considered. It is to be noted that the ratio $\frac{R}{L}$ is always greater than 3. , and bridges are considered straight for $\frac{R}{L} \geq 16$ .

### 4.1.4 Number of Girders and Girder Spacing

Most bridges consist of 2 or 3 girders, although some single span bridges have up to 5 girders. Girder spacing depends on the bridge width or the number of traffic lanes which ranges from one lane for single span bridges up to five lanes for multiple-span bridges. While the number of girders mainly affects the stiffness of the bridge in case of static analysis, it has more influence on the inertia forces, or the mass of the structure per unit length, for the dynamic analysis.

### 4.1.5 Structural Details of the Deck Cross-Section

A typical cross-section of a steel box-girder bridge deck is shown in Figure 4.1 . Thicknesses of top and bottom flanges range between 1/2 in. and 2½ in., while web thickness ranges between 1/2 in. and 1. in. .The minimum width of the top flange is 12. in., and the maximum width is 32. in. .The width of the bottom flange depends on the bridge width and the number of girders, and the web depth is approximately 1/25 of the span length. The web angle ranges between 0. and 14. degrees. It is to be noted that the bridge cross-section over the piers, which is approximately 20% of the span length on each side, is stiffer than that at the middle of the span.

### 4.1.6 Column Geometry and Stiffness

For a three-lane bridge, which dominates most of the steel box-girder bridges, a three-column bent is generally used. Such column bents are directed radially, and they generally have the following details for round concrete columns:

| | | |
|---|---|---|
| Diameter | : | 2.5' ∿ 3.0' |
| Steel Bars | : | 12 ∿ 20 #11 |
| Moment of inertia | : | 2.8 ∿ 6.0 ($ft^4$) |
| Column height | : | 10' ∿ 15' and up to 30' |
| Column spacing | : | 15' ∿ 18' |

## 4.2 Seismic Loading

El Centro earthquake accelerogram of May 18, 1940 (magnitude 7.1) will be used as a dynamic input in this study. This accelerogram is a good recording of the ground motion in

the epicentral region of a damaging earthquake. In general it may be stated that the El Centro excitation contains energy over a broad range of frequencies and has a relatively long total duration and duration of intense shaking [ 8 ]. The maximum peak acceleration of this record is .35g, where g is the gravitational acceleration.

Figures 4.2 to 4.4 show the three components of El Centro accelerogram [29]. The N-S component (S00E) is shown in Figure 4.2, while the E-W component (S90W) and the vertical component (VERT) are presented in Figures 4.3 and 4.4 respectively. The corresponding response spectra for each component are presented in Figures 4.5 to 4.7 [30].

It is to be noted that El Centro earthquake record is one of the best records obtained to date in the United States for strong ground shaking, and is usually used in seismic analysis [56]. Intensity of ground motion and site effects for different parts of the United States will be discussed later in Chapter VII.

## 4.3 Seismic Responses

Displacements, actions, and stresses at the critical points of the bridge will be studied. The following responses will be considered:

1. Attachments:
   - (i) Tangential displacement at the abutment
   - (ii) Tangential force, radial force and vertical moment at the abutment

(iii) Radial force at the pier-superstructure roller connection

It is to be noted that the tangential and radial directions are related to the horizontal alignment of the superstructure.

2. Superstructure:

(i) Steel and concrete normal stresses at the abutment

(ii) Steel and concrete normal stresses at the middle of the span length

(iii) Steel and concrete normal stresses over the pier

3. Columns:

(i) Concrete normal stress at the column base

Shear stresses will also be studied for both the superstructure and columns critical sections.

## 4.4 The Computer Program

The finite element program SAP IV for the static and dynamic response of linear systems is used in the analysis [3]. The original program is written in FORTRAN language and consists of 113 subroutines (about 15,000 cards), and is organized in a standard Fortran overlay structure to reduce the required high speed storage for program execution. A double precision arithmetic version of the program was adjusted to the University of Maryland UNIVAC 1100 system, and was successfully checked using several examples. Seven subroutines

had to be modified, two were developed, and four disk file elements were created to account for the program compilation, mapping, and the restart capabilities.

The program performs both static and dynamic analysis for linear systems. Four types of dynamic analysis can be carried out:

1. Determination of system mode shapes and frequencies only
2. Frequency calculations followed by response history analysis using mode superposition
3. Frequency calculations followed by response spectrum analysis
4. Response history analysis by direct integration

It is to be noted that in the program once the frequencies and mode shapes are obtained they are written on low speed storage, and utilizing the restart capabilities a variety of response history and response spectrum analyses can be carried out with relatively small additional cost.

The element library of SAP IV consists of nine different element types, which can be used in either static or dynamic analysis. Since both the bridge superstructure and columns will be modeled using 3-D space frame elements, that type of element will be discussed in more detail. A typical 3-D beam element is shown in Figure 4.8 . This element, which is prismatic, considers torsion, bending about two axes, axial and shearing deformations. A plane which defines the principal bending axis of the beam is specified by the plane i, j, k,

where i and j are the two nodes of the element, and point k will always be taken as the center of curvature of the superstructure. It is to be noted that forces (axial and shear) and moments (torsion and bending) are calculated in the beam local coordinate system 1, 2, and 3 .

### 4.4.1 Modification of the Program

A computer program was developed to calculate the properties of the bridge deck cross section shown in Figure 4.1. The section structural details are introduced as an input to the program, and the cross sectional area, moments of inertia, product of inertia, torsional inertia, and section moduli are calculated. Four types of lateral bracings may be used as shown in Figure 4.9 [21]. Both composite and non-composite sections are considered, where in case of composite sections, the properties of an equivalent steel cross section are obtained. Equivalent unit weight and mass, which are used to evaluate the dead load and the mass of the superstructure, are calculated for both composite and non-composite sections considering the concrete slab in both cases. The program can also compute the normal stresses due to bending for both steel and concrete at the critical points of the cross section [5]. Shear stresses due to both bending and torsion are also calculated utilizing simplified assumptions [21].

This program was introduced into SAP IV program as a set of subroutines to generate the section and material properties for the superstructure, and to calculate the normal and shearing stresses due to seismic ground-motion-acceleration

input loading. Another group of subroutines were developed to compute the column stresses. Three options are available for printing the seismic stress response: 1) print histories and maxima, 2) printer plot of histories and recovery of maxima, or 3) recover maxima only. A total of ten subroutines were created, and eleven were modified to develop the final version of the program. A partial listing of the new subroutines is presented in Reference (62).

The capacity of the program is mainly controlled by the number of nodal points of the structural system, number of frequencies considered, number of seismic input loadings, and the total number of solution time steps. Hence, several versions of the program were developed with different capacities or sizes to optimize the cost of executing the program.

### 4.4.2 Description of Input Data

A complete discussion of input data for SAP IV is presented in reference [ 3 ]. This section will discuss only the new input data for the modified version of the program, and how they are related to the original input. A sample of a complete input data is presented in Reference (62).

This set of new data is introduced in the element data section of SAP IV original input, right after the control card. It is to be noted that the number of element property (NUMETP) and the number of material property (NUMMAT), which are specified in the control card, should be the same.

(I) Superstructure

(i) Material properties [2 cards]

| Card | Format | Variable | Entry |
|---|---|---|---|
| 1 | (4F10.0) | EST | Young's modulus for steel |
| | | PRST | Poisson's ratio for steel |
| | | UTMSST | Steel mass density |
| | | UTWTST | Steel weight density |
| 2 | (4F10.0) | EC | Young's modulus for concrete |
| | | PRC | Poisson's ratio for concrete |
| | | UTMSC | Concrete mass density |
| | | UTWTC | Concrete weight density |

(ii) Bridge parameters [5 cards] (refer to Figures 4.1 and 4.9)

| Card | Format | Variable | Entry |
|---|---|---|---|
| 1 | (I5,2F10.0) | NGIRDR | Number of girders |
| | | GSPACE | Girder spacing (center to center) |
| | | BRDGWD | Bridge width |
| 2 | (I5,2F10.0) | IBRACE | Bracing type (refer to Figure 4.9) |
| | | S | Diaphragm spacing |
| | | AD | Cross sectional area of bracing |
| 3 | (3F10.0) | TS | Concrete slab thickness |
| | | ALS | Angle between slab and horizontal |
| | | DH | Depth of haunch |
| 4 | (2F10.0) | SMISC | Percentage of miscellaneous steel |
| | | CMISC | Percentage of miscellaneous concrete |
| 5 | (215,F10.0) | NUMXSB | Number of bridge deck cross sections |
| | | NUMXSC | Number of column cross sections |
| | | SPAN | Span length |

(iii) Structural details [NUMXSB sets of 4 cards each] (refer to Figure 4.1)

| Card | Format | Variable | Entry |
|---|---|---|---|
| 1 | (2I5) | NSEC | Section number (from 1 to NUMXSB) |
| | | ICOMP | Type of cross section:<br>0 noncomposite<br>1 composite |

| Card | Format | Variable | Entry |
|---|---|---|---|
| 2 | (6F10.0) | TFWL | Width of left top flange |
| | | TFTL | Thickness of left top flange |
| | | TFWR | Width of right top flange |
| | | TFTR | Thickness of right top flange |
| | | BFW | Bottom flange width |
| | | BFT | Bottom flange thickness |
| 3 | (6F10.0) | WBDL | Depth of left web |
| | | WBTL | Thickness of left web |
| | | ALL | Angle between left web and vertical |
| | | WBDR | Depth of right web |
| | | WBTR | Thickness of right web |
| | | ALR | Angle between right web and vertical |
| 4 | (I5,3F10.0) | NSTF | Number of bottom flange stiffeners |
| | | ASTF | Cross sectional area of each stiffener |
| | | IXSTF | Moment of inertia of each stiffener about a horizontal axis |
| | | YSTF | Distance between centroid of stiffeners and the bottom flange |

It is to be noted that the units used for this set of data (I) are kips, inches, and degrees.

(II) Supporting elements

Material and cross sectional properties input data of the bridge columns and other special elements will immediately follow the set of data described above in (I). They are introduced in accordance with the original input data for SAP IV, starting with the columns properties numbered as (NUMXSB + 1). The units which are used in this section, as well as the rest of the input data, are kips, feet, and degrees.

(III) Output options

The modified program can calculate both normal and shear

stresses at different cross sections for both the superstructure and the columns due to a ground-motion-acceleration dynamic input. In order to compute these stresses for some element cross section, the six action components (axial force, two shearing forces, torsional moment, and two bending moments) at that section have to be specified in the "output definition cards" input section [ 3 ]. It should also be noted that the option specified for printing these actions will consequently apply to the stresses.

## 4.5 Bridge Modeling

The bridge is modeled using 3-D space frame elemnts, with nodes selected to realistically model the stiffness and inertia effects of the structure. Masses in the deck should be lumped at least at the quarter points, while column masses may be lumped at the third points [15,31,33,49]. In both the superstructure and the columns, only the translational degrees of freedom at each node will be considered for the inertia effects. The program automatically generates a lumped mass matrix, with only translational mass coefficients, using elements geometry and material density.

Figure 4.10 shows a typical model for a three span curved bridge. Nodes and elements are numbered from left to right for the superstructure, and from bottom to top for the columns. For the deck elements, node i should always be less in number than node j , while for all bridge elements node k should be taken as the center of curvature for the superstructure.

The X-axis is taken in a direction parallel to the chord connecting the abutments. This direction will be called the longitudinal direction. The transverse direction, or the Z-axis, is perpendicular to the chord in a horizontal plane, and the Y-axis is vertical.

### 4.5.1 Curved Geometry and Boundary Conditions

To model the freedom of movement at the abutments, appropriate member releases in short elements at these locations are used. At one abutment, all degrees of freedom will be restrained except the radial rotation, while at the other one, both radial rotation and tangential translation are allowed. These short elements also insure that the superstructure mass is properly lumped, and no inertia effects are lost. The element length will be taken as 1% of the adjacent element length.

The roller supports attaching the superstructure and the bents are modeled using short vertical massless elements having neither torsional nor bendings stiffness in the radial direction. These elements, which are assumed to be 0.5 ft long, have a relatively large area to minimize the relative vertical deformations at those connections.

The three-column bents are modeled using only two columns having equivalent properties, and the base of each column is assumed to be fixed at the footing. A comparison with three-column models will be presented in Chapter V.

## 4.6 Illustrative Example

A three equal spans curved steel box girder bridge will

be analyzed. The bridge span length is 100' , and the radius of curvature is 800' . The superstructure consists of 3 girders 170" apart, and the bridge width is 42.5' (3 lanes). A horizontal concrete slab of 8" thickness is considered, with haunches of 3" depth.

The superstructure has two cross sections $XS_1$ and $XS_2$ , with the second one covering 16% of the span length on each side of the bents. These cross-sections are symmetrical, and have the following properties:

| | $XS_1$ (in.) | $XS_2$ (in.) |
|---|---|---|
| top flange width | 12.0 | 16.0 |
| top flange thickness | 1.0 | 1.5 |
| bottom flange width | 85.0 | 85.0 |
| bottom flange thickness | 0.75 | 1.0 |
| web depth | 50.0 | 50.0 |
| web thickness | 0.5 | 0.5 |

Both cross sections have inclined webs (14 degrees with vertical) and no bottom flange stiffners, and they will be considered as composite sections.

The bridge has three-column bents with round columns having the following properties:

height = 15'
spacing = 16'
area = 6 $ft^2$
stiffness = 4.5 $ft^4$

The bridge is modeled as shown in Figure 4.10, and will be first analyzed to obtain the system frequencies and mode shapes (considering 15 frequencies). A listing of input data is presented in Reference (62). Utilizing the restart capabilities, the N-S component of El Centro earthquake record and its response spectrum will be applied to the

structure in the transverse direction.

For the response history analysis, the first 10 seconds of the seismogram will be considered, and a 5% damping ratio is assumed. The seismic loading data is given in mm/sec$^2$ (adjusted to ft/sec$^2$) at equally spaced intervals of 0.02 second. Maximum displacements at the abutment, and maximum actions and stresses at the abutments, mid span, column base, and at the superstructure cross section over the pier will be considered. Maximum actions at the pier-deck roller attachments will also be obtained. A partial listing of the input data is included in Reference (62).

For the response spectrum analysis, El Centro N-S component spectrum, assuming 5% damping ratio, will be used. The spectrum units are g (the gravitational acceleration), and will be adjusted to ft/sec$^2$. A listing of input data is included in Reference (62).

The two disk file elements used for the restart technique are listed in Reference (62). The element RESTRT0 is added with the first run for computing the system frequencies and mode shapes, while the element RESTRT1 is added with each successive run for the response history or the response spectrum analyses. It is to be noted that the files TAPE1., TAPE2., TAPE7., TAPE8., TAPE9., and TAPE12. are permanent disk files that should be assigned prior to the program execution.

A partial listing of the computer program output is included in Reference (62). It is to be noted that the

actions components are computed in the element local coordinate system (Figure 4.8), while the displacements are calculated in the global coordinate system. Output units are kips and feet for both actions and displacements, and kips/in$^2$ (ksi) for stresses.

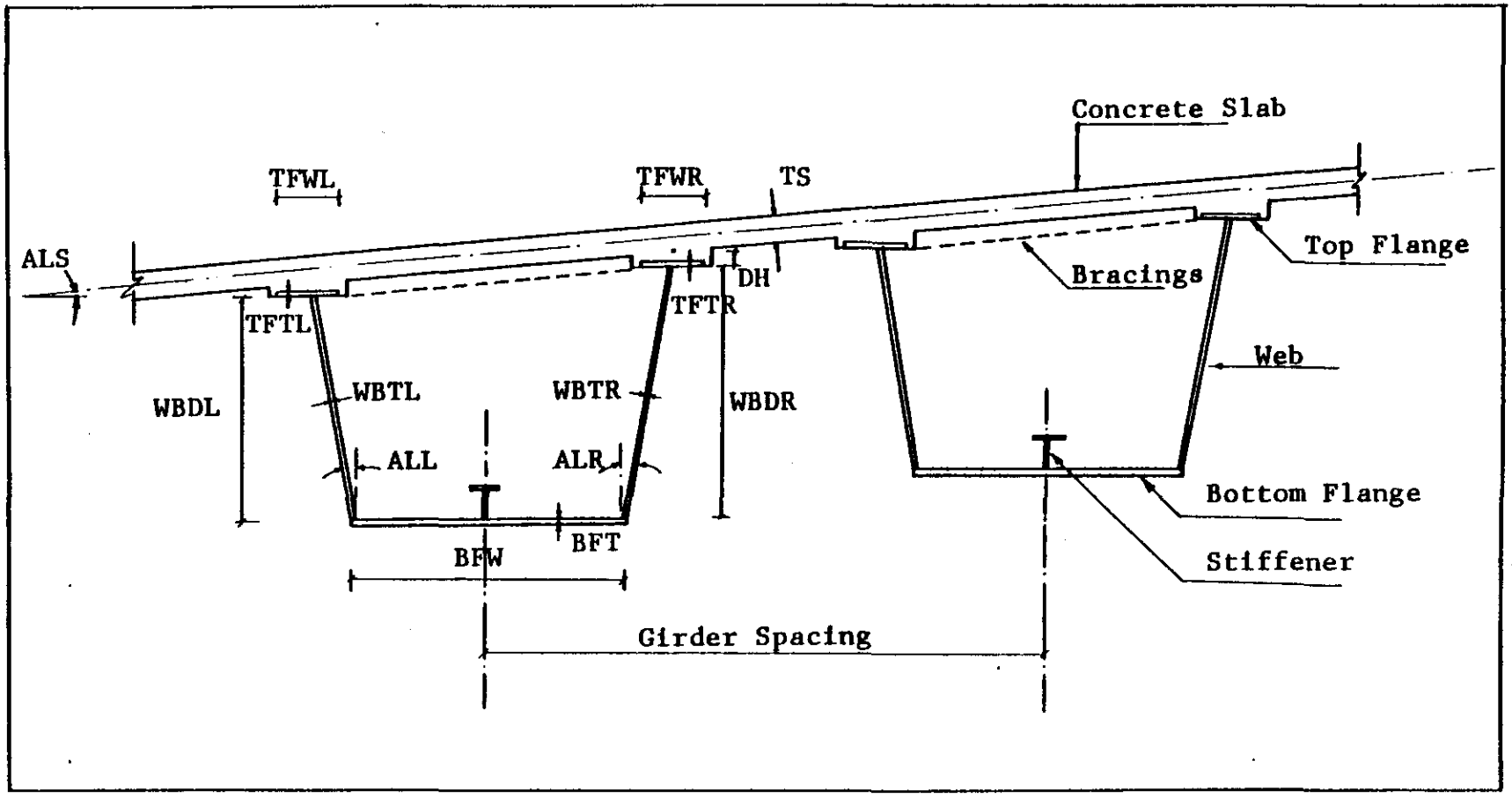


Figure 4.1 Typical Cross-Section of a Steel Box Girder Bridge Deck

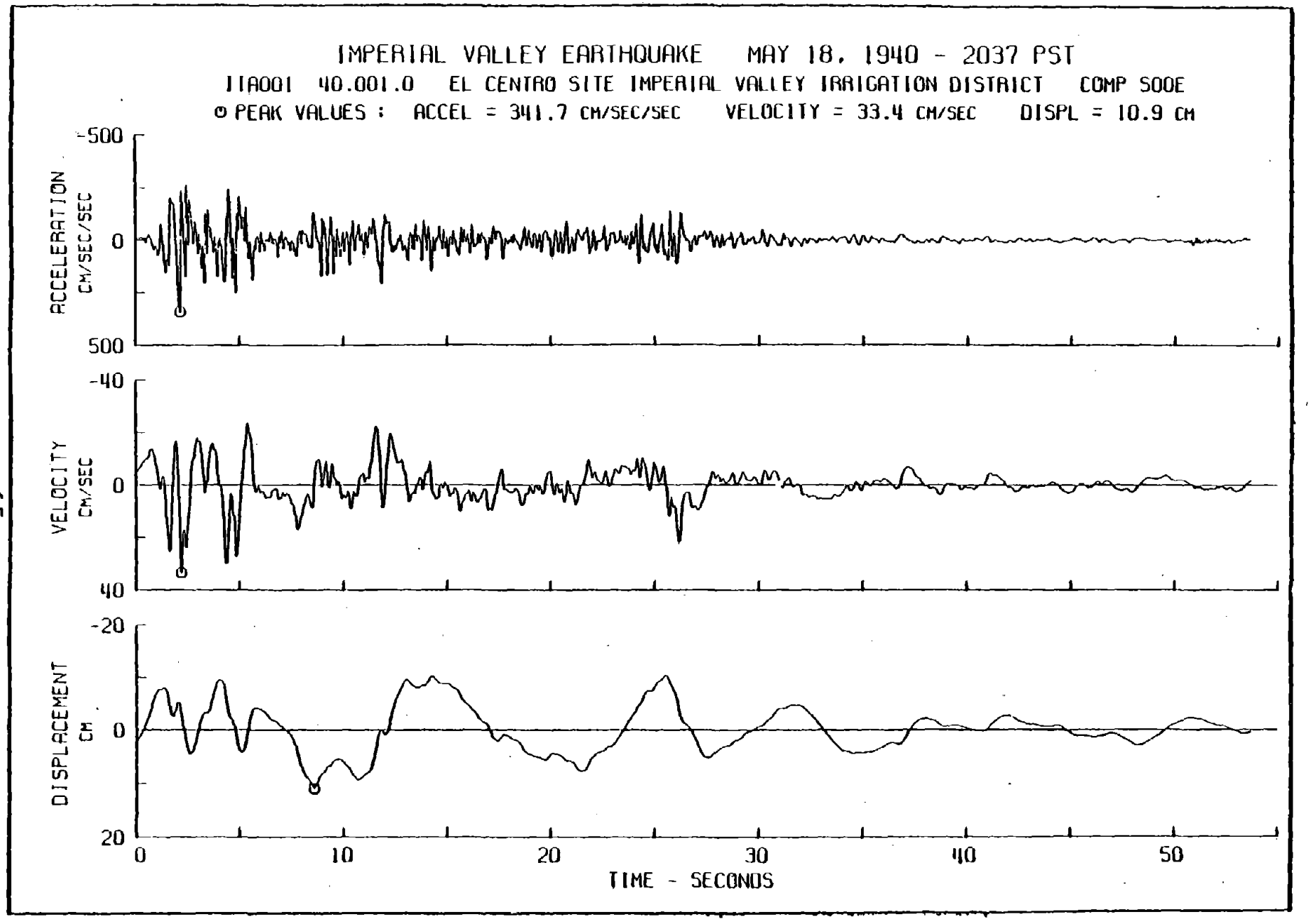


Figure 4.2 El Centro Earthquake, N-S Component [29]

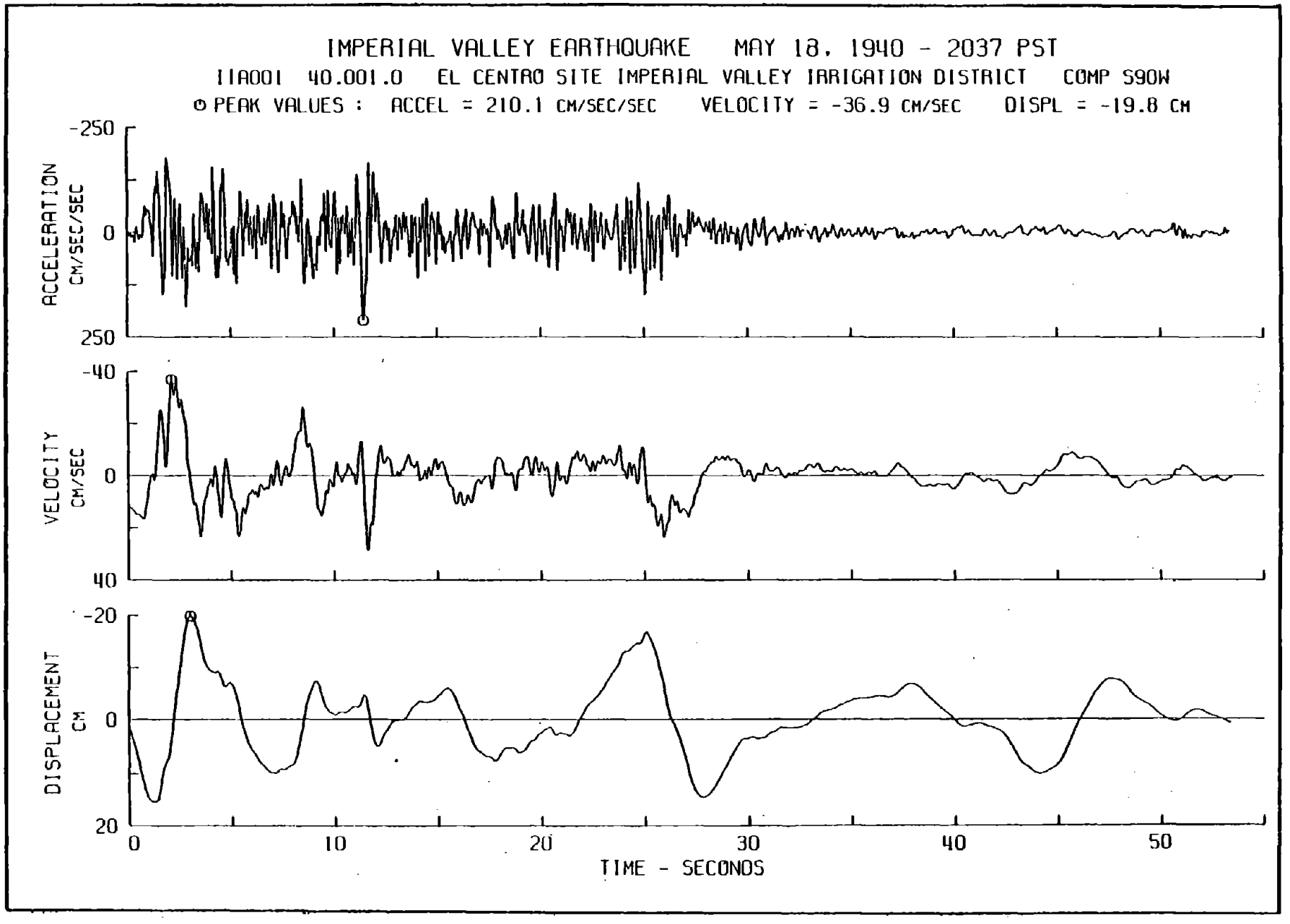


Figure 4.3 El Centro Earthquake, E-W Component [29]

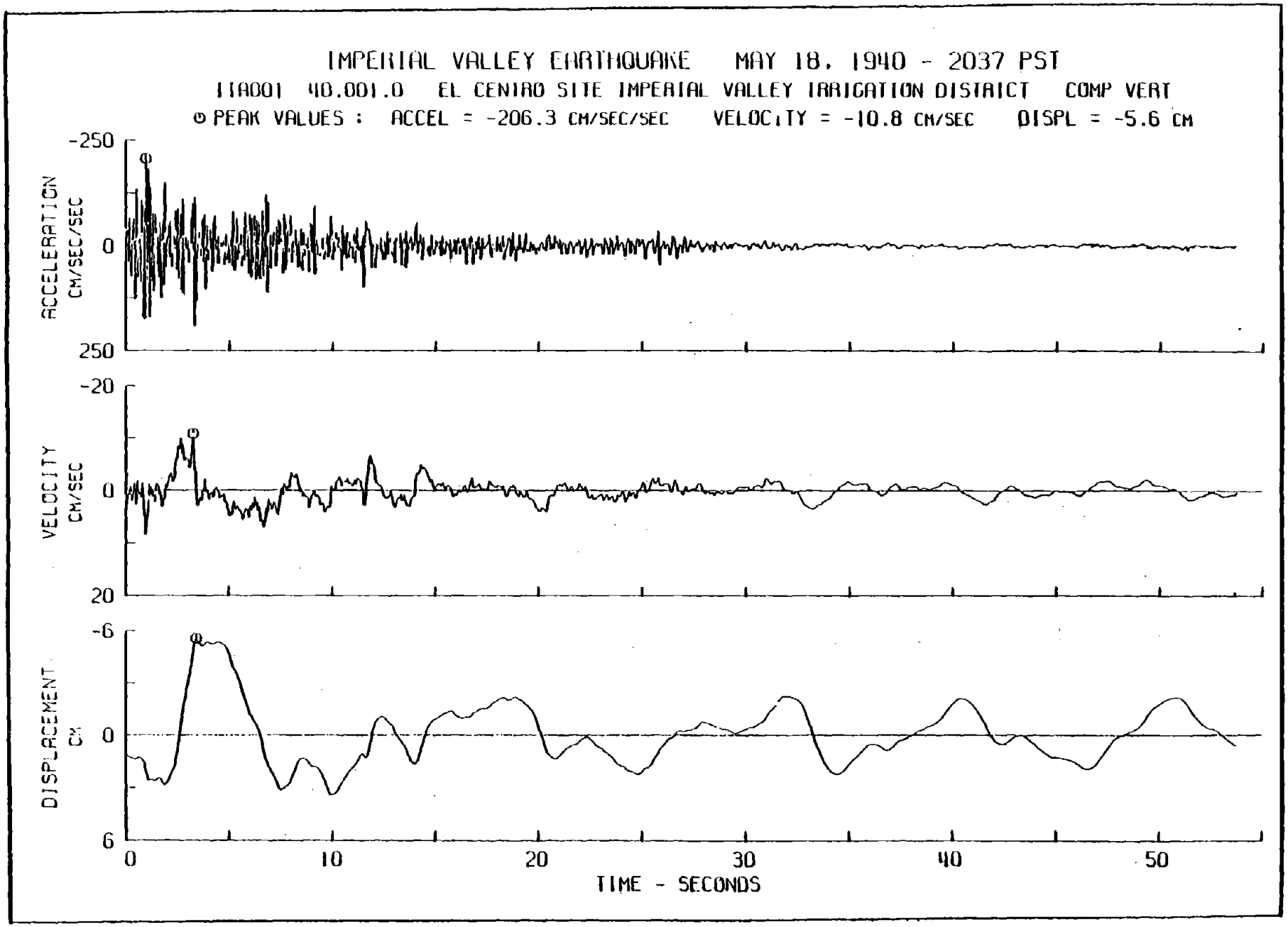


Figure 4.4 El Centro Earthquake, Vertical Component [29]

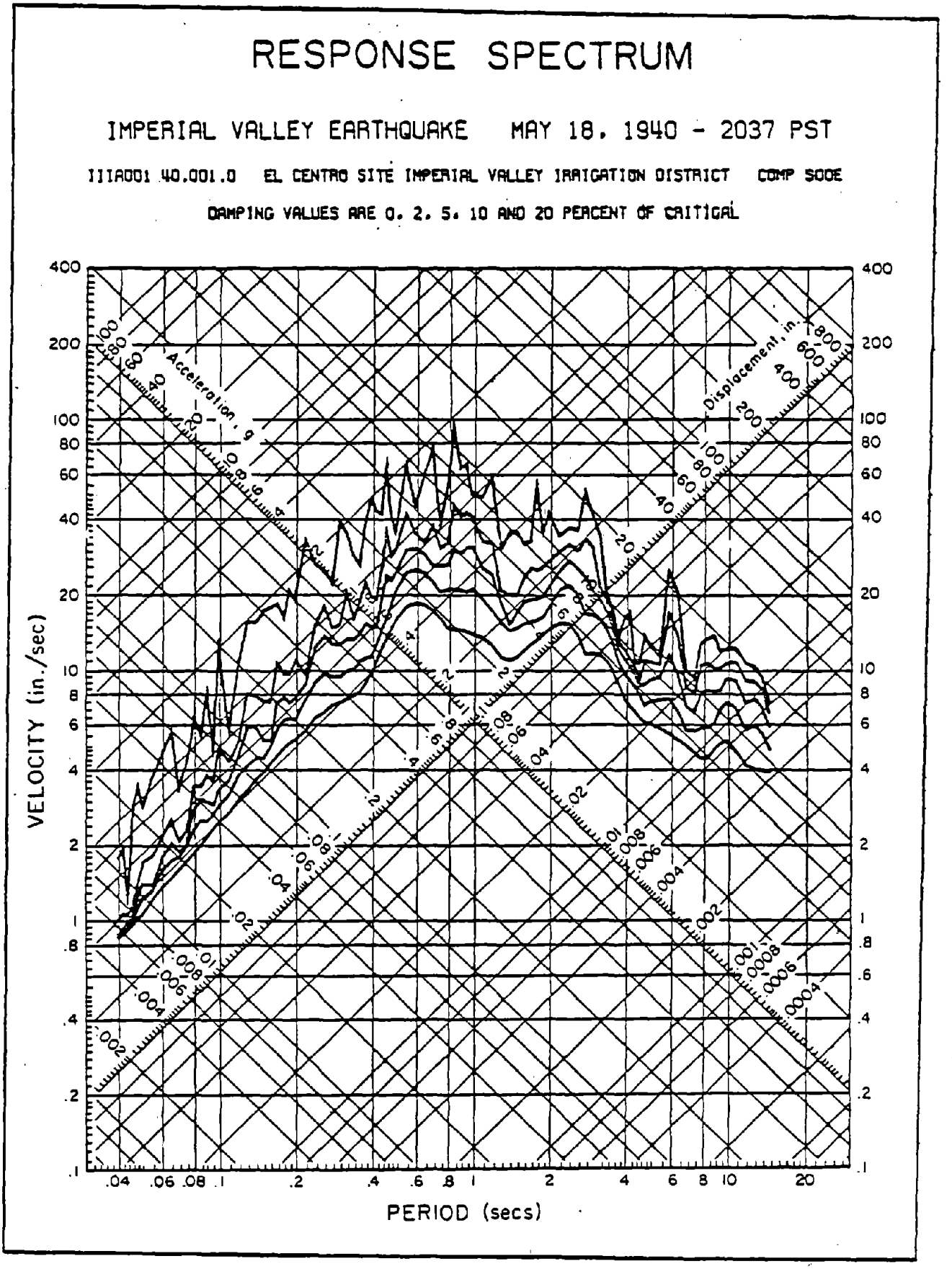


Figure 4.5 El Centro Earthquake Response Spectrum, N-S Component [30]

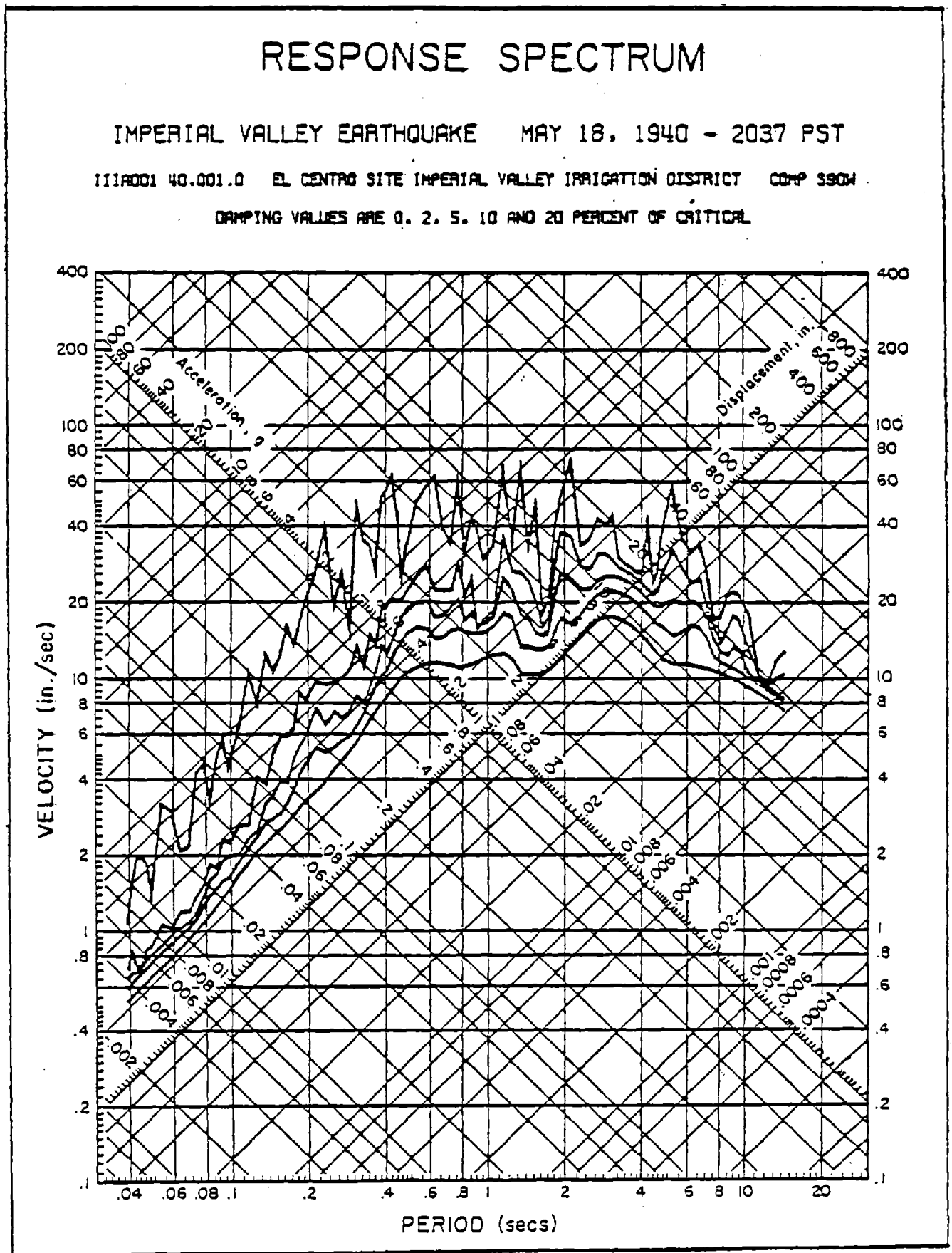


Figure 4.6 El Centro Earthquake Response Spectrum, E-W Component [30]

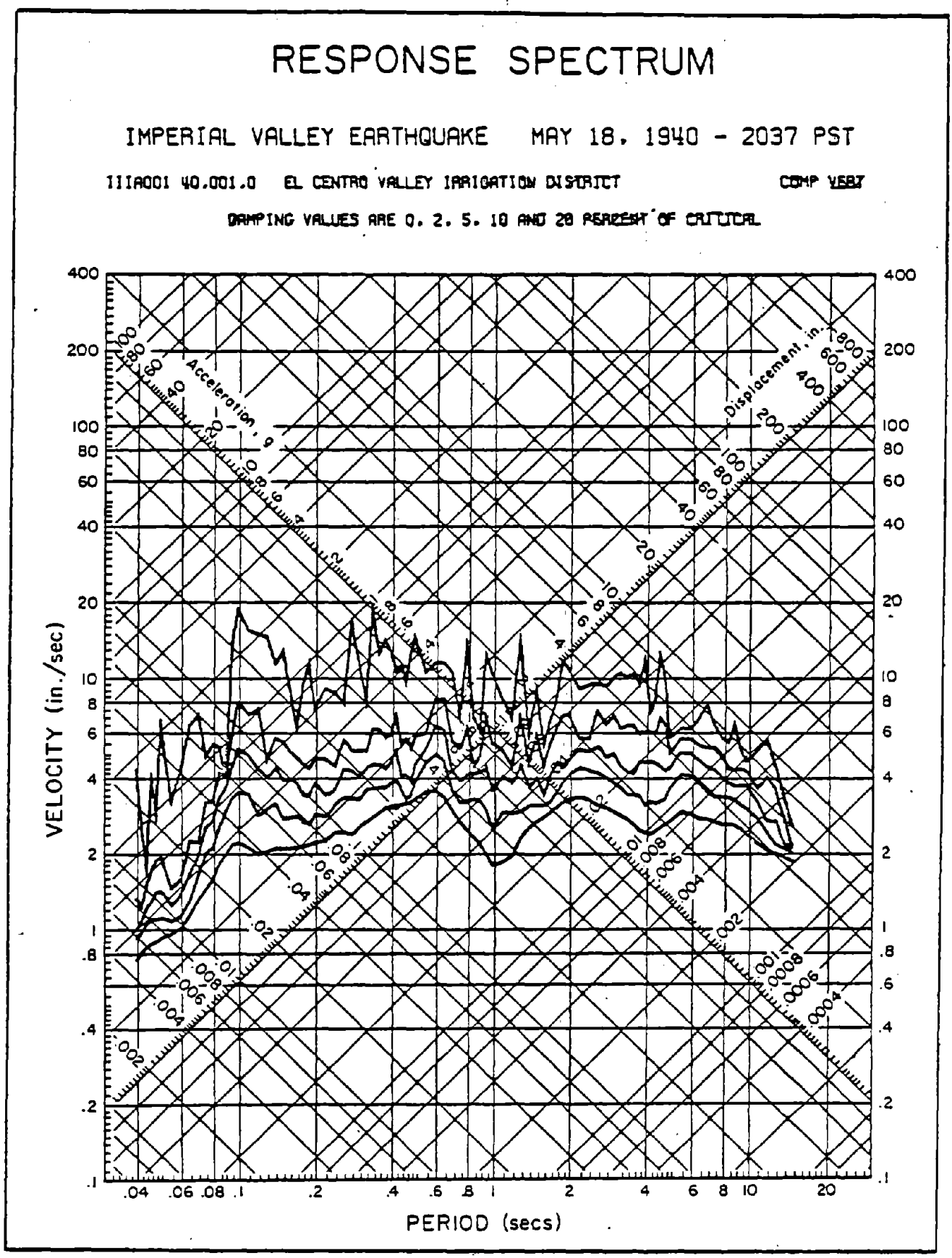


Figure 4.7 El Centro Earthquake Response Spectrum, Vertical Component [30]

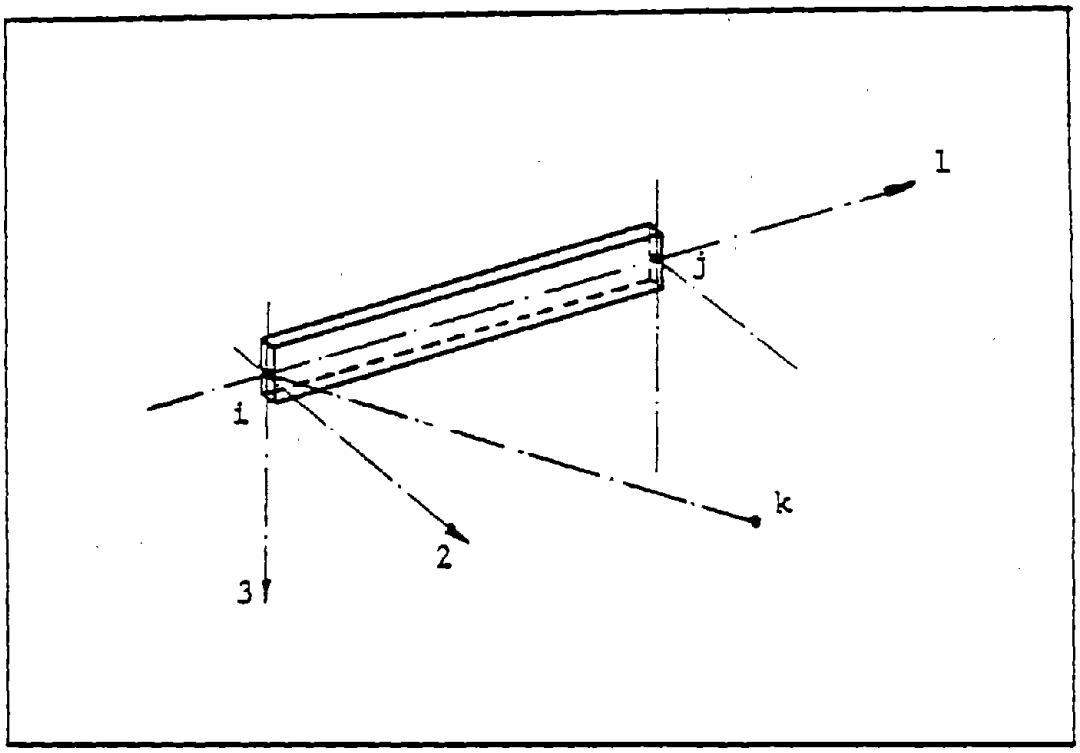


Figure 4.8 3-D Beam Element

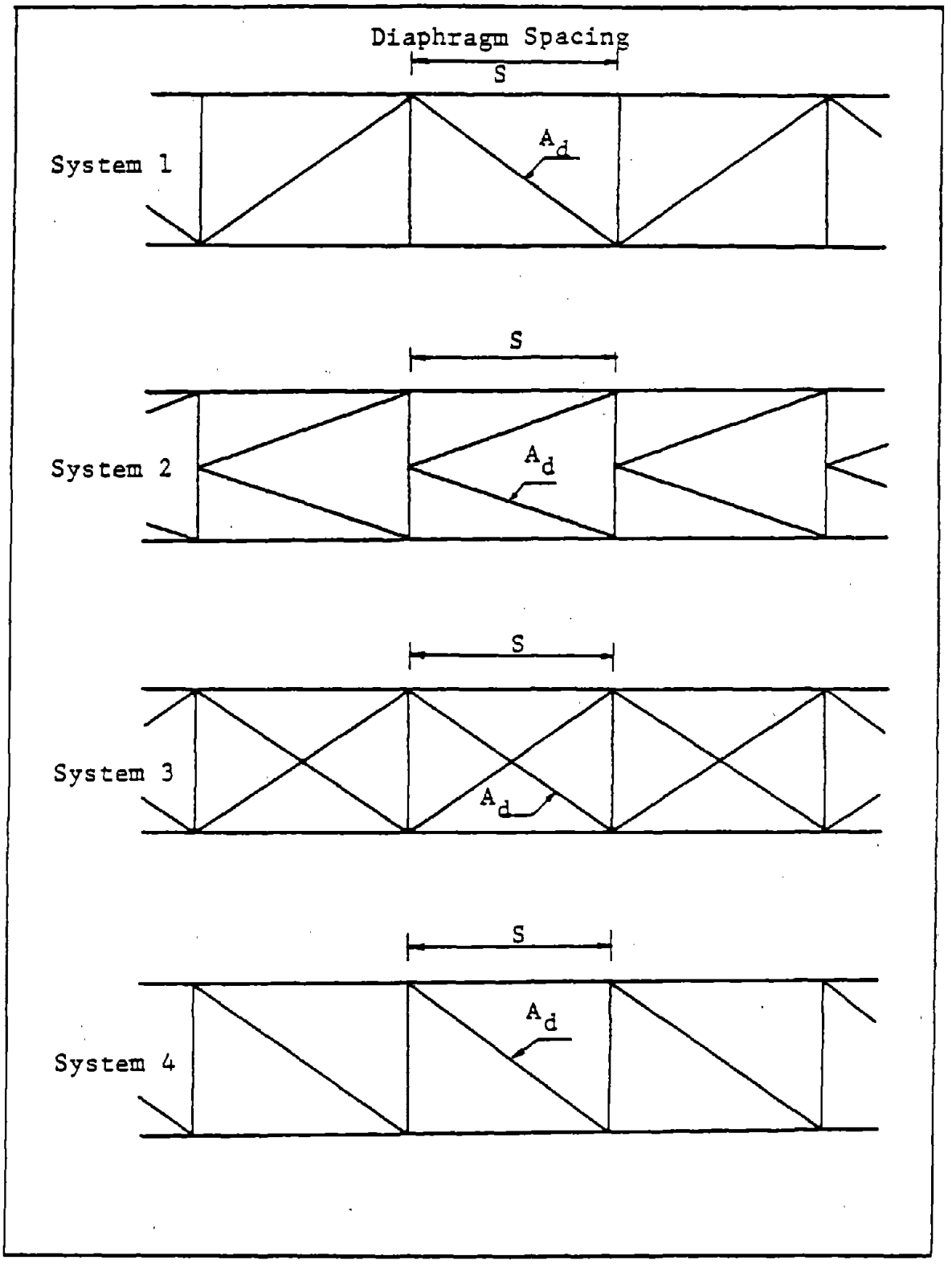


Figure 4.9 Bracing Configurations [21]

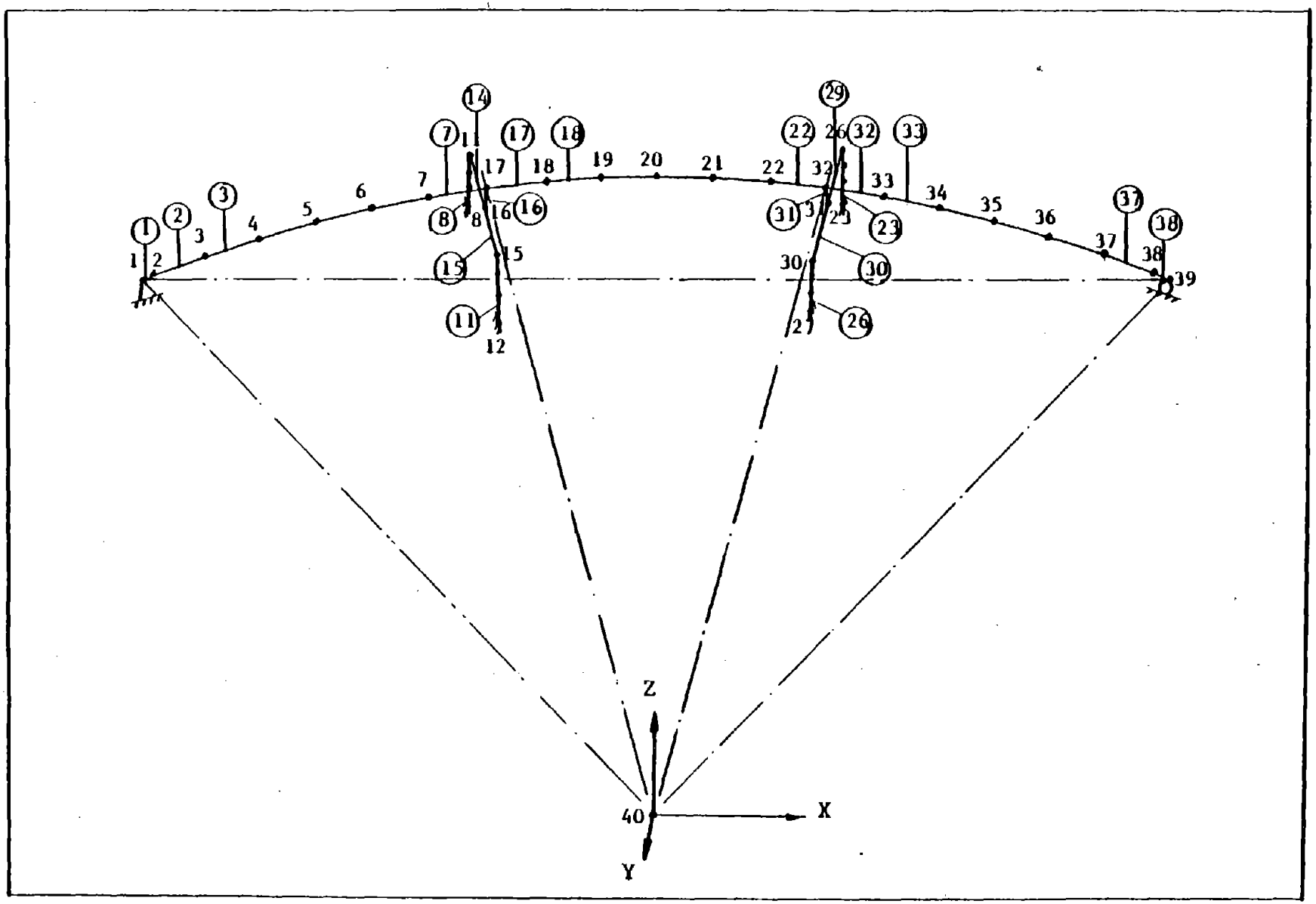


Figure 4.10 Finite Element Model For a 3-Span Curved Bridge

# CHAPTER V

## RESULTS OF THE SEISMIC ANALYSIS

In this Chapter the results of the seismic analysis of steel box-girder bridges are presented and discussed. Typical steel box-girder bridges with up to five spans are considered, and different elements of the bridge model and the seismic loading are examined for each case. A comparison between the response spectrum and the response history techniques is made, and the simultaneous application of the three components of the earthquake is discussed. Other factors influencing the seismic response are studied, including damping effects, composite and non-composite deck cross-sections, rotational inertia, and column height. A comparison with rigid-column models and closed form solutions is also made, and static analysis results due to dead loads are presented.

### 5.1 Case Studies

Typical single to five span steel box-girder bridges are analyzed, assuming the following properties:

(I) Bridge geometry

| | | |
|---|---|---|
| Span length | = | 100.' |
| Span ratio | = | 1.0 |
| Radius of curvature | = | 800.' |
| Number of girders | = | 3 |
| Girder spacing | = | 170." |
| Bridge width | | 42.5' (3 lanes) |
| Concrete slab thickness | = | 8." |
| Haunch depth | = | 3." |
| Bracing type | = | 3 |

(II) Structural details

The superstructure has two cross sections $XS_1$ and $XS_2$, with the second one covering 16% to 20% of the span length on each side of the bents. These cross sections are symmetrical, and have the following properties:

| | $XS_1$(in.) | $XS_2$(in.) |
|---|---|---|
| Top flange width | 12.0 | 16.0 |
| Top flange thickness | 1.0 | 1.5 |
| Bottom flange width | 85.0 | 85.0 |
| Bottom flange thickness | 0.75 | 1.0 |
| Web depth | 50.0 | 50.0 |
| Web thickness | 0.5 | 0.5 |

Both cross sections have inclined webs (14 degrees with vertical) and no bottom flange stiffeners, and they will be considered as composite sections.

(III) Bent geometry

Three-column bents are considered, with round columns having the following properties:

Height = 15'
Spacing = 16'
Area = 6 $ft^2$
Stiffness = 4.5 $ft^4$

It is to be noted that a 5% damping ratio is assumed for all bridges.

5.1.1 Seismic Responses

El Centro earthquake different components are applied to the bridge structures in the three global directions. The longitudinal shock is applied in the X-axis direction which is parallel to the chord connecting the abutments,

while the transverse excitation is in the Z-axis direction perpendicular to that chord. The vertical shock is directed along the Y-axis.

Displacements, actions, and stresses at the critical points of the bridge are studied. Locations of these critical sections are shown in the corresponding Figures for each case. The following responses are considered:

DT The tangential displacement at the abutment

P1 The tangential force at the abutment or the axial force at the column base

V2 The radial shearing force at the abutment or at the pier-superstructure attachment

V3 The vertical shearing force at the superstructure

M1 The twisting moment

M2 The radial moment

M3 The vertical moment at the abutments or the tangential moment at the column base.

It is to be noted that the tangential and radial directions are related to the horizontal alignment of the superstructure.

Maximum normal and shear stresses for both steel and concrete at the critical sections are also tabulated and discussed.

## 5.2 The Bridge Model

### 5.2.1 Supporting Elements

Both 2-column and 3-column bents are generally used to support steel box-girder bridges. All bents are modeled

using only two columns having equivalent properties. The intermediate column properties are equally distributed between the two exterior columns, and the concrete cap stiffness is increased to minimize the resulting deformations. A comparison between 2-column and 3-column straight models, using the (S00E) component, is presented. The response spectrum (R.S.) is applied in the longitudinal direction, while the ground motion acceleration time history (T.H.) is applied in the transverse direction.

### 5.2.2 End Boundary Conditions

The freedom of movement at the abutments is modeled using short elements with appropriate member releases. Radial moments at both abutments are released, while axial force is released only at one end. This modified end-boundary-conditions model is analyzed, considering a straight bridge and using the (S00E) component, and results are compared with the 2-column straight model with corresponding end supports restraints.

### 5.2.3 Number of Elements

The superstructure is modeled using 6 finite elements for each span length (10 elements in case of single span bridges). A comparison with a 10-element curved model (20-element curved model for single span bridges), applying the (S00E) component, is discussed.

### 5.2.4 Structure Periods and Participation Factors

The structure periods for the first modes of vibration

are tabulated, and the corresponding mode shapes are included in Appendix B.1 . The earthquake participation factors, defined by Equation (3.40), are also tabulated. These factors are useful in determining the coupling effects and the relative participation of each mode for a shock in a given direction.

### 5.2.5 Number of Mode Shapes

The mode superposition procedure yields good approximate results by considering only the contribution of the fewer lower modes. A comparison between 10, 15, and 20 mode shapes contributions is presented. The (S00E) component is applied individually in the three global directions, one at a time, and the corresponding responses are tabulated. A 3-direction shock, consisting of the three components of El Centro earthquake, is also considered.

### 5.2.6 Solution Time Step ($\Delta t$)

The computer program performs a step-by-step integration of the equations of motion using a scheme which is unconditionally stable with respect to time step $\Delta t$. The participation of the higher modes is filtered from the predicted response when large time step is used [ 3 ]. A comparison between three time steps; 0.0100, 0.0050, and 0.0025 seconds is made, applying the (S00E) component.

## 5.3 The Seismic Loading

Although the total duration of El Centro earthquake is more than 50 seconds, the intense ground shaking occurs in

the first 10 to 15 seconds of the record. Since this study is considering only linear analysis, the duration of intense shaking is of more interest. A comparison of 10 and 15 seconds shock durations is made applying both the (S00E) and the (S90W) components individually.

## 5.4 Methods of Analysis

### 5.4.1 Response Spectrum Technique (R.S.)

The (S00E) component response spectrum, assuming 5% damping ratio, is applied to the bridge structure in the three global directions, one at a time. For each case, the contribution of 10, 15, and 20 mode shapes is studied. The (S90W) component and the (VERT) component response spectra are also applied to the structure in the longitudinal and vertical directions respectively, and the results are tabulated. It is to be noted that the seismic responses obtained are maximum absolute values, which do not neccessarily occur at the same time, hence realistic values of normal and shear stresses may not be computed.

### 5.4.2 Time History Analysis (T.H.)

The first 10 seconds of the (S00E) component record is applied to the structure in the longitudinal, transverse, and vertical directions, one at a time. A solution time step $\Delta t$ of 0.0050 seconds is considered, and a 5% damping ratio is assumed. The contribution of 10 and 15 mode shapes is studied in each case, and a comparison with the response spectrum technique results is presented. Similar analysis is made using the (S90W) and the (VERT) components.

### 5.4.3 Simultaneous Application of the Earthquake Components (3-Direction Shock)

The first 10 seconds of each component is applied simultaneously to the bridge structure in the three global directions, considering the first 15 frequencies. Two cases are studied; first the (S00E) component is applied in the longitudinal direction while the (S90W) component is directed in the transverse direction and the (VERT) component is in the vertical direction. In the second case, the directions of the two horizontal components are interchanged. Seismic displacements, actions, and stresses in each case are compared with the responses obtained by applying each component individually. The time at which each maximum response occurs is also tabulated.

## 5.5 Damping, Stiffness, and Inertia Effects

The physical properties of the bridge structure, i.e., its mass, stiffness, and damping characteristics are examined. The contribution of the first 15 mode shapes is considered, and a 3-direction shock is applied to the structure. Damping ratios of 2%, 5%, and 10% are assumed and results are compared. Non-composite deck cross sections are considered, and the structure periods and participation factors and the resulting seismic responses are tabulated.

The computer program automatically forms a lumped mass matrix, containing only translational mass coefficients, using the element geometry and the material density. The effect of the bridge width is studied by introducing rotational inertia coefficients in the X-direction, and the corresponding actions

and stresses are tabulated.

Another important parameter that influence the seismic response is the height of the columns. A long-column model, with column height equals to 45' and column spacing equals to 10', is analyzed and results are compared with the short-column model case.

## 5.6 Rigid-Column Model and Exact Solution

Rigid column bents will ultimately behave as roller supports, and the bridge may be considered as a continuous beam. A rigid-column straight model is analyzed, and the structure periods are compared with closed form solutions for continuous beams [4]. A 3-direction shock is applied to the structure, and the resulting seismic responses are compared with the 2-column model case.

## 5.7 Static Analysis

Each bridge is analyzed under the effect of its own weight. The maximum stresses in the bridge deck and columns due to dead load are computed and compared with the dynamic responses.

## 5.8 Results of the Analysis

### 5.8.1 Single Span Bridges

A single span curved bridge model is shown in Figure 5.1. A comparison between a straight and a modified end-boundary-conditions model is presented in Tables A1.1 to A1.3. Results show a very good agreement between the two models. Analysis of 10-element and 20-element models is summarized in

Tables A1.4 to A1.6 , and the results indicate that increasing the number of elements does not have a significant effect on the seismic responses. The first 10 mode shapes for the 10-element model are shown in Figure B1.1 . The difference in seismic responses using 0.0050 and 0.0025 seconds time steps is less than 1% as shown in Tables A1.7 and A1.8 ,which suggests choosing the first time step to minimize the cost of excuting the computer program.

A comparison between response spectrum and time history analysis, presented in Tables A1.9 and A1.10 , shows that the first method yields much higher seismic responses which are in error. The contribution of higher modes of vibration, with relatively high frequencies, is the main reason for the failure of the response spectrum method for this model. Tables A1.11 to A1.14 present the results of the simultaneous application of the earthquake components, which show that the seismic responses due to a 3-direction schock are generally higher than individually applying each component in one direction.

The seismic responses decrease with an increase in the damping ratio as shown in Tables A1.15 and A1.16 , while the non-composite deck model, which is less stiff than the composite deck model, yields lower frequencies and higher stresses as shown in Tables A1.17 to A1.19 .

The structure periods obtained using the finite element program are in good agreement with the exact solution as shown in Table A1.20 , and both steel and concrete normal stresses due to dead loads are presented in Table A1.21 .

### 5.8.2 2-Span and 3-Span Bridges

The 2-column and 3-column models are shown in Figures 5.2 and 5.5 , and a comparison between the two models is presented in Tables A2.1 to A2.3 and A3.1 to A3.3 . Results show that the 2-column model yields conservative responses range from 1% for the superstructure to 15% for the column stresses, hence the 2-column model will be used throughout this study.

Structure periods and seismic responses for the modified end-boundary-conditions straight models are presented in Tables A2.4 to A2.6 and A3.4 to A3.6 . The good agreement between these results and the 2-column model case with end support restraints justifies the use of the short elements with member releases.

Figures 5.3 and 5.6 show 2-span and 3-span 6-element models. The slight difference in results between the 6-element and 10-element models, as presented in Tables A2.7 to A2.9 and A3.7 to A3.9 , suggests the use of the first model to minimize the problem size, and hence the program rxcution CPU time.

The structure periods and the participation factors for the first modes of vibration are included in Tables A2.10 and A3.10 , and plots of the first 10 mode shapes for both 2-span and 3-span curved bridges are shown in Figures B1.2 and B1.3 respectively. The participation factors together with the mode shape plots indicate that there is a coupling in the two horizontal directions due to the curved alignment of the bridges.

A comparison between different mode shapes contribution

to the final response for the time history technique, presented in Tables A2.11 , A2.12 , A3.11 , and A3.12 , show that increasing the number of vibration modes result in less than 4% change of the final responses.

The effect of different time steps, shown in Tables A2.13 , A2.14 , A3.13 , and A3.14 , indicates that the results are converging with the decrease in the solution time step, hence a 0.0050 seconds step will be used for the response history analysis.

The comparison between 10 and 15 seconds shock durations, presented in Tables A2.15 , A2.16 , A3.15 , and A3.16 , shows that the seismic responses have not been affected. Therefore, the 10 seconds shock, which includes the intense ground shaking, will yield satisfactory results.

Results of the response spectrum and response history analyses are presented in Tables A2.17 , A2.18 for the 2-span bridges considering the contribution of the first 15 modes of vibration, and in Tables A3.17 to A3.20 for the 3-span case considering different mode shapes. Seismic responses obtained using both techniques are in agreement when only the lower modes contribution is considered. The response spectrum method fails when higher modes are included, as a result of filtering high frequency data (greater than 25 Hz) from the earthquake record [28,42].

The 3-direction shock responses, presented in Tables A2.19 to A2.22 and A3.21 to A3.24 , are higher than the individual excitations results. Maximum tangential displacement

and forces in the superstructure correspond to a 3-direction shock with the (S00E) component in the longitudinal direction, while maximum radial forces and vertical moments occur when that component is directed in the transverse direction. This happens because the (S00E) component ground accelerations are more intense than the (S90W) component.

Tables A2.23 , A2.24 , A3.25 , and A3.26 show the decrease in seismic responses when the damping ratio increases, while Tables A2.25 to A2.27 and A3.27 to A3.29 present the results of the non-composite deck, rotational inertia, and long-column models. The less stiff non-composite deck model generally produces lower frequencies and deck actions, but higher displacements, column moments, and deck and column stresses, while including the rotational inertia coefficients in the mass matrix results only in an increase in the deck twisting moments. In long-column models, a significant increase in tangential displacements, vertical moments, and deck stresses is realized. On the other hand, column stresses are much less than the short columns case, which agrees with observed results after the San Fernando earthquake that evident fractures on the short columns were absent in the tall slender columns [18].

Rigid-column straight models for 2-span and 3-span bridges are shown in Figures 5.4 and 5.7 respectively, and the frequency analysis results are in good agreement with exact solutions as shown in Tables A2.28 and A3.30 . A comparison between the 2-column and the rigid-column models,

presented in Tables A2.29 , A2.30 , A3.31 , and A3.32 , indicates that the second model yields much less seismic responses.

Both deck and column stresses due to dead loads are presented in Tables A2.31 and A3.33 for the 2-span and the 3-span cases, respectively.

### 5.8.3 4-Span and 5-Span Bridges

Figures 5.8 and 5.9 show typical models for the 4-span and 5-span curved bridges, while seismic analysis results are included in Appendices A.4 and A.5 . Coupling in mode shapes in the two horizontal directions is more evident here (Figures B1.4 and B1.5 ), and the contribution of 15 modes of vibrations yields acceptable results.

The response spectrum method does not fail for these models because the structure frequencies are relatively low, but results are still apart from the response history analysis, and the 3-direction shock continues to yield the most satisfactory results. It can be realized from Tables A4.8 and A5.8 that both of the horizontal components have a significant contribution to the deck displacement, and axial forces, while only the transverse excitation dominates radial forces and vertical moments. The vertical component mainly affects vertical shears and radial moments for the superstructure, and axial forces in the columns.

Damping, stiffness, and rotational inertia effects are similar to the 2-span and 3-span cases, while long-column models are subjected to much higher actions and stresses.

Static analysis results are included in Tables A4.15 and A5.15 .

## 5.9 Summary

Based on the above seismic analysis of typical curved steel box-girder bridges, the following conclusions can be derived:

(I) Bridge model and seismic loading

1. A 2-column 6-element curved model having end short elements with appropriate member releases can yield satisfactory seismic responses.
2. Modes of vibration are coupled in the two horizontal directions due to the curved geometry of the bridge.
3. The contribution of the first 15 mode shapes (10 modes for single span bridges), and a solution time step of 0.0050 seconds will be considered in the response history analysis.
4. The first 10 seconds of El Centro earthquake record, which include the intense ground shaking, excite the bridge model to its maximum seismic responses.
5. Rigid-column models generally yield much less seismic responses than the 2-column models.

(II) Methods of analysis

1. The response spectrum technique fails when higher modes are considered because high frequency data (greater than 25 Hz), which is considered contaminated with erroneous noise, has been filtered out of the earthquake record [28,42] .

2. Seismic responses obtained using the response spectrum analysis are maximum absolute values that do not necessarily occur at the same time, therefore, realistic normal and shear stresses may not be computed.
3. The use of a statistical approach to replace the effects of the removed time domain in the response spectrum method may yield unrealistic results, therefore the response history technique is considered to be the most sophisticated type of analysis [33] .
4. Coupling effects due to the curved alignment of the bridges suggest that the 3-direction shock will yield the most satisfactory results.

(III) Damping, stiffness, and intertia effects

1. Seismic responses decrease with an increase in the damping ratio, and a 5% damping ratio will be considered for all bridges.
2. Non-composite deck models generally produce higher deck and column stresses.
3. Considering the rotational inertia coefficients in the mass matrix does not have a significant effect on the seismic responses.
4. A significant increase in tangential displacements, vertical moments, and deck stresses is realized in long-column models, while column stresses are much less than the short columns case.

It is to be noted that static analysis results are almost the same for all of the above case studies, while seismic responses generally increase with an increase in the number of spans.

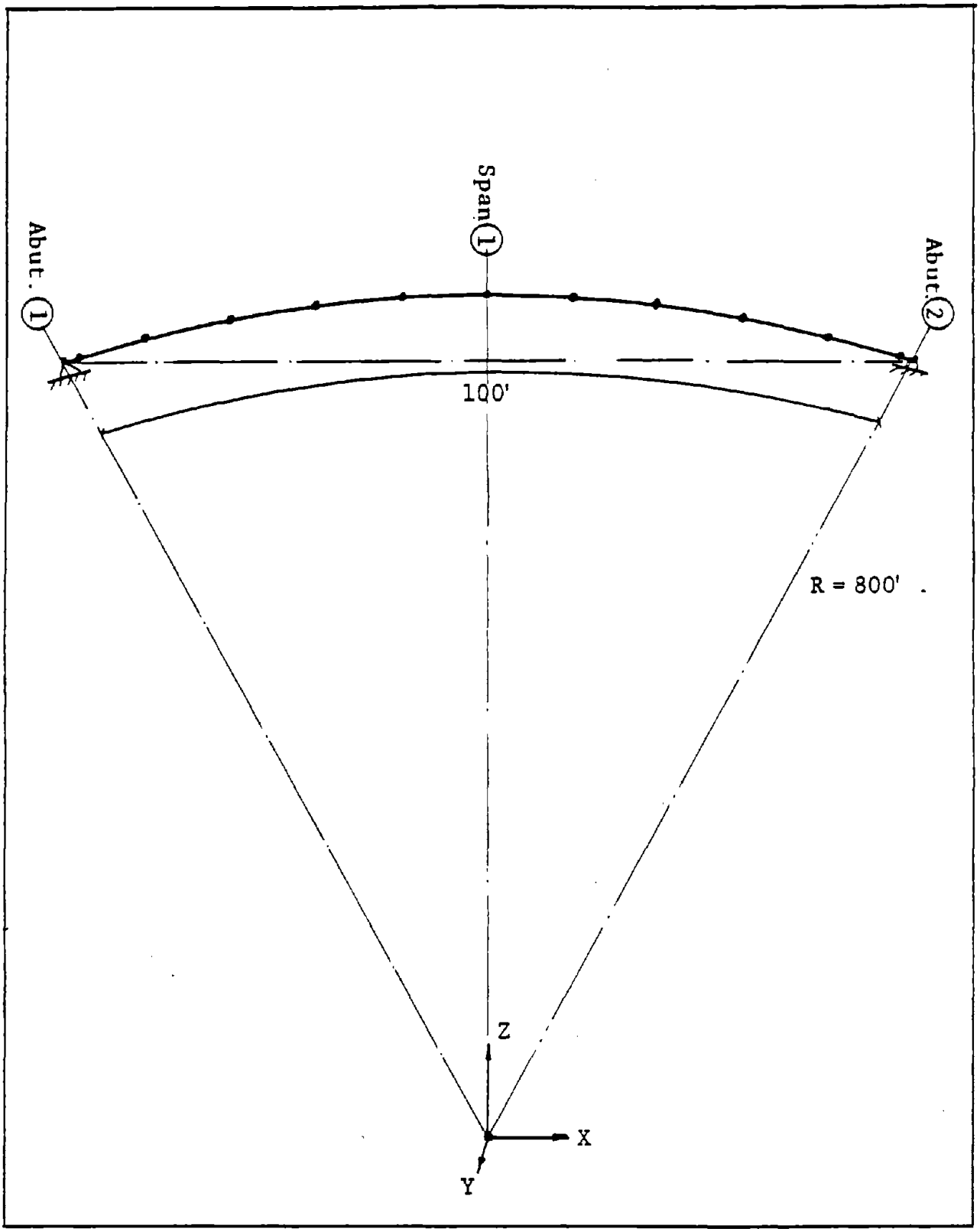


Figure 5.1 Single Span Curved Bridge Model

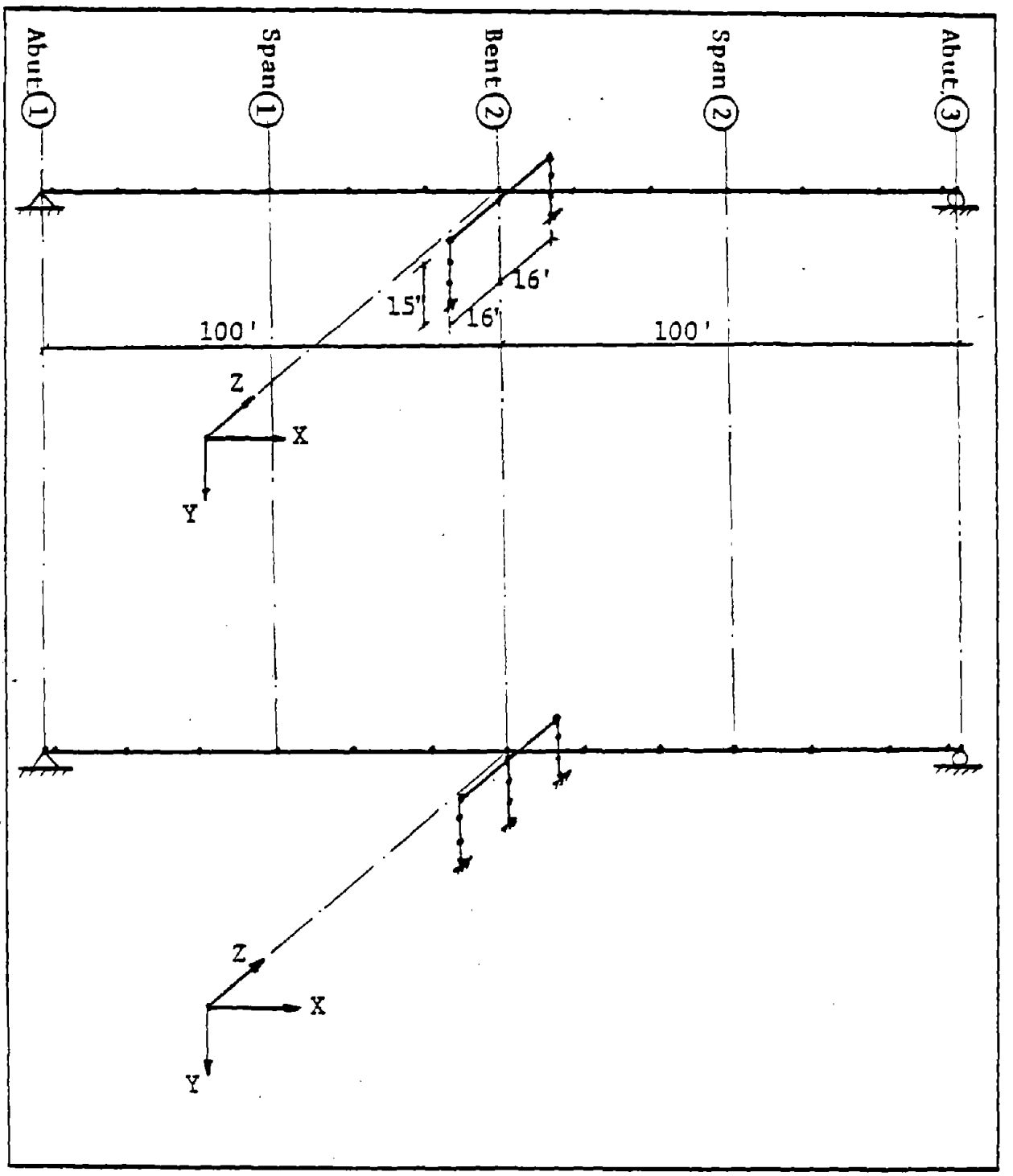


Figure 5.2 2-Column and 3-Column Models For a 2-Span Bridge

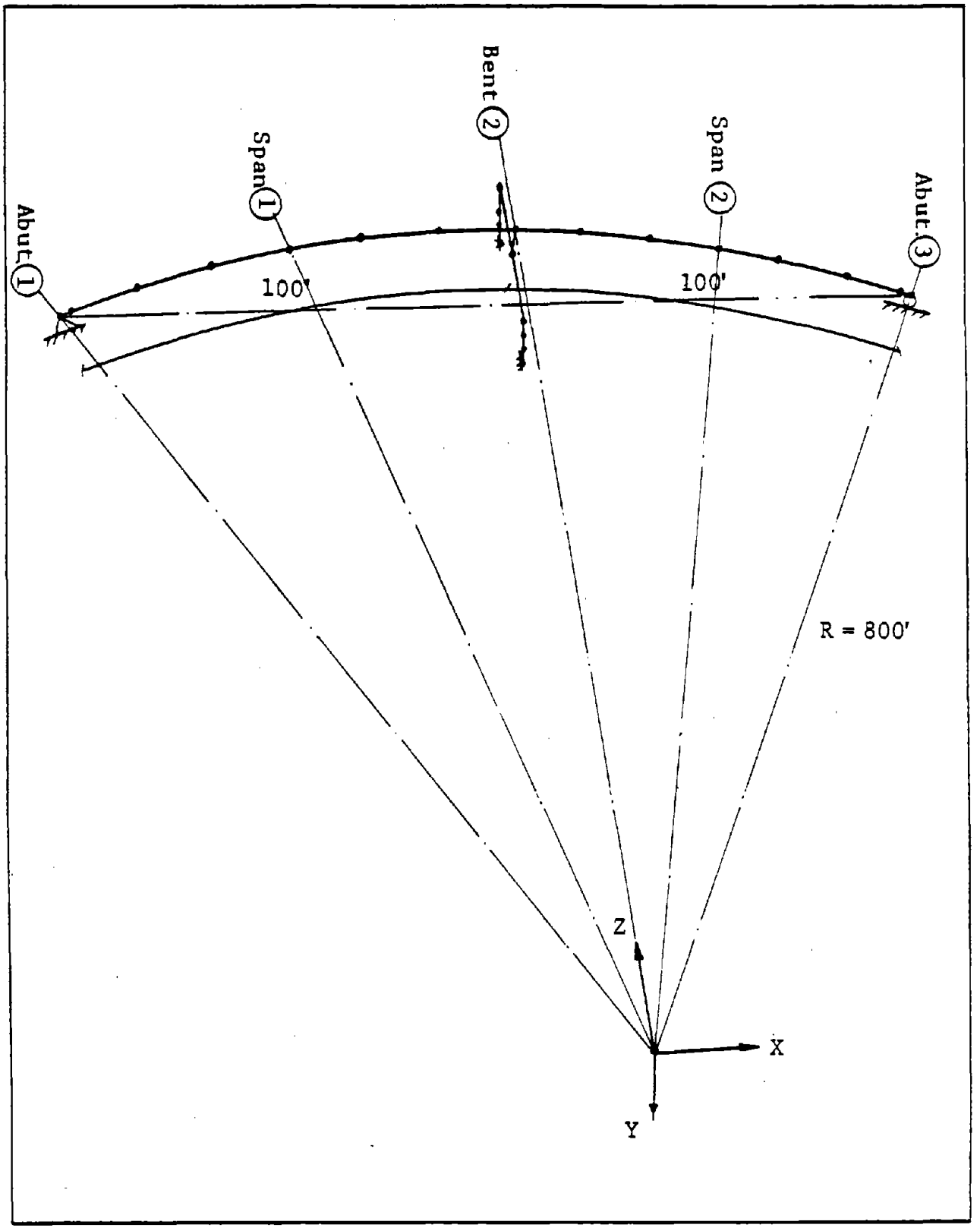


Figure 5.3 2-Span Curved Bridge Model

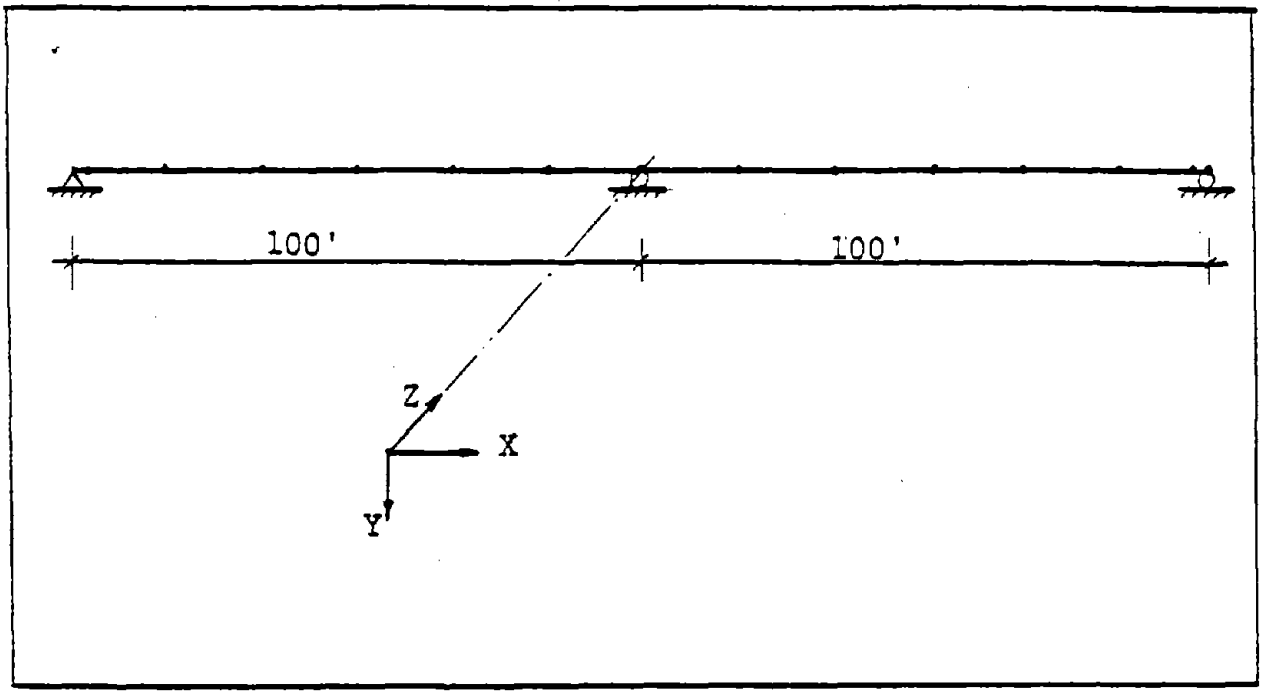


Figure 5.4 Rigid-Column Model For a 2-Span Bridge

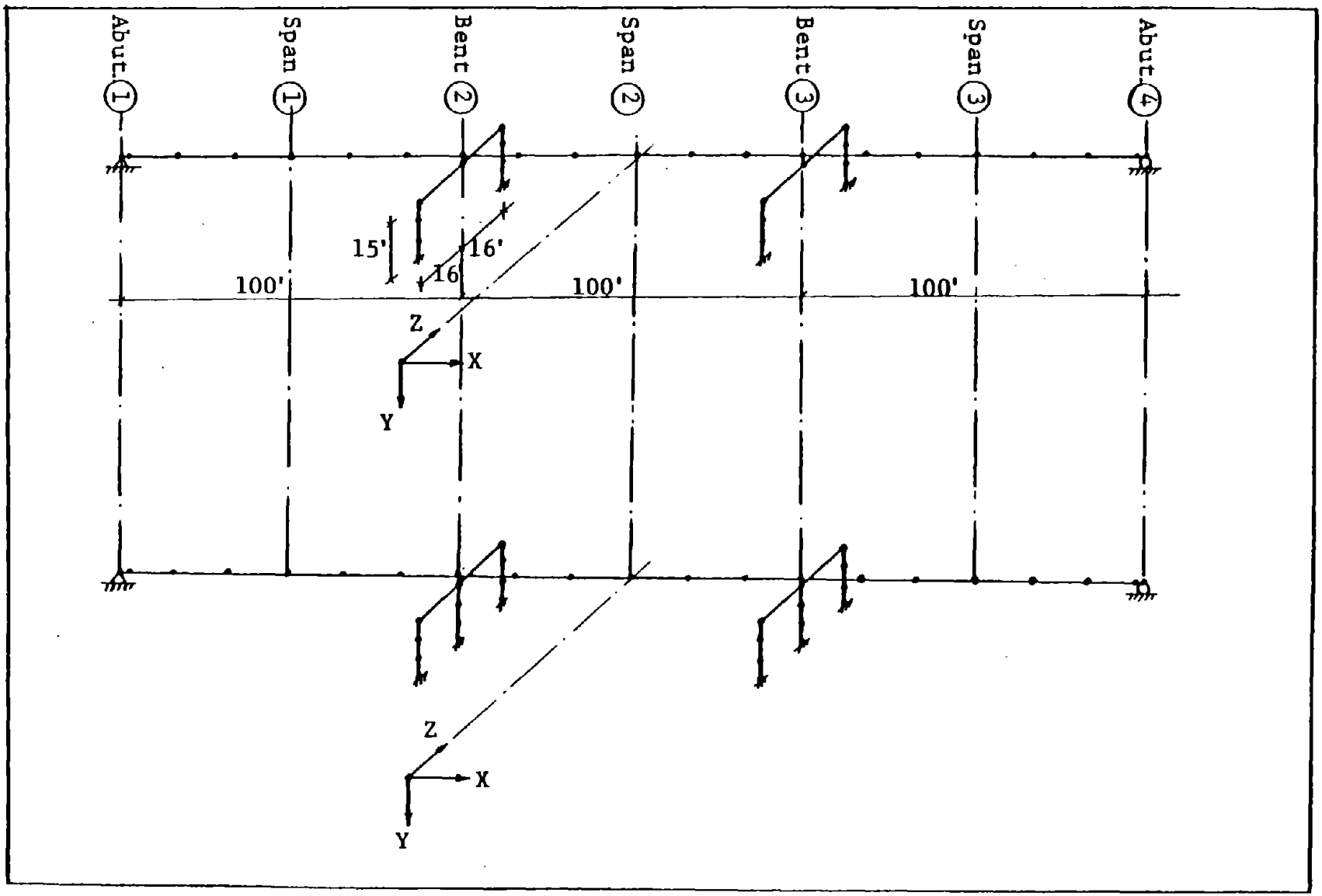


Figure 5.5 2-Column and 3-Column Models For a 3-Span Bridge

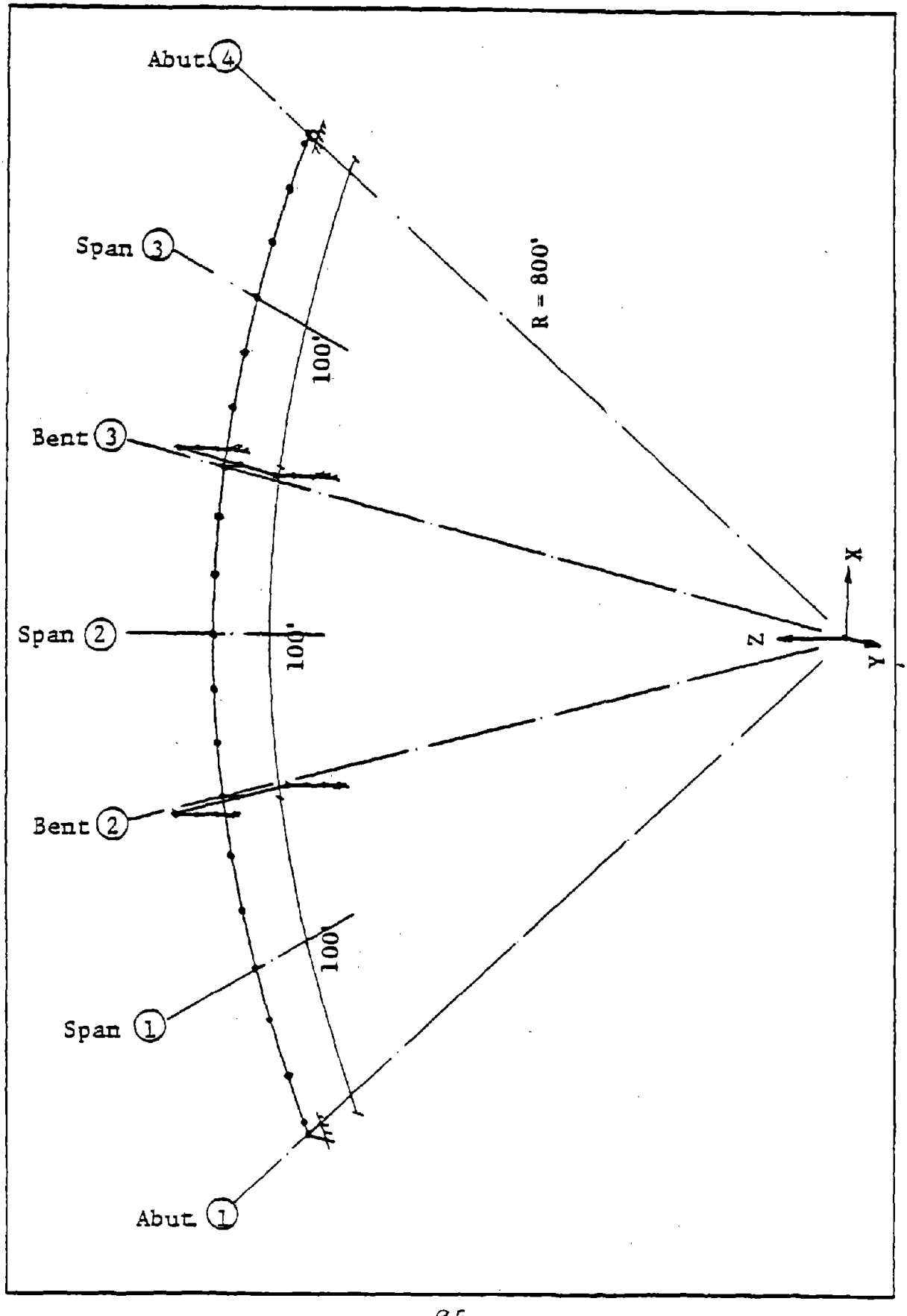


Figure 5.6 3-Span Curved Bridge Model

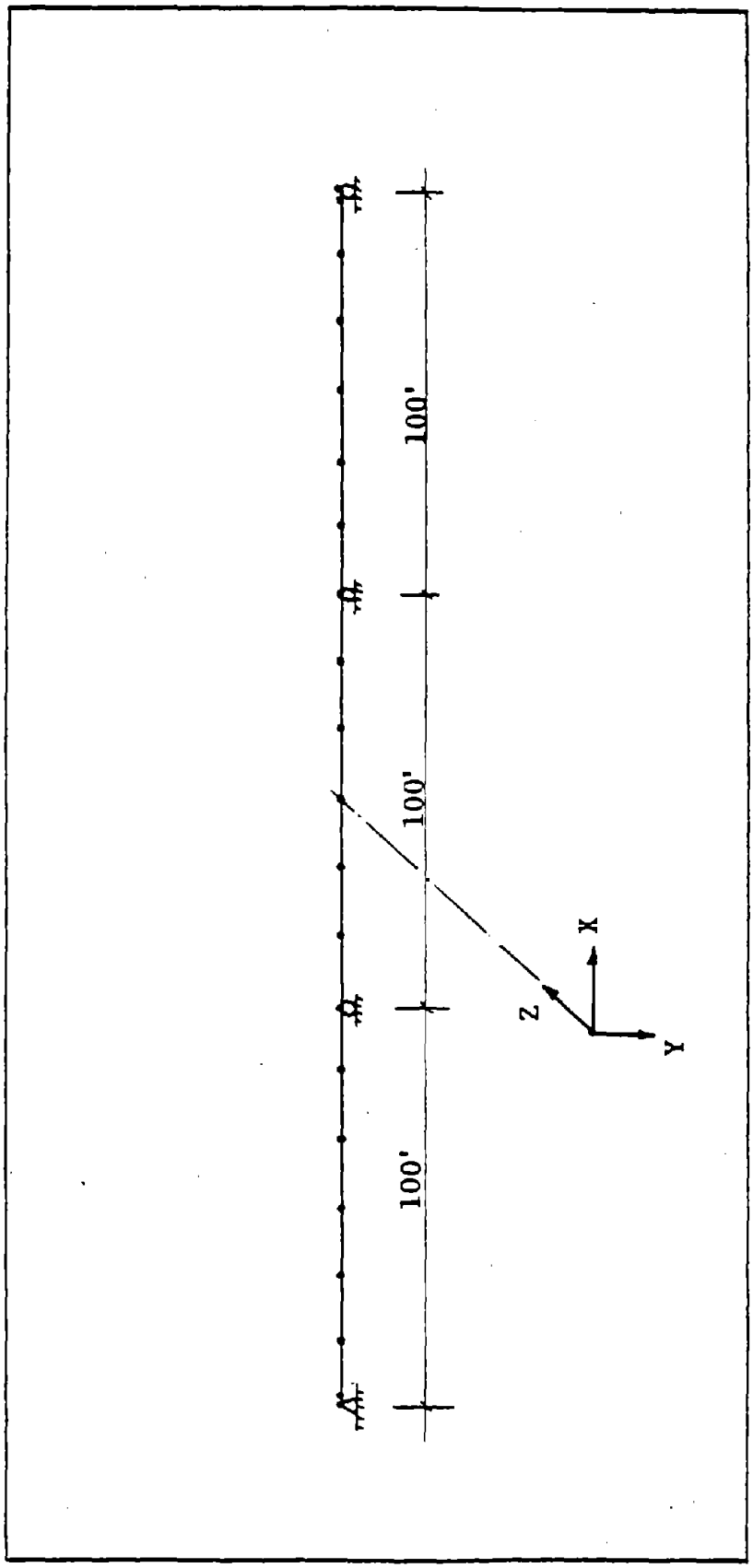


Figure 5.7 Rigid-Column Model For a 3-Span Bridge

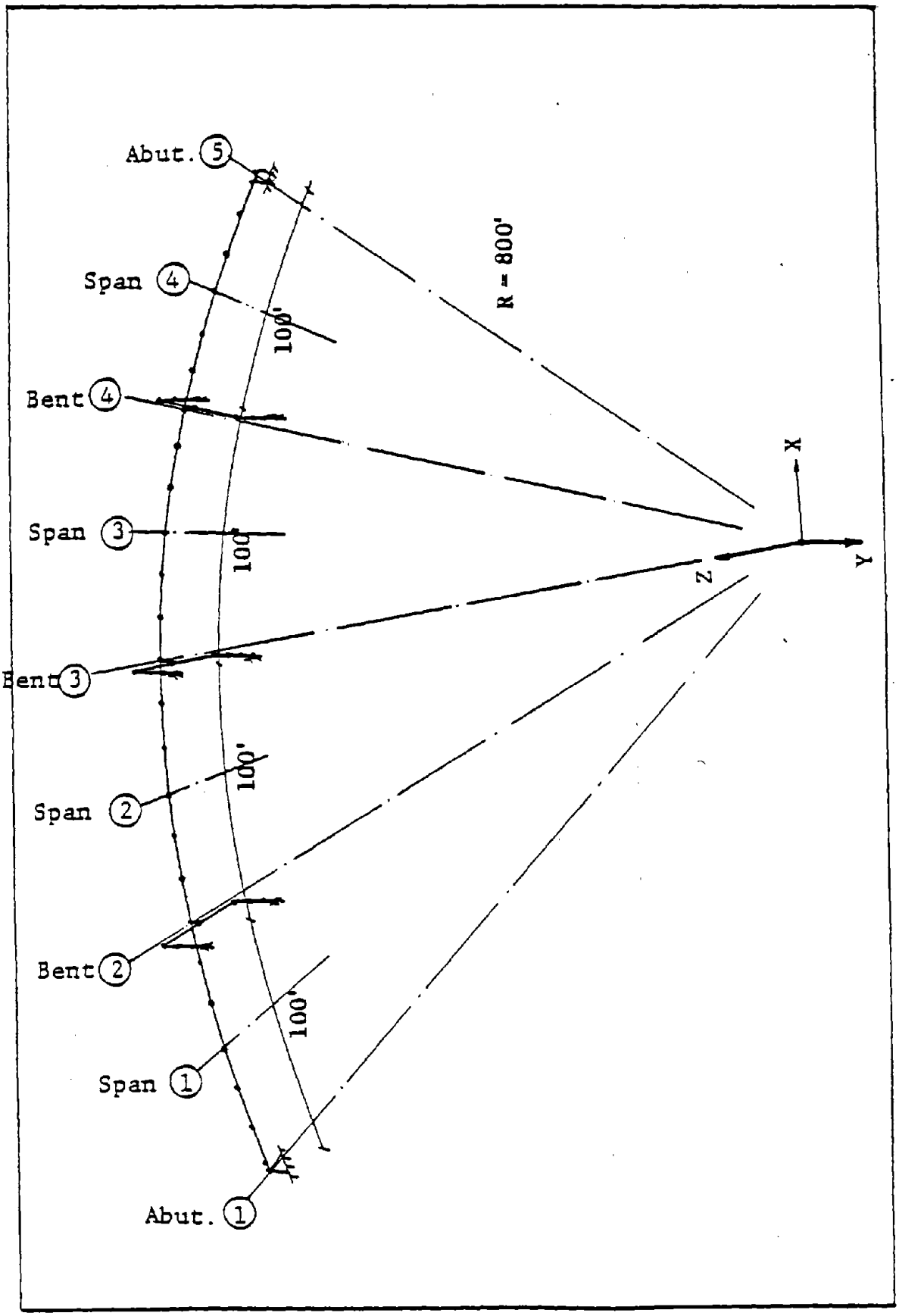


Figure 5.8 4-Span Curved Bridge Model

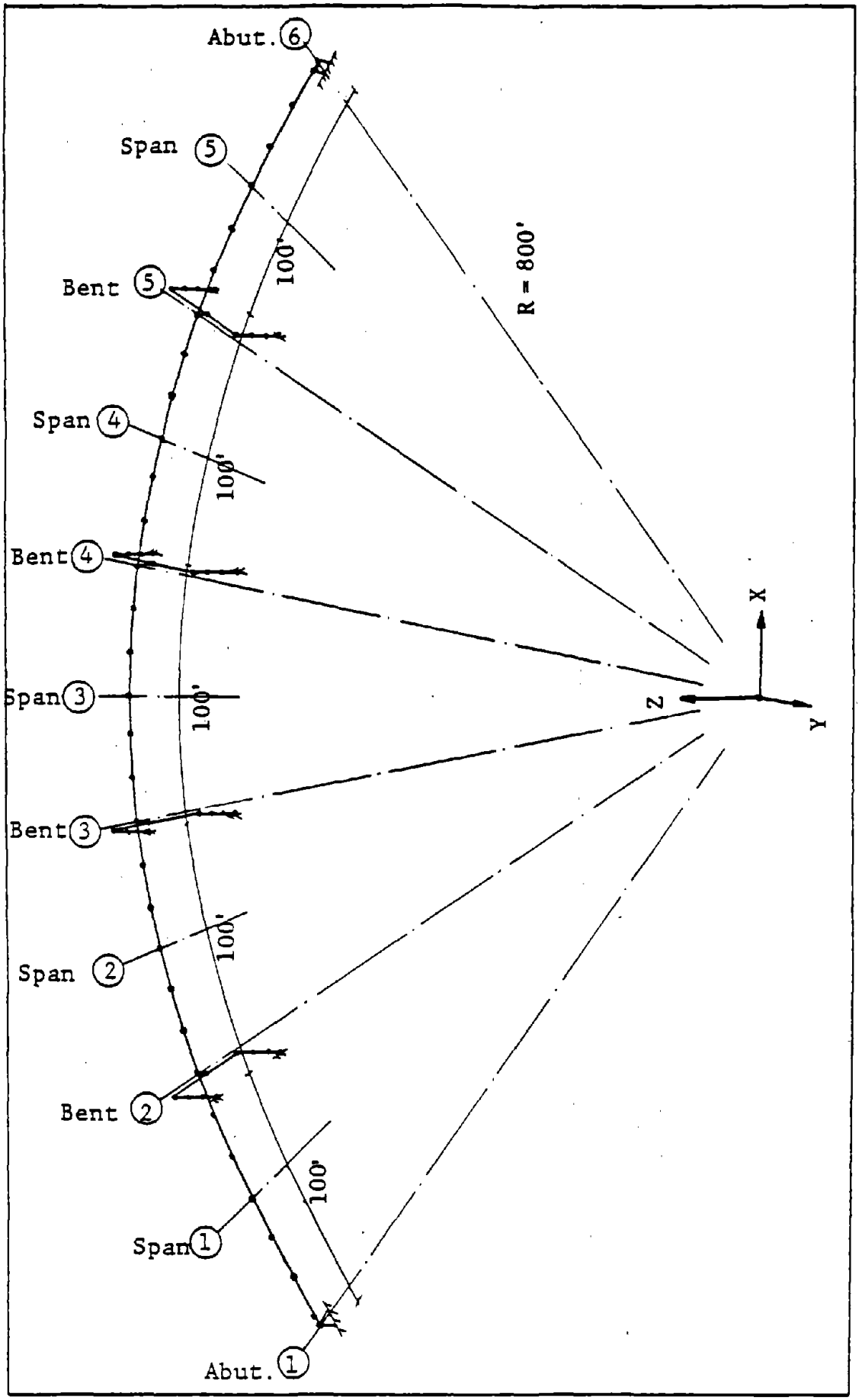


Figure 5.9 5-Span Curved Bridge Model

# CHAPTER VI

# PARAMETRIC ANALYSIS

Results of the parametric analysis of curved steel box-girder bridges under seismic loadings are presented in this Chapter. Bridge parameters are discussed, and the bridge model as well as the method of analysis are presented. Maximum seismic responses for both the superstructure and the columns are obtained, and the method of correlating these results with equivalent static loads is discussed, and design curves are developed. The influence of each parameter on the seismic responses is briefly discussed.

## 6.1 Bridge Parameters

The effects of several parameters on the seismic response of curved steel box-girder bridges are studied. These parameters include:

1. Number of spans, NS
2. Span length, L
3. Radius of curvature, R
4. Span ratio, n
5. Column height, $h_c$
6. Column stiffness, $I_c$
7. Weight of the bridge per unit length, W

Data for the above parameters are assumed based on a survey conducted by Heins et al. [20,24,25,26] on such types of bridges, as discussed before in Chapter IV. An outline of the analysis will be presented in the following Sections.

### 6.1.1 Number of Spans

Single, two, three, four, and five span bridges are studied. For each case, other parameters are varied and the seismic responses are obtained and design curves for the equivalent static loadings are developed. These curves are included in Appendix B.2 .

### 6.1.2 Span Length and Radius of Curvature

Four different span lengths are studied: 50, 100, 150, and 200 feet. The 50 ft. case is considered only for single span bridges. The radii of curvature for each case are summarized in Table 6.1, and detailed sketches for both L and R parameters are included in Figures 6.1 to 6.4 .

The central angle subtended by each span, $\theta$ ranges from 14 degrees ($\frac{R}{L} \approx 4$) for highly curved bridges to less than 3.6 degrees ($\frac{R}{L} \geq 16$) where curvature effects can be neglected and bridges are assumed to be straight. Higher values of $\theta$ were considered for single span bridges.

Values of L and R parameters are chosen such that they cover a wide range of practical data, and provide 3 to 5 points to construct each design curve.

### 6.1.3 Geometry of the Deck Cross-Section

Symmetrical 3-girder cross-sections are assumed with girder spacing of 170" and bridge width of 42.5' (3 lanes). Cross-sections with one and two girders will be discussed in Section 6.1.7 . A horizontal concrete slab of 8" thickness is considered, with haunches of 3" depth.

The cross-section geometry is generally a function of the span length. Tables 6.2 and 6.3 summarize the structural details of the deck cross-sections which are considered for the analysis. For single span bridges only one section is used, while multiple-span bridges have two cross-sections $XS_1$ and $XS_2$, with the second one covering 16% of the span length on each side of the bents. All cross-sections have inclined webs (14 degrees with vertical) and no bottom flange stiffeners, and they will be considered as composite sections. A 10% miscellaneous steel and concrete are also assumed.

### 6.1.4 Span Ratio

The span ratio n, which is the ratio between the interior span length $L_1$ and the exterior span length L, is assumed to be 1.0, i.e. equal span bridges are considered. The 3-span bridges are also analyzed for a span ratio of 1.2 . It is to be noted that unequal 2-span bridges are not a common occurrence for steel box-girder highway bridges [20].

### 6.1.5 Column Height

Three-column bents are considered, with round columns of 15' height spacing at 16'. The 2-span and 3-span bridges are also analyzed using columns of 30' height.

### 6.1.6 Column Stiffness

Three different columns are considered; $C_1$, $C_2$ and $C_3$ with the following properties (ft) :

| | $C_1$ | $C_2$ | $C_3$ |
|---|---|---|---|
| Area = | 5.0 | 6.0 | 7.0 |
| Moment of inertia, $I_c$ = | 2.5 | 4.5 | 6.5 |

Column $C_2$ is used throughout the analysis, where columns $C_1$ and $C_3$ are used to study the effect of column stiffness on the seismic response for selected cases presented in Table 6.4 . It is to be noted that the ratio R/L is equal to 8, and n is taken as 1.0 for those case studies.

### 6.1.7 Bridge Weight Per Unit Length

As mentioned in Section 6.1.3 , 3-girder 3-lane cross-sections are considered for the parametric analysis. The effect of the unit weight of the bridge is studied by analyzing 2-girder 2-lane and one-girder one-lane bridges for the same cases presented in Table 6.4 . A 2-column bent is used for both cases with column properties $C_2$. It is to be noted that the number of girders affects both the stiffness and the mass of the bridge.

## 6.2 Bridge Model

To perform the parametric analysis for multiple-span bridges, 2-column 6-element models having end short elements with appropriate member releases are utilized. The contribution of the first 15 modes of vibration is considered for each case. For single span bridges, 10-element models are used considering the first 10 mode shapes. It is to be noted that the rotational inertia effects are neglected for all bridges.

## 6.3 Method of Analysis

The response history technique is used for the parametric analysis. The first 10 seconds of El Centro earthquake record is applied to the bridge as a 3-direction shock. A solution time step of 0.0050 seconds is used, and a 5% damping ratio is assumed for all bridges.

For each case, frequency analysis is first performed to obtain the structure periods and the corresponding mode shapes. Utilizing the restart capabilities, two cases are studied. First a 3-direction shock is applied to the bridge, with the (S00E) component directing along the x-axis while the (S90W) and (VERT) components are applied in the transverse and vertical directions respectively. In the second case, the directions of the two horizontal components are interchanged. Maximum seismic responses are obtained for both cases, and the larger values are considered. The response spectrum of the (S00E) component is also applied to the structure in the longitudinal direction and both the participation factors and the seismic responses are studied.

It is to be noted that for medium-to-large size models, the frequency analysis is quite costly when compared to the forced response calculations [3]. Table 6.5 summarizes the average computer memory time required for each run for different types of analysis. Higher values are required for the frequency analysis when studying the effects of column stiffness and the bridge unit weight.

## 6.4 Seismic Responses

For design purposes, forces and moments at the attachments between the superstructure and the supporting elements, as well as stresses in both steel and concrete at the critical sections of the bridge deck and columns have to be checked. The following responses are considered:

1. Attachments

| | |
|---|---|
| $M_a$ | Vertical moment at the abutments |
| $V_a$ | Radial force at the abutments |
| $P_a$ | Tangential force at the abutment |
| $V_p$ | Radial force at the pier-superstructure roller connections |

It is to be noted that the radial and tangential directions are related to the horizontal alignment of the superstructure. Figure 6.5 shows the directions of the above actions for a 3-span bridge.

2. Superstructure

| | |
|---|---|
| $\sigma_{sa}$ | Maximum normal stress in steel at the abutments |
| $\sigma_{ca}$ | Maximum normal stress in concrete at the abutments |
| $\sigma_{sm}$ | Maximum normal stress in steel at the mid-spans cross-sections |
| $\sigma_{cm}$ | Maximum normal stress in concrete at the mid-spans cross-sections |
| $\sigma_{sp}$ | Maximum normal stress in steel at the cross-sections over the piers |

$\sigma_{cp}$ Maximum normal stress in concrete at the cross-sections over the piers

3. Columns

$\sigma_{cc}$ Maximum normal stress in concrete at the columns bases

Locations of the above critical sections are shown also in Figure 6.5 .

It is to be noted that all the above seismic responses are time absolute maximums that do not necessarily occur within the bridge at the same time.

## 6.5 Correlation With Static Analysis

To obtain equivalent static loads that produce the same maximum seismic responses at both the superstructure and the columns, the bridge is analyzed as a continuous straight beam with fixed end supports, subjected to a uniform load $w_e$ in the transverse direction as shown in Figure 6.6 for a 3-span bridge. The same span lengths and deck stiffness of the original bridge are assumed. It has been found that the difference in static results when considering the actual change in the deck cross-section is less than 2% when assuming only one section $XS_1$ for the entire bridge. Hence, the deck stiffness is computed using the section geometry of $XS_1$, assuming a constant composite section.

Two equivalent loads for computing the actions at the attachments, and another two loads for computing the normal stresses at the critical sections can be obtained by correlating the static results with the maximum dynamic responses as follows:

$$w_M = \frac{k_1}{L^2} (M_a)_{max} \tag{6.1}$$

$$w_V = \frac{k_2}{L} (V_a)_{max} \tag{6.2}$$

$$w_s = \frac{k_1}{L^2} S_s (\sigma_{sa})_{max} \tag{6.3}$$

$$w_c = \frac{k_1}{L^2} S_c m_r (\sigma_{ca})_{max} \tag{6.4}$$

where $w_M$, $w_V$ = equivalent static loads which induce the maximum seismic vertical moment and radial force, respectively, at the abutments

$w_s$, $w_c$ = equivalent static loads which induce the maximum seismic normal stresses in steel and concrete, respectively, at the abutments

$(M_a)_{max}$, $(V_a)_{max}$ = maximum values of the seismic vertical moment and radial force, respectively, at either abutments

$(\sigma_{sa})_{max}$, $(\sigma_{ca})_{max}$ = maximum values of the maximum seismic normal stresses in steel and concrete, respectively, at either abutments

$L$ = exterior span length

$S_s$, $S_c$ = section modulii for steel and concrete, respectively, about a vertical axis

$m_r$ = modular ratio = $\frac{E_s}{E_c}$

$E_s, E_c$ = Young's modulii for steel and concrete, respectively

$k_1, k_2$ = constants depend on the span ratio;

For single span or equal multiple-span bridges:

$k_1 = 12$ ,

$k_2 = 2$

For 3-span bridges with span ratio n:

$$k_1 = \frac{12\ (1+2n)}{(1+3n-n^3)} ,$$

$$k_2 = \frac{4\ (1+2n)}{(2+5n-n^3)}$$

For other unequal multiple-span bridges, $k_1$ and $k_2$ can be calculated using any classical method for solving statically indeterminate beams such as the three-moment equation [22,38].

It should be noted that the equivalent static loads are uniformly distributed, and they are applied to the structure in the transverse direction.

## 6.6 Design Curves

For each case study, the maximum seismic responses are obtained, and the corresponding equivalent static loads are computed utilizing Equations (6.1) to (6.4) . A graph

showing these equivalent loads plotted as a function of R/L is called a design curve. Such curves are developed for different span lengths, span ratios, and column heights, for single to five-span bridges, and they are included in Appendix B.2 . It should be noted that these design curves are developed assuming 3-girder 3-lane bridges with supporting columns $C_2$.

Other seismic actions at the attachments are normalized with respect to $(V_a)_{max}$, and similarly seismic normal stresses at other critical sections are related to $(\sigma_{sa})_{max}$ and $(\sigma_{ca})_{max}$, and the resulting factors are also plotted versus R/L on the design curves for each case. These factors can be defined as follows:

$$k_p = (P_a)_{max} / (V_a)_{max} \tag{6.5}$$

$$k_V = (V_p)_{max} / (V_a)_{max} \tag{6.6}$$

$$k_{sm} = (\sigma_{sm})_{max} / (\sigma_{sa})_{max} \tag{6.7}$$

$$k_{sp} = (\sigma_{sp})_{max} / (\sigma_{sa})_{max} \tag{6.8}$$

$$k_{cm} = (\sigma_{cm})_{max} / (\sigma_{ca})_{max} \tag{6.9}$$

$$k_{cp} = (\sigma_{cp})_{max} / (\sigma_{ca})_{max} \tag{6.10}$$

$$k_{cc} = (\sigma_{cc})_{max} / (\sigma_{ca})_{max} \tag{6.11}$$

where $k_p$, $k_V$ = factors used to obtain the maximum seismic tangential force at the abutment, and radial force at the pier-superstructure roller connections, respectively

$k_{sm}, k_{sp}$ = factors used to obtain the maximum seismic normal stresses in steel at the mid-spans cross-sections and at the cross-sections over the piers, respectively

$k_{cm}, k_{cp}, k_{cc}$ = factors used to obtain the maximum seismic normal stresses in concrete at the mid-spans cross-sections, at the cross-sections over the piers, and at the columns bases, respectively

$(P_a)_{max}$ = maximum value of the seismic tangential force at the abutment

$(V_p)_{max}$ = maximum value of the seismic radial force at any of the pier-superstructure roller connections

$(\sigma_{sm})_{max}, (\sigma_{sp})_{max}$ = maximum values of the maximum seismic normal stresses in steel at any of the mid-spans cross-sections and at any of the cross-sections over the piers, respectively

$(\sigma_{cm})_{max}, (\sigma_{cp})_{max}, (\sigma_{cc})_{max}$ = maximum values of the maximum seismic normal stresses in concrete at any of the mid-spans cross-sections, at any of the cross-sections over the piers, and at any of the columns bases, respectively .

The design curves are arranged in Appendix B.2 in five sets corresponding to the number of spans of the bridges. Within each set, curves for different span lengths, span ratios, and column heights, according to Section 6.1, are presented.

## 6.7 Results of the Parametric Analysis

The effects of the span length, curvature, span ratio, and the column height on the equivalent loads and factors, for bridges with different number of spans, are shown in the design curves of Appendix B.2 . On the other hand, the column stiffness and the bridge unit weight results are summarized in Table 6.6 .

For each case, it can generally be realized that $w_M$ is greater than $w_V$, while $w_c$ is greater than $w_s$. Also, the equivalent loads which induce stresses are higher than those which produce actions. For the ratio factors, $k_p$ is greater than $k_V$, while $k_{sm}$ and $k_{sp}$ are slightly higher than $k_{cm}$ and $k_{cp}$, respectively. The value of $k_{cc}$ is always higher than those for the other stresses ratio factors.

The influence of each of the bridge parameters on the equivalent loads and factors will be briefly discussed in the following Sections.

### 6.7.1 Effect of the Number of Spans

In general, higher values of equivalent loads are obtained when the number of spans increases. Similar behavior can be realized for $k_p$, $k_V$, and $k_{cc}$, while other stresses ratio factors are not affected by NS. The reason for the increase in the equivalent static loads, and consequently in the dynamic responses, is that the bridge becomes more flexible, especially in the transverse direction, when the number of spans increases, hence the values of the transverse frequencies decrease and the corresponding participation factors increase resulting in higher seismic responses.

### 6.7.2 Effect of the Span Length and the Radius of Curvature

The equivalent loads are generally affected by the ratio R/L, especially for highly curved bridges, where a sharp decrease can be realized when the radius of curvature increases. This is a result of the absence of coupling in the two horizontal directions within the modes of vibration for less curved bridges. On the other hand, the value of the tangential force at the abutment $P_a$ is higher for straight than for curved bridges because the dominant earthquake component (S00E) will be applied in the tangential direction. Other ratio factors show a slight change in their values when the radius of curvature of the bridge increases, but they are generally affected by the span length as will be discussed later in Chapter VII.

### 6.7.3 Effect of the Span Ratio

Figures B23.13 to B23.24 show the different design curves for a span ratio n = 1.2 for the 3-span bridges. A comparison with equal-span bridges indicates that the equivalent loads increase for higher values of n. On the other hand, the ratio factors are generally not affected by the span ratio.

### 6.7.4 Effect of the Column Height

A significant increase in the values of the equivalent loads, as a result of higher actions and stresses in the superstructure, can be realized for long-column models. Bridges with such type of columns are more flexible in the

transverse direction, which results in an increase in the corresponding earthquake participation factors and consequently in the superstructure seismic responses. While the values of $V_p$ and the column stress $\sigma_{cc}$ show a significant decrease when the column height increases, the tangential force at the abutment $P_a$ as well as the other stresses ratio factors are slightly affected by the column height.

### 6.7.5 Effect of the Column Stiffness

Ten cases, presented in Table 6.4, are analyzed to study the effect of the column stiffness on the seismic responses. Results of case 3 and case 8 are summarized in Table 6.6 for 2-span and 3-span bridges. Both seismic actions and stresses, except for $V_p$, decrease when the bridge columns become more stiff, and consequently smaller values for the equivalent loads are obtained when using column $C_3$ as shown in Table 6.6 . On the other hand, the ratio factors for actions increase for column $C_3$, while those for stresses show a slight change for the different column sizes. A 3-lane 3-girder (3L,3G) cross-section is considered for all cases.

### 6.7.6 Effect of the Bridge Weight Per unit Length

This parameter has a great influence on the actions at the attachments, where a sharp decrease in their values can be realized for light weight bridges (1L,1G). Accordingly, the actions equivalent loads decrease, while their ratio factors increase as shown in Table 6.6 .

Although no pattern for the deck stresses variations can be concluded, the stresses equivalent loads sharply decrease, and the stresses ratio factors generally increase when the bridge weight decreases. It should be noted that although the number of girders affects both the stiffness and the weight of the bridge, the variation in the seismic actions generally follows that of the bridge weight.

## 6.8 Summary

A comprehensive parametric analysis of curved steel box-girder bridges subjected to seismic excitations was presented. Maximum seismic responses were correlated with static analysis of the bridge, and equivalent loads and ratio factors were obtained and design curves were developed. The effects of the bridge parameters on the seismic responses were briefly discussed. It can generally be concluded that both the equivalent loads and the actions ratio factors are influenced by all parameters, while the deck stresses ratio factors are mainly affected by the span length and the bridge weight. A detailed analysis of the influence of each parameter will be presented in the following Chapter.

Table 6.1 Radii of Curvature R (ft) For Different Span Lengths L

| L (ft) | Number of Spans | | | | |
|---|---|---|---|---|---|
| | 1 | 2 | 3 | 4 | 5 |
| 50 | 200 | | | | |
| | 500 | | | | |
| | 800 | | | | |
| 100 | 300 | 400 | 400 | 400 | 400 |
| | 800 | 800 | 800 | 800 | 800 |
| | 1200 | 1200 | 1200 | 1600 | 1600 |
| | | 1600 | 1600 | | |
| | | | 2400 | | |
| 150 | 400 | 600 | 600 | 600 | 600 |
| | 1200 | 1200 | 1200 | 1200 | 1200 |
| | 1800 | 1800 | 2000 | 2400 | 2400 |
| | | 2400 | | | |
| 200 | 600 | 800 | 800 | | |
| | 1600 | 1600 | 1600 | | |
| | 2400 | 2400 | 2400 | | |
| | | 3200 | | | |

Table 6.2 Structural Details of the Deck Cross-Sections For Different Span Lengths: Single Span Bridges, (in.)

| Parameter | Span Length L (ft) | | | |
|---|---|---|---|---|
| | 50 | 100 | 150 | 200 |
| Top flange width | 12.0 | 16.0 | 20.0 | 24.0 |
| Top flange thickness | 1.0 | 1.0 | 1.0 | 1.5 |
| Bottom flange width | 85.0 | 85.0 | 85.0 | 85.0 |
| Bottom flange thickness | 0.75 | 0.75 | 0.75 | 1.5 |
| Web depth | 20.0 | 50.0 | 75.0 | 100.0 |
| Web thickness | 0.5 | 0.5 | 0.5 | 0.75 |

Table 6.3 Structural Details of the Deck Cross-Sections For Different Span Lengths: Multiple-Span Bridges, (in.)

| Parameter | Span Length L (ft) | | | | | |
|---|---|---|---|---|---|---|
| | 100 | | 150 | | 200 | |
| | $XS_1$ | $XS_2$ | $XS_1$ | $XS_2$ | $XS_1$ | $XS_2$ |
| Top flange width | 12.0 | 16.0 | 12.0 | 16.0 | 24.0 | 32.0 |
| Top flange thickness | 1.0 | 1.5 | 1.0 | 1.5 | 1.5 | 1.5 |
| Bottom flange width | 85.0 | 85.0 | 85.0 | 85.0 | 85.0 | 85.0 |
| Bottom flange thickness | 0.75 | 1.0 | 0.75 | 1.0 | 1.5 | 2.5 |
| Web depth | 50.0 | 50.0 | 75.0 | 75.0 | 100.0 | 100.0 |
| Web thickness | 0.5 | 0.5 | 0.5 | 0.5 | 0.75 | 0.75 |

Table 6.4 Cases Considered to Study the Effects of Column Stiffness and Bridge Weight on the Seismic Responses

| Number of Spans | Case Number | L (ft) | R (ft) | $h_c$ (ft) |
|---|---|---|---|---|
| 1 | 1 | 100 | 800 | |
| | 2 | 150 | 1200 | |
| 2 | 3 | 100 | 800 | 15 |
| | 4 | 150 | 1200 | 15 |
| | 5 | 150 | 1200 | 30 |
| 3 | 6 | 100 | 800 | 15 |
| | 7 | 150 | 1200 | 15 |
| | 8 | 150 | 1200 | 30 |
| 4 | 9 | 100 | 800 | 15 |
| | 10 | 150 | 1200 | 15 |

Table 6.5 Average Computer Memory Time Required For Each Run For Different Types of Analysis, (min)

| Type of Analysis | Number of Spans | | | | |
|---|---|---|---|---|---|
| | 1 | 2 | 3 | 4 | 5 |
| Frequency | 1.3 | 6.5 | 22.0 | 41.6 | 42.0 |
| Response history (3-direction shock) | 3.5 | 4.5 | 5.3 | 5.5 | 6.0 |
| Response spectrum | 0.8 | 1.6 | 2.5 | 3.0 | 3.8 |

Table 6.6 Effects of the Column Stiffness and the Bridge Weight Per Unit Length on the Seismic Responses For 2-Span and 3-Span Bridges

| NS | Column | Deck | Equivalent Loads (k/ft) | | | | Ratio Factors | | | | | | |
|---|---|---|---|---|---|---|---|---|---|---|---|---|---|
| | | | $w_M$ | $w_V$ | $w_s$ | $w_c$ | $k_P$ | $k_V$ | $k_{sm}$ | $k_{sp}$ | $k_{cm}$ | $k_{cp}$ | $k_{cc}$ |
| 2 | $C_1$ | 3L,3G | 13.19 | 5.22 | 15.65 | 21.79 | 2.00 | 0.02 | 0.80 | 1.06 | 0.32 | 0.56 | 1.35 |
| | $C_2$ | 3L,3G | 12.16 | 4.86 | 14.50 | 20.51 | 2.15 | 0.07 | 0.78 | 1.09 | 0.31 | 0.56 | 1.50 |
| | $C_3$ | 3L,3G | 11.23 | 4.62 | 13.35 | 18.58 | 2.24 | 0.16 | 0.84 | 1.17 | 0.34 | 0.59 | 1.41 |
| | $C_2$ | 3L,3G | 12.16 | 4.86 | 14.50 | 20.51 | 2.15 | 0.07 | 0.78 | 1.09 | 0.31 | 0.56 | 1.50 |
| | $C_2$ | 2L,2G | 6.67 | 2.88 | 7.73 | 10.16 | 2.32 | 0.54 | 0.80 | 1.14 | 0.29 | 0.49 | 2.06 |
| | $C_2$ | 1L,1G | 2.58 | 1.18 | 2.81 | 3.26 | 2.94 | 1.10 | 0.85 | 1.22 | 0.33 | 0.44 | 3.02 |
| 3 | $C_1$ | 3L,3G | 38.81 | 10.73 | 43.70 | 61.77 | 1.77 | 0.08 | 0.60 | 0.37 | 0.59 | 0.35 | 1.34 |
| | $C_2$ | 3L,3G | 32.31 | 9.00 | 37.30 | 52.32 | 2.23 | 0.17 | 0.63 | 0.36 | 0.63 | 0.34 | 1.43 |
| | $C_3$ | 3L,3G | 27.16 | 7.81 | 31.21 | 43.49 | 2.67 | 0.26 | 0.65 | 0.37 | 0.64 | 0.34 | 1.55 |
| | $C_2$ | 3L,3G | 32.31 | 9.00 | 37.30 | 52.32 | 2.23 | 0.17 | 0.63 | 0.36 | 0.63 | 0.34 | 1.43 |
| | $C_2$ | 2L,2G | 14.26 | 4.37 | 16.64 | 22.09 | 3.26 | 0.61 | 0.62 | 0.36 | 0.63 | 0.33 | 2.24 |
| | $C_2$ | 1L,1G | 2.66 | 1.21 | 3.77 | 4.24 | 6.31 | 2.05 | 0.85 | 0.44 | 0.96 | 0.26 | 3.83 |

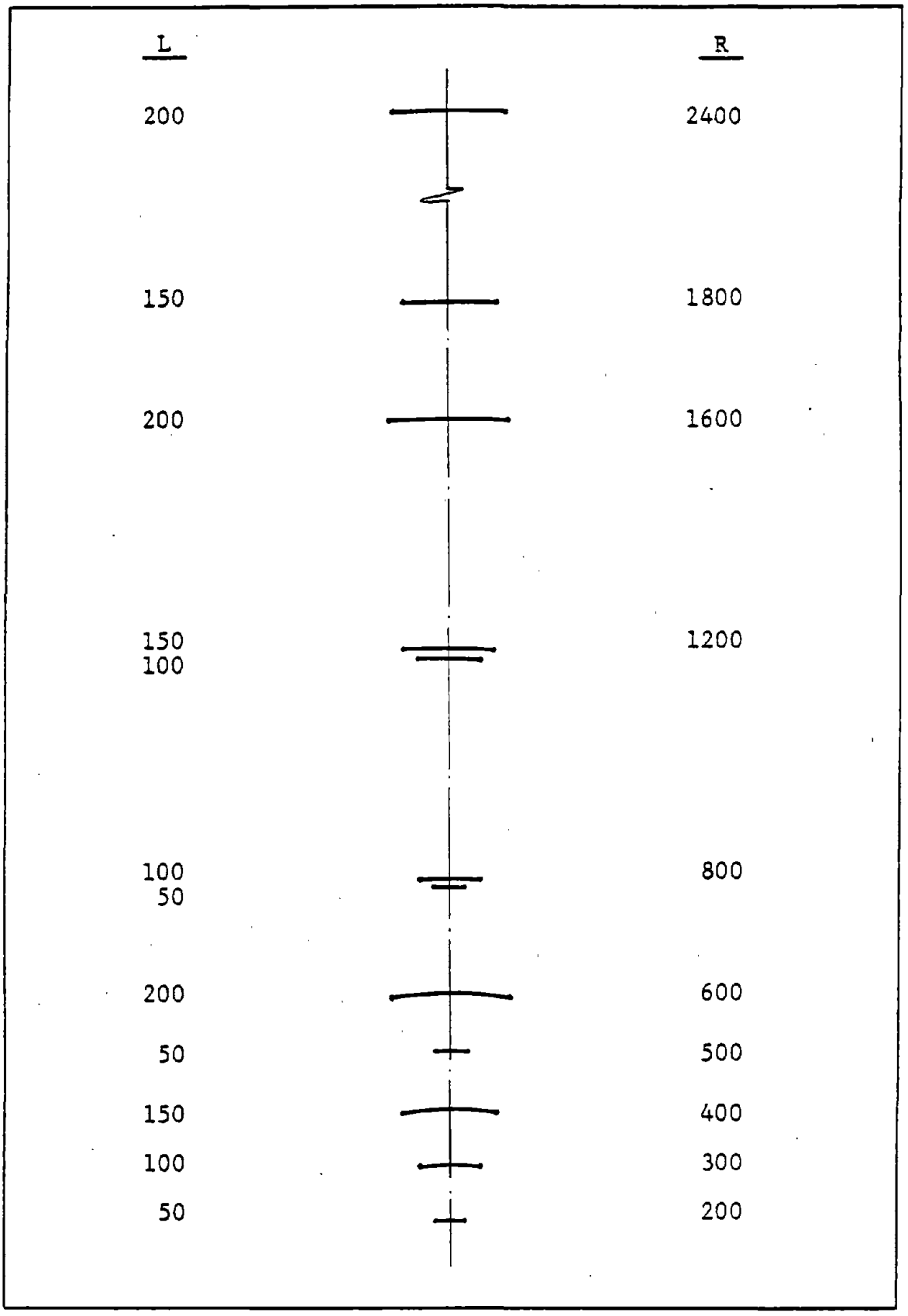


Figure 6.1 Single Span Bridges: Parameters L and R ,(ft)

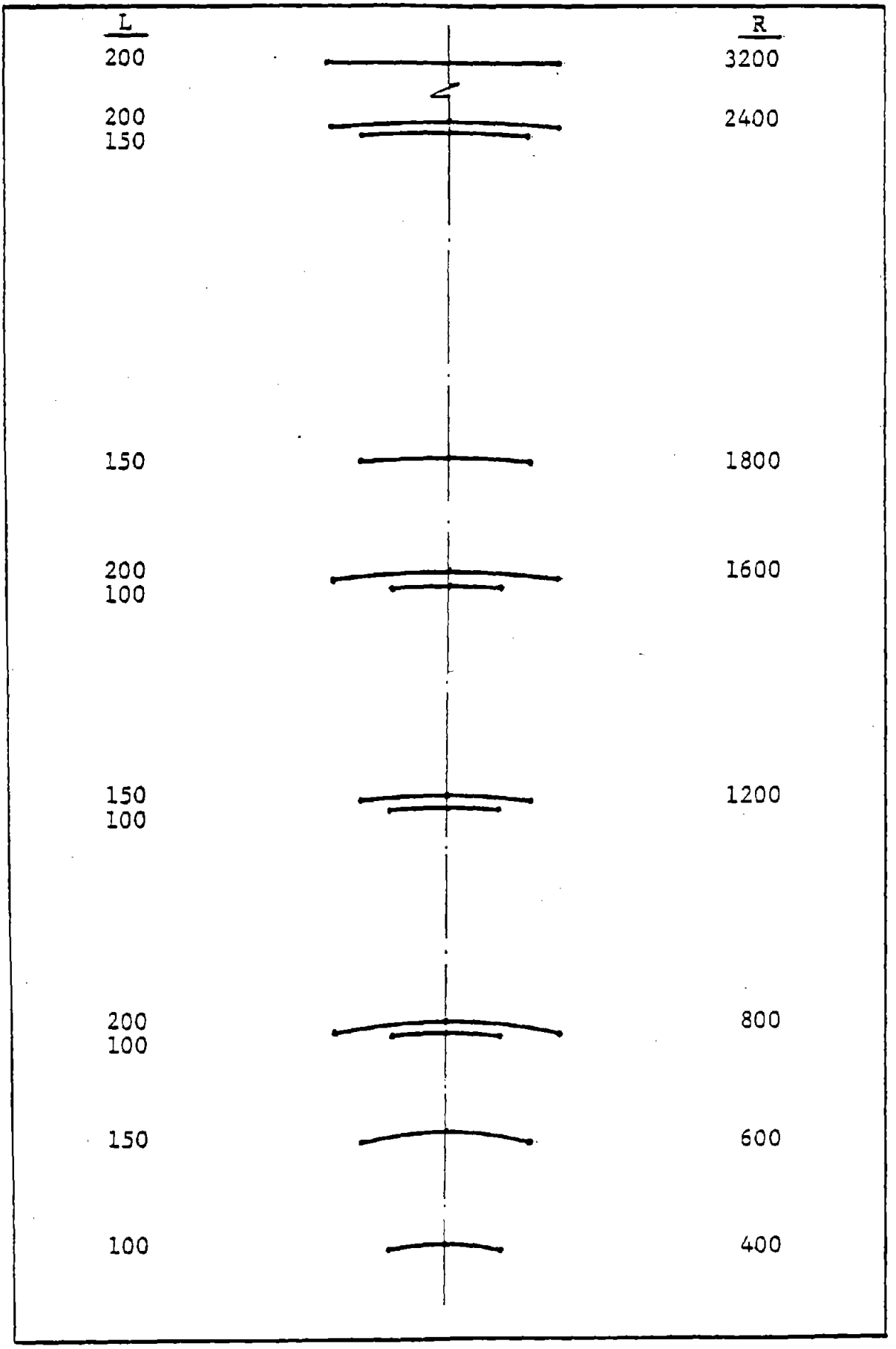


/21 Figure 6.2 2-Span Bridges: Parameters L and R ,(ft)

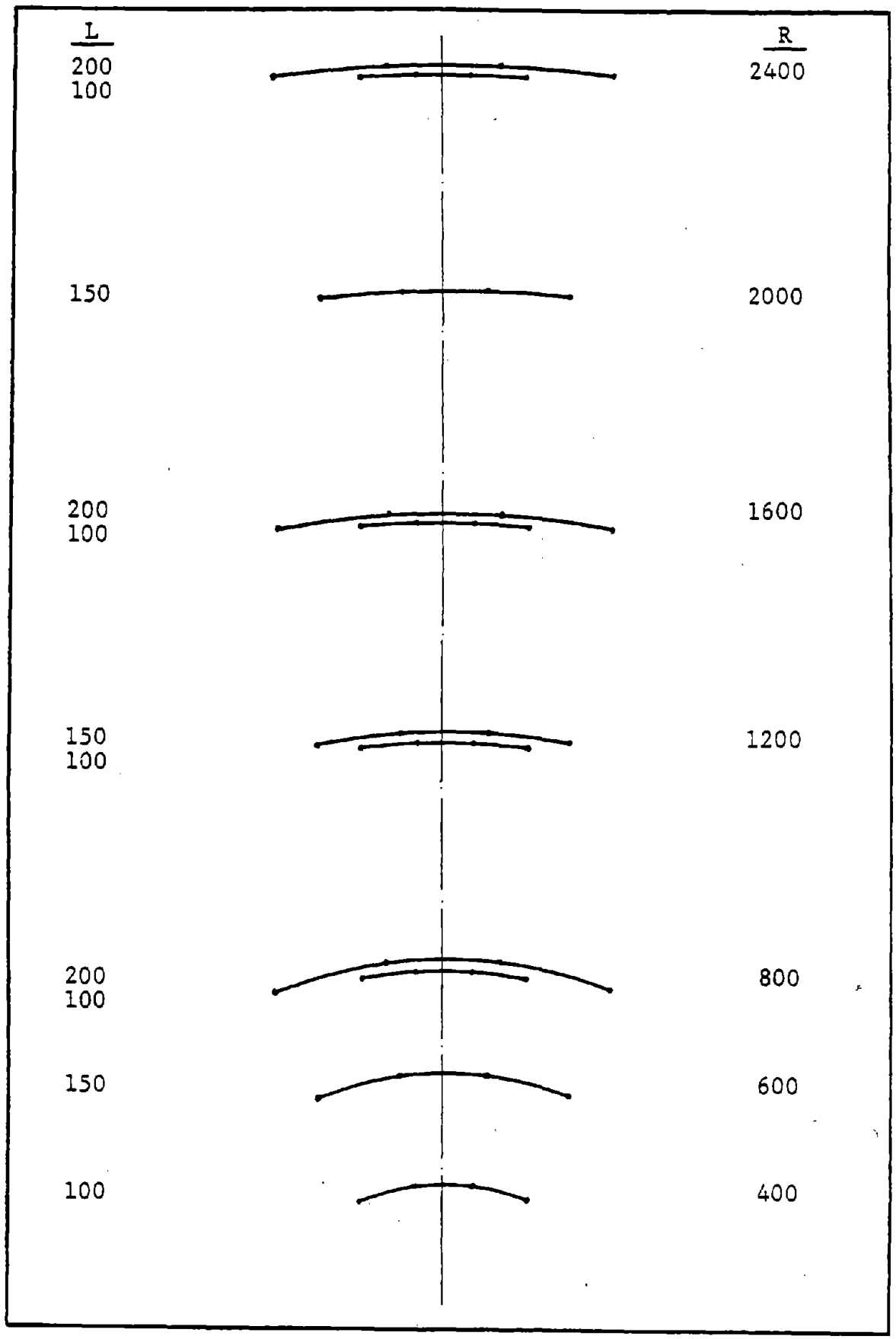


Figure 6.3 3-Span Bridges: Parameters L and R ,(ft)

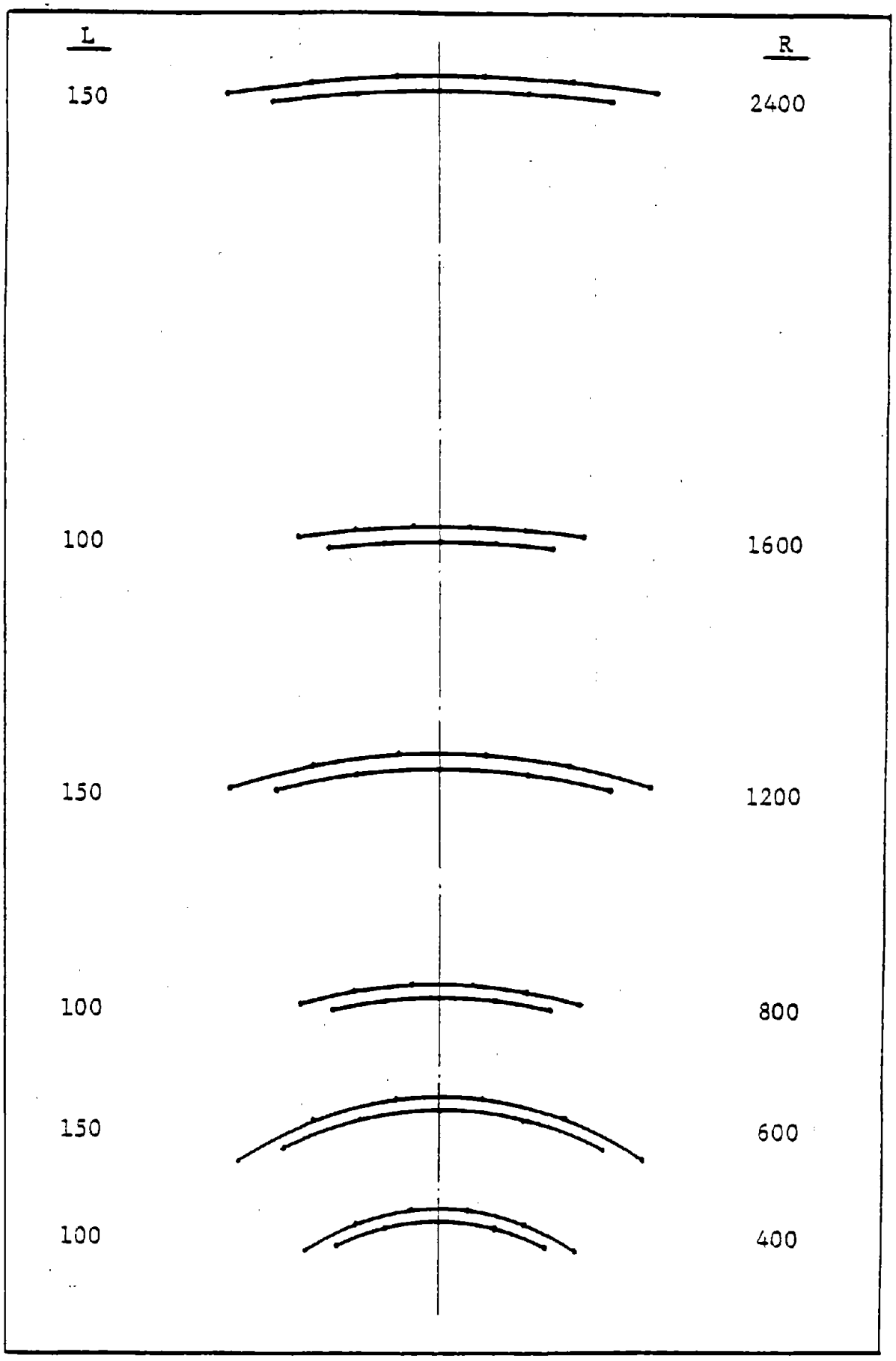






Figure 6.4 4-Span and 5-Span Bridges. Parameters L and R (ft)

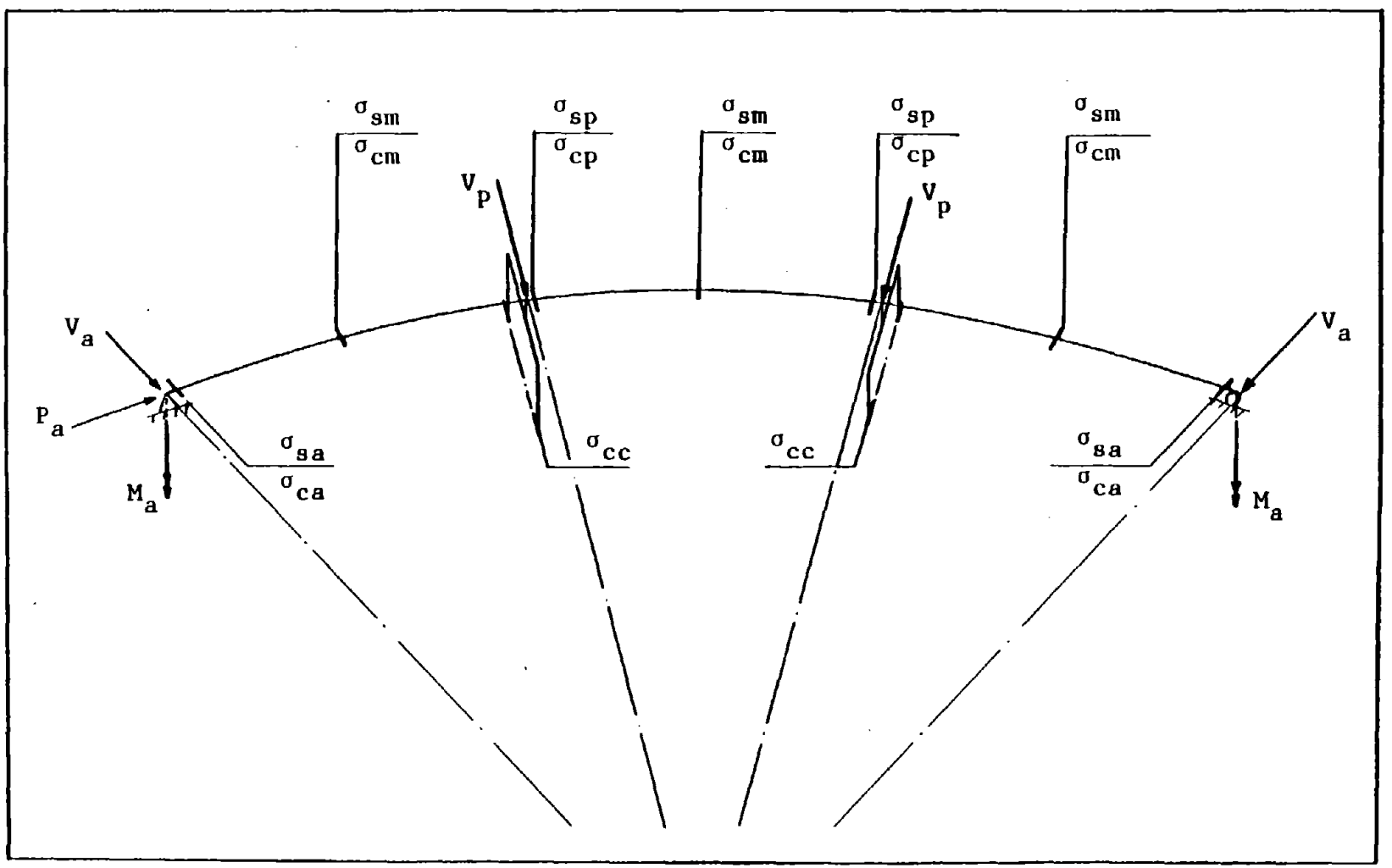


Figure 6.5 Directions of the Seismic Responses at the Attachments, and Locations of the Critical Sections For Both the Superstructure and the Columns

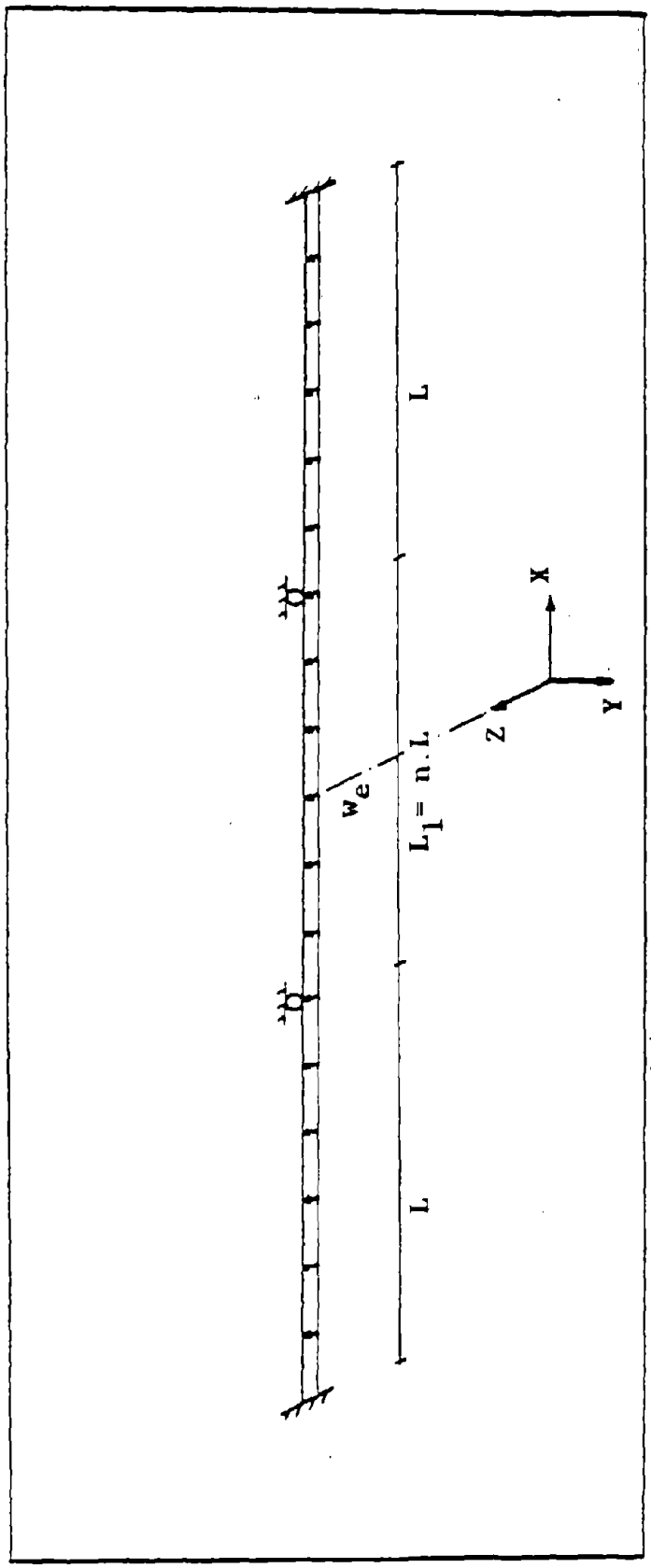


Figure 6.6 Equivalent Static Load $w_e$ For a 3-Span Bridge

# CHAPTER VII

# DESIGN CRITERIA

Results of the parametric analysis are studied to determine the influence of the bridge parameters on the seismic responses. In this Chapter, design equations for both of the equivalent loads and the ratio factors are derived, and the equivalent static analysis for bridges is presented. Practical seismic design considerations are discussed, including the intensity of ground shaking, the soil profile characteristics of the site, and the response modification factors for both the superstructure and the supporting elements. Several examples are presented, and the computer dynamic analysis is compared with the design criteria.

## 7.1 Parameters Influencing the Seismic Responses

The effects of the bridge parameters on the seismic responses were briefly discussed in Chapter VI. These parameters include:

1. Number of spans, NS
2. Span length, L
3. Radius of curvature, R
4. Span ratio, n
5. Column height, $h_c$
6. Column stiffness, $I_c$
7. Bridge weight per unit length, W

Analysis of the influence of each parameter on both of the

equivalent loads and the ratio factors will be discussed in the following Sections.

## 7.2 Design Equations

Based on the results of the parametric analysis, design equations for both of the equivalent loads and the ratio factors are derived. The derivation of the design equation for the equivalent load $w_M$ will be discussed in details. Other equations have been derived in a similar manner, and they will be presented and briefly discussed. It should be noted that the units of all the parameters used in the design equations are kips and feet.

### 7.2.1 Equivalent Load $w_M$

Tables 7.1 and 7.2 summarize the results of the equivalent load $w_M$ for all the cases considered in the parametric analysis. In Table 7.1 the average values for each subcolumn are shown between parenthesis. It can be realized that for multiple-span bridges, the values of $w_M$ are affected by all the parameters, while only the bridge weight W has a significant effect in case of single span bridges. Therefore, each case will be studied separately.

#### 7.2.1.1 Multiple-Span Bridges

i) Effect of NS

For bridges with $R/L \geq 8$, $n = 1.0$, and $h_c = 15'$, a linear relationship between $w_M$ and NS can be constructed in the form

$$w_M = C_1 NS + C_2 \qquad (a)$$

where $C_1$ and $C_2$ are constants which can be obtained by substituting the average values of $w_M$ which correspond to NS = 2 and NS = 4, respectively, in equation (a), and solving the resulting two equations simultaneously. This will yield

$$w_M = 4.5\ NS + 4 \qquad (i)$$

ii) Effect of R/L

Since no trends for $w_M$ are observed when the span length L varies, the effect of R/L is studied by averaging the values of $w_M$ for different span lengths in each sub-solumn in Table 7.1. For $R/L \geq 8$ the values of $w_M$ do not show a significant change when R/L increases, therefore, equation (i) is valid. On the other hand, the values of $w_M$ increase by approximately 10% when R/L = 4. A linear relationship is assumed in the form

$$f_1 = C_3 (R/L) + C_4 \qquad (b)$$

where $f_1$ is a modifying factor that accounts for the effects of R/L, and $C_3$ and $C_4$ are constants which can be obtained by considering the conditions

$$f_1 = 1.0 \quad \text{when} \quad R/L = 8$$

and

$$f_1 = 1.1 \quad \text{when} \quad R/L = 4$$

which yield

$$f_1 = 1.2 - \frac{R/L}{40} \qquad \text{(ii)}$$

This factor will be multiplied by equation (i) to obtain values of $w_M$ for $R/L \leq 8$ .

iii) effect of n

For the 3-span bridges which have been analyzed for $n = 1.2$ , an increase in the values of $w_M$ of approximately the same percentage of increase in n can be observed in Table 7.1 . Therefore, equation (i) will be multiplied by n to account for that effect.

iv) Effect of $h_c$

The values of $w_M$ are approximately doubled when the column height increases from 15' to 30' as shown in Table 7.1 . Therefore, a factor $f_2 = h_c/15$, where $h_c$ is in feet, will be multiplied by equation (i) to account for the column height.

v) Effect of $I_c$

The effects of the column stiffness on the equivalent load $w_M$ are presented in Table 7.2 . In general, smaller values of $w_M$ are obtained when using stiff columns. The column stiffness has more influence on the column stresses rather than the equivalent loads, therefore, this factor will be considered when analyzing the ratio factor $k_{cc}$.

vi) Effect of W

While all the cases presented in Table 7.1 consider 3-lane 3-girder (3L , 3G) bridges, Table 7.2 presents the values of $w_M$ for (2L , 2G) and (1L , 1G) bridges. It can be

realized that these values decrease with an average ratio of 1.0 : 0.5 : 0.2 when the bridge weight decreases. Table 7.3 shows the bridge weights per unit length W and the deck moments of inertia about a vertical axis $I_D$ for different cross-sections $XS_1$. It can be concluded that the variation in the values of $w_M$ generally follows that of the bridge weight. Average values for W are computed for different span lengths, and a linear relationship is assumed in the form

$$f_3 = C_5 W + C_6 \qquad (c)$$

where $f_3$ is a factor which accounts for the influence of W, and the constants $C_5$ and $C_6$ can be determined from the conditions

$$f_3 = 1.0 \quad \text{when} \quad W = 6.5 \text{ k/ft}$$

and $$f_3 = 0.2 \quad \text{when} \quad W = 2.2 \text{ k/ft}$$

which yield

$$f_3 = \frac{W}{5.4} - 0.2 \qquad (iii)$$

where the units of W are k/ft. This factor will be multiplied by equation (i) to obtain values of $w_M$ corresponding to different bridge weights W.

vii) <u>The design equation</u>

Based on the above analysis, a final design equation for $w_M$ can be obtained by multiplying equation (i) by the

factors which correspond to the different parameters. Since all these factors were derived to obtain conservative values for $w_M$, a 10% reduction in the results of the design equation will be considered. This will yield the final design equations:

For $R/L \leq 8$

$$w_M = (4.5\,NS+4)(1.2-\frac{R/L}{40})(n)(\frac{h_c}{15})(\frac{W}{6}-0.18) \qquad (7.1.a)$$

For $R/L > 8$

$$w_M = (4.5\,NS+4)(n)(\frac{h_c}{15})(\frac{W}{6}-0.18) \qquad (7.1.b)$$

It should be noted that all the units are kips and feet.

7.2.1.2 Single Span Bridges

It can be concluded from Table 7.1 that the values of $w_M$ is slightly affected by R/L, therefore an average value of $w_M = 2.5$ k/ft will be considered. The effect of W is analyzed in the same manner considered for multiple-span bridges, yielding the final design equation:

$$w_M = \frac{W}{2.33} \qquad (7.1.c)$$

7.2.2 Equivalent Load $w_V$

The following design equations for $w_V$ have been derived in a way similar to the equivalent load $w_M$ derivation, where both loads are influenced by all parameters in the same pattern:

i) Multiple-span bridges

For $R/L \leq 8$:

$$w_V = (\frac{NS}{2} + 4.5)(1.4 - \frac{R/L}{20})(n)(\frac{h_c}{15})(\frac{W}{6} - 0.18) \quad (7.2.a)$$

For $R/L > 8$:

$$w_V = (\frac{NS}{2} + 4.5)(n)(\frac{h_c}{15})(\frac{W}{6} - 0.18) \quad (7.2.b)$$

ii) Single span bridges

$$w_V = \frac{W}{2.9} \quad (7.2.c)$$

7.2.3 Equivalent Loads $w_s$ and $w_c$

The results of the stresses equivalent loads were compared to $w_M$, and direct relationships have been concluded in the form:

$$w_s = 1.35\ w_M \quad (7.3)$$

and

$$w_c = 1.8\ \ w_M \quad (7.4)$$

7.2.4 Ratio Factor $k_p$

i) Multiple-span bridges

For $R/L \leq 12$:

$$k_p = (1.5\,NS - 0.5)(\frac{R/L}{20} + 0.6)(\frac{15}{h_c})(1.9 - \frac{W}{7.2}) \quad (7.5.a)$$

For R/L > 12:

$$k_p = (1.5\,NS - 0.5)\left(\frac{18}{h_c}\right)\left(1.9 - \frac{W}{7.2}\right) \qquad (7.5.b)$$

ii) Single span bridges

$$k_p = 2.6 \qquad (7.5.c)$$

It can be realized from the above Equations that higher values for $k_p$ are obtained for straight bridges, while long-column models induce lower values for that factor.

7.2.5 Ratio Factor $k_v$

While this factor is not affected by the radius of curvature R, it sharply decreases for short-span bridges and long-column models. On the other hand, light weight bridges have higher values for $k_v$ as can be seen from the following Equation:

$$k_v = (NS - 1.5)\left(\frac{L}{100} - 0.6\right)(n)\left(1.8 - \frac{h_c}{18.9}\right)\left(4.4 - \frac{W}{2}\right) \qquad (7.6)$$

7.2.6 Deck Stresses Ratio Factors

These factors are mainly affected by the span length and the bridge weight as shown in the following Equations:

a) Ratio factor $k_{sm}$

i) Multiple-span bridges

$$k_{sm} = (0.67)(n)\left(1.76 - \frac{W}{8.6}\right) \qquad (7.7.a)$$

ii) Single span bridges

$$k_{sm} = \left(\frac{7000}{L^{1.5}}\right)\left(0.24 + \frac{W}{8.6}\right) \qquad (7.7.b)$$

b) Ratio factor $k_{cm}$

i) Multiple-span bridges

$$k_{cm} = (0.67)(n)\left(1.76 - \frac{W}{8.6}\right) \qquad (7.8.a)$$

For 2-span bridges, 50% reduction in the above Equation should be considered.

ii) Single span bridges

$$k_{cm} = \left(\frac{2000}{L^{1.4}}\right)\left(0.24 + \frac{W}{8.6}\right) \qquad (7.8.b)$$

c) Ratio factor $k_{sp}$

i) 2-span bridges

$$k_{sp} = (0.8)\left(2.2 - \frac{L}{125}\right)\left(1.76 - \frac{W}{8.6}\right) \qquad (7.9.a)$$

ii) Bridges with 3 or more spans

$$k_{sp} = (0.55)\left(1.6 - \frac{L}{250}\right)\left(1.76 - \frac{W}{8.6}\right) \qquad (7.9.b)$$

d) Ratio factor $k_{cp}$

i) 2-span bridges

$$k_{cp} = (0.55)\left(0.55 + \frac{W}{14.3}\right) \qquad (7.10.a)$$

ii) Bridges with 3 or more spans

$$k_{cp} = (0.33)(2.51 - \frac{W}{4.3}) \qquad (7.10.b)$$

7.2.7 Ratio Factor $k_{cc}$

This factor is mainly influenced by the column height and stiffness, as well as the number of spans and the span length, as can be realized from the following Equation:

$$k_{cc} = (2\,NS - 1)(\frac{L}{100} - 0.5)(1.7 - \frac{h_c}{21.4})(1.6 - \frac{I_c}{8}) \qquad (7.11)$$

7.3 Equivalent Static Analysis

In the previous Section, the equivalent loads and factors which induce the maximum seismic responses at the critical sections of the bridge have been obtained. To compute those responses, the bridge is analyzed as a continuous straight beam with fixed end supports, subjected to a uniform load $w_e = 1.0$ k/ft in the transverse direction as shown before in Figure 6.6 . The same span lengths and deck stiffness, assuming a constant composite section $XS_1$, of the original bridge are considered. Reactions and stresses at the end support are calculated as follows:

$$M_1 = \frac{L^2}{k_1} \qquad (7.12)$$

$$V_1 = \frac{L}{k_2} \qquad (7.13)$$

$$\sigma_s = \frac{L^2}{k_1}\,\frac{1}{S_s} \qquad (7.14)$$

$$\sigma_c = \frac{L^2}{k_1} \frac{1}{S_c} \frac{1}{m_r} \tag{7.15}$$

where $M_1, V_1$ = vertical moment and transverse shear, respectively, at the end support

$\sigma_s, \sigma_c$ = maximum normal stresses in steel and concrete, respectively, at the end support

Other parameters have been previously defined in Section 6.5 .

Seismic forces and moments at the attachments between the superstructure and the suporting elements, as well as seismic stresses in both steel and concrete at the critical sections of the bridge deck and columns can be computed as follows:

1. Attachments:

$$M_a = w_M \cdot M_1 \tag{7.16}$$

$$V_a = w_V \cdot V_1 \tag{7.17}$$

$$P_a = k_p \cdot V_a \tag{7.18}$$

$$V_p = k_V \cdot V_a \tag{7.19}$$

2. Superstructure

$$\sigma_{sa} = w_s \cdot \sigma_s \tag{7.20}$$

$$\sigma_{ca} = w_c \cdot \sigma_c \tag{7.21}$$

$$\sigma_{sm} = k_{sm} \cdot \sigma_{sa} \tag{7.22}$$

$$\sigma_{cm} = k_{cm} \cdot \sigma_{ca} \tag{7.23}$$

$$\sigma_{sp} = k_{sp} \cdot \sigma_{sa} \tag{7.24}$$

$$\sigma_{cp} = k_{cp} \cdot \sigma_{ca} \tag{7.25}$$

3. Columns

$$\sigma_{cc} = k_{cc} \cdot \sigma_{ca} \tag{7.26}$$

It should be noted that the seismic responses obtained from Equations (7.16) to (7.26) are absolute maximum values that do not necessarily occur within the bridge at the same time. These maximum responses are assumed to occur at all the corresponding locations shown in Figure 6.5 .

## 7.4 Seismic Design Considerations

Seismic responses, and consequently the corresponding design equations, which have been obtained throughout this study are based on El Centro earthquake excitation as a dynamic input. Intensity of ground motion and site effects for different parts of the United States are discussed in this Section. Moreover, bridges will be divided into different categories, and response modification factors for both the superstructure and the supporting elements will be presented. The following Sections are extracted from the Seismic Design Guidlines For Highway Bridges [49], with appropriate modifications.

### 7.4.1 Intensity of Ground Motion

The Guidelines present a contour map (Figure 2.6) for an acceleration coefficient that account for the design

earthquake ground motion. The development of this map is mainly based on the seismic risk map of the United States (Figure 2.4) , where the high contour lines correspond to Zone 3 . The maximum ground accelerations associated with the different zones are presented in Table 7.4 [56]. Since El Centro earthquake (peak acceleration = 0.35 g) has occurred in Zone 3 corresponding to contour line 0.40 , the contour map has been modified by dividing the contour values by 0.40 to obtain modified acceleration coefficients $A_m$, as shown in Figure 7.1 . These coefficients will be multiplied by the seismic responses which were obtained from the equivalent static analysis, presented in Section 7.3 , to account for the intensity of ground motion for different parts of the United States. It should be noted that the severity of the ground shaking is characterized by the size and shape of the pulses, i.e., the maximum accelerations and the number of zero crossings per second [56] .

### 7.4.2 Site Effects

The effects of site conditions on bridge response are determined from a site coefficient S based on soil profile types defined as follows:

i) Soil profile type I is a profile with either

1. Rock of any characteristic, either shale-like or crystalline in nature (shear wave velocity > 2500 ft/sec); or

2. Stiff soil conditions where the soil depth is less than 200 ft and the soil types overlying rock are stable deposites of sands, gravels, or stiff clays.

ii) Soil profile type II is a profile with stiff clay or deep cohesionless conditions where the soil depth exceeds 200 ft and the soil types overlying rock are stable deposites of sands, gravels, or stiff clays.

iii) Soil profile type III is a profile with soft to medium-stiff clays and sands, characterized by 30 ft or more of soft to medium-stiff clays with or without intervening layers of sand or other cohesionless soils.

In locations where the soil properties are not known in sufficient detail to determine the soil profile type, or where the profile does not fit any of the three types, the site coefficient for soil profile type II should be used.

The site coefficient S, which is given in Table 7.5 , will be multiplied by the computed seismic responses to approximate the effects of the site conditions.

7.4.3 Importance Classification

An importance classification IC shall be assigned for all bridges with $A_m > 0.72$ for the purpose of determining the seismic performance category in Section 7.4.4 as follows:

1. Essential bridges - IC = I
2. Other bridges - IC = II

Bridges shall be classified on the basis of social/ survival and security/defence requirements, guidelines for which are given in reference [49].

### 7.4.4 Seismic Performance Categories

Each bridge shall be assigned to one of four seismic performance categories SPC, A through D, based on the modified acceleration coefficient $A_m$ and the importance classification IC, as shown in Table 7.6 . Minimum design requirements are governed by the SPC as discussed in details in the Guidelines [49].

### 7.4.5 Response Modification Factors

Seismic responses for individual members and connections of bridges classified as SPC B, C, and D shall be divided by the appropriate response modification factor $R_m$ which accounts for the ductility and nonlinearity requirements. The response modification factors for the various components are given in Table 7.7 , and a detailed discussion concerning this factor is included in the Guidelines [49].

## 7.5 Design Procedures

Seismic analysis and design of steel box-girder bridges can be performed as follows:

1. Geometry and cross-sections for both the bridge deck and columns are assumed

2. Calculate the equivalent loads and ratio factors (Equations (7.1) to (7.11))
3. Perform equivalent static analysis of the bridge (Equations (7.12) to (7.15))
4. Compute the seismic responses for both the superstructure and the supporting elements (Equations (7.16) to (7.26))
5. Multiply the computed seismic responses by the modifying factor $A_m S/R_m$ (Section 7.4)
6. Calculate the dead load stresses. Also calculate stresses due to earth pressure, buoyancy, and stream flow pressure, when applicable
7. The combined stresses [Step 5 + Step 6] should not exceed 1.50 the allowable stresses for structural steel, and 1.33 for reinforced concrete [49]
8. If stresses in Step 7 are not safe, change geometry and/or cross-sections and redesign.

## 7.6 Examples

Several examples have been studied to check the proposed design criteria. Actual steel box-girder bridges are considered, where the geometry and structural details for the superstructure are obtained from reference [20], and appropriate bent geometry is assumed. Seismic responses are computed using the equivalent static analysis (steps 2 to 4 in Section 7.5) , and they are compared with the computer dynamic analysis results. Bridges are also

analyzed under the effect of their own weights and the dead load stresses are tabulated.

Single, two, three, and four-span bridges are analyzed, with different span lengths, span ratios, and radii of curvature. Various deck cross-sections are considered, including (2L , 2G), (3L , 3G), (4L , 4G), and (3L , 2G) bridges, where the girder spacing is greater for the last cross-section, and the section properties for $XS_1$ are computed. Tables 7.8 and 7.9 present the bridge geometry and the section properties, respectively, for the eight case studies.

Equivalent loads and ratio factors are calculated, utilizing Equations (7.1) to (7.11) , and they are given in Table 7.10 . Equivalent static analysis results for $w_e$ = 1.0 k/ft are included in Table 7.11 , and seismic responses for both the superstructure and the supporting elements are computed (Equations (7.16) to (7.26)) , and they are presented in Table 7.12 .

Computer dynamic analysis was performed using the modified SAP IV program. A 2-column 6-element model is used, and the first 10 seconds of El Centro earthquake record is applied to the bridge as a 3-direction shock. Results of the computer analysis are included in Table 7.12 . A comparison between the equivalent static analysis and the computer solution shows good correlation.

The modified program was also used to perform static analysis of the bridges under the effect of their own weights. Both composite sections $XS_1$ and non-composite

sections $XS_2$ are considered, and straining actions at the critical sections for both the superstructure and the columns are obtained. Dead load stresses are computed and presented in Table 7.13 .

To complete the analysis, the seismic responses in Table 7.12 can be modified, as discussed before in Section 7.4 , and the combined dead load and seismic stresses should not exceed 1.50 the allowable stresses for structural steel, and 1.33 for reinforced concrete.

Table 7.1 Equivalent Load $w_M$ (k/ft): Effects of NS , L , R , n , and $h_c$

| NS | | 1 | 2 | | 3 | | | | 4 | | 5 | |
|---|---|---|---|---|---|---|---|---|---|---|---|---|
| $h_c$(ft) | | | 15 | 30 | 15 | 30 | 15 | 30 | 15 | 30 | 15 | 30 |
| n | | | 1.0 | 1.0 | 1.0 | 1.0 | 1.2 | 1.2 | 1.0 | 1.0 | 1.0 | 1.0 |
| R/L | L(ft) | | | | | | | | | | | |
| 4 | 50 | 2.08 | | | | | | | | | | |
| | 100 | 2.10 | 13.65 | 14.47 | 22.40 | 50.14 | 36.81 | 71.79 | 34.39 | | 38.11 | |
| | 150 | 2.40 | 11.30 | 19.44 | 19.94 | 36.81 | 17.82 | 57.16 | 14.41 | | 19.29 | |
| | 200 | 3.70 | 17.28 | 23.48 | 17.49 | 62.44 | 21.03 | 62.48 | | | | |
| | | (2.60) | (14.10) | (19.10) | (19.90) | (49.80) | (25.20) | (63.80) | (24.40) | | (28.70) | |
| 8 | 50 | 1.95 | | | | | | | | | | |
| | 100 | 2.01 | 12.16 | 14.94 | 12.54 | 41.19 | 27.47 | 54.02 | 25.25 | 60.11 | 24.60 | 76.24 |
| | 150 | 2.31 | 11.15 | 18.10 | 14.78 | 32.31 | 22.33 | 38.90 | 13.75 | 61.63 | 9.45 | 51.57 |
| | 200 | 3.52 | 15.39 | 25.51 | 17.79 | 56.17 | 19.43 | 62.47 | | | | |
| | | (2.40) | (12.90) | (19.50) | (17.70) | (43.20) | (23.10) | (51.80) | (19.50) | (60.90) | (17.00) | (63.90) |
| 12 | 50 | 1.85 | | | | | | | | | | |
| | 100 | 1.98 | 11.33 | 14.77 | 22.14 | 40.68 | 23.86 | 49.60 | | | | |
| | 150 | 2.28 | 11.54 | 17.48 | 13.60 | 29.40 | 22.00 | 40.23 | | | | |
| | 200 | 3.50 | 15.01 | 25.89 | 16.66 | 53.01 | 17.62 | 61.43 | | | | |
| | | (2.40) | (12.60) | (19.40) | (17.50) | (41.00) | (21.20) | (50.40) | | | | |
| 16 | 100 | | 10.95 | 14.69 | 22.91 | 40.33 | 23.27 | 49.53 | 25.29 | | 21.54 | |
| | 150 | | 11.73 | 17.19 | | | | | 13.44 | | 9.17 | |
| | 200 | | 14.84 | 26.07 | | | | | | | | |
| | | | (12.50) | (19.30) | | | | | (19.40) | | (15.40) | |
| 24 | 100 | | | | 23.24 | 39.86 | 22.59 | | | | | |

Table 7.2 Equivalent Load $w_M$ (k/ft): Effects of $I_c$ and W

| NS | | 1 | | 2 | | | 3 | | | 4 | |
|---|---|---|---|---|---|---|---|---|---|---|---|
| L (ft) | | 100 | 150 | 100 | 150 | 150 | 100 | 150 | 150 | 100 | 150 |
| $h_c$ (ft) | | | | 15 | 15 | 30 | 15 | 15 | 30 | 15 | 15 |
| Column | Deck | | | | | | | | | | |
| $C_1$ | 3L,3G | | | 13.19 | 11.72 | 18.51 | 23.52 | 27.32 | 38.81 | 38.44 | 19.41 |
| $C_2$ | 3L,3G | | | 12.16 | 11.15 | 18.10 | 20.54 | 14.78 | 32.31 | 25.25 | 13.75 |
| $C_3$ | 3L,3G | | | 11.23 | 12.67 | 17.91 | 22.37 | 11.71 | 27.16 | 19.53 | 10.29 |
| $C_2$ | 3L,3G | 2.01 | 2.31 | 12.16 | 11.15 | 18.10 | 20.54 | 14.78 | 32.31 | 25.25 | 13.75 |
| $C_2$ | 2L,2G | 1.36 | 2.18 | 6.67 | 4.78 | 12.28 | 7.31 | 4.33 | 14.26 | 6.73 | 5.20 |
| $C_2$ | 1L,1G | 0.83 | 1.15 | 2.58 | 2.20 | 4.76 | 1.44 | 1.74 | 2.66 | 1.40 | 1.92 |

Table 7.3 Bridge Weight and Deck Stiffness, (k,ft)

| Deck | Single Span | | | | Multiple-Span | | | |
|---|---|---|---|---|---|---|---|---|
| | L=100' | | L=150' | | L=100' | | L=150' | |
| | W | $I_D$ | W | $I_D$ | W | $I_D$ | W | $I_D$ |
| 3L,3G | 6.3 | 1011. | 6.7 | 1143. | 6.2 | 985. | 6.5 | 1090. |
| 2L,2G | 4.2 | 306. | 4.5 | 355. | 4.2 | 298. | 4.3 | 337. |
| 1L,1G | 2.1 | 48. | 2.2 | 61. | 2.1 | 46. | 2.2 | 58. |

Table 7.4 Maximum Ground Accelerations [56], (g)

| Zone | Maximum Acceleration |
|---|---|
| 3 | 0.33 ∿ 0.50 |
| 2 | 0.16 |
| 1 | 0.08 |
| 0 | 0.04 |

Table 7.5 Site Coefficient, S [49]

| | Soil Profile Type | | |
|---|---|---|---|
| | I | II | III |
| S | 1.0 | 1.2 | 1.5 |

Table 7.6 Seismic Performance Category, SPC [49]

| Modified Acceleration Coefficient | | | | | Importance Classification, IC | |
|---|---|---|---|---|---|---|
| | | $A_m$ | | | I | II |
| | | $A_m$ | $\leq$ | 0.22 | A | A |
| 0.22 | < | $A_m$ | $\leq$ | 0.47 | B | B |
| 0.47 | < | $A_m$ | $\leq$ | 0.72 | C | C |
| 0.72 | < | $A_m$ | | | D | C |

Table 7.7 Response Modification Factor, $R_m$ [49]

| Substructure | $R_m$ | Connections | $R_m$ |
|---|---|---|---|
| - Wall-type pier | 2 | - Superstructure to abutment | 0.8 |
| - Reinforced concrete pile bents | | - Expansion joints within a span of the superstructure | 0.8 |
| a) vertical piles only | 3 | | |
| b) one or more batter piles | 2 | | |
| - Single columns | 3 | - Columns, piers, or pile bents to cap beam or superstructure | 1.0 |
| - Steel or composite steel and concrete pile bents | | - Columns or piers to foundations | 1.0 |
| a) vertical piles only | 5 | | |
| b) one or more batter piles | 3 | | |
| - Multiple-column bent | 5 | | |

Table 7.8 Examples: Bridge Geometry, (ft)

| Case | NS | L | n | R | R/L | $h_c$* | $I_c$ | Deck Cross-Section** |
|---|---|---|---|---|---|---|---|---|
| 1 | 1 | 140 | | 600 | 4.29 | | | 4L,4G |
| 2 | 2 | 120 | 1.00 | 700 | 5.83 | 15 | 4.5 | 3L,3G |
| 3 | 2 | 120 | 1.00 | 4000 | 33.33 | 15 | 4.5 | 3L,3G |
| 4 | 2 | 174 | 1.00 | 1000 | 5.75 | 15 | 5.5 | 3L,2G |
| 5 | 3 | 172 | 1.14 | 760 | 4.42 | 20 | 5.0 | 3L,3G |
| 6 | 3 | 172 | 1.14 | 5000 | 29.07 | 20 | 5.0 | 3L,3G |
| 7 | 3 | 116 | 1.13 | 600 | 5.17 | 15 | 3.5 | 2L,2G |
| 8 | 4 | 120 | 1.00 | 700 | 5.83 | 15 | 4.5 | 3L,3G |

* 3-Column bents are assumed for all bridges

** Structural details for the deck cross-sections are included in reference [20]

Table 7.9 Examples: Section Properties For $XS_1$ (Composite), (k,ft)

| Case | Area | Mass Density | W | $I_D$ | $S_s$ | $S_c$ |
|---|---|---|---|---|---|---|
| 1 | 15.23 | .02413 | 11.83 | 3936. | 147.8 | 141.4 |
| 2 | 5.53 | .03328 | 5.93 | 865. | 46.1 | 39.3 |
| 3 | 5.53 | .03328 | 5.93 | 865. | 46.1 | 39.3 |
| 4 | 4.74 | .03470 | 5.30 | 550. | 35.7 | 28.9 |
| 5 | 9.58 | .02570 | 7.93 | 1415. | 75.1 | 66.6 |
| 6 | 9.58 | .02570 | 7.93 | 1415. | 75.1 | 66.6 |
| 7 | 3.65 | .03724 | 4.38 | 296. | 24.2 | 17.9 |
| 8 | 6.62 | .02972 | 6.34 | 973. | 53.4 | 45.8 |

Table 7.10 Equivalent Loads and Ratio Factors

| Case | Equivalent Loads (k/ft) | | | | Ratio Factors | | | | | | |
|---|---|---|---|---|---|---|---|---|---|---|---|
| | $w_M$ | $w_V$ | $w_s$ | $w_c$ | $k_P$ | $k_V$ | $k_{sm}$ | $k_{cm}$ | $k_{sp}$ | $k_{cp}$ | $k_{cc}$ |
| 1 | 5.08 | 4.08 | 6.86 | 9.14 | 2.60 | | 6.80 | 3.20 | | | |
| 2 | 11.08 | 4.93 | 14.96 | 19.94 | 2.40 | 0.43 | 0.72 | 0.36 | 1.06 | 0.53 | 2.17 |
| 3 | 10.51 | 4.45 | 14.19 | 18.92 | 3.23 | 0.43 | 0.72 | 0.36 | 1.06 | 0.53 | 2.17 |
| 4 | 9.66 | 4.30 | 13.04 | 17.39 | 2.58 | 1.00 | 0.77 | 0.39 | 0.74 | 0.51 | 3.39 |
| 5 | 33.08 | 12.27 | 44.66 | 59.54 | 1.96 | 0.62 | 0.64 | 0.64 | 0.42 | 0.22 | 4.55 |
| 6 | 30.37 | 10.41 | 41.00 | 54.67 | 2.88 | 0.62 | 0.64 | 0.64 | 0.42 | 0.22 | 4.55 |
| 7 | 11.65 | 4.26 | 15.73 | 20.97 | 4.43 | 2.10 | 0.94 | 0.94 | 0.78 | 0.49 | 3.83 |
| 8 | 20.33 | 6.32 | 27.45 | 36.59 | 5.00 | 1.85 | 0.69 | 0.69 | 0.63 | 0.34 | 5.10 |

Table 7.11 Equivalent Static Analysis Results, $w_e = 1.0$ k/ft

| Case | $k_1$ | $k_2$ | $M_1$ (k.ft) | $V_1$ (k) | $\sigma_s$ (ksi) | $\sigma_c$* (ksi) |
|---|---|---|---|---|---|---|
| 1 | 12. | 2. | 1633. | 70. | 0.077 | 0.010 |
| 2 | 12. | 2. | 1200. | 60. | 0.181 | 0.027 |
| 3 | 12. | 2. | 1200. | 60. | 0.181 | 0.027 |
| 4 | 12. | 2. | 2523. | 87. | 0.491 | 0.076 |
| 5 | 13.39 | 2.11 | 2209. | 81.5 | 0.204 | 0.029 |
| 6 | 13.39 | 2.11 | 2209. | 81.5 | 0.204 | 0.029 |
| 7 | 13.27 | 2.10 | 1014. | 55.2 | 0.291 | 0.049 |
| 8 | 12. | 2. | 1200. | 60. | 0.156 | 0.023 |

* $n_r = 8.$

Table 7.12 Seismic Responses

| Case | Method* | Actions at the Attachments, (k,ft) | | | | Deck and Column Stresses, (ksi) | | | | | | |
|---|---|---|---|---|---|---|---|---|---|---|---|---|
| | | $M_a$ | $V_a$ | $P_a$ | $V_p$ | $\sigma_{sa}$ | $\sigma_{ca}$ | $\sigma_{sm}$ | $\sigma_{cm}$ | $\sigma_{sp}$ | $\sigma_{cp}$ | $\sigma_{cc}$ |
| 1 | S | 8296. | 286. | 743. | | 0.53 | 0.09 | 3.60 | 0.28 | | | |
| | D | 6519. | 218. | 539. | | 0.45 | 0.07 | 1.36 | 0.14 | | | |
| 2 | S | 13296. | 296. | 711. | 127. | 2.70 | 0.53 | 1.94 | 0.19 | 2.86 | 0.28 | 1.15 |
| | D | 13160. | 276. | 715. | 81. | 2.41 | 0.50 | 2.07 | 0.16 | 2.56 | 0.27 | 0.85 |
| 3 | S | 12612. | 267. | 862. | 115. | 2.56 | 0.51 | 1.84 | 0.18 | 2.71 | 0.27 | 1.10 |
| | D | 12515. | 260. | 722. | 75. | 2.28 | 0.48 | 2.08 | 0.14 | 2.49 | 0.25 | 0.76 |
| 4 | S | 24372. | 374. | 965. | 374. | 6.40 | 1.32 | 4.92 | 0.51 | 4.73 | 0.67 | 4.47 |
| | D | 18322. | 313. | 956. | 380. | 4.15 | 0.79 | 3.34 | 0.35 | 3.64 | 0.26 | 3.03 |
| 5 | S | 73074. | 1000. | 1960. | 620. | 9.11 | 1.72 | 5.83 | 1.10 | 3.83 | 0.38 | 7.82 |
| | D | 70355. | 806. | 1889. | 624. | 8.05 | 1.55 | 4.67 | 0.88 | 3.74 | 0.47 | 5.63 |
| 6 | S | 67087. | 848. | 2442. | 526. | 8.36 | 1.58 | 5.35 | 1.01 | 3.51 | 0.35 | 7.18 |
| | D | 49404. | 491. | 2469. | 510. | 6.03 | 1.14 | 4.94 | 0.94 | 3.32 | 0.37 | 4.54 |
| 7 | S | 11813. | 235. | 1041. | 493. | 4.58 | 1.03 | 4.30 | 0.96 | 3.57 | 0.50 | 3.94 |
| | D | 10483. | 235. | 986. | 350. | 5.23 | 0.95 | 3.87 | 0.67 | 2.57 | 0.25 | 3.38 |
| 8 | S | 24396. | 379. | 1895. | 701. | 4.28 | 0.84 | 2.95 | 0.57 | 2.69 | 0.28 | 4.28 |
| | D | 24900. | 385. | 1559. | 738. | 4.85 | 0.91 | 3.31 | 0.53 | 1.93 | 0.27 | 4.61 |

* S = Equivalent Static Analysis
D = Computer Dynamic Analysis

Table 7.13 Dead Load Stresses, (ksi)

| Case | $\sigma_{sm}$ | $\sigma_{cm}$ | $\sigma_{sp}$ | $\sigma_{cc}$ |
|---|---|---|---|---|
| 1 | 4.51 | 0.38 | | |
| 2 | 7.24 | 0.38 | 9.60 | 1.11 |
| 3 | 7.23 | 0.38 | 9.48 | 1.10 |
| 4 | 13.74 | 0.67 | 17.70 | 1.16 |
| 5 | 8.01 | 0.72 | 13.13 | 1.69 |
| 6 | 8.00 | 0.72 | 12.86 | 1.68 |
| 7 | 8.65 | 0.39 | 11.10 | 0.78 |
| 8 | 5.65 | 0.38 | 8.54 | 1.08 |

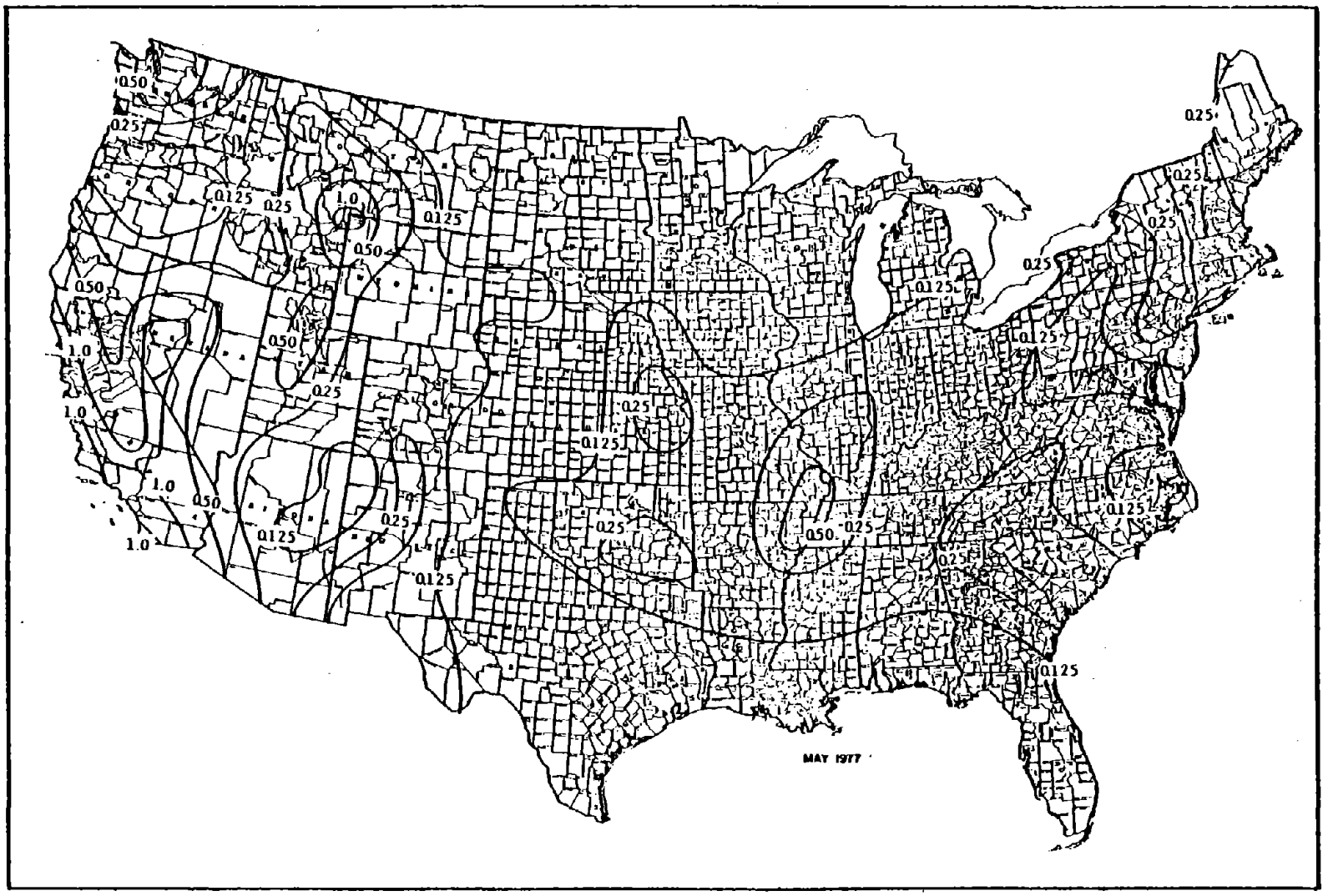


Figure 7.1 Modified Acceleration Coefficient - Continental United States

# CHAPTER VIII

## SUMMARY AND CONCLUSIONS

In this research a comprehensive study of the seismic response of curved steel box-girder bridges was presented. Single, two, three, four, and five-span bridges were considered, where the geometry and the structural details of the superstructure and the supporting elements were based on a current bridge survey of all existing box-girder bridges.

El Centro earthquake accelerogram and its corresponding response spectrum were used as a dynamic input, and maximum actions at the attachments and maximum stresses at the critical sections for both the superstructure and the columns were obtained. The finite element program SAP IV for static and dynamic responses of linear systems was modified and used in the analysis, and bridges were modeled using 3-D space frame elements.

Seismic analysis of typical curved steel box-girder bridges was performed, and different elements of the bridge model and the seismic loading were examined. 2-Column and 3-column models were compared, and the bridge curved geometry and boundary conditions were studied. Both the number of elements and the number of modes of vibration were optimized, and the solution time step as well as the seismic load duration were studied.

A comparison between the response spectrum and the response history techniques in analyzing curved steel box-

girder bridges was made, and the simultaneous application of the earthquake loadings in the three global directions was discussed.

Other factors influencing the seismic response were studied, including damping effects, composite and non-composite deck cross-sections, rotational inertia, and column height. A comparison with rigid-column models and closed form solutions was also made.

Parametric analysis was made to study the effects of the bridge geometry and materials on the seismic responses. The parameters included the number of spans, span length, span ratio, curvature, column height, deck and column stiffnesses, and the bridge weight per unit length. The response history technique was used, and the three components of El Centro earthquake were applied to the bridge structures as a 3-direction shock. Maximum dynamic responses at the critical sections were correlated with static analysis of the bridge, and equivalent loads and ratio factors were obtained and design curves were developed. The influence of each parameter on the seismic responses was also discussed.

A design criteria was proposed based on the results of the parametric analysis. Design equations for both of the equivalent loads and the ratio factors were derived, and the equivalent static analysis for bridges was presented. Practical seismic design considerations were discussed, including the intensity of ground motion, the soil profile characteristics of the site, and the response modification factors

for both the superstructure and the supporting elements. Several examples were presented, and the computer dynamic analysis was compared with the design criteria.

Based on the results of this study the following conclusions have been drawn:

(I) Bridge model and seismic loading

- A 2-column 6-element curved model having end short elements with appropriate member releases can yield satisfactory seismic responses.
- Modes of vibrations are coupled in the two horizontal directions due to the curved geometry of the bridge.
- The contribution of the first 15 mode shapes, and a solution time step of 0.0050 seconds can be considered in the response history analysis.
- Seismic responses decrease with an increase in the damping ratio, and a 5% damping ratio is generally assumed.
- Non-composite deck models produce higher deck and column stresses.
- Considering the rotational inertia coefficients in the mass matrix does not have a significant effect on the seismic responses.
- A significant increase in tangential displacements, vertical moments, and deck stresses is realized in long-column models, while column stresses are much less than the short columns case.

- Rigid-column models generally yield much less seismic responses than the 2-column models.
- Steel box-girder bridges undergo relatively small displacements when subjected to seismic loading.
- The first 10 seconds of El Centro earthquake record, which include the intense ground shaking, excite the bridge model to its maximum seismic responses.

(II) Computer program and methods of analysis

- The modified version of the finite element program SAP IV, which was developed in this study, is a powerful tool for the seismic analysis of curved steel box-girder bridges.
- The response spectrum technique fails when higher modes are considered because high frequency data (greater than 25 Hz), which is considered contaminated with erroneous noise, has been filtered out of the earthquake record.
- Seismic responses obtained using the response spectrum analysis are maximum absolute values that do not necessarily occur at the same time, therefore, realistic normal and shear stresses can not be computed.
- Combining the effects of earthquake loadings in the three orthogonal directions using the response spectrum technique will yield very conservative results.
- The use of a statistical approach to replace the effects of the removed time domain in the response spectrum method may yield unrealistic results.

Therefore, the response history technique is considered to be the most sophisticated type of analysis.

- Coupling effects due to the curved alignment of the bridges suggest that the 3-direction shock will yield the most satisfactory results.

(III) Parametric analysis and design criteria

- The most influential parameters on the seismic responses of steel box-girder bridges are the number of spans, the column height, and the bridge weight.
- The equivalent loads and the actions ratio factors are influenced by all parameters, while the deck stresses ratio factors are mainly affected by the span length and the bridge weight.
- Seismic actions and stresses for curved bridges are higher than straight bridges except for the tangential forces at the abutments.
- The design curves, which were developed in this study, can be used to obtain the equivalent loads and the ratio factors for different steel box-girder bridges.
- The proposed design criteria, which is based on the results of the parametric analysis, eliminates the need to perform computer dynamic analysis for steel box-girder bridges.
- The modifying factor $A_m S/R_m$ acounts for the intensity of ground motion and the site effects, as well as the ductility and nonlinearity requirements.

- A comparison between computer dynamic analysis and the proposed design criteria shows good correlation.

While the results of this study provided a new simplified technique for the seismic analysis of steel box-girder bridges, several important recommendations have been developed that should be pursued in future research. These are:

1) Nonlinear analysis should be considered especially when the bridge columns are subjected to higher stresses.
2) Seismic responses of long bridges under the effects of traveling seismic waves should be studied.
3) Additional research needs to be carried out to investigate the soil-structure interaction problem for bridges subjected to seismic excitations.
4) Experimental model studies, as well as dynamic tests of full-scale bridges should be conducted to support the theoretical analysis.

## REFERENCES


1. Abdel-Ghaffar, A.M. , "Earthquake Engineering" , In Process of Publication, 1982 .

2. Bathe, K. ,and Wilson, E. , "Numerical Methods in Finite Element Analysis" , Prentice-Hall Inc., N.J., 1976 .

3. Bathe, K. ,Wilson, E.L. ,and Peterson, F.E. , "SAP IV - A Structural Analysis Program for Static and Dynamic Response of Linear Systems" , Report No. EERC 73-11, University of California, Berkeley, Ca., April 1974 .

4. Blevins, R.D. , "Formulas for Natural Frequency and Mode Shape" , Litton Educational Publishing Inc., 1979 .

5 Boresi, A.P. ,Sidebottom, O.M. ,Seely, F.B. ,and Smith, J.O. , "Advanced Mechanics of Materials" , John Wiley & Sons Inc., N.Y., 1978 .

6. Chapman, H.E. , "An Overview of the State of Practice in Earthquake Resistant Design of Bridges in New Zealand" , Proceedings of a Workshop on Earthquake Resistance of Highway Bridges, ATC, Palo Alto, Ca., January 1979 .

7. Chen, M. ,and Penzien, J. , "Soil-Structure Interaction of Short Highway Bridges" , Proceedings of a Workshop on Earthquake Resistance of Highway Bridges, ATC, Palo Alto, Ca., January 1979 .

8. Clough, D.P. , "Experimental Evaluation of Seismic Design Methods for Broad Cylindrical Tanks" , Report No. UCB/ EERC - 77/10, Earthquake Engineering Research Center, College of Engineering, University of California, Berkeley, 1977 .

9. Clough, R.W. ,and Penzien, J. , "Dynamics of Structures" , McGraw-Hill Book Co., N.Y., 1975 .

10. Clough, R.W. , Penzien, J. ,and Iwasaki, T. , "Literature Survey - Seismic Effects on Highway Bridges" , Report No. EERC 72-11, Earthquake Engineering Research Center, University of California, Berkeley, November 1972 .

11. "Commentary on Draft Guidlines for Highway Bridge Seismic Design Criteria" , ATC, Palo Alto, Ca., September 1979 .

12. Desai, C.S. ,and Abel, J.F. , "Introduction to the Finite Element Method" , Litton Educational Publishing Inc., 1972 .

13. Douglas, B.M. , "Experimental Dynamic Response Investigations of Existing Highway Bridges" , Proceedings of a Workshop on Earthquake Resistance of Highway Bridges, ATC, Palo Alto, Ca., January 1979 .

14. Dowrick, D.J. , "Earthquake Resistant Design" , John Wiley & Sons Inc., N.Y., 1977 .

15. "Draft Guidlines for Highway Bridge Seismic Design Criteria", ATC, Palo Alto, Ca., July 1979 .

16. "Earthquake Resistance of Highway Bridges - Final Recommendations" , ATC, Palo Alto, Ca., January 1979 .

17. Fertis, D.G. , "Dynamics and Vibration of Structures" , John Wiley & Sons Inc., N.Y., 1973 .

18. Gates, J.H. , "Factors Considered in the Development of the California Seismic Design Criteria for Bridges" , Proceedings of a Workshop on Earthquake Resistance of Highway Bridges, ATC, Palo Alto, Ca., January 1979 .

19. Godden, W.G. , "Seismic Model Studies of Long Span Curved Bridges" , Proceedings of a Workshop on Earthquake Resistance of Highway Bridges, ATC, Palo Alto, Ca., January 1979 .

20. Heins, C.P. , "Box-Girder Bridge Design - State of the Art" , AISC Engineering Journal, Vol. 15, No. 4, 1978 .

21. Heins, C.P. , "Bending and Torsional Design in Structural Members" , Lexington Books, D.C. Heath Co., Mass., 1975 .

22. Heins, C.P. ,and Derucher, K.N. , "Structural Analysis and Design" , Marcel Dekker Inc., N.Y., 1980 .

23. Heins, C.P. ,and Firmage, D.A. , "Design of Modern Steel Highway Bridges" , J. Wiley Interscience, N.Y., 1979 .

24. Heins, C.P. ,and Hall, D.H. ,et al., "Curved Steel Box-Girder Bridges : A Survey" , ASCE Journal of the Structural Division, Vol. 104, November 1978 .

25. Heins, C.P. ,and Hall, D.H. ,et al., "Curved Steel Box-Girder Bridges : State of the Art" , ASCE Journal of the Structural Division, Vol. 104, November 1978 .

26. Heins, C.P. ,and Lin, I. , "Equivalent Seismic Design of Curved Box-Girder Bridges" , Master of Science Thesis, Civil Engineering Department, University of Maryland, December 1981 .

27. Heins, C.P. ,and Sahin, M.A. , "Natural Frequency of Curved Box-Girder Bridges" , ASCE Structural Journal, Vol. 105, No. ST12, December 1979 .

28. Hudson, D.E. , "Reading and Interpreting Strong Motion Accelerograms" , Engineering Monographs, Vol. 1, Earthquake Engineering Research Institute, Berkeley, California, 1979 .

29. Hudson, D.E. , Brady, A.G. , Trifunac, M.D.,and Vijayaraghavan, A. , "Strong Motion Earthquake Accelerograms, Corrected Accelerograms and Integrated Velocity and Displacement Curves, Vol. II, Part A" , Earthquake Engineering Research Laboratory Report No. EERL 71-50, California Institute of Technology, Pasadena, Cal., September 1971 .

30. Hudson, D.E. , Trifunac, M.D. ,and Brady, A.G. , "Strong Motion Earthquake Accelerograms, Response Spectra, Vol. III, Part A" , Earthquake Engineering Research Laboratory Report No. EERL 72-80, California Institute of Technology, Pasadena, Cal., August 1972 .

31. Imbsen, R.A. , "Seismic Design of Highway Bridges - Workshop Manual" , U.S. Department of Transportation, FHWA, Wash., D.C., January 1981 .

32. Imbsen, R.A. , Nelson, T.A. , Chittenden, R.N. , Ho, Y. , and Coats, D.W. , "Applications of the 1973 California Earthquake Design Criteria" , Report No. SM45, Office of Structures Research and Development, Structure Mechanics, September 1974 .

33. Imbsen, R.A. , Nutt, R.V. ,and Penzien, J. , "Seismic Response of Bridges - Case Studies" , Report No. UCB/EERC - 78/14, Earthquake Engineering Research Center, College of Engineering, University of California, Berkeley, June 1978 .

34. Imbsen, R.A. , Nutt, R.V. ,and Penzien, J. , "Evaluation of Analytical Procedures Used in Bridge Seismic Design Practice" , Proceedings of a Workshop on Earthquake Resistance of Highway Bridges, ATC, Palo Alto, Ca., January 1979 .

35. Johnson, N.E. ,and Galletly, R.D. , "The Comparison of Response of a Highway Bridge to Uniform and Moving Ground Excitation" , Shock & Vibration Bulletin, Vol. 42, No. 2, January 1972 .

36. Kawashima, K. ,and Penzien, J. , "Theoretical and Experimental Dynamic Behavior of a Curved Model Bridge Structure" , Earthquake Engineering & Structural Dynamics Journal, Vol. 7, No. 2, 1979 .

37. Kawashima, K. ,and Penzien, J. , "An Investigation of the Effectiveness of Existing Bridge Design Methodology in Providing Adequate Structural Resistance to Seismic Disturbances - Phase V" , Report No. FHWA-RD-77-57, Federal Highway Administration, Washington, D.C., July 1976 .

38. Laursen, H.I. , "Structural Analysis" , McGraw-Hill Book Co., N.Y., 1969 .

39. Martin, G.R. , "Seismic Design Considerations For Bridge Foundations and Site Liquifaction Potential" , Proceedings of a Workshop on Earthquake Resistance of Highway Bridges, ATC, Palo Alto, Ca., January 1979 .

40. Meirovitch, L. , "Computational Methods in Structural Dynamics" , Sijthoff & Noordhoff International Publishers, Alphen aan den Rijn, The Netherlands, 1980 .

41. Meirovitch, L. , "Analytical Methods in Vibrations" , The Macmillan Co., N.Y., 1967 .

42. Miklofsky,H.A. ,and Mancini, W.B. , "Digitization and Integration of Strong Motion Accelerograms" , Report No. FHWA-RD-77-92,Federal Highway Administration, Washington, D.C., August 1977 .

43. Miller, R.K. ,and Felszeghy, S.F. , "Engineering Features of the Santa Barbara Earthquake of August 1978" , BBRI, Berkeley, Ca., 1978 .

44. Newmark, N.M. ,and Rosenblueth, E. , "Fundamentals of Earthquake Engineering" , Prentice-Hall Inc., N.J., 1971 .

45. Okamoto, S. , "Introduction to Earthquake Engineering" , John Wiley & Sons Inc., N.Y., 1973 .

46. Park, R. ,and Blakeley, R.W. , "Seismic Design of Bridges" , RRU Bulletin 43, Vol. 3, National Roads Board, Wellington, New Zealand, 1979 .

47. Paz, M. , "Structural Dynamics - Theory & Computation" , Litton Educational Publishing Inc., 1980 .

48. Penzien, J. , Chen, M. ,and Tseng, W. , "Seismic Response of Highway Bridges" , Proceedings of the U.S. National Conference on Earthquake Engineering, Ann Arbor, June 1975 .

49. "Seismic Design Guidlines For Highway Bridges" , Applied Technology Council, Palo Alto, Ca., October 1981 .

50. Sharp, R.L. ,and Mayes, R.L. , "Development of Highway Bridge Seismic Design Criteria for the United States" , Proceedings of a Workshop on Earthquake Resistance of Highway Bridges, ATC, Palo Alto, Ca., January 1979 .

51. "Standard Specifications for Highway Bridges - Twelfth Edition" , AASHTO, Washington, D.C., 1977 .

52. Tseng, W.S. ,and Penzien, J. , "Seismic Analysis of Long Multiple Span Highway Bridges" , Earthquake Engineering & Structural Dynamics Journal, Vol. 4, 1975 .

53. Tseng, W.S. ,and Penzien, J. , "Analytical Investigations of the Seismic Response of Long Multiple Span Highway Bridges" , Report No. EERC 73-12, Earthquake Engineering Research Center, University of California, Berkeley, June 1973 .

54. Weaver, W. ,and Gere, J.M. , "Matrix Analysis of Framed Structures" , Litton Educational Publishing Inc., 1980 .

55. Werner, S.D. , Lee, L.C. , Wong, H.L. ,and Trifunac, M.D. , "Effects of Travelling Seismic Waves on the Response of Bridges" , Proceedings of a Workshop on Earthquake Resistance of Highway Bridges, ATC, Palo Alto, Ca., January 1979 .

56. Wiegel, R.L. (Editor) , "Earthquake Engineering" , Prentice-Hall Inc., N.J., 1970 .

57. Williams, D. ,and Godden,W.G. , "Seismic Response of Long Curved Bridge Structures: Experimental Model Studies" , Earthquake Engineering & Structural Dynamics Journal, Vol. 7, No. 2, 1979 .

58. Williams, D. ,and Godden, W.G. , "An Investigation of the Effectiveness of Existing Bridge Design Methodology in Providing Adequate Structural Resistance to Seismic Disturbances - Phase IV" , Report No. FHWA-RD-77-91, Federal Highway Administration, Washington, D.C., June 1976 .

59. Williams, D. ,and Godden, W.G. , "Seismic Behavior of High Curved Overcrossings" , Proceedings of the U.S. National Conference on Earthquake Engineering, Ann Arbor, June 1975 .

60. Williams, D.,and Godden, W.G. , "Seismic Response of a Curved Highway Bridge Model" , 54th Annual Meeting, Transportation Research Board, Wash., D.C., January 1975 .

61. Zienkiewicz, O.C. , "The Finite Element Method" , McGraw-Hill Book Co., U.K., 1977 .

62. "Seismic Analysis and Design of Curved Steel Box-Girder Bridges", M. N. Abdel-Salam, Ph.D. Thesis, University of Maryland, College Park, MD, 1982.

# APPENDIX A

## TABLES

## SHOWING THE RESULTS OF THE SEISMIC ANALYSIS

## A.1 Single Span Curved Bridges

Table A1.1 Structure Period and Participation Factors For Straight and Modified End-Boundary-Conditions Models

| Mode | Straight | | | | | Modified End-Boundary-Conditions | | | | |
|---|---|---|---|---|---|---|---|---|---|---|
| | Period (sec) | Frequency (Hz) | Participation Factor X | Y | Z | Period (sec) | Frequency (Hz) | Participation Factor X | Y | Z |
| 1 | .265 | 3.77 | 0. | -3.93 | 0. | .265 | 3.77 | 0. | -3.93 | 0. |
| 2 | .066 | 15.09 | 0. | 0. | 0. | .066 | 15.09 | 0. | 0. | 0. |
| 3 | .033 | 29.93 | -3.96 | 0. | 0. | .033 | 29.95 | -3.95 | 0. | 0. |
| 4 | .029 | 33.95 | 0. | 1.23 | 0. | .029 | 33.95 | 0. | 1.23 | 0. |
| 5 | .019 | 52.77 | 0. | 0. | 3.66 | .019 | 52.77 | 0. | 0. | 3.66 |
| 6 | .017 | 60.26 | 0. | 0. | 0. | .017 | 60.26 | 0. | 0. | 0. |

Table A1.2 Maximum Actions and Displacements at the Attachments For Straight and Modified End-Boundary-Conditions Models, (k,ft)

| Location | Component | Straight | Mod. End-Bound.-Cond. |
|---|---|---|---|
| Abut. 1 | P1 | 124. | 124. |
| | V2 | 75. | 75. |
| | V3 | 75. | 75. |
| | M3 | 1,619. | 1,619. |
| Abut. 2 | V2 | 75. | 75. |
| | M3 | 1,619. | 1,619. |
| | DT | .00028 | .00028 |

Table A1.3 Maximum Stresses in Bridge Deck For Straight and Modified End-Boundary-Conditions Models, (ksi)

| Location | Material | Straight | Mod. End Bound Cond. |
|---|---|---|---|
| Abut. 1 | Steel | 0.27 | 0.27 |
| | Conc. | 0.05 | 0.05 |
| Span 1 | Steel | 2.13 | 2.13 |
| | Conc. | 0.15 | 0.15 |

Table A1.4 Structure Period and Participation Factors For 10-Element and 20-Element Models

| Mode | 10-Element | | | | | 20-Element | | | | |
|---|---|---|---|---|---|---|---|---|---|---|
| | Period (sec) | Frequency (Hz) | Participation Factor X | Y | Z | Period (sec) | Frequency (Hz) | Participation Factor X | Y | Z |
| 1 | .266 | 3.76 | 0. | -3.93 | 0. | .266 | 3.76 | 0. | -3.95 | 0. |
| 2 | .066 | 15.09 | 0. | 0. | 0. | .066 | 15.09 | 0. | 0. | 0. |
| 3 | .033 | 29.89 | -3.94 | 0. | 0.27 | .033 | 29.91 | -3.95 | 0. | 0.27 |
| 4 | .029 | 33.96 | 0. | 1.23 | 0. | .029 | 33.96 | 0. | 1.30 | 0. |
| 5 | .019 | 52.83 | 0.27 | 0. | 3.65 | .019 | 52.83 | 0.27 | 0. | 3.65 |
| 6 | .017 | 60.28 | 0. | 0. | 0. | .017 | 60.39 | 0. | 0. | 0. |
| 7 | .011 | 89.16 | -1.30 | 0. | 0.02 | .011 | 89.78 | -1.31 | 0. | 0.02 |
| 8 | .010 | 93.75 | 0. | -0.63 | 0. | .010 | 94.37 | 0. | -0.75 | 0. |
| 9 | .007 | 133.5 | 0. | 0. | 0. | .007 | 135.9 | 0. | 0. | 0. |
| 10 | .006 | 144.0 | -0.42 | 0. | 0. | .006 | 144.8 | 0.23 | 0. | 0. |

Table A1.5 Maximum Actions and Displacements at the Attachments For 10-Element and 20-Element Models, (k,ft)

| Location | Component | Excitation Direction | 10-Element | 20-Element |
|---|---|---|---|---|
| Abut. 1 | P1 | Long. (R.S.) | 7,461. | 7,485. |
| | V2 | Trans. (T.H.) | 99. | 99. |
| | M3 | Trans. (T.H.) | 2,126. | 2,126. |
| Abut. 2 | V2 | Trans. (T.H.) | 99. | 99. |
| | M3 | Trans. (T.H.) | 2,119. | 2,118. |
| | DT | Long. (R.S.) | .0172 | .0172 |

Table A1.6 Maximum Stresses in Bridge Deck for 10-Element and 20-Element Models, (ksi)

| Location | Material | Excitation Direction | 10-Element | 20-Element |
|---|---|---|---|---|
| Abut. 1 | Steel | Trans. (T.H.) | 0.31 | 0.31 |
| | Conc. | Trans. (T.H.) | 0.06 | 0.06 |
| Span 1 | Steel | Trans. (T.H.) | 0.20 | 0.20 |
| | Conc. | Trans. (T.H.) | 0.04 | 0.04 |

Table A1.7 Maximum Actions at the Attachments
For Different Time Steps (Δt), (k,ft)

| Location | Component | Long. Shock (T.H.) | | | Trans. Shock (T.H.) | | | Vert. Shock (T.H.) | | |
|---|---|---|---|---|---|---|---|---|---|---|
| | | .0100 | .0050 | .0025 | .0100 | .0050 | .0025 | .0100 | .0050 | .0025 |
| Abut. 1 | P1 | 215. | 201. | 199 | 6.8 | 6.6 | 6.2 | 0. | 0. | 0. |
| | V2 | 10.3 | 10.2 | 9.7 | 79. | 75. | 75. | 0. | 0. | 0. |
| | V3 | 0. | 0. | 0. | 0. | 0. | 0. | 212. | 217. | 217. |
| | M3 | 225. | 219. | 213. | 1,692. | 1,622. | 1,627. | 0. | 0. | 0. |
| Abut. 2 | V2 | 7.1 | 6.6 | 6.8 | 78. | 75. | 75. | 0. | 0. | 0. |
| | M3 | 84. | 78. | 81. | 1,684. | 1,614. | 1,620. | 0. | 0. | 0. |

Table A1.8 Maximum Stresses in Bridge Deck
For Different Time Steps (Δt), (ksi)

| Location | Material | Long. Shock (T.H.) | | | Trans. Shock (T.H.) | | | Vert. Shock (T.H.) | | |
|---|---|---|---|---|---|---|---|---|---|---|
| | | .0100 | .0050 | .0025 | .0100 | .0050 | .0025 | .0100 | .0050 | .0025 |
| Abut. 1 | Steel | 0.26 | 0.24 | 0.24 | 0.25 | 0.24 | 0.24 | 0. | 0. | 0. |
| | Conc. | 0.04 | 0.03 | 0.03 | 0.05 | 0.05 | 0.05 | 0. | 0. | 0. |
| Span 1 | Steel | 0.16 | 0.15 | 0.14 | 0.16 | 0.15 | 0.16 | 6.13 | 6.21 | 6.25 |
| | Conc. | 0.02 | 0.02 | 0.02 | 0.03 | 0.03 | 0.03 | 0.41 | 0.42 | 0.42 |

Table A1.9 Maximum Actions and Displacements at the Attachments Due to El Centro Earthquake (SOOE) Component,(R.S. & T.H. Analysis), (k,ft)

| Location | Component | Longitudinal Shock | | Transverse Shock | | Vertical Shock | |
|---|---|---|---|---|---|---|---|
| | | R. S. | T. H. | R. S. | T. H. | R. S. | T. H. |
| Abut. 1 | P1 | 7,461. | 199. | 688. | 6.2 | 0. | 0. |
| | V2 | 702. | 9.7 | 3,084. | 76. | 0. | 0. |
| | V3 | 0. | 0. | 0. | 0. | 425. | 217. |
| | M1 | 0. | 0. | 0. | 0. | 278. | 275. |
| | M3 | 14,340. | 213. | 66,490. | 1,627. | 0. | 0. |
| Abut. 2 | V2 | 441. | 6.8 | 3,100. | 75. | 0. | 0. |
| | M3 | 7,373. | 81. | 66,740. | 1,620. | 0. | 0. |
| | DT | .0172 | .0004 | .00120 | .00003 | 0. | 0. |
| Span 1 | M2 | 0. | 0. | 0. | 0. | 8,234. | 6,971. |

Table A1.10 Maximum Actions and Displacements at the Attachments Due to El Centro Earthquake (S90W) and (VERT) Components, (R. S. & T.H. Analysis), (k,ft)

| Location | Component | Longitudinal Shock (S90W) | | Vertical Shock (VERT) | |
|---|---|---|---|---|---|
| | | R. S. | T. H. | R. S. | T. H. |
| Abut. 1 | P1 | 7,461. | 132. | 0. | 0. |
| | V2 | 702. | 7.5 | 0. | 0. |
| | V3 | 0. | 0. | 374. | 75. |
| | M1 | 0. | 0. | 103. | 92. |
| | M3 | 14,340. | 160. | 0. | 0. |
| Abut. 2 | V2 | 441. | 4.7 | 0. | 0. |
| | M3 | 7,373. | 55. | 0. | 0. |
| | DT | .0172 | .0003 | 0. | 0. |
| Span 1 | M2 | 0. | 0. | 5,003. | 2,337. |

Table A1.11 Maximum Actions at the Attachments Due to El Centro Earthquake Different Components, (k,ft)

| Location | Component | Long.Shock(S00E) | | Trans.Shock(S90W) | | Vert.Shock(VERT) | | 3-Direction Shock | |
|---|---|---|---|---|---|---|---|---|---|
| | | Response | Time(sec) | Response | Time(sec) | Response | Time(sec) | Response | Time(sec) |
| Abut. 1 | P1 | 199. | 2.122 | 4. | 4.150 | 0. | 0.985 | 200. | 2.122 |
| | V2 | 9.7 | 2.450 | 41. | 1.905 | 0. | 0.985 | 42. | 2.865 |
| | V3 | 0. | 2.460 | 0. | 4.145 | 75. | 3.365 | 75. | 3.365 |
| | M1 | 0. | 2.460 | 0. | 4.145 | 92. | 3.372 | 92. | 3.372 |
| | M3 | 213. | 2.450 | 883. | 1.905 | 0. | 0.985 | 900. | 2.865 |
| Abut. 2 | V2 | 6.8 | 2.450 | 41. | 1.905 | 0. | 0.985 | 41. | 2.865 |
| | M3 | 81. | 2.450 | 881. | 1.905 | 0. | 0.985 | 875. | 1.905 |
| Span 1 | M2 | 0. | 2.440 | 0. | 4.145 | 2,337. | 3.375 | 2,337. | 3.375 |

Table A1.12 Maximum Stresses in Bridge Deck Due to El Centro Earthquake Different Components, (ksi)

| Location | Material | Long.Shock(S00E) | | Trans. Shock(S90W) | | Vert.Shock(VERT) | | 3-Direction Shock | |
|---|---|---|---|---|---|---|---|---|---|
| | | Stress | Time(sec) | Stress | Time(sec) | Stress | Time(sec) | Stress | Time(sec) |
| Abut. 1 | Steel | 0.24 | 2.122 | 0.13 | 1.905 | 0. | 0.985 | 0.29 | 2.447 |
| | Conc. | 0.03 | 2.122 | 0.03 | 1.905 | 0. | 0.985 | 0.04 | 2.447 |
| Span 1 | Steel | 0.14 | 2.450 | 0.08 | 1.905 | 2.10 | 3.375 | 2.10 | 3.372 |
| | Conc. | 0.02 | 2.450 | 0.02 | 1.905 | 0.14 | 3.375 | 0.15 | 3.377 |

Table A1.13 Maximum Actions at the Attachments Due to El Centro Earthquake Different Components, (k,ft)

| Location | Component | Long. Shock(S90W) | | Trans. Shock(S00E) | | Vert. Shock(VERT) | | 3-Direction Shock | |
|---|---|---|---|---|---|---|---|---|---|
| | | Response | Time(sec) | Response | Time(sec) | Response | Time(sec) | Response | Time(sec) |
| Abut. 1 | P1 | 132. | 4.147 | 6.2 | 3.347 | 0. | 0.985 | 133. | 4.147 |
| | V2 | 7.5 | 4.147 | 76. | 2.122 | 0. | 0.985 | 77. | 2.122 |
| | V3 | 0. | 1.905 | 0. | 2.122 | 75. | 3.365 | 75. | 3.365 |
| | M1 | 0. | 4.160 | 0. | 2.122 | 92. | 3.372 | 92. | 3.372 |
| | M3 | 160. | 4.147 | 1,627. | 2.122 | 0. | 0.985 | 1,662. | 2.122 |
| Abut. 2 | V2 | 4.7 | 4.150 | 75. | 2.122 | 0. | 0.985 | 77. | 2.122 |
| | M3 | 55. | 4.150 | 1,620. | 2.122 | 0. | 0.985 | 1,632. | 2.122 |
| Span 1 | M2 | 0. | 4.145 | 0. | 2.447 | 2,337. | 3.375 | 2,337. | 3.375 |

Table A1.14 Maximum Stresses in Bridge Deck Due to El Centro Earthquake Different Components, (ksi)

| Location | Material | Long.Shock(S90W) | | Trans.Shock(S00E) | | Vert. Shock(VERT) | | 3-Direction Shock | |
|---|---|---|---|---|---|---|---|---|---|
| | | Stress | Time(sec) | Stress | Time(sec) | Stress | Time(sec) | Stress | Time(sec) |
| Abut. 1 | Steel | 0.17 | 4.147 | 0.24 | 2.122 | 0. | 0.985 | 0.29 | 2.087 |
| | Conc. | 0.02 | 4.147 | 0.05 | 2.122 | 0. | 0.985 | 0.05 | 2.122 |
| Span 1 | Steel | 0.10 | 4.147 | 0.16 | 2.122 | 2.10 | 3.375 | 2.14 | 3.375 |
| | Conc. | 0.01 | 4.147 | 0.03 | 2.122 | 0.14 | 3.375 | 0.15 | 3.367 |

Table A1.15 Maximum Actions at the Attachments For Different Damping Ratios, (k,ft)

| Location | Component | 2% | 5% | 10% |
|---|---|---|---|---|
| Abut. 1 | P1 | 136. | 133. | 127. |
| | V2 | 78. | 77. | 76. |
| | V3 | 101. | 75. | 57. |
| | M1 | 125. | 92. | 69. |
| | M3 | 1,670. | 1,662. | 1,657. |
| Abut. 2 | V2 | 77. | 77. | 76. |
| | M3 | 1,636. | 1,632. | 1,629. |
| Span 1 | M2 | 3,201. | 2,337. | 1,745. |

Table A1.16 Maximum Stresses in Bridge Deck For Different Damping Ratios, (ksi)

| Location | Material | 2% | 5% | 10% |
|---|---|---|---|---|
| Abut. 1 | Steel | 0.29 | 0.29 | 0.28 |
| | Conc. | 0.05 | 0.05 | 0.05 |
| Span 1 | Steel | 2.91 | 2.14 | 1.60 |
| | Conc. | 0.20 | 0.15 | 0.11 |

Table A1.17 Structure Period For Composite and Non-Composite Deck Models

| Mode | Composite Deck | | | Non-Composite Deck | | |
|---|---|---|---|---|---|---|
| | Period (sec) | Frequency (Hz) | Mode Shape Direction | Period (sec) | Frequency (Hz) | Mode Shape Direction |
| 1 | .266 | 3.76 | Y | .459 | 2.18 | Y |
| 2 | .066 | 15.09 | Y | .114 | 8.75 | Y |
| 3 | .033 | 29.89 | X | .051 | 19.69 | Y |
| 4 | .029 | 33.96 | Y | .050 | 20.06 | X |
| 5 | .019 | 52.83 | Z | .029 | 34.59 | Z |
| 6 | .017 | 60.28 | Y | .028 | 34.95 | Y |
| 7 | .011 | 89.16 | X | .018 | 54.36 | Y |
| 8 | .010 | 93.75 | Y | .017 | 59.83 | X |
| 9 | .007 | 133.50 | Y | .013 | 77.38 | Y |
| 10 | .006 | 144.00 | Z & X | .011 | 94.85 | Z & X |

Table A1.18 Maximum Actions at the Attachments For Composite and Non-Composite Deck Models, (k,ft)

| Location | Component | Composite Deck | Non-Composite Deck |
|---|---|---|---|
| Abut. 1 | P1 | 133. | 140. |
| | V2 | 77. | 80. |
| | V3 | 75. | 40. |
| | M1 | 92. | 48. |
| | M3 | 1,662. | 1,718. |
| Abut. 2 | V2 | 77. | 79. |
| | M3 | 1,632. | 1,672. |
| Span 1 | M2 | 2,337. | 1,255. |

Table A1.19 Maximum Stresses in Bridge Deck For Composite and Non-Composite Deck Models, (ksi)

| Location | Material | Composite Deck | Non-Composite Deck |
|---|---|---|---|
| Abut. 1 | Steel | 0.29 | 0.71 |
| | Conc. | 0.05 | 0. |
| Span 1 | Steel | 2.14 | 2.76 |
| | Conc. | 0.15 | 0. |

Table A1.20 Structure Period:
Finite Element and Exact Solutions

| Mode | Finite Element | | | Exact | | |
|---|---|---|---|---|---|---|
| | Period (sec) | Frequency (Hz) | Mode Shape Direction | Period (sec) | Frequency (Hz) | Mode Shape Direction |
| 1 | .265 | 3.77 | Y | .265 | 3.77 | Y |
| 2 | .066 | 15.09 | Y | .066 | 15.09 | Y |
| 3 | .033 | 29.95 | X | | | |
| 4 | .029 | 33.95 | Y | .029 | 33.95 | Y |
| 5 | .019 | 52.77 | Z | .019 | 52.77 | Z |
| 6 | .017 | 60.26 | Y | .017 | 60.36 | Y |

Table A1.21 Maximum Stresses in Bridge Deck
Due to Dead Load, (ksi)

| Location | Material | Stress |
|---|---|---|
| Span 1 | Steel | 7.1 |
| | Conc. | 0.44 |

## A.2 2-Span Curved Bridges

Table A2.1 Structure Period and Participation Factors For 2-Column and 3-Column Models

| Mode | 2-Column | | | | | 3-Column | | | | |
|---|---|---|---|---|---|---|---|---|---|---|
| | Period (sec) | Frequency (Hz) | Participation Factor X | Y | Z | Period (sec) | Frequency (Hz) | Participation Factor X | Y | Z |
| 1 | .265 | 3.78 | 0. | 0. | 0. | .265 | 3.78 | 0. | 0. | 0. |
| 2 | .188 | 5.33 | 0. | -5.76 | 0. | .170 | 5.87 | 0. | -5.44 | 0. |
| 3 | .079 | 12.64 | 0. | 1.21 | 0. | .074 | 13.49 | 0. | 0. | 5.44 |
| 4 | .074 | 13.45 | 0. | 0. | 5.44 | .073 | 13.59 | 0. | 0. | 0. |
| 5 | .069 | 14.52 | 0. | 0. | 0. | .068 | 14.70 | 5.86 | 0. | 0. |
| 6 | .068 | 14.70 | 5.86 | 0. | 0. | .066 | 15.14 | -0.09 | 0. | 0. |
| 7 | .066 | 15.14 | -0.09 | 0. | 0. | .059 | 16.97 | 0. | 1.40 | 0. |
| 8 | .042 | 23.62 | -0.13 | 0. | 0. | .042 | 23.71 | -1.58 | 0. | 0. |
| 9 | .040 | 24.94 | 0. | 1.50 | 0. | .034 | 29.78 | 0. | -2.36 | 0. |
| 10 | .029 | 34.01 | 0. | 0. | 0. | .029 | 34.01 | 0. | 0. | 0. |

Table A2.2 Maximum Actions and Displacements at the Attachments For 2-Column and 3-Column Models, (k,ft)

| Location | Component | Excitation Direction | 2-Column | 3-Column |
|---|---|---|---|---|
| Abut. 1 | P1 | Long. (R.S.) | 511. | 510. |
| | V2 | Trans. (T.H.) | 176. | 175. |
| | M3 | Trans. (T.H.) | 7472. | 7409. |
| Bent 2 | V2 | Trans. (T.H.) | 11. | 13. |
| Abut. 3 | V2 | Trans. (T.H.) | 176. | 175. |
| | M3 | Trans. (T.H.) | 7472. | 7409. |
| | DT | Long. (R.S.) | .00225 | .00225 |

Table A2.3 Maximum Stresses in Bridge Deck and Columns For 2-Column and 3-Column Models, (ksi)

| Location | Material | Excitation Direction | 2-Column | 3-Column |
|---|---|---|---|---|
| Deck: | | | | |
| Abut. 1 | Steel | Trans. (T.H.) | 1.10 | 1.09 |
| | Conc. | Trans. (T.H.) | 0.22 | 0.22 |
| Span 1 | Steel | Trans. (T.H.) | 0.13 | 0.13 |
| | Conc. | Trans. (T.H.) | 0.03 | 0.03 |
| Bent 2 | Steel | Trans. (T.H.) | 0.62 | 0.62 |
| | Conc. | Trans. (T.H.) | 0.12 | 0.12 |
| Column Base: | | | | |
| Bent 2 | Conc. | Trans. (T.H.) | 0.32 | 0.27 |

Table A2.4 Structure Period and Participation Factors For the Modified End-Boundary-Conditions Model

| Mode | Period (sec) | Frequency (Hz) | Participation Factor | | |
|---|---|---|---|---|---|
| | | | X | Y | Z |
| 1 | .265 | 3.78 | 0. | 0. | 0. |
| 2 | .188 | 5.33 | 0. | -5.76 | 0. |
| 3 | .079 | 12.64 | 0. | 1.21 | 0. |
| 4 | .074 | 13.45 | 0. | 0. | 5.44 |
| 5 | .069 | 14.52 | 0. | 0. | 0. |
| 6 | .068 | 14.71 | 5.86 | 0. | 0. |
| 7 | .066 | 15.14 | -0.09 | 0. | 0. |
| 8 | .042 | 23.62 | 0.13 | 0. | 0. |
| 9 | .040 | 24.94 | 0. | 1.50 | 0. |
| 10 | .029 | 34.01 | 0. | 0. | 0. |

Table A2.5 Maximum Actions and Displacements at the Attachments For the Modified End-Boundary-Conditions Model , (k,ft)

| Location | Component | Excitation Direction | Response |
|---|---|---|---|
| Abut. 1 | P1 | Long. (R.S.) | 511. |
| | V2 | Trans. (T.H.) | 176. |
| | M3 | Trans. (T.H.) | 7472. |
| Bent 2 | V2 | Trans. (T.H.) | 11. |
| Abut. 3 | V2 | Trans. (T.H.) | 176. |
| | M3 | Trans. (T.H.) | 7472. |
| | DT | Long. (R.S.) | .00224 |

Table A2.6 Maximum Stresses in Bridge Deck and Columns For the Modified End-Boundary-Conditions Model, (ksi)

| Location | Material | Excitation Direction | Stress |
|---|---|---|---|
| Deck: | | | |
| Abut. 1 | Steel | Trans. (T.H.) | 1.10 |
| | Conc. | Trans. (T.H.) | 0.22 |
| Span 1 | Steel | Trans. (T.H.) | 0.13 |
| | Conc. | Trans. (T.H.) | 0.03 |
| Bent 2 | Steel | Trans. (T.H.) | 0.62 |
| | Conc. | Trans. (T.H.) | 0.12 |
| Column Base: | | | |
| Bent 2 | Conc. | Trans. (T.H.) | 0.32 |

Table A2.7 Structure Period and Participation Factors For 6-Element and 10-Element Models

| Mode | 6-Element | | | | | 10-Element | | | | |
|---|---|---|---|---|---|---|---|---|---|---|
| | Period (sec) | Frequency (Hz) | Participation Factor X | Y | Z | Period (sec) | Frequency (Hz) | Participation Factor X | Y | Z |
| 1 | .265 | 3.77 | 0. | 0. | 0. | .265 | 3.77 | 0. | 0. | 0. |
| 2 | .188 | 5.33 | 0. | 5.76 | 0. | .188 | 5.33 | 0. | 5.80 | 0. |
| 3 | .079 | 12.64 | 0.01 | 1.21 | -0.01 | .079 | 12.64 | -0.01 | -1.18 | 0.02 |
| 4 | .078 | 12.86 | 2.90 | 0. | -4.80 | .078 | 12.85 | 2.89 | 0. | -4.80 |
| 5 | .069 | 14.52 | 0. | 0. | 0. | .069 | 14.52 | 0. | 0. | 0. |
| 6 | .066 | 15.15 | 0.19 | 0. | 0.10 | .066 | 15.25 | 0.45 | 0. | 0.23 |
| 7 | .065 | 15.33 | -5.07 | 0. | -2.58 | .065 | 15.32 | -5.06 | 0. | -2.56 |
| 8 | .042 | 23.63 | -0.15 | 0. | -0.11 | .042 | 23.63 | 0.15 | 0. | 0.11 |
| 9 | .040 | 24.97 | 0. | -1.50 | 0. | .040 | 24.78 | 0. | -1.59 | 0. |
| 10 | .029 | 34.06 | 0. | 0. | 0. | .029 | 34.26 | 0. | 0. | 0. |

Table A2.8 Maximum Actions and Displacements at the Attachments For 6-Element and 10-Element Models, (k,ft)

| Location | Component | Excitation Direction | 6-Element | 10-Element |
|---|---|---|---|---|
| Abut. 1 | P1 | Long. (R.S.) | 438. | 438. |
| | V2 | Trans. (T.H.) | 175. | 175. |
| | M3 | Trans. (T.H.) | 7373. | 7388. |
| Bent 2 | V2 | Trans. (T.H.) | 12. | 12. |
| Abut. 3 | V2 | Trans. (T.H.) | 172. | 172. |
| | M3 | Trans. (T.H.) | 7230. | 7244. |
| | DT | Long. (R.S.) | .00185 | .00185 |

Table A2.9 Maximum Stresses in Bridge Deck and Columns For 6-Element and 10-Element Models, (ksi)

| Location | Material | Excitation Direction | 6-Element | 10-Element |
|---|---|---|---|---|
| Deck: | | | | |
| Abut. 1 | Steel | Trans. (T.H.) | 1.14 | 1.14 |
| | Conc. | Trans. (T.H.) | 0.22 | 0.22 |
| Span 1 | Steel | Trans. (T.H.) | 0.19 | 0.19 |
| | Conc. | Trans. (T.H.) | 0.03 | 0.03 |
| Bent 2 | Steel | Trans. (T.H.) | 0.66 | 0.66 |
| | Conc. | Trans. (T.H.) | 0.12 | 0.12 |
| Column Base: | | | | |
| Bent 2 | Conc. | Trans. (T.H.) | 0.32 | 0.32 |

Table A2.10 Structure Period and Participation Factors
(The Lowest Fifteen Frequencies)

| Mode | Period (sec) | Frequency (Hz) | Participation Factor | | |
|---|---|---|---|---|---|
| | | | X | Y | Z |
| 1 | .265 | 3.77 | 0. | 0. | 0. |
| 2 | .188 | 5.33 | 0. | 5.76 | 0. |
| 3 | .079 | 12.64 | 0.01 | 1.21 | -0.01 |
| 4 | .078 | 12.86 | 2.90 | 0. | -4.80 |
| 5 | .069 | 14.52 | 0. | 0. | 0. |
| 6 | .066 | 15.15 | 0.19 | 0. | 0.10 |
| 7 | .065 | 15.33 | -5.07 | 0. | -2.58 |
| 8 | .042 | 23.63 | -0.15 | 0. | -0.11 |
| 9 | .040 | 24.97 | 0. | -1.50 | 0. |
| 10 | .029 | 34.06 | 0. | 0. | 0. |
| 11 | .028 | 36.27 | -0.48 | 0. | -0.01 |
| 12 | .022 | 45.29 | -1.70 | 0. | -0.16 |
| 13 | .021 | 45.85 | 0. | 0.37 | 0. |
| 14 | .017 | 59.10 | 0. | 0. | 0. |
| 15 | .016 | 64.12 | 0.40 | 0. | -0.02 |

Table A2.11 Maximum Actions at the Attachments and Column Base, (k,ft) (10 and 15 Frequencies)

| Location | Component | Long. Shock (T.H.) | | Trans. Shock (T.H.) | |
|---|---|---|---|---|---|
| | | 10 | 15 | 10 | 15 |
| Abut. 1 | P1 | 522. | 542. | 79. | 78. |
| | V2 | 57. | 63. | 216. | 216. |
| | M3 | 2055. | 2140. | 9155. | 9155. |
| Bent 2 | V2 | 8. | 8. | 14. | 14. |
| Abut. 3 | V2 | 42. | 41. | 215. | 215. |
| | M3 | 1690. | 1660. | 9050. | 9048. |
| Column Base: | | | | | |
| Bent 2 | M2 | 99. | 99. | 18. | 18. |
| | M3 | 45. | 45. | 221. | 221. |

Table A2.12 Maximum Stresses in Bridge Deck and Columns, (ksi) (10 and 15 Frequencies)

| Location | Material | Long. Shock (T.H.) | | Trans. Shock (T.H.) | |
|---|---|---|---|---|---|
| | | 10 | 15 | 10 | 15 |
| Deck: | | | | | |
| Abut. 1 | Steel | 0.83 | 0.87 | 1.37 | 1.37 |
| | Conc. | 0.12 | 0.13 | 0.27 | 0.27 |
| Span 1 | Steel | 0.57 | 0.59 | 0.20 | 0.20 |
| | Conc. | 0.07 | 0.08 | 0.04 | 0.04 |
| Bent 2 | Steel | 0.46 | 0.45 | 0.80 | 0.80 |
| | Conc. | 0.06 | 0.06 | 0.15 | 0.15 |
| Column Base: | | | | | |
| Bent 2 | Conc. | 0.17 | 0.17 | 0.40 | 0.40 |

Table A2.13 Maximum Actions at the Attachments
For Different Time Steps ($\Delta t$), (k, ft)

| Location | Component | Long. Shock (T.H.) | | |
|---|---|---|---|---|
| | | .0100 | .0050 | .0025 |
| Abut. 1 | P1 | 498. | 525. | 553. |
| | V2 | 83. | 85. | 91. |
| | M3 | 3072. | 3467. | 3702. |
| Bent 2 | V2 | 9. | 9. | 9. |
| Abut. 3 | V2 | 59. | 78. | 84. |
| | M3 | 2343. | 3250. | 3525. |

Table A2.14 Maximum Stresses in Bridge Deck and Columns
For Different Time Steps ($\Delta t$), (ksi)

| Location | Material | Long. Shock (T.H.) | | |
|---|---|---|---|---|
| | | .0100 | .0050 | .0025 |
| Deck: | | | | |
| Abut. 1 | Steel | 0.89 | 0.93 | 0.88 |
| | Conc. | 0.14 | 0.14 | 0.13 |
| Span 1 | Steel | 0.55 | 0.58 | 0.60 |
| | Conc. | 0.07 | 0.08 | 0.08 |
| Bent 2 | Steel | 0.50 | 0.52 | 0.48 |
| | Conc. | 0.08 | 0.07 | 0.07 |
| Column Base: | | | | |
| Bent 2 | Conc. | 0.18 | 0.19 | 0.19 |

Table A2.15 Maximum Actions at the Attachments For 10 and 15 sec. Shock Durations, (k,ft)

| Location | Component | Longitudinal Shock (S00E) | | Longitudinal Shock (S90W) | |
|---|---|---|---|---|---|
| | | 10 sec. | 15 sec. | 10 sec. | 15 sec. |
| Abut. 1 | P1 | 542. | 542. | 295. | 295. |
| | V2 | 63. | 63. | 41. | 41. |
| | M3 | 2140. | 2140. | 1533. | 1533. |
| Bent 2 | V2 | 8. | 8. | 5. | 5. |
| Abut. 3 | V2 | 41. | 41. | 28. | 28. |
| | M3 | 1660. | 1660. | 1195. | 1195. |

Table A2.16 Maximum Stresses in Bridge Deck and Columns For 10 and 15 sec. Shock Durations, (ksi)

| Location | Material | Longitudinal Shock (S00E) | | Longitudinal Shock (S90W) | |
|---|---|---|---|---|---|
| | | 10 sec. | 15 sec. | 10 sec. | 15 sec. |
| Deck: | | | | | |
| Abut. 1 | Steel | 0.87 | 0.87 | 0.49 | 0.49 |
| | Conc. | 0.13 | 0.13 | 0.08 | 0.08 |
| Span 1 | Steel | 0.59 | 0.59 | 0.32 | 0.32 |
| | Conc. | 0.08 | 0.08 | 0.04 | 0.04 |
| Bent 2 | Steel | 0.45 | 0.45 | 0.27 | 0.27 |
| | Conc. | 0.06 | 0.06 | 0.04 | 0.04 |
| Column Base: | | | | | |
| Bent 2 | Conc. | 0.17 | 0.17 | 0.10 | 0.10 |

Table A2.17 Maximum Actions and Displacements at the Attachments and Column Base Due to El Centro Earthquake (S00E) Component, (R.S. & T.H. Analysis), (k,ft)

| Location | Component | Longitudinal Shock | | Transverse Shock | | Vertical Shock | |
|---|---|---|---|---|---|---|---|
| | | R. S. | T. H. | R. S. | T. H. | R. S. | T. H. |
| Abut. 1 | P1 | 1409. | 514. | 337. | 122. | 0.2 | 0. |
| | V2 | 390. | 84. | 194. | 222. | 0.2 | 0. |
| | V3 | 3. | 0. | 1. | 0. | 335. | 121. |
| | M1 | 3. | 1. | 4. | 5. | 122. | 103. |
| | M3 | 11000. | 3083. | 8041. | 9372. | 9. | 1. |
| Bent 2 | V2 | 17. | 9. | 14. | 15. | 0.2 | 0. |
| | M2 (Deck) | 9. | 2. | 3. | 1. | 7174. | 4903. |
| Abut. 3 | V2 | 402. | 59. | 184. | 219. | 0.2 | 0. |
| | M3 | 11360. | 2337. | 7686. | 9222. | 9. | 1. |
| | DT | .0029 | .0023 | .0017 | .0010 | 0. | 0. |
| Column Base: | | | | | | | |
| Bent 2 | P1 | 8. | 4. | 12. | 13. | 327. | 227. |
| | M2 | 127. | 95. | 63. | 26. | 0. | 0. |
| | M3 | 140. | 66. | 191. | 226. | 303. | 209. |

Table A2.18 Maximum Actions and Displacements at the Attachments Due To El Centro Earthquake (S90W) and (VERT) Components, (R.S. & T.H. Analysis),(k,ft)

| Location | Component | Longitudinal Shock (S90W) | | Vertical Shock (VERT) | |
|---|---|---|---|---|---|
| | | R. S. | T. H. | R. S. | T. H. |
| Abut. 1 | P1 | 1420. | 295. | 0.3 | 0. |
| | V2 | 374. | 41. | 0.2 | 0. |
| | V3 | 2. | 0. | 317. | 55. |
| | M1 | 2. | 0.7 | 75. | 49. |
| | M3 | 9897. | 1533. | 10. | 1. |
| Bent 2 | V2 | 16. | 5. | 0.2 | 0. |
| | V3 (Deck) | 2. | 0. | 195. | 101. |
| | M2 (Deck) | 8. | 1. | 5477. | 2430. |
| Abut. 3 | V2 | 384. | 28. | 0.2 | 0. |
| | M3 | 10210. | 1195. | 9. | 1. |
| | DT | .0025 | .0013 | 0. | 0. |
| Column Base: | | | | | |
| Bent 2 | P1 | 4. | 2. | 250. | 108. |
| | M2 | 105. | 54. | 0. | 0. |
| | M3 | 75. | 33. | 232. | 100. |

Table A2.19 Maximum Actions and Displacements at the Attachments and Column Base Due To El Centro Earthquake Different Components, (k,ft)

| Location | Component | Longitudinal Shock (S00E) | | Transverse Shock (S90W) | | Vertical Shock (VERT) | | 3-Direction Shock | |
|---|---|---|---|---|---|---|---|---|---|
| | | Response | Time (sec) | Response | Time (sec) | Response | Time (sec) | Response | Time (sec) |
| Abut. 1 | P1 | 514. | 2.46 | 58. | 4.30 | 0. | 1.17 | 538. | 2.46 |
| | V2 | 84. | 2.47 | 123. | 4.17 | 0. | 1.25 | 141. | 4.16 |
| | V3 | 0. | 2.45 | 0. | 4.67 | 55. | 0.88 | 55. | 0.88 |
| | M1 | 1. | 4.98 | 3. | 4.17 | 49. | 0.89 | 50. | 0.89 |
| | M3 | 3083. | 2.47 | 5186. | 4.17 | 1. | 1.25 | 5910. | 4.16 |
| Bent 2 | V2 | 9. | 2.47 | 8. | 4.17 | 0. | 1.00 | 11. | 2.46 |
| | V3 (Deck) | 0. | 2.56 | 0. | 4.67 | 101. | 0.89 | 101. | 0.89 |
| | M2 (Deck) | 2. | 2.46 | 1. | 4.16 | 2430. | 0.89 | 2430. | 0.89 |
| Abut. 3 | V2 | 59. | 2.47 | 121. | 4.17 | 0. | 1.25 | 136. | 4.16 |
| | M3 | 2337. | 2.47 | 5083. | 4.17 | 1. | 1.25 | 5750. | 4.16 |
| | DT | .0023 | 2.46 | .0005 | 4.17 | 0. | 1.26 | .0025 | 2.46 |
| Column Base; | | | | | | | | | |
| Bent 2 | P1 | 4. | 2.47 | 7. | 4.17 | 108. | 0.88 | 108. | 0.88 |
| | M2 | 95. | 2.46 | 14. | 4.30 | 0. | 1.26 | 101. | 2.46 |
| | M3 | 66. | 2.47 | 125. | 4.17 | 100. | 0.88 | 175. | 4.16 |

Table A2.20 Maximum Stresses in Bridge Deck and Columns
Due to El Centro Earthquake Different Components, (ksi)

| Location | Material | Longitudinal Shock (SOOE) | | Transverse Shock (S90W) | | Vertical Shock (VERT) | | 3-Direction Shock | |
|---|---|---|---|---|---|---|---|---|---|
| | | Stress | Time (sec) | Stress | Time (sec) | Stress | Time (sec) | Stress | Time (sec) |
| Abut. 1 | Steel | 0.90 | 2.46 | 0.80 | 4.17 | 0. | 1.26 | 1.17 | 2.46 |
| | Conc. | 0.15 | 2.47 | 0.16 | 4.17 | 0. | 1.25 | 0.19 | 2.46 |
| Span 1 | Steel | 0.57 | 2.46 | 0.14 | 4.17 | 1.26 | 0.89 | 1.34 | 0.89 |
| | Conc. | 0.07 | 2.46 | 0.02 | 4.17 | 0.09 | 0.89 | 0.10 | 3.36 |
| Bent 2 | Steel | 0.50 | 2.47 | 0.47 | 4.17 | 1.75 | 0.89 | 1.74 | 0.89 |
| | Conc. | 0.08 | 2.47 | 0.09 | 4.17 | 0.13 | 0.89 | 0.15 | 0.89 |
| Column Base: | | | | | | | | | |
| Bent 2 | Conc. | 0.18 | 2.47 | 0.22 | 4.17 | 0.26 | 0.88 | 0.34 | 4.16 |

Table A2.21 Maximum Actions and Displacements at the Attachments and Column Base Due to El Centro Earthquake Different Components, (k,ft)

| Location | Component | Longitudinal Shock (S90W) | | Transverse Shock (S00E) | | Vertical Shock (VERT) | | 3-Direction Shock | |
|---|---|---|---|---|---|---|---|---|---|
| | | Response | Time (sec) | Response | Time (sec) | Response | Time (sec) | Response | Time (sec) |
| Abut. 1 | P1 | 295. | 4.16 | 122. | 2.52 | 0. | 1.17 | 335. | 4.16 |
| | V2 | 41. | 4.30 | 222. | 2.46 | 0. | 1.25 | 241. | 2.46 |
| | V3 | 0. | 4.22 | 0. | 2.65 | 55. | 0.88 | 55. | 0.88 |
| | M1 | 0.7 | 4.30 | 5. | 2.46 | 49. | 0.89 | 49. | 0.89 |
| | M3 | 1533. | 4.30 | 9372. | 2.46 | 1. | 1.25 | 10063. | 2.46 |
| Bent 2 | V2 | 5. | 4.17 | 15. | 2.47 | 0. | 1.00 | 16. | 2.46 |
| | V3 (Deck) | 0. | 1.02 | 0. | 2.66 | 101. | 0.89 | 101. | 0.89 |
| | M2 (Deck) | 1. | 4.16 | 1. | 2.46 | 2430. | 0.89 | 2430. | 0.89 |
| Abut. 3 | V2 | 28. | 4.30 | 219. | 2.46 | 0. | 1.25 | 231. | 2.46 |
| | M3 | 1195. | 4.30 | 9222. | 2.46 | 1. | 1.25 | 9726. | 2.46 |
| | DT | .0013 | 4.16 | .0010 | 2.47 | 0. | 1.26 | .0015 | 4.16 |
| Column Base: Bent 2 | P1 | 2. | 4.30 | 13. | 2.46 | 108. | 0.88 | 110. | 0.88 |
| | M2 | 54. | 4.16 | 26. | 4.98 | 0. | 1.26 | 63. | 4.16 |
| | M3 | 33. | 4.30 | 226. | 2.46 | 100. | 0.88 | 256. | 2.46 |

Table A2.22 Maximum Stresses in Bridge Deck and Columns Due to El Centro Earthquake Different Components, (ksi)

| Location | Material | Longitudinal Shock (S90W) | | Transverse Shock (S00E) | | Vertical Shock (VERT) | | 3-Direction Shock | |
|---|---|---|---|---|---|---|---|---|---|
| | | Stress | Time (sec) | Stress | Time (sec) | Stress | Time (sec) | Stress | Time (sec) |
| Abut. 1 | Steel | 0.49 | 4.17 | 1.46 | 2.47 | 0. | 1.26 | 1.61 | 2.46 |
| | Conc. | 0.08 | 4.17 | 0.28 | 2.47 | 0. | 1.25 | 0.31 | 2.46 |
| Span 1 | Steel | 0.32 | 4.16 | 0.28 | 2.47 | 1.26 | 0.89 | 1.24 | 0.89 |
| | Conc. | 0.04 | 4.16 | 0.05 | 2.47 | 0.09 | 0.89 | 0.09 | 0.89 |
| Bent 2 | Steel | 0.27 | 4.17 | 0.85 | 2.47 | 1.75 | 0.89 | 1.83 | 0.89 |
| | Conc. | 0.04 | 4.17 | 0.16 | 2.47 | 0.13 | 0.89 | 0.18 | 2.21 |
| Column Base: | | | | | | | | | |
| Bent 2 | Conc. | 0.10 | 4.17 | 0.40 | 2.46 | 0.26 | 0.88 | 0.47 | 2.46 |

Table A2.23 Maximum Actions and Displacements at the Attachments and Column Base for Different Damping Ratios, (k,ft)

| Location | Component | 2% | 5% | 10% |
|---|---|---|---|---|
| Abut. 1 | P1 | 344. | 335. | 309. |
| | V2 | 268. | 241. | 210. |
| | V3 | 71. | 55. | 41. |
| | M1 | 62. | 49. | 37. |
| | M3 | 11164. | 10063. | 8798. |
| Bent 2 | V2 | 18. | 16. | 14. |
| | M2 (Deck) | 3020. | 2430. | 1875. |
| Abut. 3 | V2 | 256. | 231. | 202. |
| | M3 | 10761. | 9726. | 8510. |
| | DT | .0016 | .0015 | .0014 |
| Column Base: | | | | |
| Bent 2 | P1 | 138. | 110. | 85. |
| | M2 | 64. | 63. | 57. |
| | M3 | 305. | 256. | 218. |

Table A2.24 Maximum Stresses in Bridge Deck and Columns For Different Damping Ratios, (ksi)

| Location | Material | 2% | 5% | 10% |
|---|---|---|---|---|
| Deck: | | | | |
| Abut. 1 | Steel | 1.80 | 1.61 | 1.40 |
| | Conc. | 0.35 | 0.31 | 0.27 |
| Span 1 | Steel | 1.55 | 1.24 | 1.03 |
| | Conc. | 0.11 | 0.09 | 0.08 |
| Bent 2 | Steel | 2.25 | 1.83 | 1.43 |
| | Conc. | 0.22 | 0.18 | 0.16 |
| Column Base: | | | | |
| Bent 2 | Conc. | 0.58 | 0.47 | 0.39 |

Table A2.25 Structure Period For Composite Deck, Non-Composite Deck, Rotational Inertia, and Long Columns Models

| Mode | Composite Deck | | | Non-Composite Deck | | | Rotational Inertia | | | Long Columns | | |
|---|---|---|---|---|---|---|---|---|---|---|---|---|
| | Period (sec) | Frequency (Hz) | Mode Shape Direction | Period (sec) | Frequency (Hz) | Mode Shape Direction | Period (sec) | Frequency (Hz) | Mode Shape Direction | Period (sec) | Frequency (Hz) | Mode Shape Direction |
| 1 | .265 | 3.77 | Y | .457 | 2.19 | Y | .266 | 3.76 | Y | .265 | 3.77 | Y |
| 2 | .188 | 5.33 | Y | .286 | 3.50 | Y | .188 | 5.31 | Y | .175 | 5.76 | Y |
| 3 | .079 | 12.64 | Y | .113 | 8.87 | Y | .164 | 6.11 | X[Rot.] | .125 | 7.99 | X(Col.) |
| 4 | .078 | 12.86 | Z&X | .109 | 9.18 | Z&X | .149 | 6.73 | X[Rot.] | .103 | 9.74 | X(Col.) |
| 5 | .069 | 14.52 | X(Col.) | .104 | 9.60 | Y | .084 | 11.87 | X[Rot.] | .086 | 11.65 | Z |
| 6 | .066 | 15.15 | Y | .094 | 10.66 | X&Z | .079 | 12.70 | Y | .071 | 14.18 | Z(Col.) |
| 7 | .065 | 15.33 | X&Z | .069 | 14.52 | X(Col.) | .078 | 12.87 | Z&X | .070 | 14.21 | X |
| 8 | .042 | 23.63 | X(Col.) | .060 | 16.77 | Y | .077 | 12.88 | X[Rot.] | .066 | 15.15 | Y |
| 9 | .040 | 24.97 | Y | .050 | 20.07 | Y | .069 | 14.52 | X(Col.) | .064 | 15.56 | X&Z |
| 10 | .029 | 34.06 | Y | .044 | 22.91 | X(Col.) | .066 | 15.17 | Y | .063 | 15.85 | Y |
| 11 | .028 | 36.27 | Z | .042 | 23.91 | X(Col.) | .065 | 15.33 | X&Z | .057 | 17.53 | X(Col.) |
| 12 | .022 | 45.29 | X | .036 | 28.00 | Y | .058 | 17.23 | X[Rot.] | .037 | 27.22 | Y |
| 13 | .021 | 45.85 | Y | .032 | 31.17 | X | .055 | 18.25 | X[Rot.] | .036 | 27.83 | X(Col.) |
| 14 | .017 | 59.10 | Y | .029 | 34.91 | Y | .046 | 21.56 | X[Rot.] | .031 | 32.42 | Z(Col.) |
| 15 | .016 | 64.12 | X(Col.) | .023 | 42.83 | Y | .045 | 22.24 | X[Rot.] | .030 | 33.23 | Z(Col.) |

Table A2.26 Maximum Actions and Displacements at the Attachments and Column Base For Composite Deck, Non-Composite Deck, Rotational Inertia, and Long Columns Models, (k,ft)

| Location | Component | Composite Deck | Non-Composite Deck | Rotational Inertia | Long Columns |
|---|---|---|---|---|---|
| Abut. 1 | P1 | 335. | 354. | 326. | 323. |
| | V2 | 241. | 218. | 239. | 244. |
| | V3 | 55. | 52. | 55. | 62. |
| | M1 | 49. | 37. | 259. | 55. |
| | M3 | 10063. | 8811. | 10009. | 10461. |
| Bent 2 | V2 | 16. | 72. | 17. | 47. |
| | M2(Deck) | 2430. | 2139. | 2400. | 2579. |
| Abut. 3 | V2 | 231. | 211. | 232. | 238. |
| | M3 | 9726. | 8541. | 9743. | 10211. |
| | DT | .0015 | .0039 | .0015 | .0016 |
| Column Base: | | | | | |
| Bent 2 | P1 | 110. | 102. | 117. | 103. |
| | M2 | 63. | 108. | 64. | 118. |
| | M3 | 256. | 459. | 255. | 186. |

Table A2.27 Maximum Stresses in Bridge Deck and Columns For Composite Deck, Non-Composite Deck, Rotational Inertia, and Long Columns Models, (ksi)

| Location | Material | Composite Deck | Non-Composite Deck | Rotational Inertia | Long Columns |
|---|---|---|---|---|---|
| Deck: | | | | | |
| Abut.1 | Steel | 1.61 | 3.39 | 1.59 | 1.64 |
| | Conc. | 0.31 | 0. | 0.31 | 0.32 |
| | Steel(τ) | 0.94 | 2.27 | 0.92 | 0.97 |
| | Conc.(τ) | 0.04 | 0. | 0.04 | 0.04 |
| Span 1 | Steel | 1.24 | 2.22 | 1.19 | 1.33 |
| | Conc. | 0.09 | 0. | 0.09 | 0.09 |
| Bent 2 | Steel | 1.83 | 3.30 | 1.81 | 1.89 |
| | Conc. | 0.18 | 0. | 0.18 | 0.20 |
| Column Base: | | | | | |
| Bent 2 | Conc. | 0.47 | 0.82 | 0.47 | 0.33 |
| | Conc.(τ) | 0.04 | 0.06 | 0.04 | 0.02 |

Table A2.28 Structure Period For 2-Column and Rigid-Column Straight Models

| Mode | 2-Column | | | Rigid-Column | | | Exact Solution | | |
|---|---|---|---|---|---|---|---|---|---|
| | Period (sec) | Frequency (Hz) | Mode Shape Direction | Period (sec) | Frequency (Hz) | Mode Shape Direction | Period (sec) | Frequency (Hz) | Mode Shape Direction |
| 1 | .265 | 3.77 | Y | .265 | 3.77 | Y | .265 | 3.77 | Y |
| 2 | .191 | 5.23 | Y | .170 | 5.89 | Y | .170 | 5.89 | Y |
| 3 | .078 | 12.78 | Y | .067 | 14.97 | X | | | |
| 4 | .074 | 13.47 | Z | .066 | 15.08 | Y | .066 | 15.08 | Y |
| 5 | .069 | 14.52 | X(Col.) | .052 | 19.07 | Y | .052 | 19.10 | Y |
| 6 | .068 | 14.65 | X | .030 | 33.73 | Y | .029 | 33.95 | Y |
| 7 | .066 | 15.08 | Y | .028 | 36.36 | Z | .027 | 36.37 | Z |
| 8 | .042 | 23.59 | X(Col.) | .025 | 39.33 | Y | .025 | 39.85 | Y |
| 9 | .040 | 24.81 | Y | .022 | 44.66 | X | | | |
| 10 | .030 | 33.73 | Y | .019 | 52.75 | Z | .019 | 52.77 | Z |

Table A2.29 Maximum Actions at the Attachments For 2-Column and Rigid-Column Straight Models, (k,ft)

| Location | Component | 2-Column | Rigid-Column |
|---|---|---|---|
| Abut. 1 | P1 | 296. | 282. |
| | V2 | 228. | 78. |
| | V3 | 57. | 63. |
| | M1 | 5. | 0. |
| | M3 | 9754. | 1683. |
| Bent 2 | M2(Deck) | 2380. | 2442 |
| Abut. 3 | V2 | 228. | 78. |
| | M3 | 9754. | 1683. |

Table A2.30 Maximum Stresses in Bridge Deck For 2-Column and Rigid-Column Straight Models, (ksi)

| Location | Material | 2-Column | Rigid-Column |
|---|---|---|---|
| Abut. 1 | Steel | 1.49 | 0.37 |
| | Conc. | 0.29 | 0.06 |
| Span 1 | Steel | 1.34 | 1.38 |
| | Conc. | 0.10 | 0.09 |
| Bent 2 | Steel | 2.22 | 2.19 |
| | Conc. | 0.19 | 0.15 |

Table A2.31 Maximum Stresses in Bridge Deck and Columns Due to Dead Load, (ksi)

| Location | Material | Stresses |
|---|---|---|
| Deck: | | |
| Span 1 | Steel | 4.47 |
| | Conc. | 0.28 |
| Bent 2 | Steel | 7.93 |
| Column Base: | | |
| Bent 2 | Conc. | 0.95 |

## A.3 3-Span Curved Bridges

Table A3.1 Structure Period and Participation Factors For 2-Column and 3-Column Models

| Mode | 2-Column | | | | | 3-Column | | | | |
|---|---|---|---|---|---|---|---|---|---|---|
| | Period | Frequency | Participation Factor | | | Period | Frequency | Participation Factor | | |
| | (sec) | (Hz) | X | Y | Z | (sec) | (Hz) | X | Y | Z |
| 1 | .265 | 3.78 | 0. | 2.24 | 0. | .265 | 3.78 | 0. | 2.24 | 0. |
| 2 | .217 | 4.61 | 0. | 0. | 0. | .206 | 4.85 | 0. | 0. | 0. |
| 3 | .167 | 5.98 | 0. | 6.88 | 0. | .144 | 6.95 | 0. | 6.33 | 0. |
| 4 | .138 | 7.25 | 0. | 0. | 6.76 | .136 | 7.33 | 0. | 0. | -6.76 |
| 5 | .101 | 9.94 | 7.24 | 0. | 0. | .101 | 9.94 | 7.24 | 0. | 0. |
| 6 | .083 | 12.08 | 0. | 0. | 0. | .066 | 15.15 | 0. | 0. | 0. |
| 7 | .074 | 13.48 | 0. | -1.35 | 0. | .062 | 16.18 | 0. | -1.56 | 0. |
| 8 | .066 | 15.15 | 0. | 0. | 0. | .057 | 17.63 | 0. | 0. | 0. |
| 9 | .045 | 22.38 | 0.22 | -1.83 | 0. | .044 | 22.54 | -1.14 | 0.01 | 0. |
| 10 | .044 | 22.48 | 1.11 | 0.38 | 0. | .042 | 23.67 | -0.28 | 0. | 0. |

Table A3.2 Maximum Actions and Displacements at the Attachments For 2-Column and 3-Column Models, (k,ft)

| Location | Component | Excitation Direction | 2-Column | 3-Column |
|---|---|---|---|---|
| Abut. 1 | P1 | Long. (R.S.) | 908. | 907. |
| | V2 | Trans. (T.H.) | 219. | 212. |
| | M3 | Trans. (T.H.) | 13770. | 13376. |
| Bent 2 | V2 | Trans. (T.H.) | 115. | 119. |
| Abut. 4 | V2 | Trans. (T.H.) | 219. | 212. |
| | M3 | Trans. (T.H.) | 13770. | 13376. |
| | DT | Long. (R.S.) | .0060 | .0060 |

Table A3.3 Maximum Stresses in Bridge Deck and Columns For 2-Column and 3-Column Models, (ksi)

| Location | Material | Excitation Direction | 2-Column | 3-Column |
|---|---|---|---|---|
| Deck: | | | | |
| Abut. 1 | Steel | Trans. (T.H.) | 2.02 | 1.96 |
| | Conc. | Trans. (T.H.) | 0.41 | 0.39 |
| Span 1 | Steel | Trans. (T.H.) | 0.46 | 0.44 |
| | Conc. | Trans. (T.H.) | 0.09 | 0.09 |
| Bent 2 | Steel | Trans. (T.H.) | 0.58 | 0.56 |
| | Conc. | Trans. (T.H.) | 0.11 | 0.11 |
| Span 2 | Steel | Trans. (T.H.) | 1.39 | 1.36 |
| | Conc. | Trans. (T.H.) | 0.28 | 0.27 |
| Column Base: | | | | |
| Bent 2 | Conc. | Trans. (T.H.) | 1.03 | 0.86 |

Table A3.4 Structure Period and Participation Factors For the Modified End-Boundary-Conditions Model

| Mode | Period (sec) | Frequency (Hz) | Participation Factor | | |
|---|---|---|---|---|---|
| | | | X | Y | Z |
| 1 | .265 | 3.78 | 0. | 2.24 | 0. |
| 2 | .217 | 4.61 | 0. | 0. | 0. |
| 3 | .167 | 5.98 | 0. | 6.88 | 0. |
| 4 | .138 | 7.25 | 0. | 0. | 6.77 |
| 5 | .101 | 9.95 | 7.24 | 0. | 0. |
| 6 | .083 | 12.08 | 0. | 0. | 0. |
| 7 | .074 | 13.48 | 0. | 1.35 | 0. |
| 8 | .066 | 15.15 | 0. | 0. | 0. |
| 9 | .045 | 22.38 | -0.22 | 1.83 | 0. |
| 10 | .044 | 22.49 | 1.11 | 0.38 | 0. |

Table A3.5 Maximum Actions and Displacements at the Attachments For The Modified End-Boundary-Conditions Model, (k,ft)

| Location | Component | Excitation Direction | Response |
|---|---|---|---|
| Abut. 1 | P1 | Long. (R.S.) | 907. |
| | V2 | Trans. (T.H.) | 218. |
| | M3 | Trans. (T.H.) | 13770. |
| Bent 2 | V2 | Trans. (T.H.) | 115. |
| Abut. 4 | V2 | Trans. (T.H.) | 218. |
| | M3 | Trans. (T.H.) | 13770. |
| | DT | Long. (R.S.) | .0060 |

Table A3.6 Maximum Stresses in Bridge Deck and Columns For The Modified End-Boundary-Conditions Model, (ksi)

| Location | Material | Excitation Direction | Stress |
|---|---|---|---|
| Deck: | | | |
| Abut. 1 | Steel | Trans. (T.H.) | 2.02 |
| | Conc. | Trans. (T.H.) | 0.40 |
| Span 1 | Steel | Trans. (T.H.) | 0.46 |
| | Conc. | Trans. (T.H.) | 0.09 |
| Bent 2 | Steel | Trans. (T.H.) | 0.58 |
| | Conc. | Trans. (T.H.) | 0.11 |
| Span 2 | Steel | Trans. (T.H.) | 1.39 |
| | Conc. | Trans. (T.H.) | 0.28 |
| Column Base: | | | |
| Bent 2 | Conc. | Trans. (T.H.) | 1.03 |

Table A3.7 Structure Period and Participation Factors For 6-Element and 10-Element Models

| Mode | 6-Element | | | | | 10-Element | | | | |
|---|---|---|---|---|---|---|---|---|---|---|
| | Period (sec) | Frequency (Hz) | Participation Factor X | Y | Z | Period (sec) | Frequency (Hz) | Participation Factor X | Y | Z |
| 1 | .265 | 3.77 | 0. | 2.24 | 0. | .265 | 3.77 | 0. | 2.28 | 0. |
| 2 | .217 | 4.60 | 0. | 0. | 0. | .217 | 4.60 | 0. | 0. | 0. |
| 3 | .167 | 5.98 | 0. | 6.87 | 0. | .167 | 5.98 | 0. | 6.89 | 0. |
| 4 | .144 | 6.95 | -2.39 | 0. | 6.48 | .144 | 6.95 | -2.39 | 0. | 6.48 |
| 5 | .097 | 10.30 | 6.81 | 0. | 1.99 | .097 | 10.30 | -6.81 | 0. | -1.99 |
| 6 | .083 | 12.08 | 0. | 0. | 0. | .083 | 12.10 | 0. | 0. | 0. |
| 7 | .074 | 13.49 | 0. | 1.35 | 0. | .074 | 13.51 | 0. | -1.32 | 0. |
| 8 | .069 | 14.52 | 0. | 0. | 0. | .069 | 14.52 | 0. | 0. | 0. |
| 9 | .066 | 15.16 | 0. | 0. | 0. | .069 | 14.52 | 0. | 0. | 0. |
| 10 | .062 | 16.10 | 0.57 | 0. | -0.03 | .065 | 15.30 | 0. | 0. | 0. |

Table A3.8 Maximum Actions and Displacements At the Attachments For 6-Element and 10-Element Models, (k,ft)

| Location | Component | Excitation Direction | 6-Element | 10-Element |
|---|---|---|---|---|
| Abut. 1 | P1 | Long. (R.S.) | 765. | 766. |
| | V2 | Trans. (T.H.) | 244. | 244. |
| | M3 | Trans. (T.H.) | 15303. | 15310. |
| Bent 2 | V2 | Trans. (T.H.) | 129. | 130. |
| Abut. 4 | V2 | Trans. (T.H.) | 240. | 240. |
| | M3 | Trans. (T.H.) | 14935. | 14963. |
| | DT | Long. (R.S.) | .0049 | .0049 |

Table A3.9 Maximum Stresses in Bridge Deck and Columns For 6-Element and 10-Element Models, (ksi)

| Location | Material | Excitation Direction | 6-Element | 10-Element |
|---|---|---|---|---|
| Deck: | | | | |
| Abut. 1 | Steel | Trans. (T.H.) | 2.32 | 2.32 |
| | Conc. | Trans. (T.H.) | 0.46 | 0.46 |
| Span 1 | Steel | Trans. (T.H.) | 0.66 | 0.66 |
| | Conc. | Trans. (T.H. | 0.12 | 0.12 |
| Bent 2 | Steel | Trans. (T.H.) | 0.76 | 0.75 |
| | Conc. | Trans. (T.H.) | 0.14 | 0.13 |
| Span 2 | Steel | Trans. (T.H.) | 1.64 | 1.63 |
| | Conc. | Trans. (T.H.) | 0.32 | 0.32 |
| Column Base: | | | | |
| Bent 2 | Conc. | Trans. (T.H.) | 1.14 | 1.14 |

Table A3.10 Structure Period and Participation Factors (The Lowest Twenty Frequencies)

| Mode | Period (sec) | Frequency (Hz) | Participation Factor | | |
|---|---|---|---|---|---|
| | | | X | Y | Z |
| 1 | .265 | 3.77 | 0. | 2.24 | 0. |
| 2 | .217 | 4.60 | 0. | 0. | 0. |
| 3 | .167 | 5.98 | 0. | 6.87 | 0. |
| 4 | .144 | 6.95 | -2.39 | 0. | 6.48 |
| 5 | .097 | 10.30 | 6.81 | 0. | 1.99 |
| 6 | .083 | 12.08 | 0. | 0. | 0. |
| 7 | .074 | 13.49 | 0. | 1.35 | 0. |
| 8 | .069 | 14.52 | 0. | 0. | 0. |
| 9 | .069 | 14.52 | 0. | 0. | 0. |
| 10 | .066 | 15.16 | 0. | 0. | 0. |
| 11 | .062 | 16.10 | -0.57 | 0. | 0.03 |
| 12 | .045 | 22.39 | -0.21 | 1.83 | -0.01 |
| 13 | .044 | 22.50 | 1.07 | 0.37 | 0.06 |
| 14 | .042 | 23.58 | 0.31 | -0.02 | 0.04 |
| 15 | .036 | 27.91 | -0.01 | 0. | 0. |
| 16 | .032 | 31.02 | -1.97 | 0. | -0.09 |
| 17 | .031 | 31.54 | -0.23 | 0. | -2.80 |
| 18 | .029 | 34.11 | 0.01 | 0.60 | 0. |
| 19 | .024 | 41.98 | 0. | 0. | 0. |
| 20 | .020 | 50.05 | -0.07 | -0.18 | -0.01 |

Table A3.11 Maximum Actions at the Attachments and Column Base, (k,ft)
(10, 15, and 20 Frequencies)

| Location | Component | Long. Shock (T.H.) | | Trans. Shock (T.H.) | | Vert. Shock (T.H.) | | 3-Direction Shock (T.H.) | |
|---|---|---|---|---|---|---|---|---|---|
| | | 10 | 15 | 10 | 15 | 10 | 15 | 15 | 20 |
| Abut. 1 | P1 | 794. | 798. | 313. | 313. | 0. | 0.2 | 518. | 539. |
| | V2 | 111. | 111. | 268. | 268. | 0. | 0. | 291. | 303. |
| | V3 | 0. | 0. | 0. | 0. | 107. | 112. | 47. | 48. |
| | M3 | 6344. | 6347. | 16220. | 16220. | 4. | 4. | 17179. | 17511. |
| Bent 2 | V2 | 53. | 53. | 136. | 136. | 0. | 0. | 142. | 142. |
| | M2(Deck) | 2. | 4. | 5. | 5. | 4607. | 4551. | 2558. | 2557. |
| Abut. 4 | V2 | 96. | 97. | 245. | 245. | 0. | 0. | 250. | 262. |
| | M3 | 6124. | 6133. | 15215. | 15214. | 4. | 4. | 15526. | 15859. |
| Column Base: | | | | | | | | | |
| Bent 2 | P1 | 16. | 16. | 41. | 41. | 226. | 229. | 124. | 124. |
| | M2 | 109. | 118. | 58. | 57. | 5. | 5. | 89. | 85. |
| | M3 | 265. | 265. | 664. | 664. | 209. | 212. | 699. | 699. |

Table A3.12 Maximum Stresses in Bridge Deck and Columns, (ksi)
(10, 15, and 20 Frequencies)

| Location | Material | Long. Shock (T.H.) | | Trans. Shock (T.H.) | | Vert. Shock (T.H.) | | 3-Direction Shock (T.H.) | |
|---|---|---|---|---|---|---|---|---|---|
| | | 10 | 15 | 10 | 15 | 10 | 15 | 15 | 20 |
| Deck: | | | | | | | | | |
| Abut. 1 | Steel | 1.31 | 1.31 | 2.68 | 2.68 | 0. | 0. | 2.96 | 3.01 |
| | Conc. | 0.21 | 0.21 | 0.51 | 0.51 | 0. | 0. | 0.56 | 0.57 |
| Span 1 | Steel | 1.00 | 1.01 | 0.85 | 0.85 | 2.43 | 2.40 | 1.22 | 1.28 |
| | Conc. | 0.12 | 0.14 | 0.14 | 0.14 | 0.16 | 0.16 | 0.17 | 0.16 |
| Bent 2 | Steel | 0.73 | 0.73 | 0.94 | 0.94 | 3.31 | 3.27 | 1.88 | 1.89 |
| | Conc. | 0.10 | 0.10 | 0.16 | 0.16 | 0.25 | 0.25 | 0.18 | 0.19 |
| Span 2 | Steel | 0.97 | 0.97 | 1.84 | 1.84 | 3.31 | 3.27 | 1.96 | 1.93 |
| | Conc. | 0.15 | 0.15 | 0.35 | 0.35 | 0.22 | 0.22 | 0.36 | 0.36 |
| Column Base: | | | | | | | | | |
| Bent 2 | Conc. | 0.47 | 0.47 | 1.19 | 1.19 | 0.54 | 0.55 | 1.26 | 1.26 |

Table A3.13 Maximum Actions at the Attachments
For Different Time Steps ($\Delta t$), (k,ft)

| Location | Component | Long. Shock (T.H.) | | | Trans. Shock (T.H.) | | | Vert. Shock (T.H.) | | |
|---|---|---|---|---|---|---|---|---|---|---|
| | | .0100 | .0050 | .0025 | .0100 | .0050 | .0025 | .0100 | .0050 | .0025 |
| Abut. 1 | P1 | 827. | 798. | 783. | 331. | 313. | 301. | 0.1 | 0.2 | 0.2 |
| | V2 | 98. | 111. | 114. | 262. | 268. | 276. | 0. | 0. | 0. |
| | V3 | 0. | 0. | 0. | 0. | 0. | 0. | 116. | 112. | 109. |
| | M3 | 6244. | 6347. | 6518. | 15616. | 16220. | 16705. | 5. | 4. | 4. |
| Bent 2 | V2 | 53. | 53. | 51. | 131. | 136. | 140. | 0. | 0. | 0. |
| | M2(Deck) | 4. | 4. | 4. | 5. | 5. | 5. | 4667. | 4551. | 4463. |
| Abut. 4 | V2 | 102. | 97. | 93. | 233. | 245. | 253. | 0. | 0. | 0. |
| | M3 | 6480. | 6133. | 5807. | 14432. | 15214. | 15680. | 4. | 4. | 4. |

Table A3.14 Maximum Stresses in Bridge Deck and Columns For Different Time Steps ($\Delta t$), (ksi)

| Location | Material | Long. Shock (T.H.) | | | Trans. Shock (T.H.) | | | Vert. Shock (T.H.) | | |
|---|---|---|---|---|---|---|---|---|---|---|
| | | .0100 | .0050 | .0025 | .0100 | .0050 | .0025 | .0100 | .0050 | .0025 |
| Deck: | | | | | | | | | | |
| Abut. 1 | Steel | 1.32 | 1.31 | 1.33 | 2.65 | 2.68 | 2.73 | 0. | 0. | 0. |
| | Conc. | 0.21 | 0.21 | 0.21 | 0.50 | 0.51 | 0.52 | 0. | 0. | 0. |
| Span 1 | Steel | 0.92 | 1.01 | 0.99 | 0.85 | 0.85 | 0.83 | 2.45 | 2.40 | 2.39 |
| | Conc. | 0.12 | 0.14 | 0.14 | 0.14 | 0.14 | 0.14 | 0.17 | 0.16 | 0.16 |
| Bent 2 | Steel | 0.77 | 0.73 | 0.74 | 0.94 | 0.94 | 0.93 | 3.35 | 3.27 | 3.20 |
| | Conc. | 0.10 | 0.10 | 0.10 | 0.16 | 0.16 | 0.16 | 0.25 | 0.25 | 0.24 |
| Span 2 | Steel | 0.91 | 0.97 | 0.97 | 1.81 | 1.84 | 1.88 | 3.38 | 3.27 | 3.26 |
| | Conc. | 0.15 | 0.15 | 0.15 | 0.34 | 0.35 | 0.36 | 0.23 | 0.22 | 0.22 |
| Column Base: | | | | | | | | | | |
| Bent 2 | Conc. | 0.48 | 0.47 | 0.47 | 1.13 | 1.19 | 1.22 | 0.56 | 0.55 | 0.54 |

Table A3.15 Maximum Actions at the Attachments for 10 and 15 sec. Shock Durations, (k,ft)

| Location | Component | Longitudinal Shock (SOOE) | | Transverse Shock (SOOE) | |
|---|---|---|---|---|---|
| | | 10 sec. | 15 sec. | 10 sec. | 15 sec. |
| Abut. 1 | P1 | 825. | 825. | 263. | 263. |
| | V2 | 110. | 110. | 244. | 244. |
| | M3 | 4880. | 4880. | 15303. | 15303. |
| Bent 2 | V2 | 39. | 39. | 129. | 129. |
| Abut. 4 | V2 | 80. | 80. | 240. | 240. |
| | M3 | 4962. | 4962. | 14934. | 14934. |

Table A3.16 Maximum Stresses in Bridge Deck and Columns For 10 and 15 sec. Shock Durations, (ksi)

| Location | Material | Longitudinal Shock (SOOE) | | Transverse Shock (SOOE) | |
|---|---|---|---|---|---|
| | | 10 sec. | 15 sec. | 10 sec. | 15 sec. |
| Deck: | | | | | |
| Abut. 1 | Steel | 1.46 | 1.46 | 2.32 | 2.32 |
| | Conc. | 0.24 | 0.24 | 0.46 | 0.46 |
| Span 1 | Steel | 0.97 | 0.97 | 0.66 | 0.66 |
| | Conc. | 0.13 | 0.13 | 0.12 | 0.12 |
| Bent 2 | Steel | 0.80 | 0.80 | 0.76 | 0.76 |
| | Conc. | 0.11 | 0.11 | 0.14 | 0.14 |
| Span 2 | Steel | 0.84 | 0.84 | 1.64 | 1.64 |
| | Conc. | 0.14 | 0.14 | 0.32 | 0.32 |
| Column Base: | | | | | |
| Bent 2 | Conc. | 0.35 | 0.35 | 1.14 | 1.14 |

Table A3.17 Maximum Actions and Displacements at the Attachments and Column Base Due to a Longitudinal Shock (S00E), (R.S. & T.H. Analysis), (k,ft)

| Location | Component | 10 Frequencies | | 15 Frequencies | | 20 Frequencies |
|---|---|---|---|---|---|---|
| | | R.S. | T.H. | R.S. | T.H. | R.S. |
| Abut. 1 | P1 | 765. | 794. | 765. | 798. | 2098. |
| | V2 | 112. | 111. | 112. | 111. | 253. |
| | V3 | 0. | 0. | 2. | 0. | 7. |
| | M1 | 6. | 5. | 6. | 5. | 6. |
| | M3 | 6743. | 6344. | 6743. | 6347. | 8602. |
| Bent 2 | V2 | 57. | 53. | 57. | 53. | 58. |
| | M2 (Deck) | 3. | 2. | 30. | 4. | 113. |
| Abut. 4 | V2 | 115. | 96. | 115. | 97. | 210. |
| | M3 | 7187. | 6124. | 7187. | 6133. | 9136. |
| | DT | .0049 | .0052 | .0049 | .0052 | .0065 |
| Column Base: | | | | | | |
| Bent 2 | P1 | 18. | 16. | 18. | 16. | 18. |
| | M2 | 106. | 109. | 108. | 118. | 340. |
| | M3 | 288. | 265. | 288. | 265. | 289. |

Table A3.18 Maximum Actions and Displacements at the Attachments and Column Base Due to a Transverse Shock (S00E), (R.S. & T.H. Analysis), (k,ft)

| Location | Component | 10 Frequencies | | 15 Frequencies | | 20 Frequencies |
|---|---|---|---|---|---|---|
| | | R.S. | T.H. | R.S. | T.H. | R.S. |
| Abut. 1 | P1 | 372. | 313. | 372. | 313. | 498. |
| | V2 | 296. | 268. | 296. | 268. | 1840. |
| | V3 | 0. | 0. | 0.3 | 0. | 1. |
| | M1 | 15. | 14. | 15. | 14. | 16. |
| | M3 | 17910. | 16220. | 17910. | 16220. | 52870. |
| Bent 2 | V2 | 150. | 136. | 150. | 136. | 181. |
| | M2 (Deck) | 6. | 5. | 7. | 5. | 19. |
| Abut. 4 | V2 | 272. | 245. | 272. | 245. | 1850. |
| | M3 | 16850. | 15215. | 16850. | 15214. | 52470. |
| | DT | .0051 | .0047 | .0051 | .0047 | .0052 |
| Column Base: | | | | | | |
| Bent 2 | P1 | 46. | 41. | 46. | 41. | 46. |
| | M2 | 65. | 58. | 65. | 57. | 67. |
| | M3 | 733. | 664. | 733. | 664. | 748. |

Table A3.19 Maximum Actions at the Attachments and Column Base Due to a Vertical Shock (SOOE), (R.S. & T.H. Analysis), (k,ft)

| Location | Component | 10 Frequencies | | 15 Frequencies | |
|---|---|---|---|---|---|
| | | R.S. | T.H. | R.S. | T.H. |
| Abut. 1 | P1 | 0. | 0. | 6. | 0.2 |
| | V2 | 0. | 0. | 0.3 | 0. |
| | V3 | 103. | 107. | 103. | 112. |
| | M1 | 105. | 98. | 105. | 99. |
| | M3 | 6. | 4. | 8. | 4. |
| Bent 2 | V2 | 0. | 0. | 0. | 0. |
| | V3 (Deck) | 171. | 182. | 171. | 177. |
| | M2 (Deck) | 4339. | 4607. | 4341. | 4551. |
| Abut. 4 | V2 | 0. | 0. | 0.5 | 0. |
| | M3 | 6. | 4. | 19. | 4. |
| Column Base: | | | | | |
| Bent 2 | P1 | 215. | 226. | 216. | 229. |
| | M2 | 6. | 5. | 12. | 5. |
| | M3 | 200. | 209. | 200. | 212. |

Table A3.20 Maximum Actions at the Attachments and Column Base Due To El Centro Earthquake (S90W) and (VERT) Components, (R.S. & T.H. Analysis), (k,ft)

| Location | Component | Longitudinal Shock (S90W) | | Vertical Shock (VERT) | |
|---|---|---|---|---|---|
| | | R. S. | T. H. | R. S. | T. H. |
| Abut. 1 | P1 | 477. | 519. | 7. | 0.2 |
| | V2 | 66. | 73. | 0.4 | 0. |
| | V3 | 2. | 0. | 53. | 47. |
| | M1 | 4. | 3. | 44. | 46. |
| | M3 | 3969. | 3725. | 7. | 3. |
| Bent 2 | V2 | 34. | 29. | 0. | 0. |
| | V3 (Deck) | 1. | 0. | 96. | 89. |
| | M2 (Deck) | 26. | 2. | 2585. | 2558. |
| Abut. 4 | V2 | 68. | 44. | 0.6 | 0. |
| | M3 | 4290. | 2746. | 23. | 3. |
| Column Base: | | | | | |
| Bent 2 | P1 | 11. | 9. | 129. | 126. |
| | M2 | 68. | 73. | 14. | 2. |
| | M3 | 171. | 139. | 120. | 117. |

Table A3.21 Maximum Actions and Displacements at the Attachments and Column Base Due to El Centro Earthquake Different Components, (k,ft)

| Location | Component | Longitudinal Shock (S00E) | | Transverse Shock (S90W) | | Vertical Shock (VERT) | | 3-Direction Shock | |
|---|---|---|---|---|---|---|---|---|---|
| | | Response | Time (sec) | Response | Time (sec) | Response | Time (sec) | Response | Time (sec) |
| Abut. 1 | P1 | 798. | 5.00 | 130. | 4.02 | 0.2 | 1.08 | 767. | 5.00 |
| | V2 | 111. | 2.65 | 173. | 1.94 | 0. | 0.74 | 207. | 2.08 |
| | V3 | 0. | 2.61 | 0. | 2.89 | 47. | 3.36 | 47. | 3.36 |
| | M1 | 6. | 3.54 | 9. | 1.93 | 46. | 3.36 | 43. | 3.36 |
| | M3 | 6347. | 2.65 | 10589. | 1.94 | 3. | 0.74 | 12134. | 1.93 |
| Bent 2 | V2 | 53. | 3.54 | 89. | 1.94 | 0. | 0.82 | 101. | 1.93 |
| | V3 (Deck) | 0. | 2.52 | 0. | 3.48 | 89. | 0.64 | 89. | 0.64 |
| | M2 (Deck) | 4. | 2.59 | 3. | 1.93 | 2558. | 0.64 | 2558. | 0.64 |
| Abut. 4 | V2 | 97. | 3.54 | 163. | 1.93 | 0. | 0.74 | 179. | 1.93 |
| | M3 | 6113. | 3.54 | 10117. | 1.93 | 3. | 0.74 | 11115. | 1.93 |
| | DT | .0052 | 4.90 | .0026 | 1.94 | 0. | 0.74 | .0056 | 2.22 |
| Column Base: | | | | | | | | | |
| Bent 2 | P1 | 16. | 3.54 | 27. | 1.94 | 126. | 0.64 | 125. | 0.64 |
| | M2 | 118. | 5.00 | 26. | 1.94 | 2. | 3.40 | 116. | 4.49 |
| | M3 | 265. | 3.54 | 437. | 1.94 | 117. | 0.64 | 490. | 1.93 |

Table A3.22 Maximum Stresses in Bridge Deck and Columns Due to El Centro Earthquake Different Components, (ksi)

| Location | Material | Longitudinal Shock (S00E) | | Transverse Shock (S90W) | | Vertical Shock (VERT) | | 3-Direction Shock | |
|---|---|---|---|---|---|---|---|---|---|
| | | Stress | Time (sec) | Stress | Time (sec) | Stress | Time (sec) | Stress | Time (sec) |
| Abut. 1 | Steel | 1.31 | 2.23 | 1.68 | 1.94 | 0. | 0.74 | 2.23 | 2.08 |
| | Conc. | 0.21 | 2.23 | 0.33 | 1.94 | 0. | 0.74 | 0.40 | 2.08 |
| Span 1 | Steel | 1.01 | 5.00 | 0.48 | 1.94 | 1.16 | 3.35 | 1.15 | 3.34 |
| | Conc. | 0.14 | 5.00 | 0.09 | 1.94 | 0.08 | 3.35 | 0.15 | 3.36 |
| Bent 2 | Steel | 0.73 | 2.22 | 0.56 | 1.94 | 1.84 | 0.64 | 1.90 | 0.64 |
| | Conc. | 0.10 | 2.22 | 0.10 | 1.94 | 0.14 | 0.64 | 0.15 | 0.56 |
| Span 2 | Steel | 0.97 | 4.99 | 1.17 | 1.94 | 1.78 | 0.64 | 1.89 | 0.56 |
| | Conc. | 0.15 | 5.00 | 0.22 | 1.94 | 0.12 | 0.64 | 0.26 | 1.94 |
| Column Base: | | | | | | | | | |
| Bent 2 | Conc. | 0.47 | 3.54 | 0.78 | 1.94 | 0.30 | 0.64 | 0.88 | 1.94 |

Table A3.23 Maximum Actions and Displacements at the Attachments and Column Base Due to El Centro Earthquake Different Components, (k,ft)

| Location | Component | Longitudinal Shock (S90W) | | Transverse Shock (S00E) | | Vertical Shock (VERT) | | 3-Direction Shock | |
|---|---|---|---|---|---|---|---|---|---|
| | | Response | Time (sec) | Response | Time (sec) | Response | Time (sec) | Response | Time (sec) |
| Abut. 1 | P1 | 519. | 4.18 | 313. | 3.54 | 0.2 | 1.08 | 518. | 1.91 |
| | V2 | 73. | 1.93 | 268. | 2.65 | 0. | 0.74 | 291. | 2.65 |
| | V3 | 0. | 4.24 | 0. | 2.25 | 47. | 3.36 | 47. | 3.36 |
| | M1 | 3. | 1.94 | 14. | 2.65 | 46. | 3.36 | 49. | 3.36 |
| | M3 | 3725. | 1.94 | 16220. | 2.65 | 3. | 0.74 | 17179. | 2.65 |
| Bent 2 | V2 | 29. | 1.94 | 136. | 2.65 | 0. | 0.82 | 142. | 2.65 |
| | V3 (Deck) | 0. | 2.82 | 0. | 2.64 | 89. | 0.64 | 89. | 0.64 |
| | M2 (Deck) | 2. | 1.89 | 5. | 2.64 | 2558. | 0.64 | 2558. | 0.64 |
| Abut. 4 | V2 | 44. | 1.94 | 245. | 2.65 | 0. | 0.74 | 250. | 2.65 |
| | M3 | 2746. | 1.94 | 15214. | 2.65 | 3. | 0.74 | 15526. | 2.65 |
| | DT | .0037 | 4.18 | .0047 | 3.54 | 0. | 0.74 | .0054 | 2.65 |
| Column Base: | | | | | | | | | |
| Bent 2 | P1 | 9. | 1.94 | 41. | 2.65 | 126. | 0.64 | 124. | 0.64 |
| | M2 | 73. | 4.18 | 57. | 3.54 | 2. | 3.40 | 89. | 1.91 |
| | M3 | 139. | 1.94 | 664. | 2.65 | 117. | 0.64 | 699. | 2.65 |

Table A3.24 Maximum Stresses in Bridge Deck and Columns Due To El Centro Earthquake Different Components, (ksi)

| Location | Material | Longitudinal Shock (S90W) | | Transverse Shock (S00E) | | Vertical Shock (VERT) | | 3-Direction Shock | |
|---|---|---|---|---|---|---|---|---|---|
| | | Stress | Time (sec) | Stress | Time (sec) | Stress | Time (sec) | Stress | Time (sec) |
| Deck: | | | | | | | | | |
| Abut. 1 | Steel | 0.96 | 4.17 | 2.68 | 3.54 | 0. | 0.74 | 2.96 | 2.65 |
| | Conc. | 0.15 | 4.17 | 0.51 | 3.54 | 0. | 0.74 | 0.56 | 2.65 |
| Span 1 | Steel | 0.57 | 4.18 | 0.85 | 3.54 | 1.16 | 3.35 | 1.22 | 3.36 |
| | Conc. | 0.07 | 4.18 | 0.14 | 3.54 | 0.08 | 3.35 | 0.17 | 2.65 |
| Bent 2 | Steel | 0.53 | 4.17 | 0.94 | 3.54 | 1.84 | 0.64 | 1.88 | 0.64 |
| | Conc. | 0.07 | 4.17 | 0.16 | 3.54 | 0.14 | 0.64 | 0.18 | 2.64 |
| Span 2 | Steel | 0.54 | 1.93 | 1.84 | 3.54 | 1.78 | 0.64 | 1.97 | 2.65 |
| | Conc. | 0.08 | 4.18 | 0.35 | 2.65 | 0.12 | 0.64 | 0.36 | 2.65 |
| Column Base: | | | | | | | | | |
| Bent 2 | Conc. | 0.25 | 1.94 | 1.19 | 2.65 | 0.30 | 0.64 | 1.26 | 2.65 |

Table A3.25 Maximum Actions and Displacements at the Attachments and Column Base for Different Damping Ratios, (k,ft)

| Location | Component | 2% | 5% | 10% |
|---|---|---|---|---|
| Abut. 1 | P1 | 684. | 518. | 460. |
| | V2 | 360. | 291. | 241. |
| | V3 | 59. | 47. | 39. |
| | M1 | 66. | 49. | 38. |
| | M3 | 22215. | 17179. | 14851. |
| Bent 2 | V2 | 188. | 142. | 125. |
| | M2 (Deck) | 3259. | 2558. | 1879. |
| Abut. 4 | V2 | 347. | 250. | 229. |
| | M3 | 21456. | 15526. | 14222. |
| | DT | .0068 | .0054 | .0044 |
| Column Base: | | | | |
| Bent 2 | P1 | 156. | 124. | 93. |
| | M2 | 112. | 89. | 78. |
| | M3 | 943. | 699. | 610. |

Table A3.26 Maximum Stresses in Bridge Deck and Columns For Different Damping Ratios, (ksi)

| Location | Material | 2% | 5% | 10% |
|---|---|---|---|---|
| Deck: | | | | |
| Abut. 1 | Steel | 3.52 | 2.96 | 2.38 |
| | Conc. | 0.68 | 0.56 | 0.45 |
| Span 1 | Steel | 1.78 | 1.22 | 1.12 |
| | Conc. | 0.23 | 0.17 | 0.13 |
| Bent 2 | Steel | 2.39 | 1.88 | 1.37 |
| | Conc. | 0.28 | 0.18 | 0.15 |
| Span 2 | Steel | 2.78 | 1.97 | 1.62 |
| | Conc. | 0.44 | 0.36 | 0.31 |
| Column Base: | | | | |
| Bent 2 | Conc. | 1.70 | 1.26 | 1.09 |

Table A3.27 Structure Period For Composite Deck, Non-Composite Deck, Rotational Inertia, and Long Columns Models

| Mode | Composite Deck | | | Non-Composite Deck | | | Rotational Inertia | | | Long Columns | | |
|---|---|---|---|---|---|---|---|---|---|---|---|---|
| | Period (sec) | Frequency (Hz) | Mode Shape Direction | Period (sec) | Frequency (Hz) | Mode Shape Direction | Period (sec) | Frequency (Hz) | Mode Shape Direction | Period (sec) | Frequency (Hz) | Mode Shape Direction |
| 1 | .265 | 3.77 | Y | .457 | 2.19 | Y | .266 | 3.76 | Y | .265 | 3.77 | Y |
| 2 | .217 | 4.60 | Y | .349 | 2.86 | Y | .218 | 4.58 | Y | .208 | 4.80 | Y |
| 3 | .167 | 5.98 | Y | .240 | 4.17 | Y | .173 | 5.79 | Y | .185 | 5.40 | Z&X |
| 4 | .144 | 6.95 | Z&X | .178 | 5.60 | Z&X | .166 | 6.04 | Y | .148 | 6.78 | Y |
| 5 | .097 | 10.30 | X&Z | .138 | 7.25 | X&Z | .156 | 6.43 | X[Rot.] | .125 | 7.99 | X&Z(Col.) |
| 6 | .083 | 12.08 | Y | .112 | 8.90 | Y | .148 | 6.77 | X[Rot.] | .125 | 7.99 | X&Z(Col.) |
| 7 | .074 | 13.49 | Y | .107 | 9.30 | Y | .144 | 6.95 | Z&X | .107 | 9.39 | X&Z(Col.) |
| 8 | .069 | 14.52 | X&Z(Col.) | .101 | 9.87 | Y | .097 | 10.30 | X&Z | .102 | 9.78 | X&Z(Col.) |
| 9 | .069 | 14.52 | X&Z(Col.) | .087 | 11.47 | Z&X | .087 | 11.51 | X[Rot.] | .095 | 10.56 | X&Z |
| 10 | .066 | 15.16 | Y | .069 | 14.52 | X&Z(Col.) | .082 | 12.12 | Y | .076 | 13.08 | Z&X(Col.) |
| 11 | .062 | 16.10 | Z&X | .069 | 14.52 | X&Z(Col.) | .081 | 12.39 | X[Rot.] | .072 | 13.86 | Z&X(Col.) |
| 12 | .045 | 22.39 | Y | .063 | 15.99 | Y | .077 | 12.96 | X[Rot.] | .071 | 14.18 | Z&X(Col.) |
| 13 | .044 | 22.50 | X&Z(Col.) | .056 | 17.98 | Y | .074 | 13.51 | Y | .070 | 14.19 | Z&X(Col.) |
| 14 | .042 | 23.58 | X&Z(Col.) | .052 | 19.24 | X&Z | .066 | 15.10 | Y | .066 | 15.16 | Y |
| 15 | .036 | 27.91 | Y | .049 | 20.23 | Y | .062 | 16.10 | Z&X | .064 | 15.57 | Y |

Table A3.28 Maximum Actions and Displacements at the Attachments and Column Base For Composite Deck, Non-Composite Deck, Rotational Inertia and Long Columns Models, (k,ft)

| Location | Component | Composite Deck | Non-Composite Deck | Rotational Inertia | Long Columns |
|---|---|---|---|---|---|
| Abut. 1 | P1 | 518. | 712. | 512. | 492. |
| | V2 | 291. | 233. | 291. | 551. |
| | V3 | 47. | 45. | 49. | 69. |
| | M1 | 49. | 28. | 193. | 61. |
| | M3 | 17179. | 13881. | 17188. | 34894. |
| Bent 2 | V2 | 142. | 294. | 142. | 33. |
| | M2(Deck) | 2558. | 1668. | 2510. | 2867. |
| Abut. 4 | V2 | 250. | 222. | 250. | 535. |
| | M3 | 15526. | 13311. | 15528. | 33878. |
| | DT | .0054 | .0112 | .0054 | .0074 |
| Column Base: Bent 2 | P1 | 124. | 111. | 119. | 126. |
| | M2 | 89. | 206. | 78. | 132. |
| | M3 | 699. | 1308. | 694. | 250. |

Table A3.29 Maximum Stresses in Bridge Deck and Columns For Composite Deck, Non-Composite Deck, Rotational Inertia and Long Columns Models, (ksi)

| Location | Material | Composite Deck | Non-Composite Deck | Rotational Inertia | Long Columns |
|---|---|---|---|---|---|
| Deck: | | | | | |
| Abut. 1 | Steel | 2.96 | 5.25 | 2.95 | 5.33 |
| | Conc. | 0.56 | 0. | 0.56 | 1.05 |
| | Steel($\tau$) | 1.15 | 2.43 | 1.15 | 2.16 |
| | Conc.($\tau$) | 0.05 | 0. | 0.05 | 0.09 |
| Span 1 | Steel | 1.22 | 2.64 | 1.24 | 1.61 |
| | Conc. | 0.17 | 0. | 0.17 | 0.29 |
| Bent 2 | Steel | 1.88 | 2.70 | 1.84 | 2.26 |
| | Conc. | 0.18 | 0. | 0.18 | 0.39 |
| Span 2 | Steel | 1.97 | 4.58 | 1.98 | 3.37 |
| | Conc. | 0.36 | 0. | 0.37 | 0.66 |
| Column Base: | | | | | |
| Bent 2 | Conc. | 1.26 | 2.33 | 1.24 | 0.46 |
| | Conc.($\tau$) | 0.10 | 0.18 | 0.10 | 0.02 |

Table A3.30 Structure Period For 2-Column and Rigid-Column Straight Models

| Mode | 2-Column | | | Rigid-Column | | | Exact Solution | | |
|---|---|---|---|---|---|---|---|---|---|
| | Period (sec) | Frequency (Hz) | Mode Shape Direction | Period (sec) | Frequency (Hz) | Mode Shape Direction | Period (sec) | Frequency (Hz) | Mode Shape Direction |
| 1 | .265 | 3.77 | Y | .265 | 3.77 | Y | .265 | 3.77 | Y |
| 2 | .220 | 4.54 | Y | .201 | 4.84 | Y | .206 | 4.84 | Y |
| 3 | .171 | 5.85 | Y | .142 | 7.06 | Y | .142 | 7.06 | Y |
| 4 | .137 | 7.31 | Z | .100 | 9.99 | X | | | |
| 5 | .101 | 9.89 | X | .066 | 15.08 | Y | .118 | 8.49 | Y |
| 6 | .082 | 12.25 | Y | .058 | 17.18 | Y | .058 | 17.19 | Y |
| 7 | .074 | 13.57 | Y | .047 | 21.04 | Y | .047 | 21.10 | Y |
| 8 | .069 | 14.52 | X(Col.) | .034 | 29.83 | Z | .034 | 29.84 | Z |
| 9 | .069 | 14.52 | X(Col.) | .033 | 29.88 | X | | | |
| 10 | .066 | 15.08 | Y | .030 | 33.72 | Y | | | |

Table A3.31 Maximum Actions at the Attachments For 2-Column and Rigid-Column Straight Models, (k,ft)

| Location | Component | 2-Column | Rigid-Column |
|---|---|---|---|
| Abut. 1 | P1 | 535. | 524. |
| | V2 | 312. | 0. |
| | V3 | 47. | 68. |
| | M1 | 17. | 0. |
| | M3 | 19852. | 0. |
| Bent 2 | M2(Deck) | 2303. | 2861. |
| Abut. 4 | V2 | 312. | 0. |
| | M3 | 19852. | 0. |

Table A3.32 Maximum Stresses in Bridge-Deck For 2-Column and Rigid-Column Straight Models, (ksi)

| Location | Material | 2-Column | Rigid-Column |
|---|---|---|---|
| Abut. 1 | Steel | 3.06 | 0.56 |
| | Conc. | 0.60 | 0.07 |
| Span 1 | Steel | 1.31 | 1.20 |
| | Conc. | 0.14 | 0.12 |
| Bent 2 | Steel | 2.10 | 2.58 |
| | Conc. | 0.21 | 0.17 |
| Span 2 | Steel | 1.99 | 2.05 |
| | Conc. | 0.40 | 0.14 |

Table A3.33 Maximum Stresses in Bridge Deck and Columns Due to Dead Load, (ksi)

| Location | Material | Stress |
|---|---|---|
| Deck: | | |
| Span 1 | Steel | 4.80 |
| | Conc. | 0.30 |
| Bent 2 | Steel | 6.80 |
| Span 2 | Steel | 2.60 |
| | Conc. | 0.16 |
| Column Base: | | |
| Bent 2 | Conc. | 0.88 |

## A.4 4-Span Curved Bridges

Table A4.1 Structure Period and Participation Factors

| Mode | Period (sec) | Frequency (Hz) | Participation Factor | | |
|---|---|---|---|---|---|
| | | | X | Y | Z |
| 1 | .266 | 3.76 | 0. | 0. | 0. |
| 2 | .235 | 4.27 | 0. | 3.00 | 0. |
| 3 | .190 | 5.26 | 3.31 | 0. | -7.38 |
| 4 | .188 | 5.32 | -0.02 | 0. | 0.05 |
| 5 | .161 | 6.23 | 0. | 7.89 | 0. |
| 6 | .126 | 7.96 | -7.69 | 0. | -2.69 |
| 7 | .102 | 9.81 | 0.22 | 0. | -0.24 |
| 8 | .084 | 11.89 | 0. | 0.43 | 0. |
| 9 | .079 | 12.63 | 0. | 0. | 0. |
| 10 | .072 | 13.98 | 0. | 1.37 | 0. |
| 11 | .069 | 14.52 | 0. | 0. | 0. |
| 12 | .069 | 14.52 | 0. | 0. | 0. |
| 13 | .069 | 14.52 | 0. | 0. | 0. |
| 14 | .066 | 15.14 | 0. | 0. | 0. |
| 15 | .057 | 17.61 | 0.14 | 0. | 3.24 |
| 16 | .049 | 20.53 | -2.41 | 0.04 | -0.53 |
| 17 | .047 | 21.24 | 0.05 | 2.22 | 0. |
| 18 | .044 | 22.78 | 0.42 | 0.01 | 0.12 |
| 19 | .042 | 23.57 | 0.45 | -0.02 | -0.08 |
| 20 | .040 | 24.98 | 0.04 | 0. | 0. |

Table A4.2 Maximum Actions at the Attachments and Column Base, (k,ft),(10,15, and 20 Frequencies)

| Location | Component | Long. Shock (T.H.) | | Trans. Shock (T.H.) | | Vert. Shock (T.H.) | | 3-Direction Shock (T.H.) | |
|---|---|---|---|---|---|---|---|---|---|
| | | 10 | 15 | 10 | 15 | 10 | 15 | 15 | 20 |
| Abut. 1 | P1 | 1387. | 1387. | 648. | 647. | 0. | 0. | 871. | 888. |
| | V2 | 201. | 202. | 244. | 267. | 0. | 0. | 301. | 302. |
| | V3 | 0. | 0. | 0. | 0. | 110. | 110. | 52. | 49. |
| | M3 | 8459. | 8483. | 17184. | 18548. | 9. | 10. | 21038. | 21032. |
| Bent 2 | V2 | 95. | 95. | 193. | 191. | 0. | 0. | 221. | 221. |
| | M2(Deck) | 3. | 3. | 6. | 6. | 3844. | 3844. | 2099. | 2085. |
| Bent 3 | V2 | 190. | 190. | 349. | 351. | 0. | 0. | 408. | 408. |
| | M2(Deck) | 6. | 6. | 11. | 11. | 4508. | 4508. | 3238. | 3217. |
| Abut. 5 | V2 | 123. | 123. | 189. | 236. | 0. | 0. | 268. | 268. |
| | M3 | 10031. | 10018. | 15501. | 16984. | 8. | 8. | 19520. | 19523. |
| Column Base: | | | | | | | | | |
| Bent 2 | P1 | 26. | 26. | 53. | 54. | 188. | 188. | 119. | 116. |
| | M2 | 182. | 182. | 98. | 98. | 4. | 4. | 129. | 140. |
| | M3 | 423. | 423. | 845. | 873. | 174. | 174. | 1007. | 1007. |
| Bent 3 | P1 | 54. | 54. | 96. | 95. | 225. | 225. | 156. | 157. |
| | M2 | 341. | 341. | 239. | 239. | 0. | 0. | 305. | 310. |
| | M3 | 867. | 866. | 1534. | 1515. | 208. | 208. | 1759. | 1758. |

Table A4.3 Maximum Stresses in Bridge Deck and Columns, (ksi),(10,15, and 20 Frequencies)

| Location | Material | Long. Shock (T.H.) | | Trans. Shock (T.H.) | | Vert. Shock (T.H.) | | 3-Direction Shock (T.H.) | |
|---|---|---|---|---|---|---|---|---|---|
| | | 10 | 15 | 10 | 15 | 10 | 15 | 15 | 20 |
| Deck: | | | | | | | | | |
| Abut. 1 | Steel | 2.74 | 2.74 | 3.20 | 3.23 | 0. | 0. | 3.93 | 3.95 |
| | Conc. | 0.43 | 0.44 | 0.59 | 0.59 | 0. | 0. | 0.72 | 0.72 |
| Span 1 | Steel | 1.69 | 1.69 | 1.59 | 1.58 | 2.83 | 2.83 | 2.06 | 2.08 |
| | Conc. | 0.24 | 0.24 | 0.27 | 0.26 | 0.19 | 0.19 | 0.34 | 0.35 |
| Bent 2 | Steel | 1.51 | 1.51 | 0.70 | 0.73 | 2.76 | 2.76 | 1.49 | 1.49 |
| | Conc. | 0.21 | 0.21 | 0.09 | 0.10 | 0.21 | 0.21 | 0.15 | 0.15 |
| Span 2 | Steel | 1.69 | 1.69 | 1.94 | 1.93 | 2.25 | 2.25 | 2.45 | 2.46 |
| | Conc. | 0.24 | 0.24 | 0.34 | 0.34 | 0.15 | 0.15 | 0.43 | 0.43 |
| Bent 3 | Steel | 1.24 | 1.24 | 1.29 | 1.28 | 3.24 | 3.24 | 2.34 | 2.33 |
| | Conc. | 0.18 | 0.18 | 0.22 | 0.21 | 0.24 | 0.24 | 0.25 | 0.24 |
| Column Base: | | | | | | | | | |
| Bent 2 | Conc. | 0.76 | 0.76 | 1.51 | 1.56 | 0.45 | 0.45 | 1.80 | 1.80 |
| Bent 3 | Conc. | 1.55 | 1.55 | 2.75 | 2.71 | 0.54 | 0.54 | 3.15 | 3.15 |

Table A4.4 Maximum Actions and Displacements at the Attachments and Column Base Due to a Longitudinal Shock (S00E), (R.S. & T.H. Analysis), (k,ft)

| Location | Component | 10 Frequencies | | 15 Frequencies | | 20 Frequencies |
|---|---|---|---|---|---|---|
| | | R.S. | T.H. | R.S. | T.H. | R.S. |
| Abut. 1 | P1 | 1249. | 1387. | 1249. | 1387. | 1251. |
| | V2 | 149. | 201. | 149. | 202. | 149. |
| | V3 | 0. | 0. | 0. | 0. | 6. |
| | M1 | 8. | 9. | 8. | 9. | 8. |
| | M3 | 7884. | 8459. | 7885. | 8483. | 7885. |
| Bent 2 | V2 | 90. | 95. | 90. | 95. | 90. |
| | M2(Deck) | 18. | 3. | 18. | 3. | 91. |
| Bent 3 | V2 | 173. | 190. | 173. | 190. | 173. |
| | M2(Deck) | 5. | 6. | 5. | 6. | 7. |
| Abut. 5 | V2 | 119. | 123. | 119. | 123. | 119. |
| | M3 | 9623. | 10031. | 9624. | 10018. | 9624. |
| | DT | .0104 | .0133 | .0104 | .0133 | .0104 |
| Column Base: | | | | | | |
| Bent 2 | P1 | 25. | 26. | 25. | 26. | 26. |
| | M2 | 159. | 182. | 159. | 182. | 164. |
| | M3 | 397. | 423. | 397. | 423. | 397. |
| Bent 3 | P1 | 49. | 54. | 49. | 54. | 49. |
| | M2 | 281. | 341. | 281. | 341. | 282. |
| | M3 | 789. | 867. | 789. | 866. | 789. |

Table A4.5 Maximum Actions and Displacements at the Attachments and Column Base Due to a Transverse Shock (S00E), (R.S. & T.H. Analysis), (k,ft)

| Location | Component | 10 Frequencies | | 15 Frequencies | | 20 Frequencies |
|---|---|---|---|---|---|---|
| | | R.S. | T.H. | R.S. | T.H. | R.S. |
| Abut. 1 | P1 | 614. | 648. | 614. | 647. | 615. |
| | V2 | 233. | 244. | 244. | 267. | 244. |
| | V3 | 1. | 0. | 1. | 0. | 15. |
| | M1 | 18. | 18. | 18. | 19. | 18. |
| | M3 | 17270. | 17184. | 17470. | 18548. | 17470. |
| Bent 2 | V2 | 196. | 193. | 196. | 191. | 196. |
| | M2(Deck) | 39. | 6. | 39. | 6. | 43. |
| Bent 3 | V2 | 353. | 349. | 353. | 351. | 353. |
| | M2(Deck) | 10. | 11. | 10. | 11. | 10. |
| Abut. 5 | V2 | 186. | 189. | 200. | 236. | 200. |
| | M3 | 15160. | 15501. | 15380. | 16984. | 15380. |
| | DT | .0107 | .0115 | .0107 | .0116 | .0107 |
| Column Base: | | | | | | |
| Bent 2 | P1 | 55. | 53. | 55. | 54. | 55. |
| | M2 | 90. | 98. | 90. | 98. | 91. |
| | M3 | 860. | 845. | 861. | 873. | 861. |
| Bent 3 | P1 | 97. | 96. | 97. | 95. | 97. |
| | M2 | 218. | 239. | 218. | 239. | 218. |
| | M3 | 1547. | 1534. | 1548. | 1515. | 1548. |

Table A4.6 Maximum Actions at the Attachments and Column Base Due to a Vertical Shock (S00E), (R.S. & T.H. Analysis), (k,ft)

| Location | Component | 10 Frequencies | | 15 Frequencies | |
|---|---|---|---|---|---|
| | | R.S. | T.H. | R.S. | T.H. |
| Abut. 1 | P1 | 0. | 0. | 0. | 0. |
| | V2 | 0. | 0. | 0. | 0. |
| | V3 | 98. | 110. | 98. | 110. |
| | M1 | 104. | 116. | 104. | 116. |
| | M3 | 12. | 9. | 12. | 10. |
| Bent 2 | V2 | 0. | 0. | 0. | 0. |
| | V3(Deck) | 150. | 177. | 150. | 177. |
| | M2(Deck) | 3179. | 3844. | 3179. | 3844. |
| Bent 3 | V2 | 0. | 0. | 0. | 0. |
| | V3(Deck) | 200. | 202. | 200. | 202. |
| | M2(Deck) | 4495. | 4508. | 4495. | 4508. |
| Abut. 5 | V2 | 0. | 0. | 0. | 0. |
| | M3 | 11. | 8. | 11. | 8. |
| Column Base: | | | | | |
| Bent 2 | P1 | 158. | 188. | 158. | 188. |
| | M2 | 5. | 4. | 5. | 4. |
| | M3 | 146. | 174. | 146. | 174. |
| Bent 3 | P1 | 223. | 225. | 223. | 225. |
| | M2 | 0. | 0. | 0. | 0. |
| | M3 | 206. | 208. | 206. | 208. |

Table A4.7 Maximum Actions at the Attachments and Column Base Due to El Centro Earthquake (S90W) and (VERT) Components, (R.S. & T.H. Analysis), (k,ft)

| Location | Component | Longitudinal Shock (S90W) | | Vertical Shock (VERT) | |
|---|---|---|---|---|---|
| | | R.S. | T.H. | R.S. | T.H. |
| Abut. 1 | P1 | 586. | 626. | 0. | 0. |
| | V2 | 91. | 97. | 0. | 0. |
| | V3 | 0. | 0. | 46. | 52. |
| | M1 | 6. | 6. | 40. | 46. |
| | M3 | 5797. | 5958. | 6. | 5. |
| Bent 2 | V2 | 66. | 63. | 0. | 0. |
| | V3(Deck) | 0. | 0. | 85. | 83. |
| | M2(Deck) | 13. | 2. | 2251. | 2099. |
| Bent 3 | V2 | 122. | 109. | 0. | 0. |
| | V3(Deck) | 0. | 0. | 145. | 147. |
| | M2(Deck) | 4. | 3. | 3185. | 3237. |
| Abut. 5 | V2 | 73. | 52. | 0. | 0. |
| | M3 | 5912. | 4292. | 5. | 4. |
| Column Base: | | | | | |
| Bent 2 | P1 | 19. | 17. | 115. | 109. |
| | M2 | 75. | 82. | 2. | 2. |
| | M3 | 290. | 277. | 106. | 101. |
| Bent 3 | P1 | 34. | 30. | 163. | 164. |
| | M2 | 139. | 156. | 0. | 0. |
| | M3 | 543. | 474. | 151. | 152. |

Table A4.8 Maximum Actions and Displacements at the Attachments and Column Base Due to El Centro Earthquake Different Components, (k,ft)

| Location | Component | Longitudinal Shock (S90W) | | Transverse Shock (S00E) | | Vertical Shock (VERT) | | 3-Direction Shock | |
|---|---|---|---|---|---|---|---|---|---|
| | | Response | Time (sec) | Response | Time (sec) | Response | Time (sec) | Response | Time (sec) |
| Abut. 1 | P1 | 626. | 1.92 | 647. | 2.68 | 0. | 0.95 | 871. | 2.68 |
| | V2 | 97. | 1.93 | 267. | 2.26 | 0. | 0.86 | 301. | 2.67 |
| | V3 | 0. | 2.85 | 0. | 2.88 | 52. | 3.35 | 52. | 3.35 |
| | M1 | 6. | 4.61 | 19. | 2.26 | 46. | 3.35 | 43. | 1.04 |
| | M3 | 5958. | 4.60 | 18548. | 2.26 | 5. | 0.86 | 21038. | 2.26 |
| Bent 2 | V2 | 63. | 4.61 | 191. | 2.26 | 0. | 0.78 | 221. | 2.26 |
| | V3(Deck) | 0. | 4.83 | 0. | 2.99 | 83. | 3.34 | 83. | 3.34 |
| | M2(Deck) | 2. | 4.84 | 6. | 2.25 | 2099. | 0.63 | 2099. | 0.63 |
| Bent 3 | V2 | 109. | 4.61 | 351. | 2.26 | 0. | 0.77 | 408. | 2.26 |
| | V3(Deck) | 0. | 4.55 | 0. | 2.73 | 147. | 0.63 | 147. | 0.63 |
| | M2(Deck) | 3. | 4.60 | 11. | 2.67 | 3237. | 0.63 | 3238. | 0.63 |
| Abut. 5 | V2 | 52. | 4.61 | 236. | 2.26 | 0. | 0.86 | 268. | 2.26 |
| | M3 | 4292. | 4.61 | 16984. | 2.26 | 4. | 0.86 | 19520. | 2.26 |
| | DT | .0062 | 1.93 | .0116 | 2.68 | 0. | 0.95 | .0144 | 2.67 |
| Column Base: | | | | | | | | | |
| Bent 2 | P1 | 17. | 4.61 | 54. | 2.26 | 109. | 0.63 | 119. | 3.34 |
| | M2 | 82. | 1.92 | 98. | 2.68 | 2. | 0.63 | 129. | 2.68 |
| | M3 | 277. | 4.61 | 873. | 2.26 | 101. | 0.63 | 1007. | 2.26 |
| Bent 3 | P1 | 30. | 4.61 | 95. | 2.48 | 164. | 0.63 | 156. | 0.63 |
| | M2 | 156. | 1.93 | 239. | 2.68 | 0. | 0.95 | 305. | 2.67 |
| | M3 | 474. | 4.61 | 1515. | 2.48 | 152. | 0.63 | 1759. | 2.26 |

Table A4.9 Maximum Stresses in Bridge Deck and Columns Due to El Centro Earthquake Different Components, (ksi)

| Location | Material | Longitudinal Shock (S90W) | | Transverse Shock (S00E) | | Vertical Shock (VERT) | | 3-Direction Shock | |
|---|---|---|---|---|---|---|---|---|---|
| | | Stress | Time (sec) | Stress | Time (sec) | Stress | Time (sec) | Stress | Time (sec) |
| Deck: | | | | | | | | | |
| Abut. 1 | Steel | 1.32 | 1.93 | 3.23 | 2.68 | 0. | 0.86 | 3.93 | 2.67 |
| | Conc. | 0.22 | 4.60 | 0.59 | 2.68 | 0. | 0.86 | 0.72 | 2.67 |
| Span 1 | Steel | 0.75 | 1.93 | 1.58 | 2.67 | 1.13 | 3.35 | 2.06 | 2.67 |
| | Conc. | 0.10 | 4.60 | 0.26 | 2.67 | 0.08 | 3.35 | 0.34 | 2.67 |
| Bent 2 | Steel | 0.68 | 1.93 | 0.73 | 2.68 | 1.51 | 0.63 | 1.49 | 0.55 |
| | Conc. | 0.09 | 1.93 | 0.10 | 2.68 | 0.11 | 0.63 | 0.15 | 3.47 |
| Span 2 | Steel | 0.82 | 1.93 | 1.93 | 2.67 | 1.61 | 0.63 | 2.45 | 2.67 |
| | Conc. | 0.13 | 4.60 | 0.34 | 2.67 | 0.11 | 0.63 | 0.43 | 2.67 |
| Bent 3 | Steel | 0.49 | 4.60 | 1.28 | 2.67 | 2.32 | 0.63 | 2.34 | 0.63 |
| | Conc. | 0.08 | 4.60 | 0.21 | 2.67 | 0.17 | 0.63 | 0.25 | 2.88 |
| Column Base: | | | | | | | | | |
| Bent 2 | Conc. | 0.50 | 4.61 | 1.56 | 2.26 | 0.26 | 0.63 | 1.80 | 2.26 |
| Bent 3 | Conc. | 0.85 | 4.61 | 2.71 | 2.48 | 0.39 | 0.63 | 3.15 | 2.26 |

Table A4.10 Maximum Actions and Displacements at the Attachments and Column Base For Different Damping Ratios, (k,ft)

| Location | Component | 2% | 5% | 10% |
|---|---|---|---|---|
| Abut. 1 | P1 | 1147. | 871. | 646. |
| | V2 | 389. | 301. | 249. |
| | V3 | 67. | 52. | 46. |
| | M1 | 56. | 43. | 37. |
| | M3 | 26540. | 21038. | 18060. |
| Bent 2 | V2 | 290. | 221. | 191. |
| | M2(Deck) | 2665. | 2099. | 1655. |
| Bent 3 | V2 | 507. | 408. | 354. |
| | M2(Deck | 4152. | 3238. | 2273. |
| Abut. 5 | V2 | 296. | 268. | 231. |
| | M3 | 22240. | 19520. | 16995. |
| | DT | .0187 | .0144 | .0105 |
| Column Base: | | | | |
| Bent 2 | P1 | 167. | 119. | 97. |
| | M2 | 165. | 129. | 96. |
| | M3 | 1289. | 1007. | 863. |
| Bent 3 | P1 | 212. | 156. | 111. |
| | M2 | 393. | 305. | 223. |
| | M3 | 2222. | 1759. | 1527. |

Table A4.11 Maximum Stresses in Bridge Deck and Columns For Different Damping Ratios, (ksi)

| Location | Material | 2% | 5% | 10% |
|---|---|---|---|---|
| Deck: | | | | |
| Abut. 1 | Steel | 5.08 | 3.93 | 2.92 |
| | Conc. | 0.93 | 0.72 | 0.56 |
| Span 1 | Steel | 2.67 | 2.06 | 1.50 |
| | Conc. | 0.45 | 0.34 | 0.25 |
| Bent 2 | Steel | 2.04 | 1.49 | 1.17 |
| | Conc. | 0.18 | 0.15 | 0.13 |
| Span 2 | Steel | 3.12 | 2.45 | 1.81 |
| | Conc. | 0.54 | 0.43 | 0.32 |
| Bent 3 | Steel | 2.98 | 2.34 | 1.65 |
| | Conc. | 0.35 | 0.25 | 0.19 |
| Column Base: | | | | |
| Bent 2 | Conc. | 2.33 | 1.80 | 1.54 |
| Bent 3 | Conc. | 3.99 | 3.15 | 2.73 |

Table A4.12 Structure Period For Composite Deck, Non-Composite Deck, Rotational Inertia, and Long Columns Models

| Mode | Composite Deck | | | Non-Composite Deck | | | Rotational Inertia | | | Long Columns | | |
|---|---|---|---|---|---|---|---|---|---|---|---|---|
| | Period (sec) | Frequency (Hz) | Mode Shape Direction | Period (sec) | Frequency (Hz) | Mode Shape Direction | Period (sec) | Frequency (Hz) | Mode Shape Direction | Period (sec) | Frequency (Hz) | Mode Sha Directio |
| 1 | .266 | 3.76 | Y | .457 | 2.19 | Y | .267 | 3.75 | Y | .327 | 3.06 | Z&X |
| 2 | .235 | 4.27 | Y | .386 | 2.59 | Y | .236 | 4.24 | Y | .266 | 3.76 | Y |
| 3 | .190 | 5.26 | Z&X | .286 | 3.50 | Y | .190 | 5.25 | Z&X | .228 | 4.38 | Y |
| 4 | .188 | 5.32 | Y | .224 | 4.46 | Y | .189 | 5.30 | Y | .173 | 5.77 | Y |
| 5 | .161 | 6.23 | Y | .217 | 4.61 | Z&X | .174 | 5.76 | X[Rot.] | .139 | 7.21 | Y |
| 6 | .126 | 7.96 | X&Z | .171 | 5.84 | X&Z | .162 | 6.18 | X[Rot.] | .133 | 7.49 | X&Z |
| 7 | .102 | 9.81 | Z | .136 | 7.36 | Z | .160 | 6.24 | Y | .125 | 7.99 | X(Col.) |
| 8 | .084 | 11.89 | Y | .112 | 8.90 | Y | .151 | 6.62 | X[Rot.] | .125 | 7.99 | X(Col.) |
| 9 | .079 | 12.63 | Y | .109 | 9.14 | Y | .147 | 6.81 | X[Rot.] | .125 | 7.99 | X(Col.) |
| 10 | .072 | 13.98 | Y | .104 | 9.63 | Y | .126 | 7.96 | X&Z | .116 | 8.63 | Z |
| 11 | .069 | 14.52 | X(Col.) | .101 | 9.95 | Y | .102 | 9.81 | Z | .103 | 9.77 | X(Col.) |
| 12 | .069 | 14.52 | X(Col.) | .080 | 12.48 | Z | .088 | 11.36 | X[Rot.] | .102 | 9.79 | X(Col.) |

Table A4.13 Maximum Actions and Displacements at the Attachments and Column Base For Composite Deck, Non-Composite Deck, Rotational Inertia, and Long Columns Models, (k,ft)

| Location | Component | Composite Deck | Non-Composite Deck | Rotational Inertia | Long Columns |
|---|---|---|---|---|---|
| Abut. 1 | P1 | 871. | 1122. | 870. | 819. |
| | V2 | 301. | 222. | 297. | 767. |
| | V3 | 52. | 48. | 48. | 63. |
| | M1 | 43. | 35. | 146. | 69. |
| | M3 | 21038. | 12375. | 20249. | 60917. |
| Bent 2 | V2 | 221. | 290. | 221. | 2. |
| | M2(Deck) | 2099. | 1401. | 2061. | 2929. |
| Bent 3 | V2 | 408. | 510. | 402. | 9. |
| | M2(Deck) | 3238. | 2070. | 3194. | 3644. |
| Abut. 5 | V2 | 268. | 154. | 217. | 635. |
| | M3 | 19520. | 9372. | 17635. | 53755. |
| | DT | .0144 | .0291 | .0144 | .0287 |
| Column Base: | | | | | |
| Bent 2 | P1 | 119. | 81. | 114. | 143. |
| | M2 | 129. | 311. | 129. | 101. |
| | M3 | 1007. | 1217. | 980. | 393. |
| Bent 3 | P1 | 156. | 139. | 148. | 187. |
| | M2 | 305. | 637. | 304. | 137. |
| | M3 | 1759. | 2186. | 1778. | 696. |

Table A4.14 Maximum Stresses in Bridge Deck and Columns For Composite Deck, Non-Composite Deck, Rotational Inertia, and Long Columns Models, (ksi)

| Location | Material | Composite Deck | Non-Composite Deck | Rotational Inertia | Long Columns |
|---|---|---|---|---|---|
| Deck: | | | | | |
| Abut. 1 | Steel | 3.93 | 6.80 | 3.90 | 9.81 |
| | Conc. | 0.72 | 0. | 0.71 | 1.89 |
| | Steel (τ) | 1.18 | 2.32 | 1.22 | 2.97 |
| | Conc. (τ) | 0.05 | 0. | 0.04 | 0.13 |
| Span 1 | Steel | 2.06 | 3.63 | 2.05 | 4.44 |
| | Conc. | 0.34 | 0. | 0.34 | 0.82 |
| Bent 2 | Steel | 1.49 | 3.59 | 1.47 | 2.32 |
| | Conc. | 0.15 | 0. | 0.13 | 0.29 |
| Span 2 | Steel | 2.45 | 4.84 | 2.44 | 5.01 |
| | Conc. | 0.43 | 0. | 0.43 | 0.94 |
| Bent 3 | Steel | 2.34 | 3.54 | 2.31 | 5.25 |
| | Conc. | 0.25 | 0. | 0.26 | 0.97 |
| Column Base: | | | | | |
| Bent 2 | Conc. | 1.80 | 2.17 | 1.77 | 0.73 |
| | Conc. (τ) | 0.14 | 0.17 | 0.14 | 0.02 |
| Bent 3 | Conc. | 3.15 | 3.90 | 3.18 | 1.29 |
| | Conc. (τ) | 0.24 | 0.30 | 0.24 | 0.03 |

Table A4.15 Maximum Stresses in Bridge Deck and Columns Due to Dead Load, (ksi)

| Location | Material | Stress |
|---|---|---|
| Deck: | | |
| Span 1 | Steel | 4.69 |
| | Conc. | 0.29 |
| Bent 2 | Steel | 7.06 |
| Span 2 | Steel | 2.85 |
| | Conc. | 0.18 |
| Bent 3 | Steel | 5.65 |
| Column Base: | | |
| Bent 2 | Conc. | 0.89 |
| Bent 3 | Conc. | 0.79 |

## A.5 5-Span Curved Bridges

Table A5.1 Structure Period and Participation Factors

| Mode | Period (sec) | Frequency (Hz) | Participation Factor X | Y | Z |
|---|---|---|---|---|---|
| 1 | .266 | 3.76 | 0. | 1.73 | 0. |
| 2 | .244 | 4.10 | 0. | 0. | 0. |
| 3 | .217 | 4.62 | 4.81 | 0. | -7.87 |
| 4 | .205 | 4.88 | 0. | 3.13 | 0.01 |
| 5 | .174 | 5.74 | 0. | 0. | 0. |
| 6 | .158 | 6.34 | 0. | -8.81 | 0. |
| 7 | .151 | 6.62 | 7.83 | 0. | 3.69 |
| 8 | .137 | 7.28 | -1.79 | 0. | -1.33 |
| 9 | .085 | 11.81 | 0. | 0. | 0. |
| 10 | .084 | 11.84 | 0.41 | 0. | 3.73 |
| 11 | .082 | 12.27 | 0. | -0.61 | 0. |
| 12 | .076 | 13.11 | 0. | 0. | 0. |
| 13 | .070 | 14.30 | 0. | 1.35 | 0. |
| 14 | .069 | 14.52 | 0. | 0. | 0. |
| 15 | .069 | 14.52 | 0. | 0. | 0. |
| 16 | .066 | 15.14 | 0.02 | 0. | 0. |
| 17 | .058 | 17.24 | 3.11 | 0. | 0.72 |
| 18 | .054 | 18.63 | -0.06 | 0. | 0.20 |
| 19 | .048 | 20.64 | 0. | 2.54 | 0. |
| 20 | .045 | 22.39 | -0.77 | -0.02 | -0.21 |

Table A5.2 Maximum Actions at the Attachments and Column Base, (k,ft),(10,15, and 20 Frequencies)

| Location | Component | Long Shock (T.H.) | | Trans. Shock (T.H.) | | Vert. Shock (T.H.) | | 3-Direction Shock (T.H.) | |
|---|---|---|---|---|---|---|---|---|---|
| | | 10 | 15 | 10 | 15 | 10 | 15 | 15 | 20 |
| Abut. 1 | P1 | 1130. | 1130. | 779. | 779. | 0. | 0. | 1175. | 1188. |
| | V2 | 196. | 195. | 252. | 253. | 0. | 0. | 290. | 290. |
| | V3 | 0. | 0. | 0. | 0. | 94. | 92. | 52. | 47. |
| | M3 | 10640. | 10641. | 15719. | 15718. | 6. | 7. | 20506. | 20651. |
| Bent 2 | V2 | 106. | 106. | 189. | 189. | 0. | 0. | 248. | 248. |
| | M2(Deck) | 5. | 5. | 7. | 7. | 3227. | 3227. | 1909. | 1902. |
| Bent 3 | V2 | 240. | 240. | 436. | 436. | 0. | 0. | 534. | 534. |
| | M2(Deck) | 6. | 6. | 12. | 12. | 3560. | 3551. | 3000. | 2981. |
| Abut. 6 | V2 | 101. | 101. | 160. | 160. | 0. | 0. | 183. | 187. |
| | M3 | 8629. | 8629. | 12229. | 12230. | 5. | 5. | 15613. | 15692. |
| Column Base: | | | | | | | | | |
| Bent 2 | P1 | 29. | 29. | 49. | 49. | 159. | 162. | 95. | 96. |
| | M2 | 146. | 146. | 107. | 107. | 4. | 4. | 160. | 161. |
| | M3 | 459. | 459. | 786. | 786. | 147. | 150. | 1077. | 1078. |
| Bent 3 | P1 | 66. | 66. | 119. | 119. | 185. | 185. | 160. | 158. |
| | M2 | 302. | 302. | 248 | 248. | 4. | 4. | 375. | 375. |
| | M3 | 1047. | 1047. | 1889. | 1889. | 171. | 172. | 2292. | 2289. |

Table A5.3 Maximum Stresses in Bridge Deck and Columns, (ksi),(10,15, and 20 Frequencies)

| Location | Material | Long Shock (T.H.) | | Trans. Shock (T.H.) | | Vert. Shock (T.H.) | | 3-Direction Shock (T.H.) | |
|---|---|---|---|---|---|---|---|---|---|
| | | 10 | 15 | 10 | 15 | 10 | 15 | 15 | 20 |
| Deck: | | | | | | | | | |
| Abut. 1 | Steel | 2.76 | 2.76 | 3.05 | 3.05 | 0. | 0. | 4.15 | 4.15 |
| | Conc. | 0.46 | 0.46 | 0.55 | 0.55 | 0. | 0. | 0.73 | 0.74 |
| Span 1 | Steel | 1.62 | 1.62 | 1.55 | 1.55 | 2.28 | 2.28 | 2.68 | 2.72 |
| | Conc. | 0.23 | 0.23 | 0.26 | 0.26 | 0.15 | 0.15 | 0.39 | 0.39 |
| Bent 2 | Steel | 1.36 | 1.36 | 0.93 | 0.93 | 2.32 | 2.32 | 1.65 | 1.68 |
| | Conc. | 0.19 | 0.19 | 0.14 | 0.14 | 0.17 | 0.17 | 0.25 | 0.26 |
| Span 2 | Steel | 1.74 | 1.74 | 1.59 | 1.59 | 2.24 | 2.21 | 2.33 | 2.41 |
| | Conc. | 0.27 | 0.27 | 0.26 | 0.26 | 0.15 | 0.15 | 0.36 | 0.36 |
| Bent 3 | Steel | 1.09 | 1.09 | 0.88 | 0.88 | 2.56 | 2.55 | 2.20 | 2.19 |
| | Conc. | 0.15 | 0.15 | 0.15 | 0.15 | 0.19 | 0.19 | 0.26 | 0.26 |
| Span 3 | Steel | 1.28 | 1.28 | 2.04 | 2.04 | 2.67 | 2.67 | 2.48 | 2.47 |
| | Conc. | 0.21 | 0.21 | 0.38 | 0.38 | 0.18 | 0.18 | 0.45 | 0.45 |
| Column Base: | | | | | | | | | |
| Bent 2 | Conc. | 0.82 | 0.82 | 1.41 | 1.41 | 0.38 | 0.39 | 1.94 | 1.94 |
| Bent 3 | Conc. | 1.87 | 1.87 | 3.38 | 3.38 | 0.44 | 0.44 | 4.11 | 4.11 |

Table A5.4 Maximum Actions and Displacements at the Attachments and Column Base Due to a Longitudinal Shock (S00E), (R.S. & T.H. Analysis), (k,ft)

| Location | Component | 10 Frequencies | | 15 Frequencies | | 20 Frequencies |
|---|---|---|---|---|---|---|
| | | R.S. | T.H. | R.S. | T.H. | R.S. |
| Abut. 1 | P1 | 1027. | 1130. | 1027. | 1130. | 1036. |
| | V2 | 209. | 196. | 209. | 195. | 210. |
| | V3 | 0. | 0. | 0. | 0. | 0. |
| | M1 | 11. | 10. | 11. | 10. | 11. |
| | M3 | 11440. | 10640. | 11440. | 10641. | 11460. |
| Bent 2 | V2 | 118. | 106. | 118. | 106. | 118. |
| | M2(Deck) | 9. | 5. | 9. | 5. | 9. |
| Bent 3 | V2 | 246. | 240. | 246. | 240. | 246. |
| | M2(Deck) | 4. | 6. | 4. | 6. | 4. |
| Abut. 6 | V2 | 145. | 101. | 145. | 101. | 146. |
| | M3 | 11770. | 8629. | 11770. | 8629. | 11780. |
| | DT | .0128 | .0165 | .0128 | .0165 | .0128 |
| Column Base: | | | | | | |
| Bent 2 | P1 | 32. | 29. | 32. | 29. | 32. |
| | M2 | 132. | 146. | 132. | 146. | 137. |
| | M3 | 511. | 459. | 511. | 459. | 511. |
| Bent 3 | P1 | 66. | 66. | 66. | 66. | 66. |
| | M2 | 263. | 302. | 263. | 302. | 265. |
| | M3 | 1053. | 1047. | 1053. | 1047. | 1053. |

Table A5.5 Maximum Actions and Displacements at the Attachments and Column Base Due to a Transverse Shock (S00E), (R.S. & T.H. Analysis), (k,ft)

| Location | Component | 10 Frequencies | | 15 Frequencies | | 20 Frequencies |
|---|---|---|---|---|---|---|
| | | R.S. | T.H. | R.S. | T.H. | R.S. |
| Abut. 1 | P1 | 789. | 779. | 789. | 779. | 790. |
| | V2 | 234. | 252. | 234. | 253. | 234. |
| | V3 | 0. | 0. | 0. | 0. | 0. |
| | M1 | 17. | 17. | 17. | 17. | 17. |
| | M3 | 15930. | 15719. | 15930. | 15718. | 15930. |
| Bent 2 | V2 | 182. | 189. | 182. | 189. | 182. |
| | M2(Deck) | 15. | 7. | 15. | 7. | 15. |
| Bent 3 | V2 | 393. | 436. | 393. | 436. | 393. |
| | M2(Deck) | 7. | 12. | 7. | 12. | 7. |
| Abut. 6 | V2 | 168. | 160. | 168. | 160. | 168. |
| | M3 | 12410. | 12229. | 12410. | 12230. | 12410. |
| | DT | .0168 | .0159 | .0168 | .0159 | .0168 |
| Column Base: | | | | | | |
| Bent 2 | P1 | 49. | 49. | 49. | 49. | 49. |
| | M2 | 108. | 107. | 108. | 107. | 109. |
| | M3 | 788. | 786. | 788. | 786. | 788. |
| Bent 3 | P1 | 105. | 119. | 105. | 119. | 105. |
| | M2 | 258. | 248. | 258. | 248. | 258. |
| | M3 | 1672. | 1889. | 1672. | 1889. | 1672. |

Table A5.6 Maximum Actions at the Attachments and Column Base Due to a Vertical Shock (S00E), (R.S. & T.H. Analysis), (k,ft)

| Location | Component | 10 Frequencies | | 15 Frequencies | |
|---|---|---|---|---|---|
| | | R.S. | T.H. | R.S. | T.H. |
| Abut. 1 | P1 | 0. | 0. | 0. | 0. |
| | V2 | 0. | 0. | 0. | 0. |
| | V3 | 74. | 94. | 75. | 92. |
| | M1 | 77. | 94. | 77. | 92. |
| | M3 | 11. | 6. | 11. | 7. |
| Bent 2 | V2 | 0. | 0. | 0. | 0. |
| | V3(Deck) | 120. | 151. | 121. | 152. |
| | M2(Deck) | 2866. | 3227. | 2866. | 3227. |
| Bent 3 | V2 | 0. | 0. | 0. | 0. |
| | V3(Deck) | 171. | 161. | 171. | 164. |
| | M2(Deck) | 3964. | 3560. | 3964. | 3551. |
| Abut. 6 | V2 | 0. | 0. | 0. | 0. |
| | M3 | 8. | 5. | 8. | 5. |
| Column Base: | | | | | |
| Bent 2 | P1 | 142. | 159. | 142. | 162. |
| | M2 | 4. | 4. | 4. | 4. |
| | M3 | 131. | 147. | 132. | 150. |
| Bent 3 | P1 | 205. | 185. | 205. | 185. |
| | M2 | 4. | 4. | 4. | 4. |
| | M3 | 189. | 171. | 189. | 172. |

Table A5.7 Maximum Actions at the Attachments and Column Base Due to El Centro Earthquake (S90W) and (VERT) Components, (R.S. & T.H. Analysis), (k,ft)

| Location | Component | Longitudinal Shock (S90W) | | Vertical Shock (VERT) | |
|---|---|---|---|---|---|
| | | R.S. | T.H. | R.S. | T.H. |
| Abut. 1 | P1 | 727. | 782. | 0. | 0. |
| | V2 | 152. | 135. | 0. | 0. |
| | V3 | 0. | 0. | 40. | 51. |
| | M1 | 9. | 9. | 35. | 46. |
| | M3 | 8953. | 8473. | 6. | 3. |
| Bent 2 | V2 | 98. | 98. | 0. | 0. |
| | V3(Deck) | 0. | 0. | 75. | 81. |
| | M2(Deck) | 7. | 5. | 1993. | 1909. |
| Bent 3 | V2 | 209. | 208. | 0. | 0. |
| | V3(Deck) | 0. | 0. | 130. | 130. |
| | M2(Deck) | 3. | 3. | 3019. | 2999. |
| Abut. 6 | V2 | 100. | 75. | 0. | 0. |
| | M3 | 8503. | 6715. | 4. | 2. |
| Column Base: | | | | | |
| Bent 2 | P1 | 26. | 26. | 102. | 96. |
| | M2 | 95. | 99. | 2. | 2. |
| | M3 | 420. | 418. | 94. | 89. |
| Bent 3 | P1 | 56. | 55. | 157. | 156. |
| | M2 | 194. | 196. | 2. | 1. |
| | M3 | 892. | 880. | 145. | 144. |

Table A5.8 Maximum Actions and Displacements at the Attachments and Column Base Due to El Centro Earthquake Different Components, (k,ft)

| Location | Component | Longitudinal Shock (S90W) | | Transverse Shock (S00E) | | Vertical Shock (VERT) | | 3-Direction Shock | |
|---|---|---|---|---|---|---|---|---|---|
| | | Response | Time (sec) | Response | Time (sec) | Response | Time (sec) | Response | Time (sec) |
| Abut. 1 | P1 | 782. | 1.95 | 779. | 2.72 | 0. | 0.95 | 1175. | 2.71 |
| | V2 | 135. | 3.35 | 253. | 4.98 | 0. | 0.89 | 290. | 3.26 |
| | V3 | 0. | 3.59 | 0. | 3.37 | 51. | 3.35 | 52. | 3.35 |
| | M1 | 9. | 2.91 | 17. | 2.50 | 46. | 3.35 | 58. | 3.35 |
| | M3 | 8473. | 2.91 | 15718. | 4.98 | 3. | 0.69 | 20506. | 2.92 |
| Bent 2 | V2 | 98. | 2.91 | 189. | 2.51 | 0. | 0.70 | 248. | 2.92 |
| | V3(Deck) | 0. | 3.35 | 0. | 3.50 | 81. | 3.34 | 81. | 3.34 |
| | M2(Deck) | 5 | 3.36 | 7. | 3.27 | 1909. | 0.56 | 1909. | 0.56 |
| Bent 3 | V2 | 208. | 2.92 | 436. | 2.51 | 0. | 0.70 | 534. | 2.92 |
| | V3(Deck) | 0. | 3.58 | 0. | 3.36 | 130. | 0.63 | 130. | 0.63 |
| | M2(Deck) | 3. | 2.91 | 12. | 2.51 | 2999. | 0.63 | 3000. | 0.63 |
| Abut. 6 | V2 | 75. | 3.58 | 160. | 2.47 | 0. | 1.11 | 183. | 3.57 |
| | M3 | 6715. | 3.58 | 12230. | 2.08 | 2. | 0.69 | 15613. | 3.03 |
| | DT | .0104 | 2.90 | .0159 | 2.72 | 0. | 0.98 | .0239 | 2.71 |
| Column Base: | | | | | | | | | |
| Bent 2 | P1 | 26. | 2.91 | 49. | 2.50 | 96. | 0.63 | 95. | 0.55 |
| | M2 | 99. | 1.95 | 107. | 2.72 | 2. | 3.40 | 160. | 2.71 |
| | M3 | 418. | 2.91 | 786. | 2.50 | 89. | 0.63 | 1077. | 2.92 |
| Bent 3 | P1 | 55. | 2.92 | 119. | 2.51 | 156. | 0.63 | 160. | 2.93 |
| | M2 | 196. | 1.95 | 248. | 2.72 | 1. | 1.11 | 375. | 2.71 |
| | M3 | 880. | 2.92 | 1889. | 2.51 | 144. | 0.63 | 2292. | 2.92 |

Table A5.9 Maximum Stresses in Bridge Deck and Columns Due to El Centro Earthquake Different Components, (ksi)

| Location | Material | Longitudinal Shock (S90W) | | Transverse Shock (S00E) | | Vertical Shock (VERT) | | 3-Direction Shock | |
|---|---|---|---|---|---|---|---|---|---|
| | | Stress | Time (sec) | Stress | Time (sec) | Stress | Time (sec) | Stress | Time (sec) |
| Deck: | | | | | | | | | |
| Abut. 1 | Steel | 1.86 | 2.90 | 3.05 | 4.98 | 0. | 0.89 | 4.15 | 2.71 |
| | Conc. | 0.32 | 2.90 | 0.55 | 4.98 | 0. | 0.89 | 0.73 | 2.71 |
| Span 1 | Steel | 1.06 | 2.90 | 1.55 | 2.72 | 1.10 | 3.35 | 2.68 | 3.35 |
| | Conc. | 0.17 | 2.90 | 0.26 | 2.51 | 0.07 | 3.35 | 0.39 | 2.71 |
| Bent 2 | Steel | 0.93 | 4.19 | 0.93 | 4.89 | 1.37 | 0.56 | 1.65 | 3.34 |
| | Conc. | 0.14 | 4.19 | 0.14 | 4.89 | 0.10 | 0.56 | 0.25 | 3.34 |
| Span 2 | Steel | 1.17 | 3.35 | 1.59 | 4.98 | 1.35 | 0.55 | 2.33 | 3.34 |
| | Conc. | 0.18 | 3.35 | 0.26 | 4.98 | 0.09 | 0.55 | 0.36 | 3.26 |
| Bent 3 | Steel | 0.73 | 3.35 | 0.88 | 2.51 | 2.15 | 0.63 | 2.20 | 0.63 |
| | Conc. | 0.10 | 3.35 | 0.15 | 2.51 | 0.16 | 0.63 | 0.26 | 3.34 |
| Span 3 | Steel | 1.03 | 2.92 | 2.04 | 2.51 | 1.74 | 0.70 | 2.48 | 2.93 |
| | Conc. | 0.18 | 2.92 | 0.38 | 2.51 | 0.12 | 0.70 | 0.45 | 2.93 |
| Column Base: | | | | | | | | | |
| Bent 2 | Conc. | 0.75 | 2.91 | 1.41 | 2.50 | 0.23 | 0.63 | 1.94 | 2.92 |
| Bent 3 | Conc. | 1.58 | 2.92 | 3.38 | 2.51 | 0.37 | 0.63 | 4.11 | 2.93 |

Table A5.10 Maximum Actions and Displacements at the Attachments and Column Base For Different Damping Ratios, (k,ft)

| Location | Component | 2% | 5% | 10% |
|---|---|---|---|---|
| Abut. 1 | P1 | 1688. | 1175. | 879. |
| | V2 | 458. | 290. | 224. |
| | V3 | 59. | 52. | 45. |
| | M1 | 77. | 58. | 43. |
| | M3 | 30167. | 20506. | 15757. |
| Bent 2 | V2 | 338. | 248. | 192. |
| | M2(Deck) | 2303. | 1909. | 1655. |
| Bent 3 | V2 | 728. | 534. | 434. |
| | M2(Deck) | 3894. | 3000. | 2096. |
| Abut. 6 | V2 | 316. | 183. | 148. |
| | M3 | 26548. | 15613. | 11783. |
| | DT | .0323 | .0239 | .0173 |
| Column Base: | | | | |
| Bent 2 | P1 | 126. | 95. | 81. |
| | M2 | 229. | 160. | 120. |
| | M3 | 1480. | 1077. | 817. |
| Bent 3 | P1 | 254. | 160. | 117. |
| | M2 | 533. | 375. | 277. |
| | M3 | 3150. | 2292. | 1863. |

Table A5.11 Maximum Stresses in Bridge Deck and Columns For Different Damping Ratios, (ksi)

| Location | Material | 2% | 5% | 10% |
|---|---|---|---|---|
| Deck: | | | | |
| Abut. 1 | Steel | 6.18 | 4.15 | 3.05 |
| | Conc. | 1.10 | 0.73 | 0.54 |
| Span 1 | Steel | 3.86 | 2.68 | 1.75 |
| | Conc. | 0.51 | 0.39 | 0.28 |
| Bent 2 | Steel | 2.15 | 1.65 | 1.21 |
| | Conc. | 0.33 | 0.25 | 0.20 |
| Span 2 | Steel | 3.81 | 2.33 | 1.66 |
| | Conc. | 0.58 | 0.36 | 0.27 |
| Bent 3 | Steel | 2.92 | 2.20 | 1.53 |
| | Conc. | 0.40 | 0.26 | 0.17 |
| Span 3 | Steel | 3.45 | 2.48 | 1.93 |
| | Conc. | 0.63 | 0.45 | 0.36 |
| Column Base: | | | | |
| Bent 2 | Conc. | 2.67 | 1.94 | 1.46 |
| Bent 3 | Conc. | 5.66 | 4.11 | 3.33 |

Table A5.12 Structure Period For Composite Deck, Non-Composite Deck, Rotational Inertia, and Long Columns Models

| Mode | Composite Deck | | | Non-Composite Deck | | | Rotational Inertia | | | Long Columns | | |
|---|---|---|---|---|---|---|---|---|---|---|---|---|
| | Period (sec) | Frequency (Hz) | Mode Shape Direction | Period (sec) | Frequency (Hz) | Mode Shape Direction | Period (sec) | Frequency (Hz) | Mode Shape Direction | Period (sec) | Frequency (Hz) | Mode Shaı Directioı |
| 1 | .266 | 3.76 | Y | .457 | 2.19 | Y | .267 | 3.75 | Y | .495 | 2.02 | Z&X |
| 2 | .244 | 4.10 | Y | .408 | 2.45 | Y | .246 | 4.07 | Y | .266 | 3.76 | Y |
| 3 | .217 | 4.62 | Z&X | .322 | 3.11 | Y | .217 | 4.62 | Z&X | .240 | 4.17 | Y |
| 4 | .205 | 4.88 | Y | .256 | 3.91 | Y | .206 | 4.86 | Y | .193 | 5.17 | Y |
| 5 | .174 | 5.74 | Y | .246 | 4.07 | X&Z | .176 | 5.69 | Y | .183 | 5.46 | Z&X |
| 6 | .158 | 6.34 | Y | .217 | 4.61 | Y | .175 | 5.72 | X[Rot.] | .160 | 6.25 | X&Z |
| 7 | .151 | 6.62 | X&Z | .191 | 5.23 | Z&X | .165 | 6.06 | X[Rot.] | .157 | 6.38 | Y |
| 8 | .137 | 7.28 | Z&X | .170 | 5.88 | Z&X | .158 | 6.35 | Y | .135 | 7.43 | Y |
| 9 | .085 | 11.81 | Y | .116 | 8.61 | Z | .156 | 6.40 | X[Rot.] | .125 | 7.99 | X(Col.) |
| 10 | .084 | 11.84 | Z | .112 | 8.91 | Y | .151 | 6.62 | X&Z | .125 | 7.99 | X(Col.) |
| 11 | .082 | 12.27 | Y | .110 | 9.06 | Y | .148 | 6.75 | X[Rot.] | .125 | 7.99 | X(Col.) |
| 12 | .076 | 13.11 | Y | .106 | 9.46 | Y | .146 | 6.86 | X[Rot.] | .125 | 7.99 | X(Col.) |

Table A5.13 Maximum Actions and Displacements at the Attachments and Column Base For Composite Deck, Non-Composite Deck, Rotational Inertia, and Long Columns Models, (k,ft)

| Location | Component | Composite Deck | Non-Composite Deck | Rotational Inertia | Long Columns |
|---|---|---|---|---|---|
| Abut. 1 | P1 | 1175. | 1337. | 1173. | 1323. |
| | V2 | 290. | 190. | 268. | 1216. |
| | V3 | 52. | 38. | 47. | 65. |
| | M1 | 58. | 24. | 168. | 173. |
| | M3 | 20506. | 10771. | 20406. | 121540. |
| Bent 2 | V2 | 248. | 284. | 247. | 40. |
| | M2(Deck) | 1909. | 1320. | 1879. | 3016. |
| Bent 3 | V2 | 534. | 634. | 531. | 92. |
| | M2(Deck) | 3000. | 1895. | 2964. | 3201. |
| Abut. 6 | V2 | 183. | 156. | 167. | 1063. |
| | M3 | 15613. | 9805. | 15661. | 109060. |
| | DT | .0239 | .0387 | .0238 | .0940 |
| Column Base: | | | | | |
| Bent 2 | P1 | 95. | 97. | 94. | 183. |
| | M2 | 160. | 348. | 159. | 88. |
| | M3 | 1077. | 1211. | 1069. | 834. |
| Bent 3 | P1 | 160. | 157. | 149. | 372. |
| | M2 | 375. | 693. | 373. | 191. |
| | M3 | 2292. | 2669. | 2282. | 1895. |

Table A5.14 Maximum Stresses in Bridge Deck and Columns For Composite Deck, Non-Composite Deck, Rotational Inertia, and Long Columns Models, (ksi)

| Location | Material | Composite Deck | Non-Composite Deck | Rotational Inertia | Long Columns |
|---|---|---|---|---|---|
| Deck: | | | | | |
| Abut. 1 | Steel | 4.15 | 6.11 | 4.02 | 18.79 |
| | Conc. | 0.73 | 0. | 0.71 | 3.68 |
| | Steel (τ) | 1.16 | 1.98 | 1.09 | 4.68 |
| | Conc. (τ) | 0.04 | 0. | 0.04 | 0.20 |
| Span 1 | Steel | 2.68 | 4.29 | 2.64 | 10.27 |
| | Conc. | 0.39 | 0. | 0.39 | 1.96 |
| Bent 2 | Steel | 1.65 | 2.52 | 1.70 | 2.49 |
| | Conc. | 0.25 | 0. | 0.27 | 0.40 |
| Span 2 | Steel | 2.33 | 4.34 | 2.35 | 6.25 |
| | Conc. | 0.36 | 0. | 0.35 | 1.17 |
| Bent 3 | Steel | 2.20 | 2.84 | 2.18 | 9.06 |
| | Conc. | 0.26 | 0. | 0.25 | 1.68 |
| Span 3 | Steel | 2.48 | 5.13 | 2.46 | 11.29 |
| | Conc. | 0.45 | 0. | 0.44 | 2.19 |
| Column Base: | | | | | |
| Bent 2 | Conc. | 1.94 | 2.17 | 1.91 | 1.59 |
| | Conc. (τ) | 0.15 | 0.17 | 0.15 | 0.04 |
| Bent 3 | Conc. | 4.11 | 4.77 | 4.09 | 3.59 |
| | Conc. (τ) | 0.31 | 0.37 | 0.31 | 0.09 |

Table A5.15 Maximum Stresses in Bridge Deck and Columns Due to Dead Load, (ksi)

| Location | Material | Stress |
|---|---|---|
| Deck: | | |
| Span 1 | Steel | 4.70 |
| | Conc. | 0.29 |
| Bent 2 | Steel | 7.01 |
| Span 2 | Steel | 2.79 |
| | Conc. | 0.17 |
| Bent 3 | Steel | 5.88 |
| Span 3 | Steel | 3.16 |
| | Conc. | 0.20 |
| Column Base: | | |
| Bent 2 | Conc. | 0.89 |
| Bent 3 | Conc. | 0.81 |

# APPENDIX B

## FIGURES

## B.1 Mode Shapes

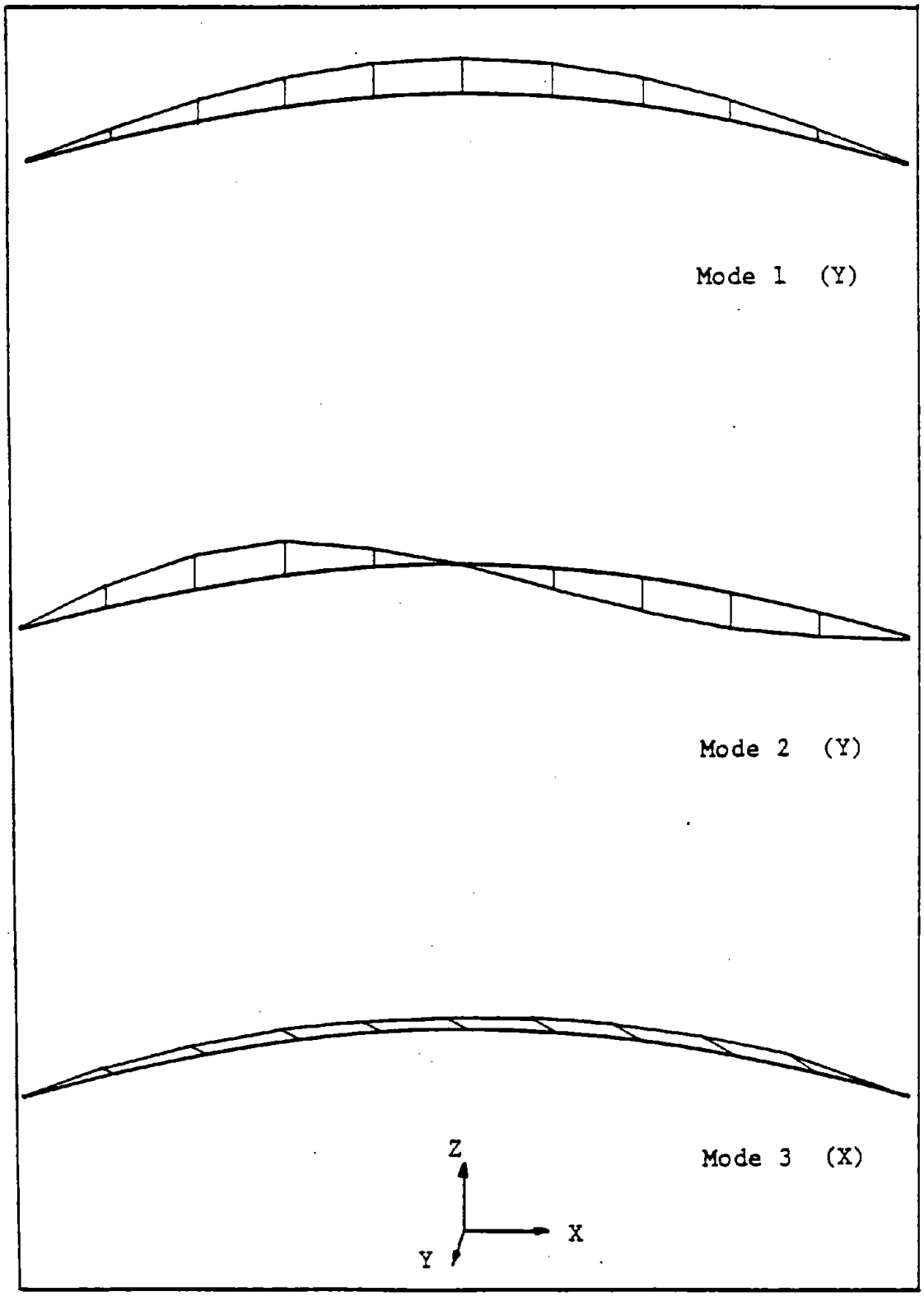


Figure B1.1 Single Span Curved Bridge Mode Shapes

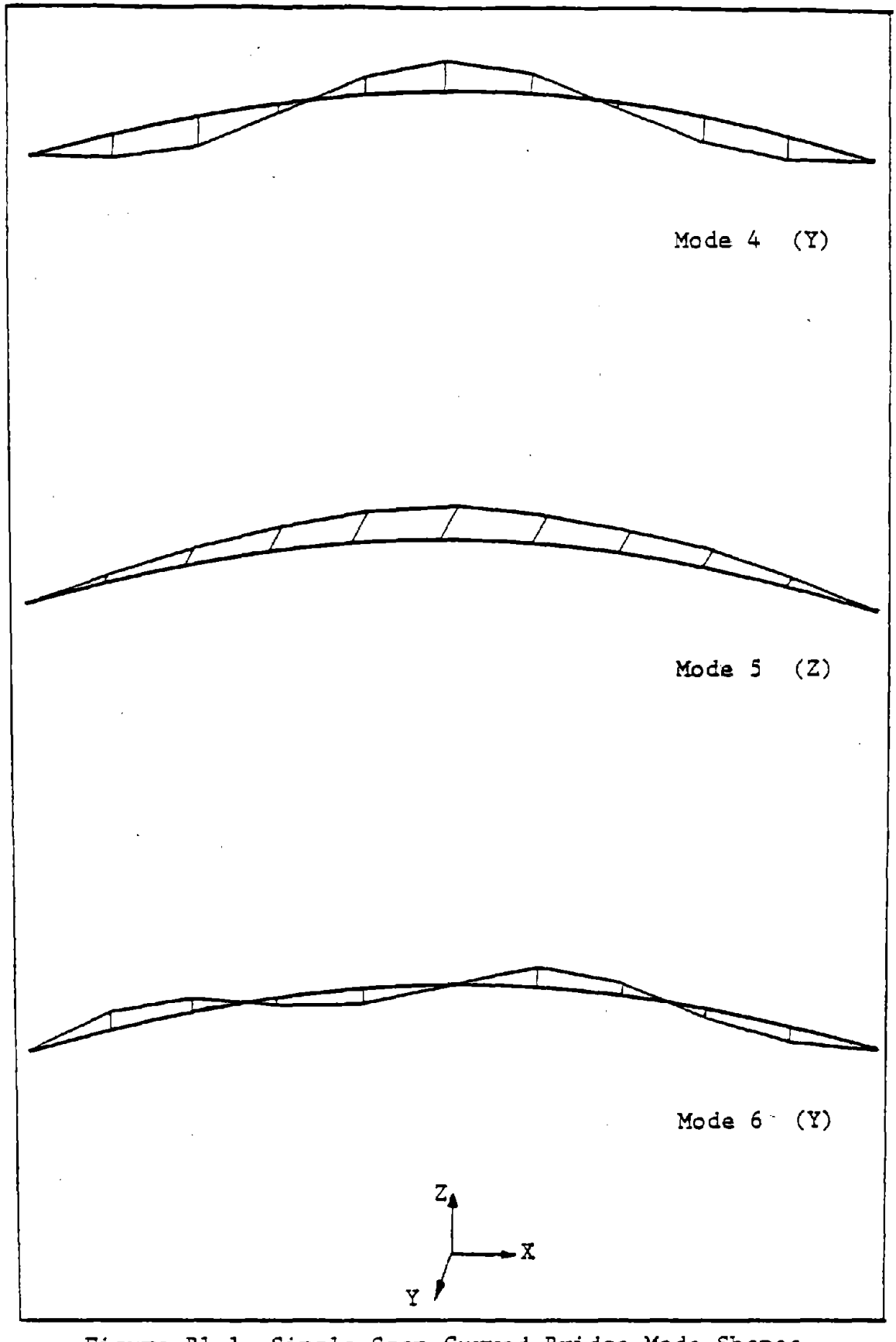


Figure B1.1 Single Span Curved Bridge Mode Shapes

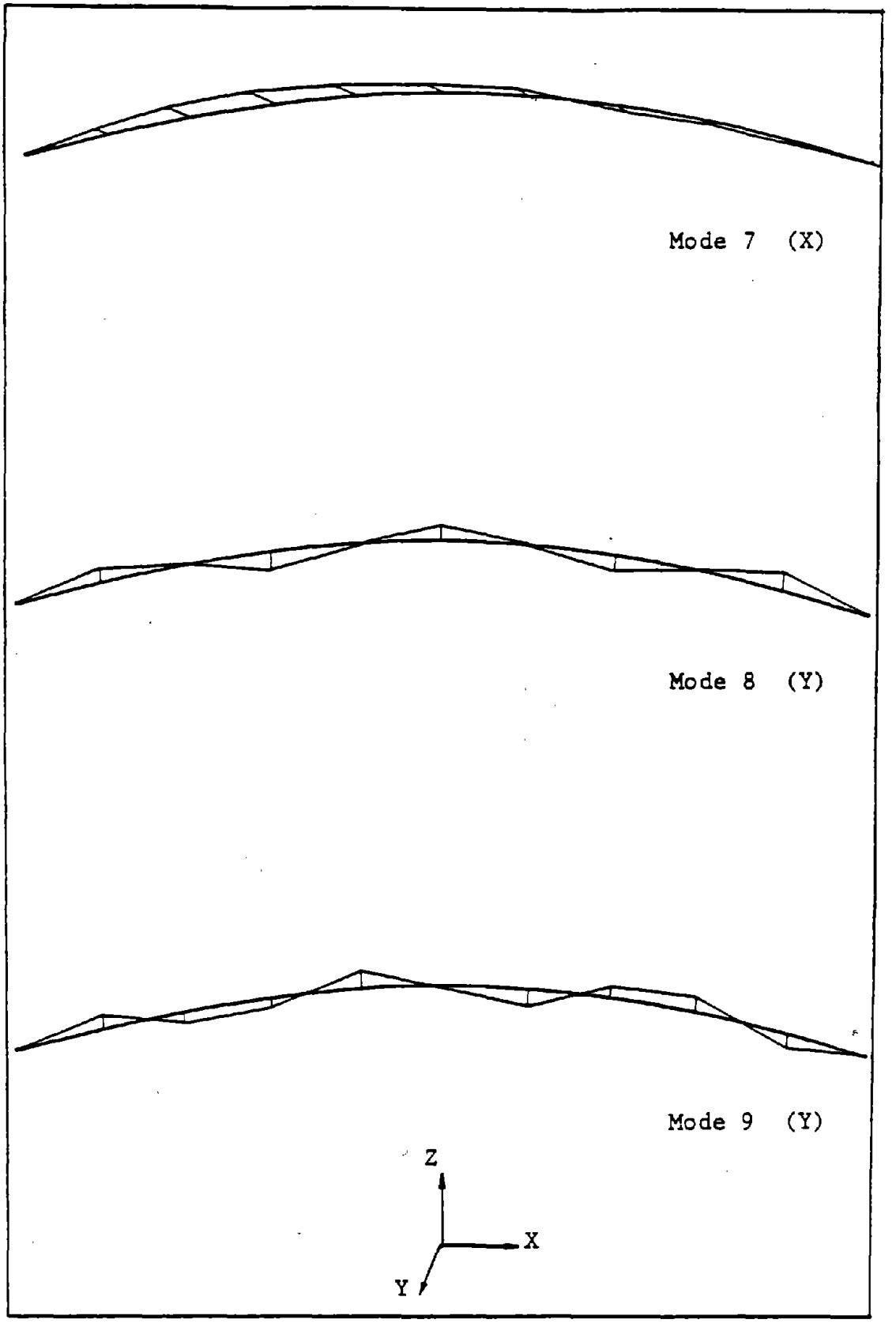


Figure B1.1 Single Span Curved Bridge Mode Shapes

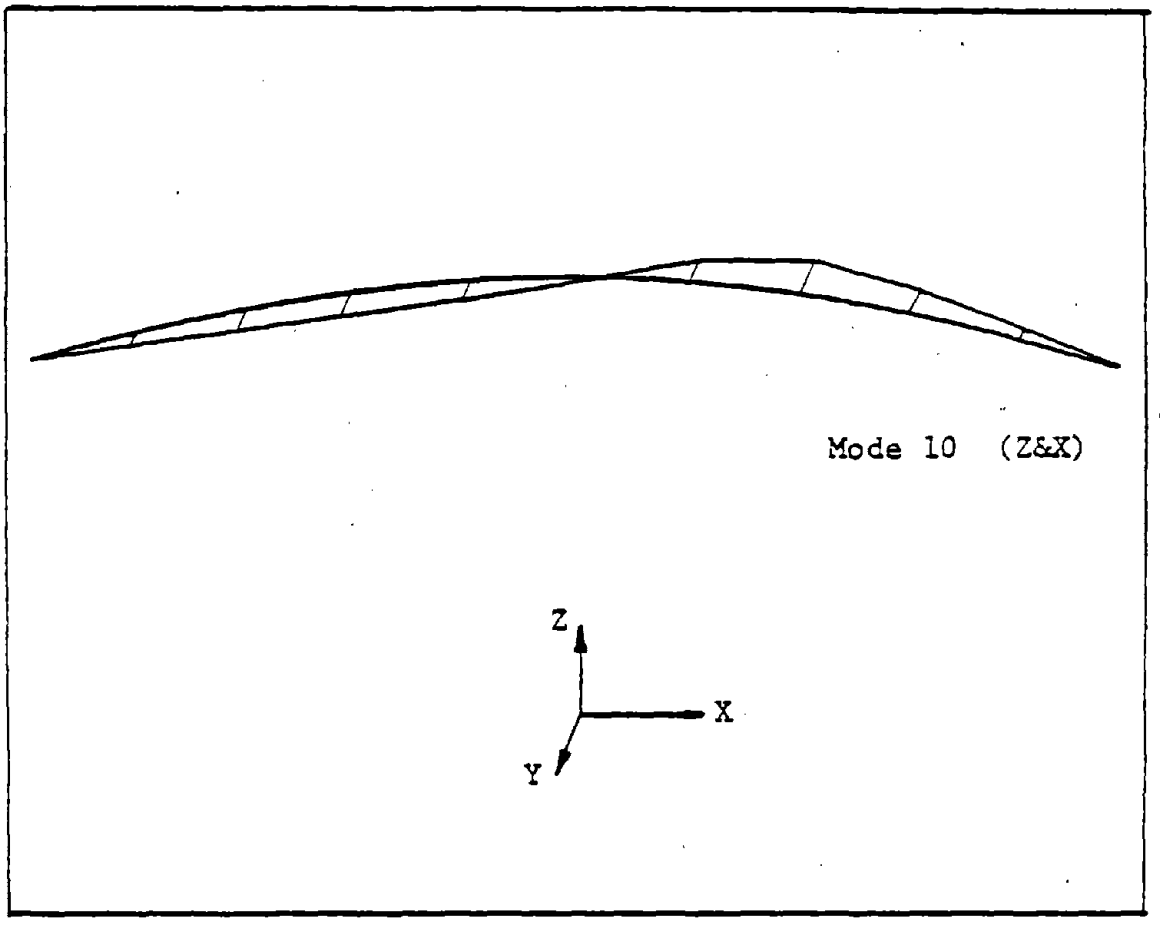


Figure B1.1 Single Span Curved Bridge Mode Shapes

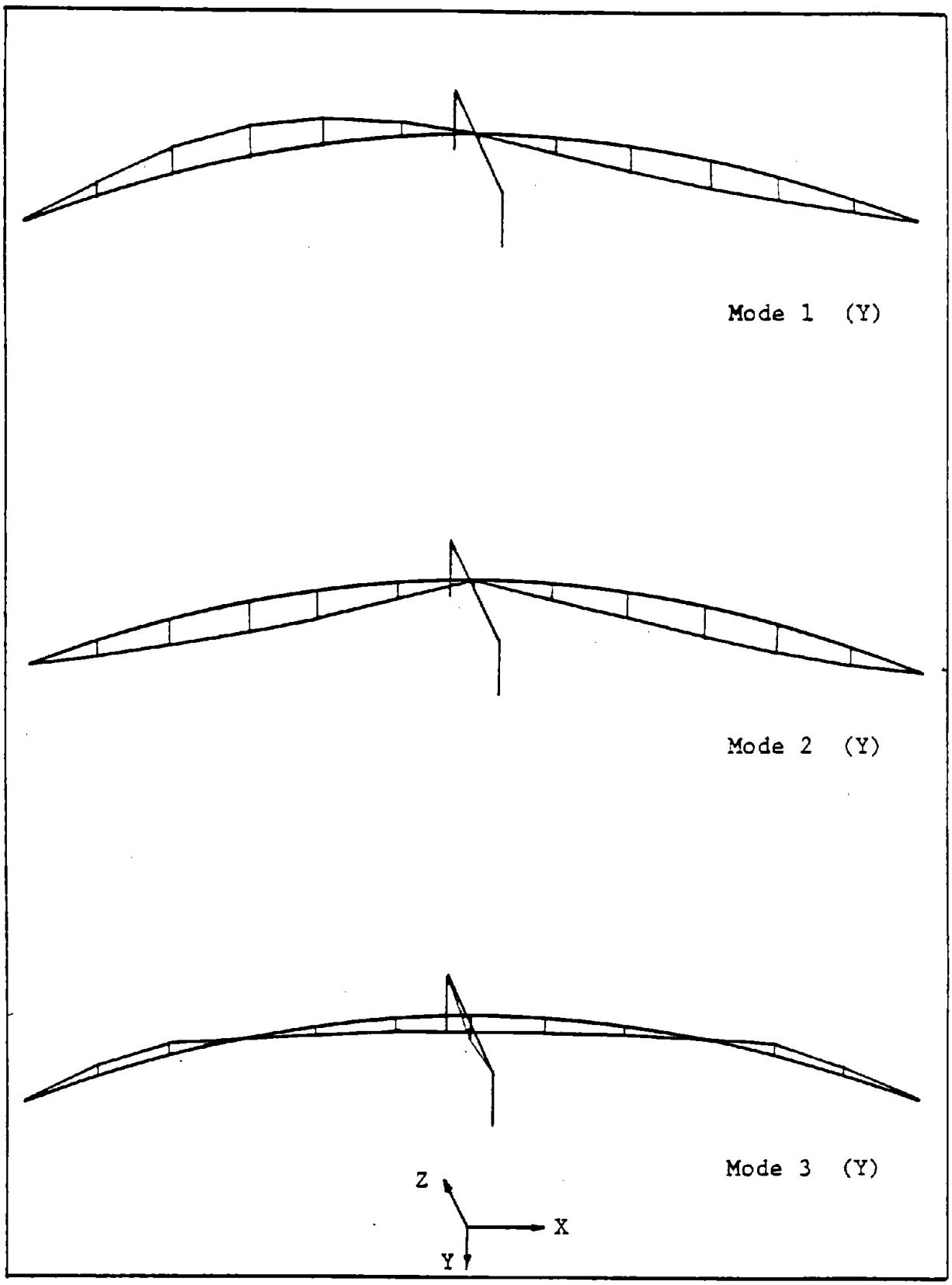


Figure B1.2 2-Span Curved Bridge Mode Shapes

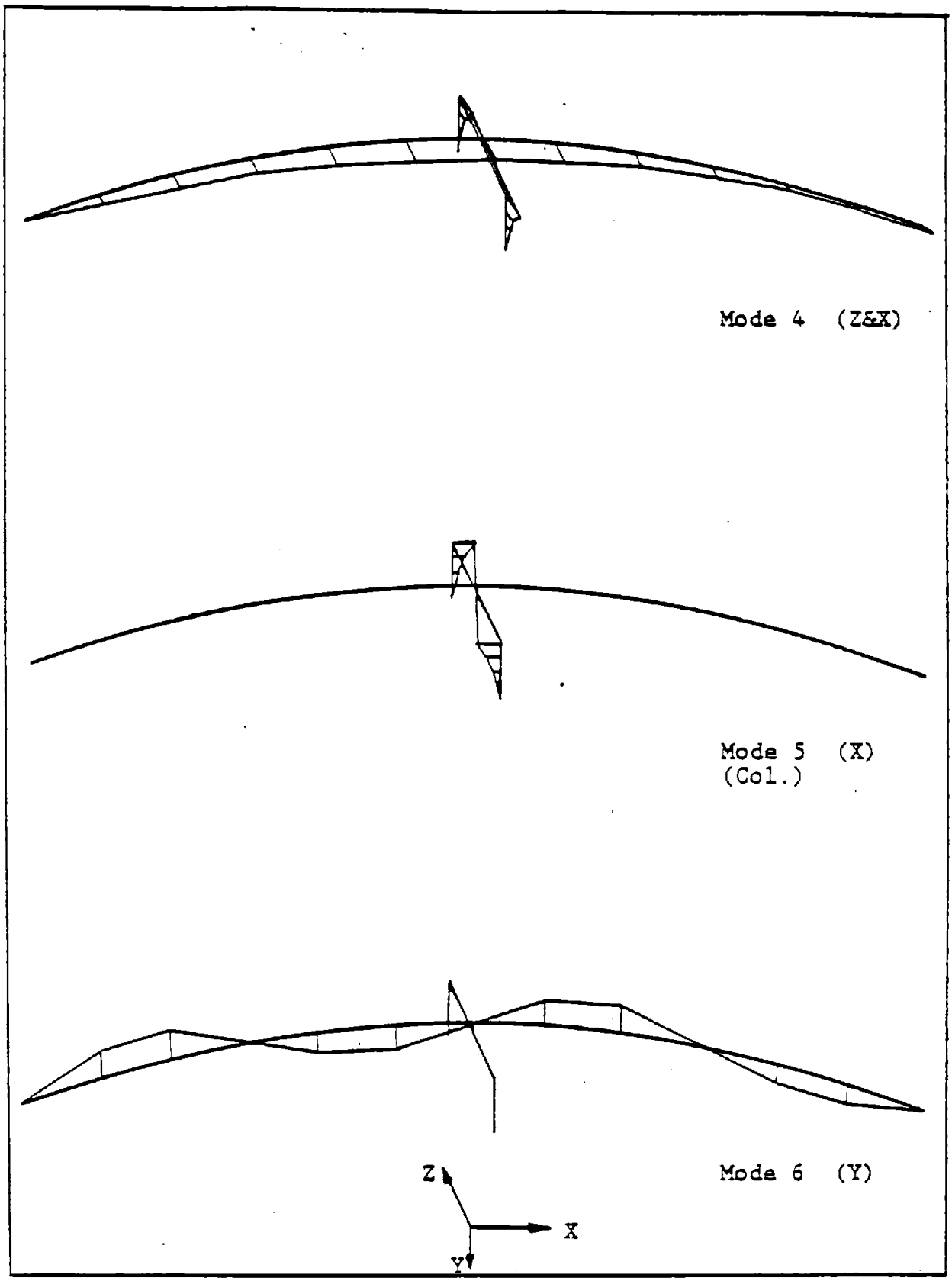


Figure B1.2 2-Span Curved Bridge Mode Shapes

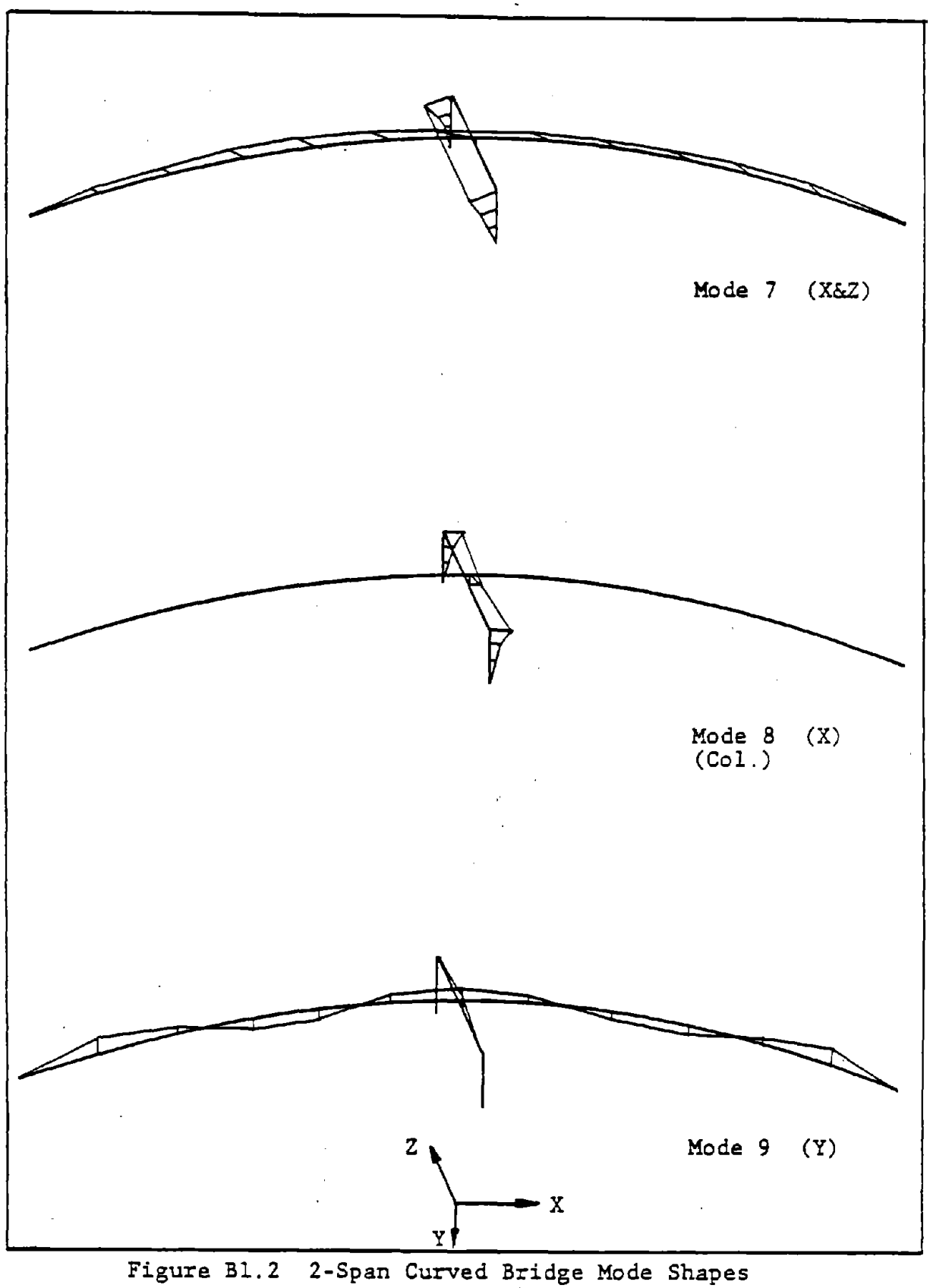


Figure B1.2 2-Span Curved Bridge Mode Shapes

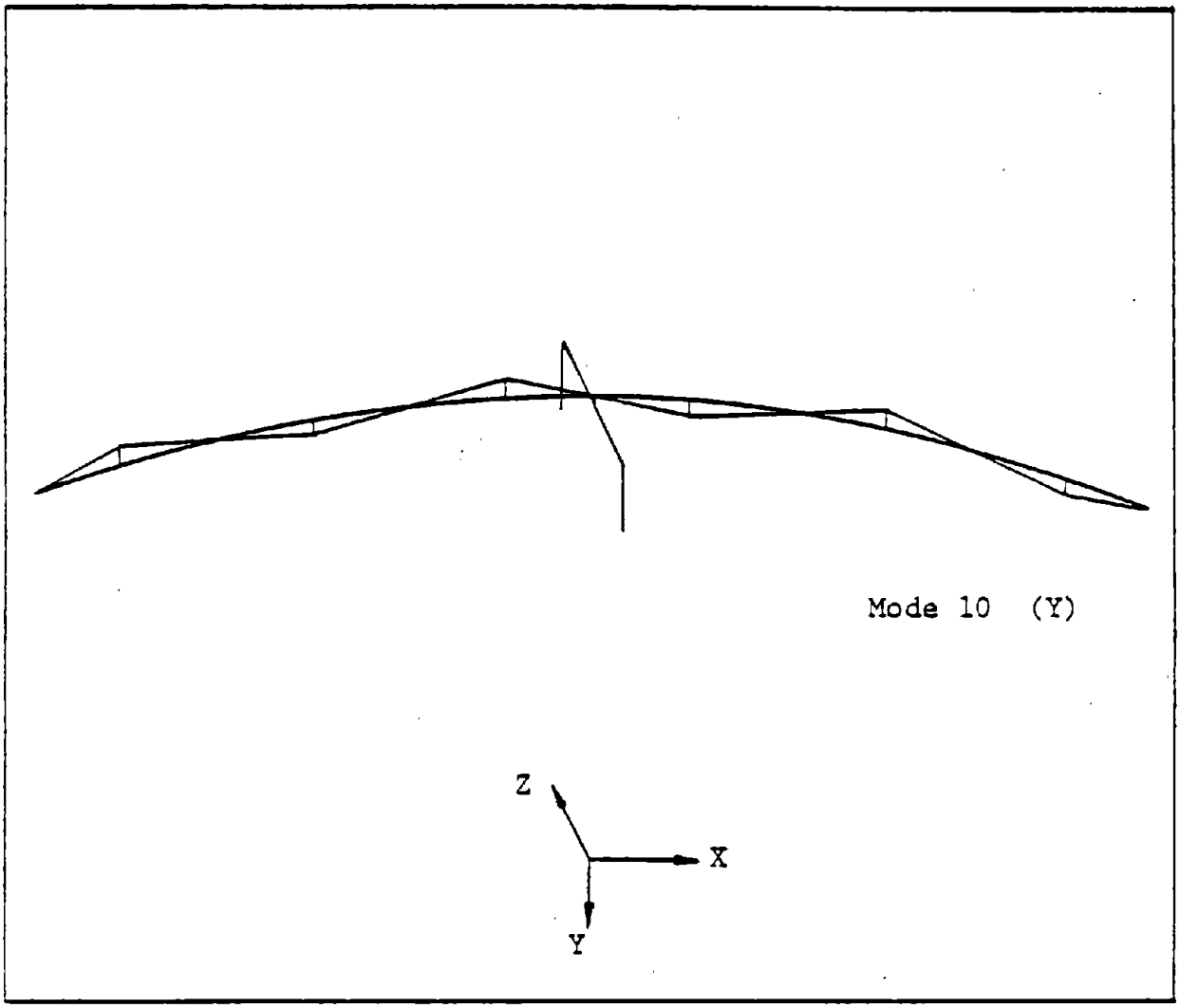


Figure B1.2 2-Span Curved Bridge Mode Shapes

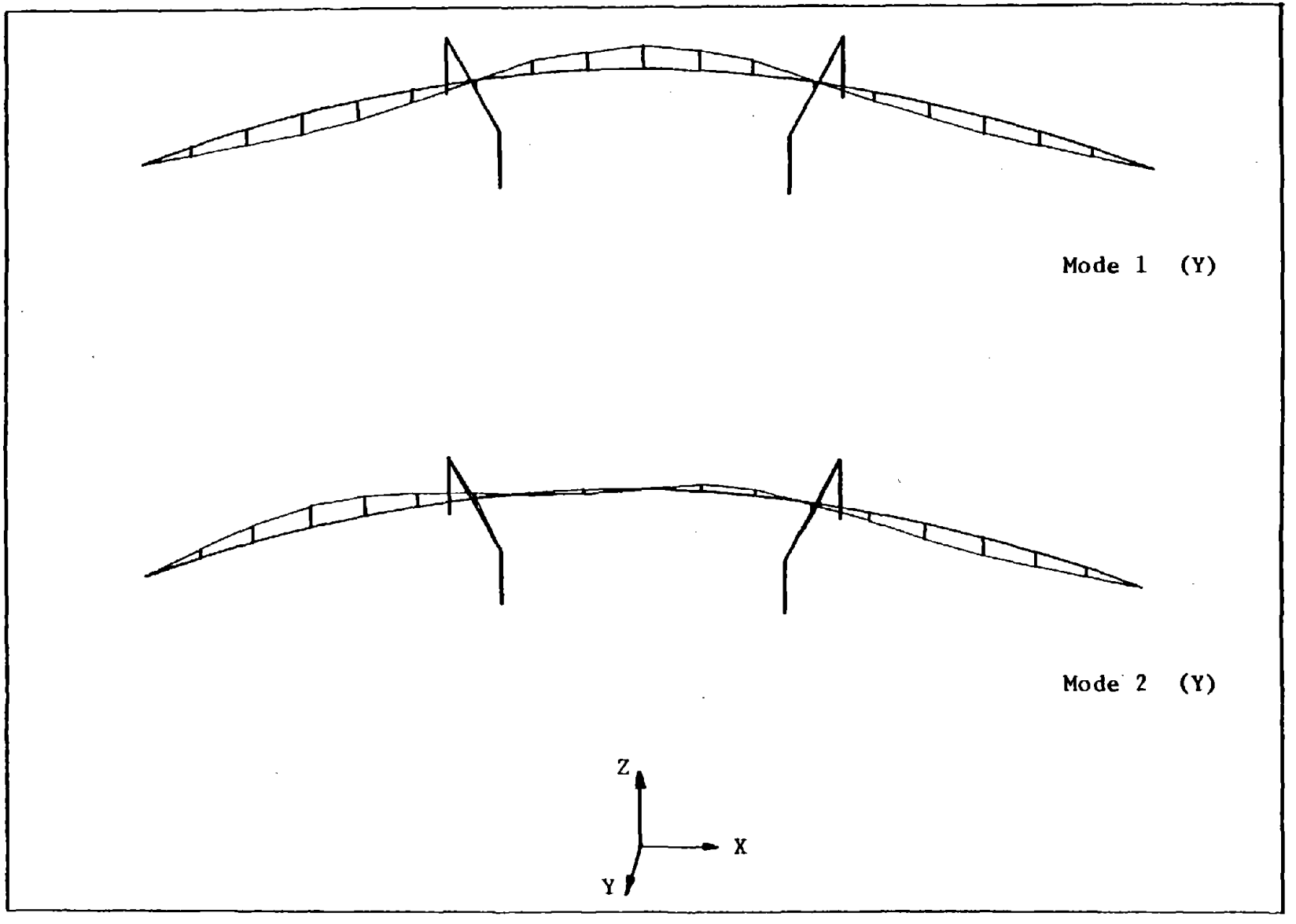


Figure B1.3 3-Span Curved Bridge Mode Shapes

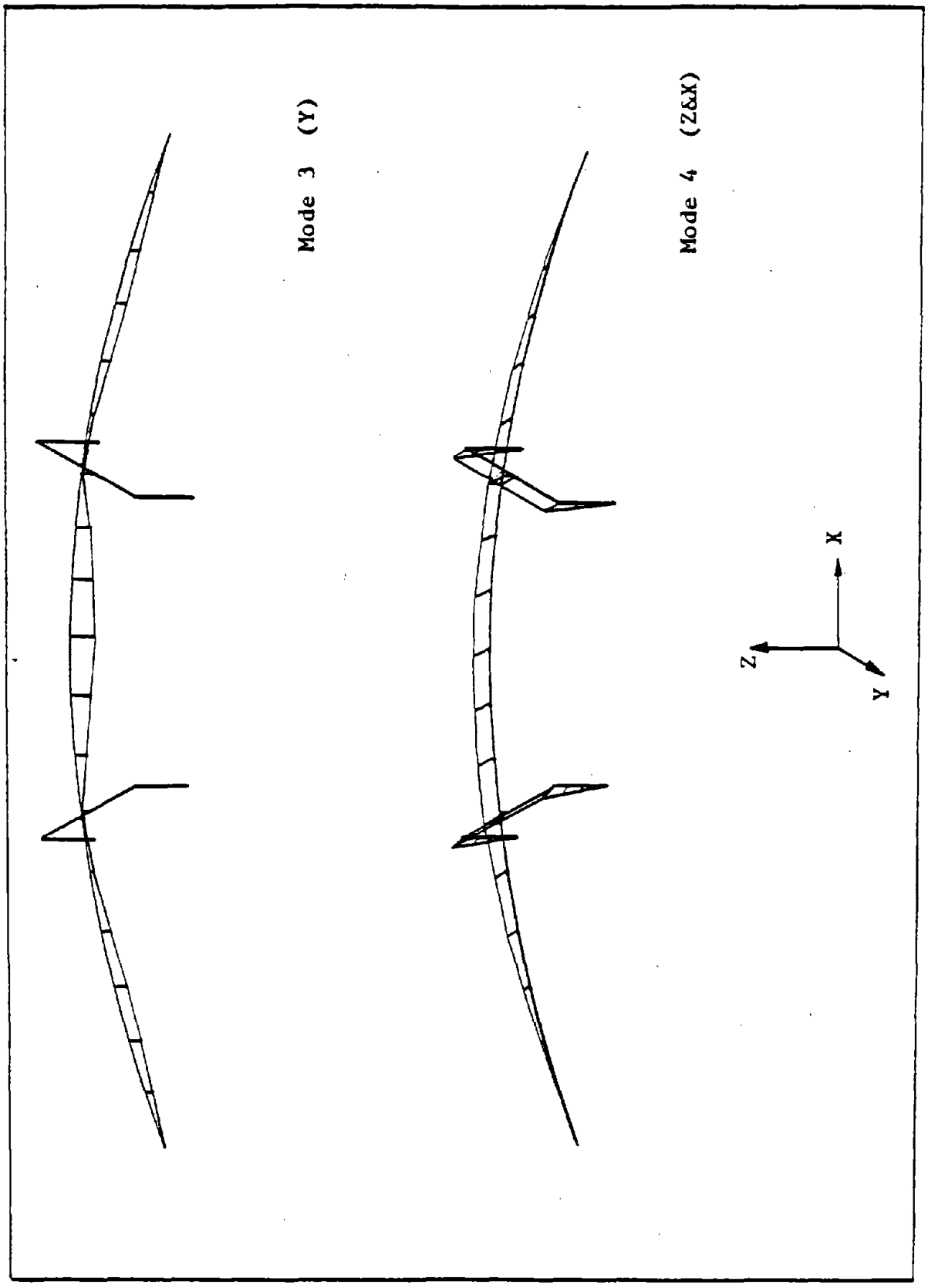


Figure B1.3 3-Span Curved Bridge Mode Shapes

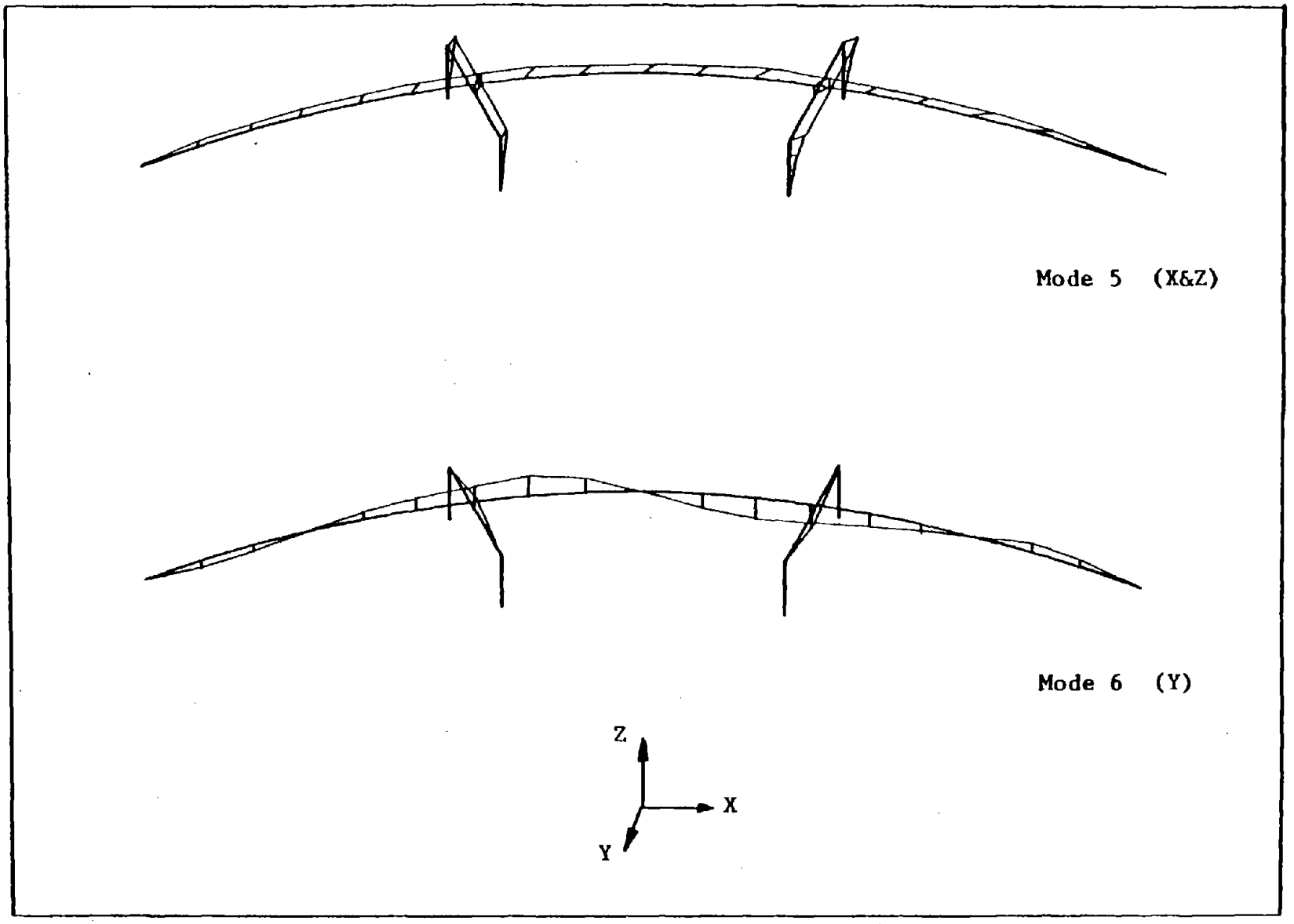


Figure B1.3 3-Span Curved Bridge Mode Shapes

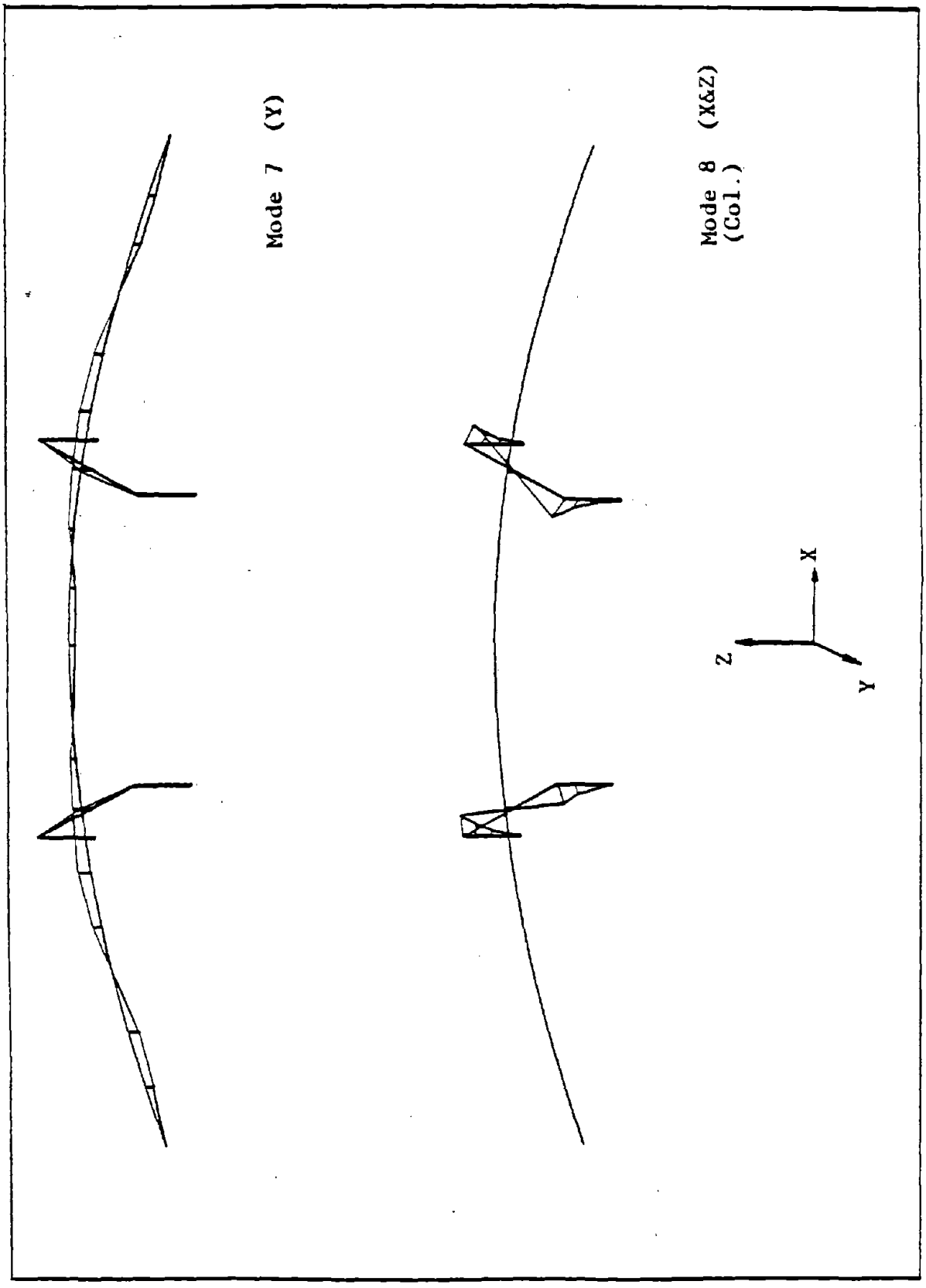


Figure B1.3 3-Span Curved Bridge Mode Shapes

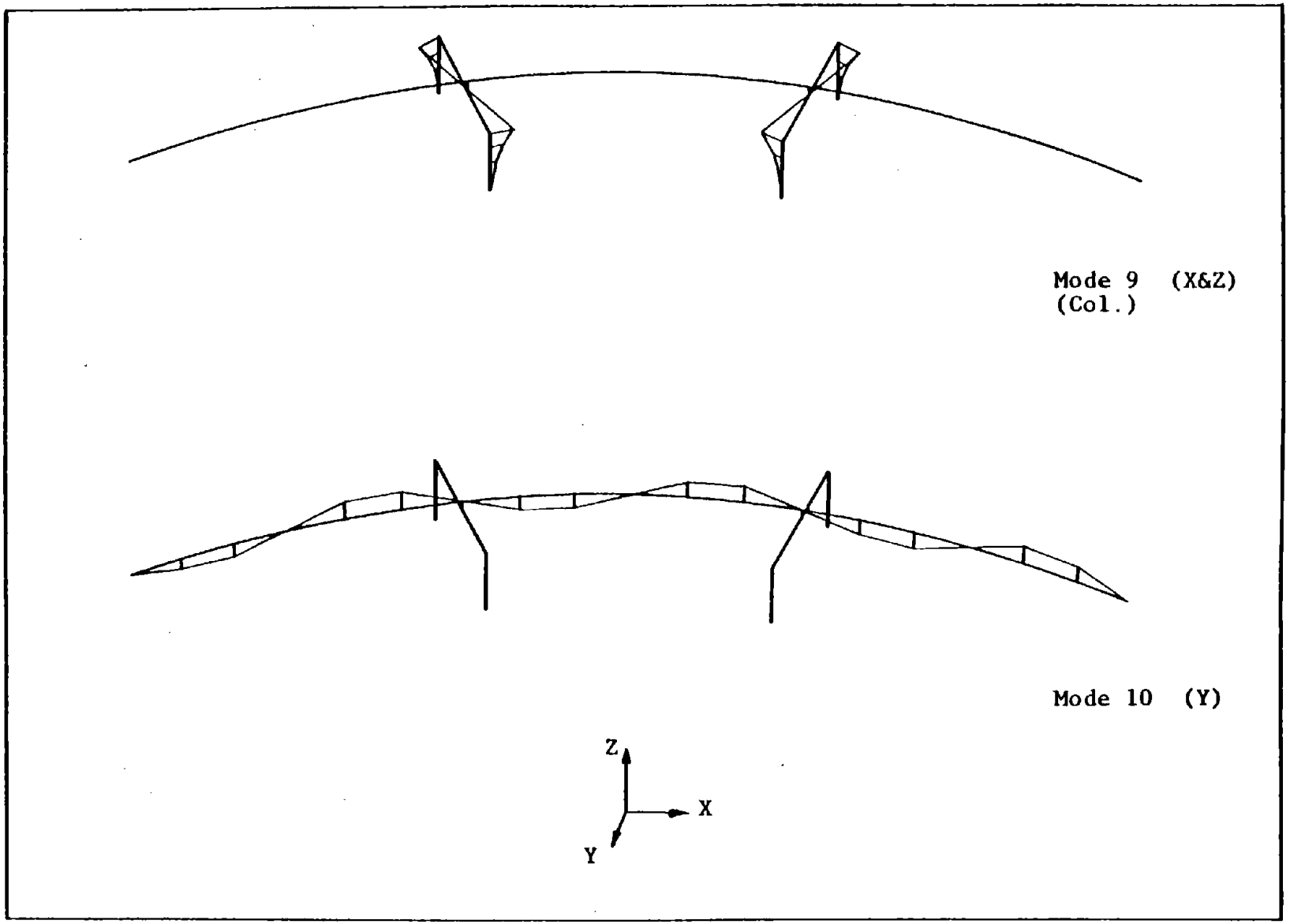


Figure B1.3 3-Span Curved Bridge Mode Shapes

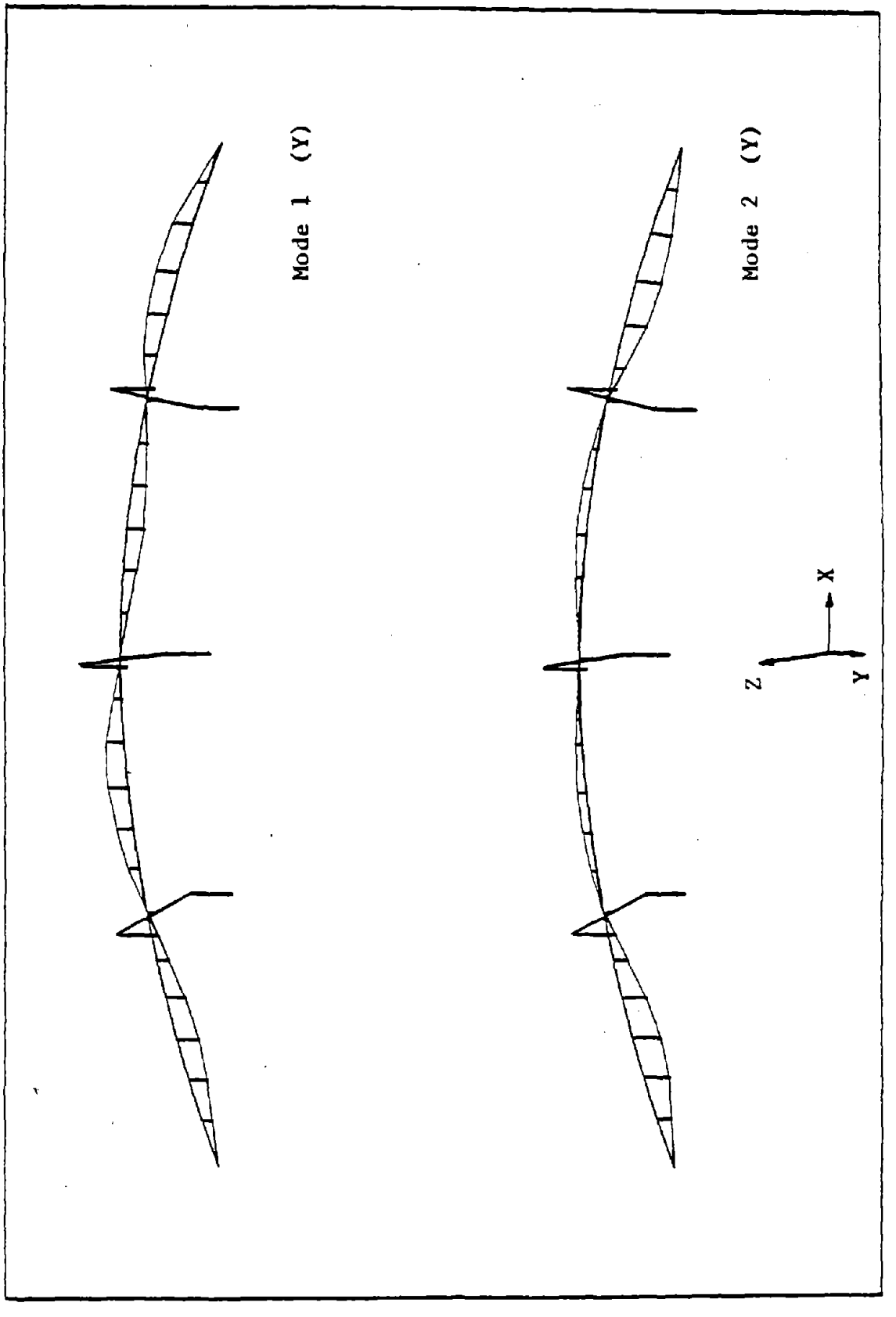


Figure B1.4 4-Span Curved Bridge Mode Shapes

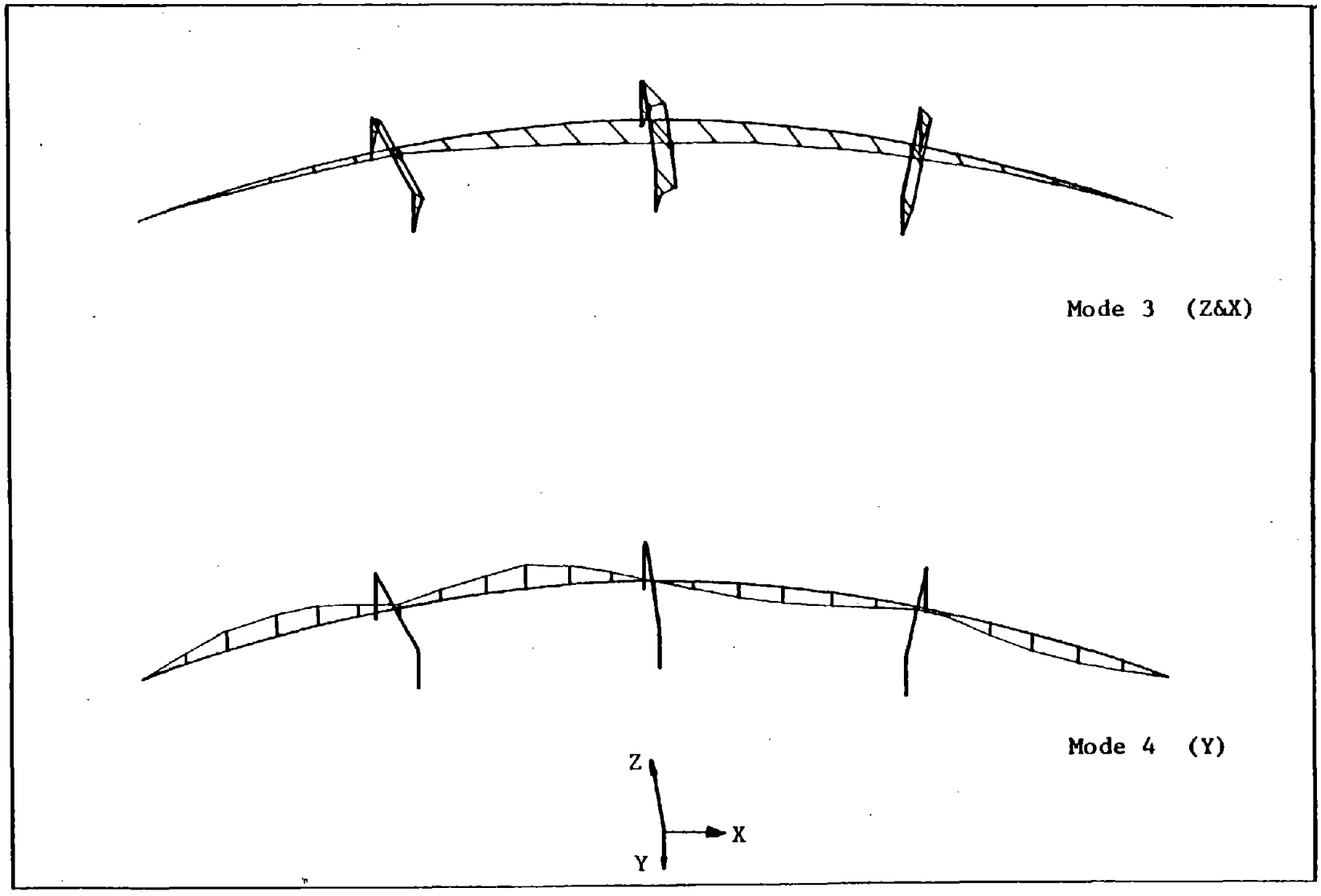


Figure B1.4 4-Span Curved Bridge Mode Shapes

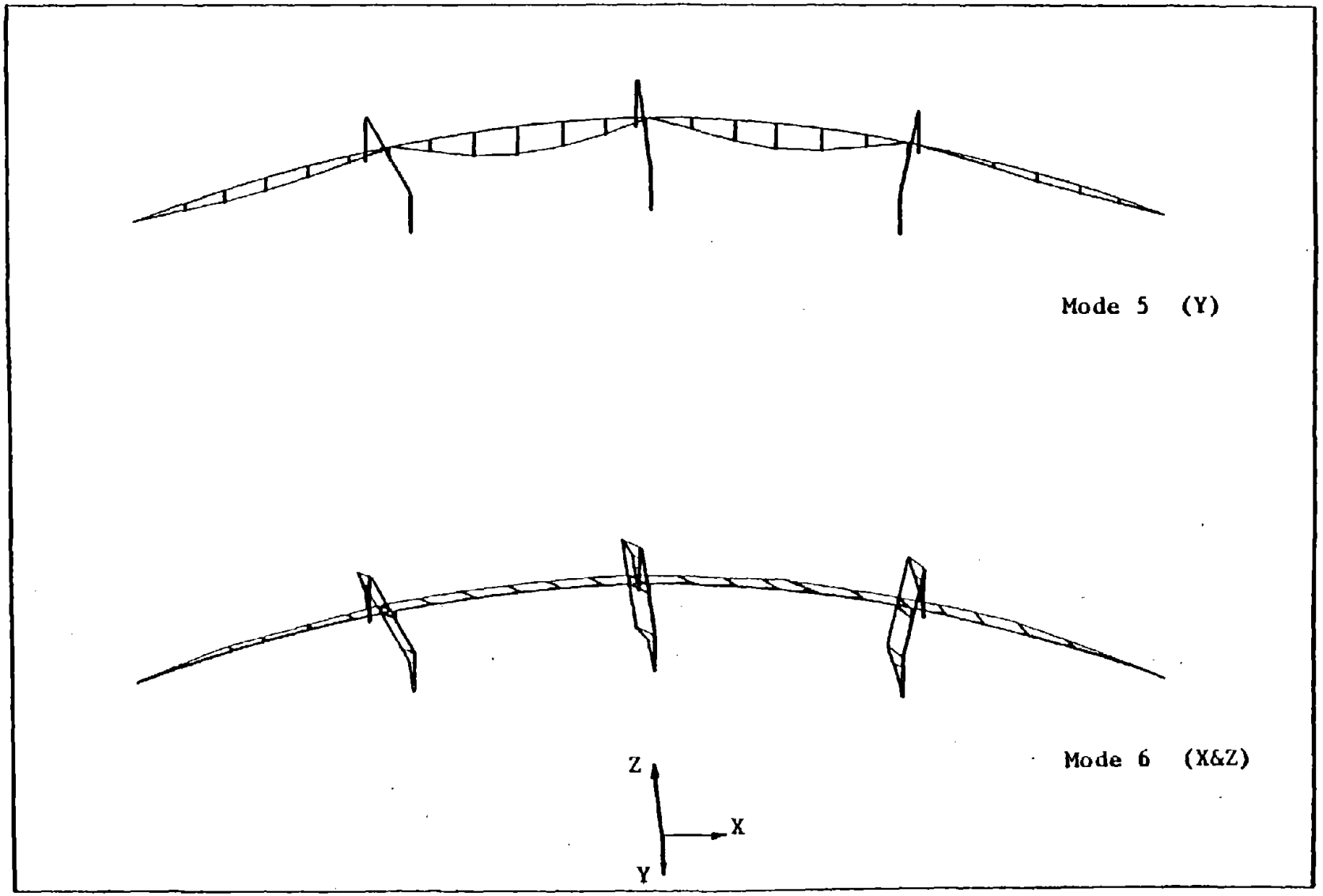


Figure B1.4 4-Span Curved Bridge Mode Shapes

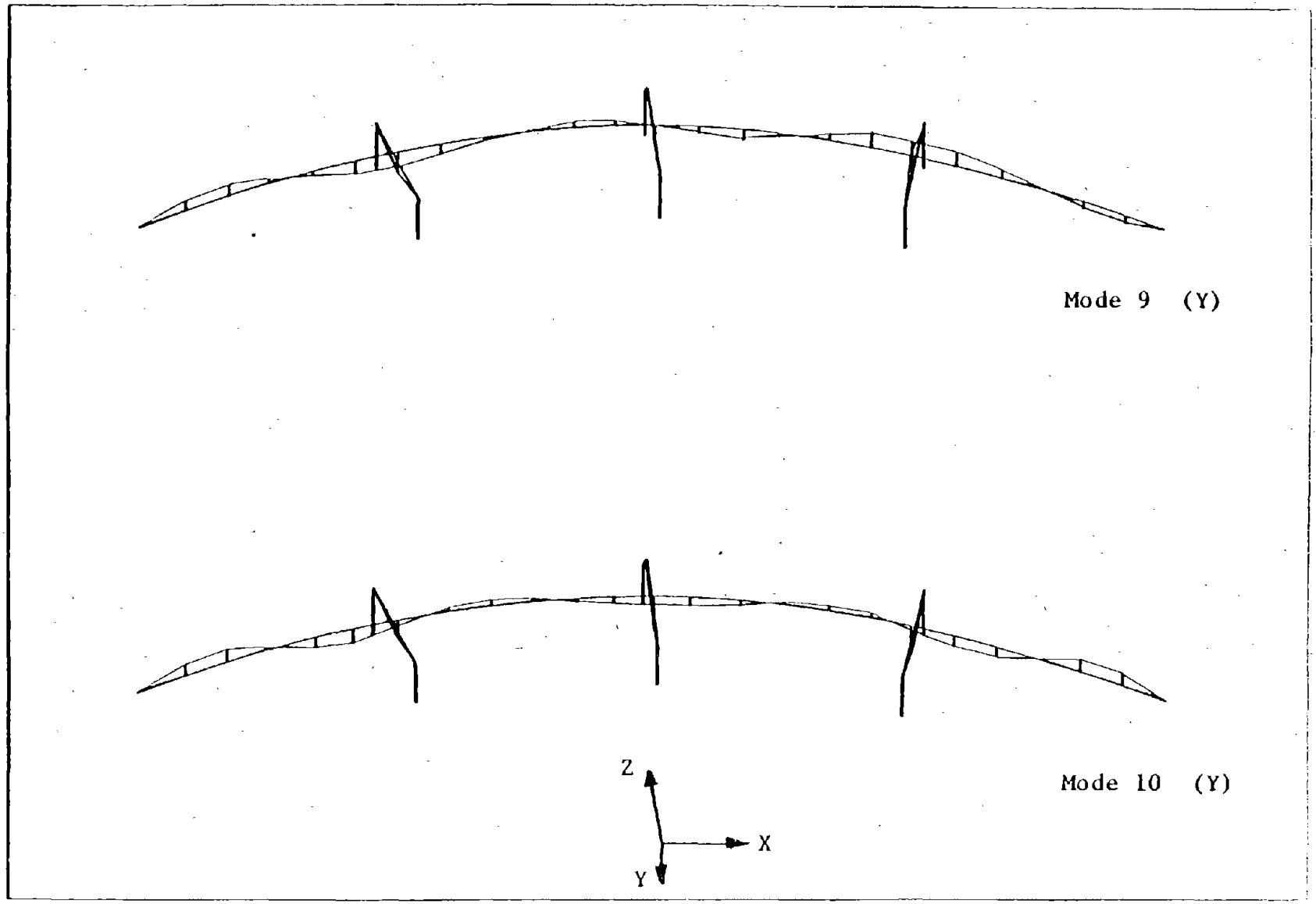


Figure B1.4 4-Span Curved Bridge Mode Shapes

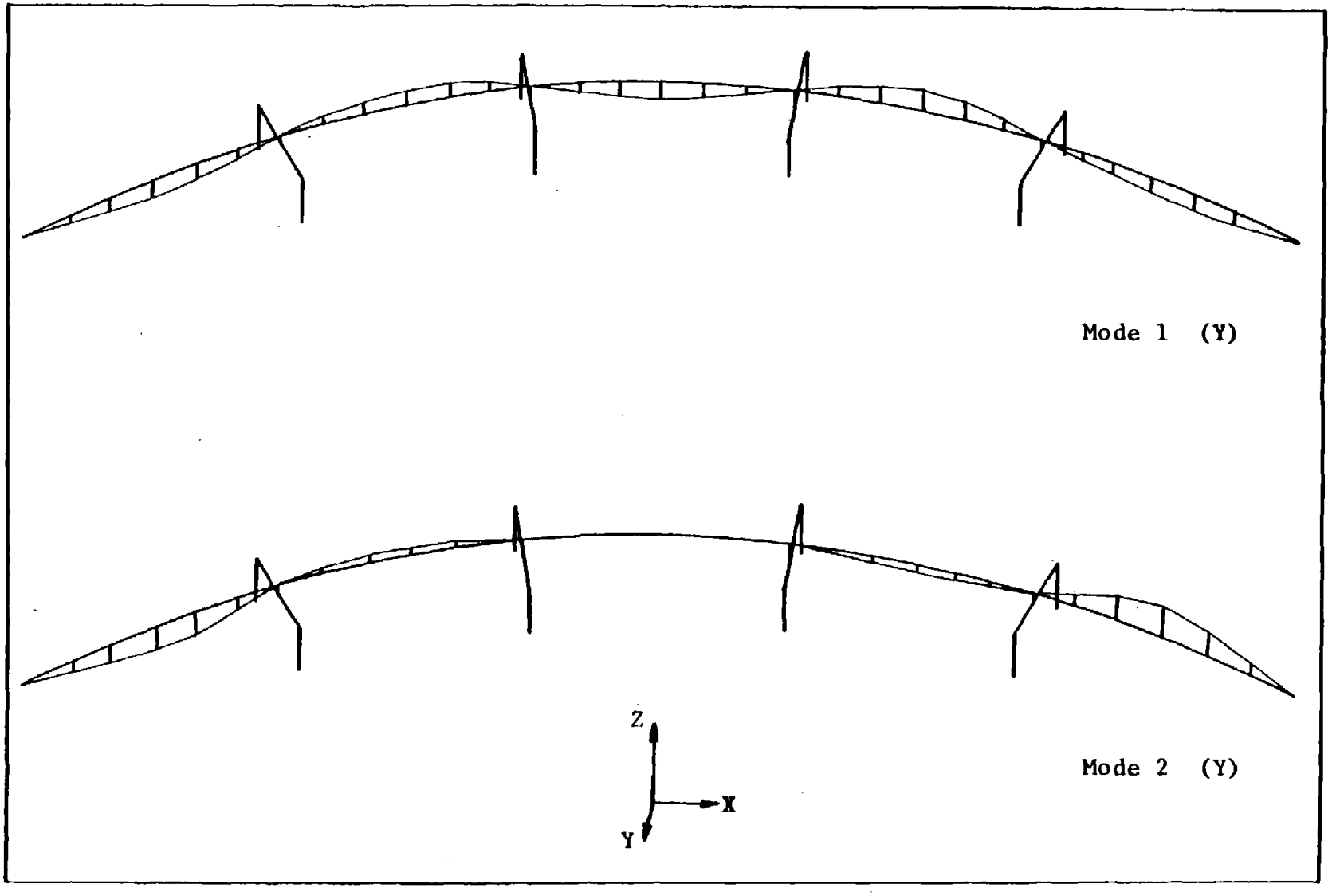


Figure B1.5 5-Span Curved Bridge Mode Shapes

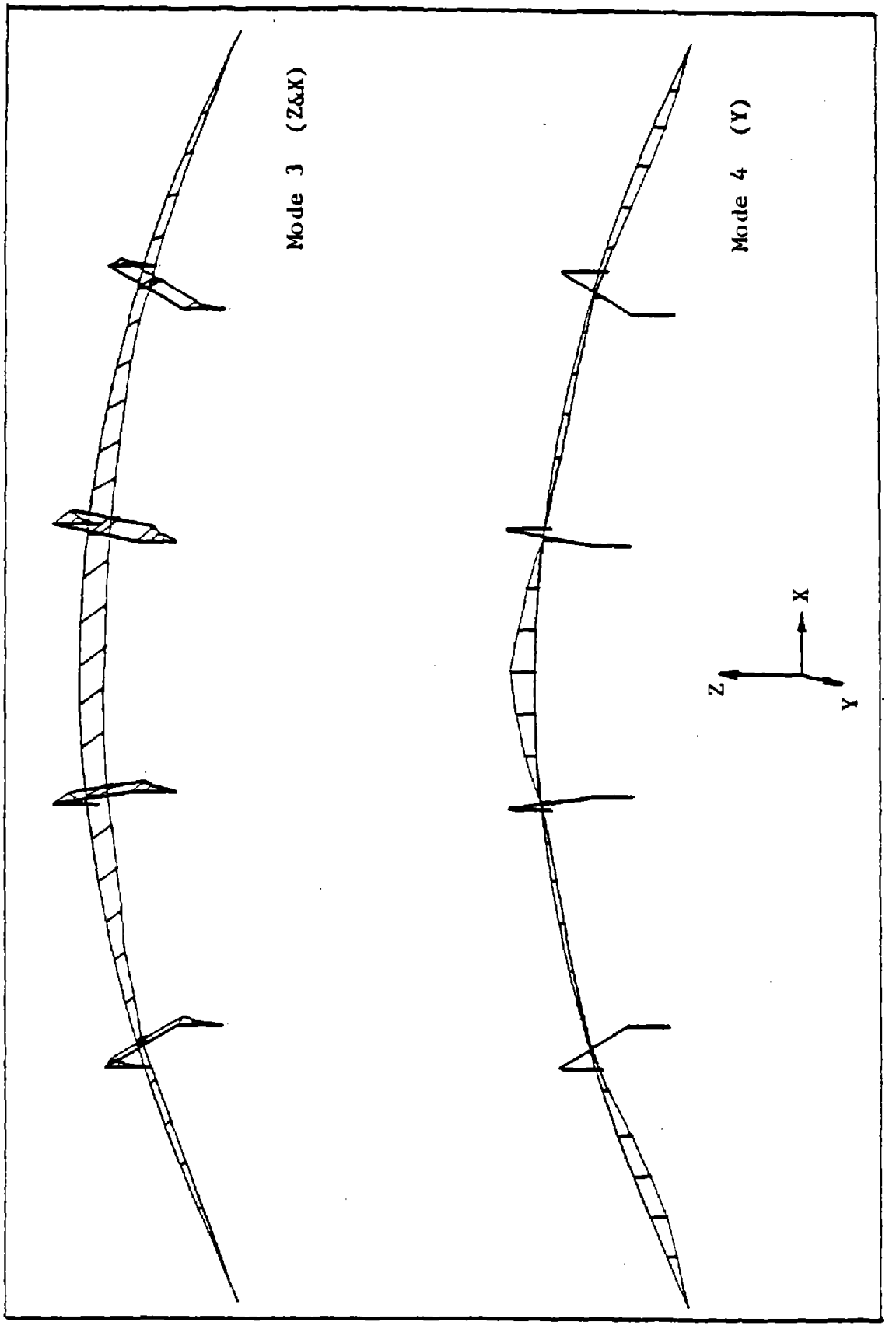


Figure B1.5 5-span Curved Bridge Mode Shapes

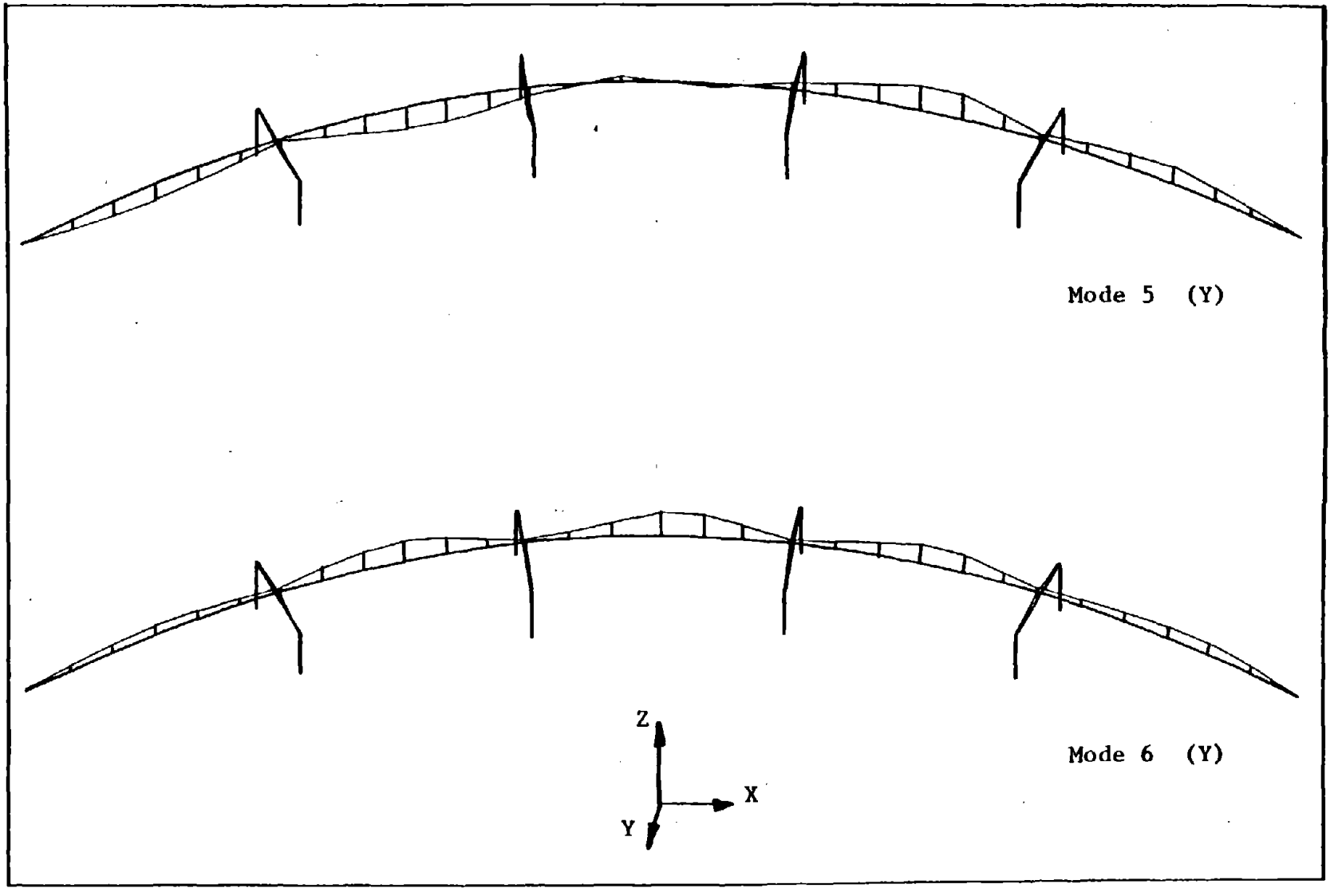


Figure B1.5 5-Span Curved Bridge Mode Shapes

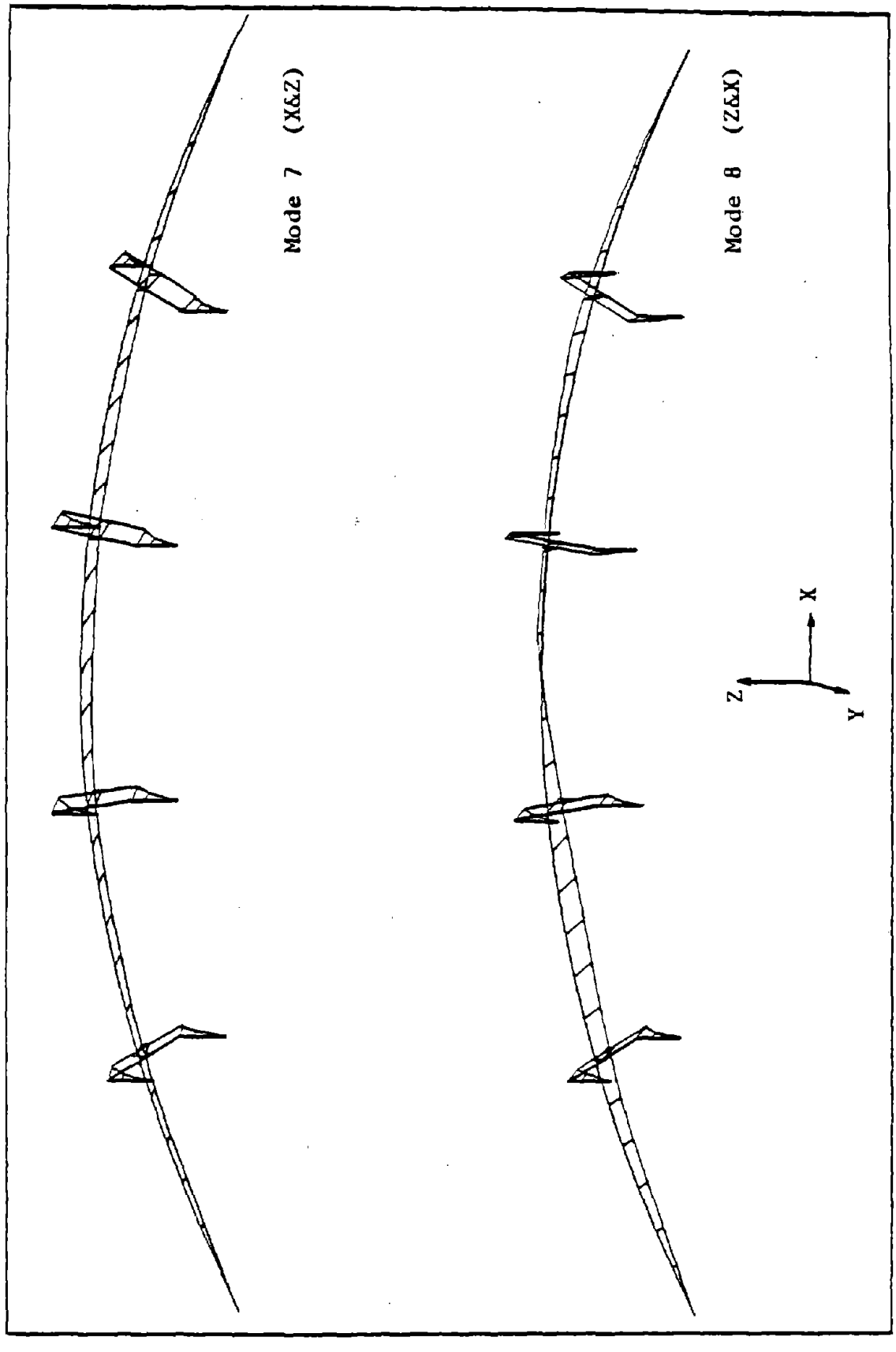


Figure B1.5 5-Span Curved Bridge Mode Shapes

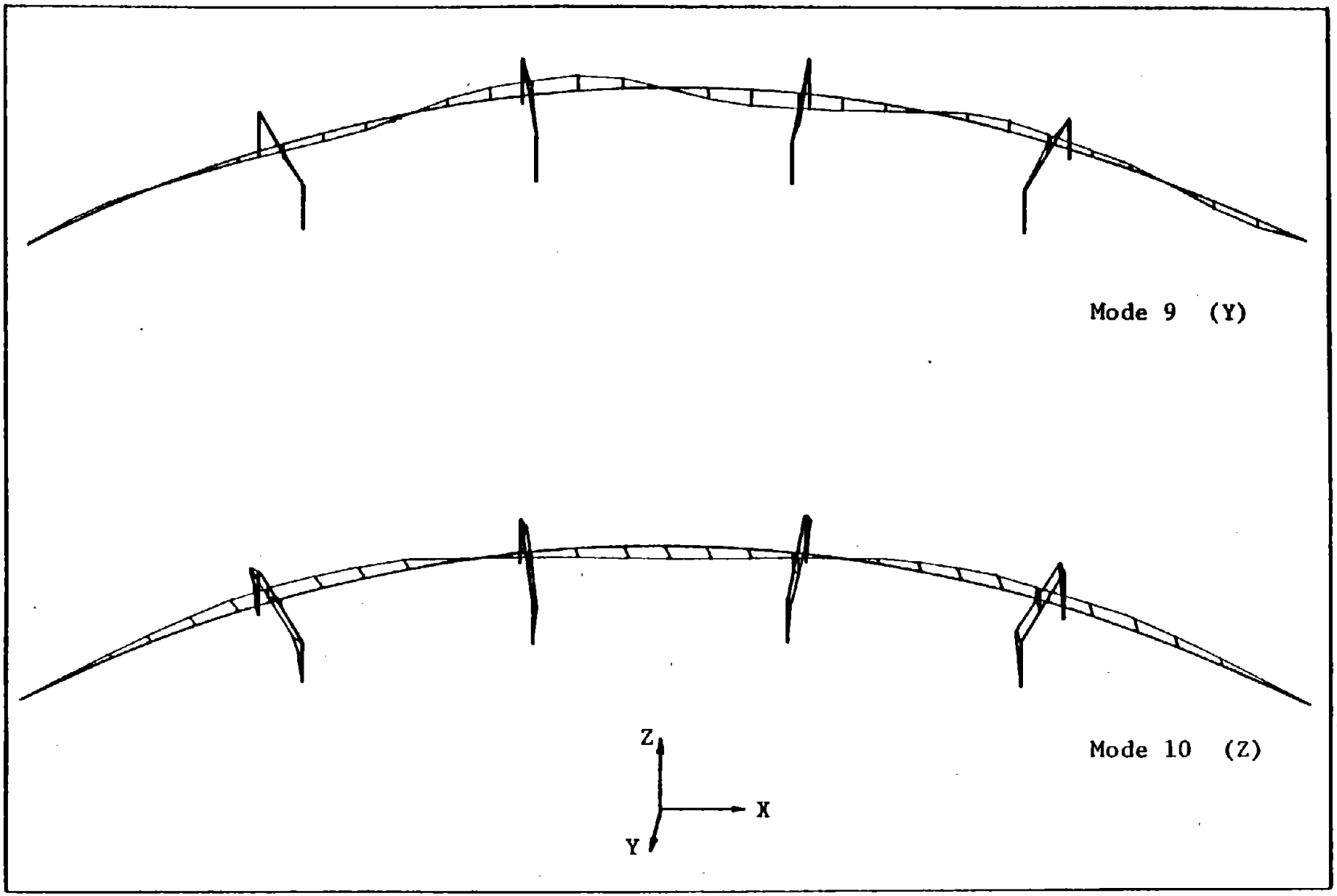


Figure B1.5 5-Span Curved Bridge Mode Shapes

## B.2 Design Curves

### B.2.1 Single Span Bridges

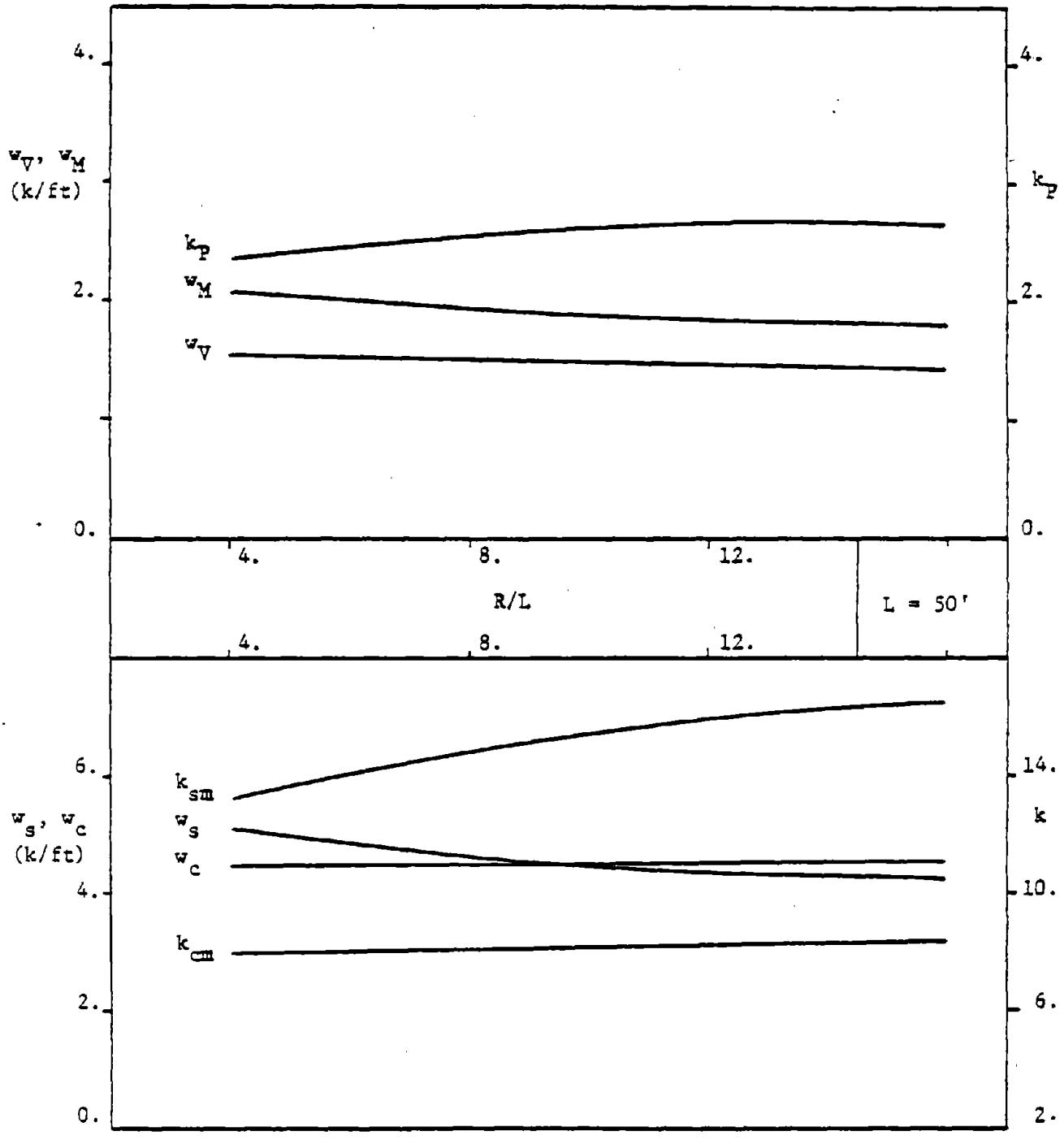


Figure B21.1 Actions at the Attachments and Deck Stresses

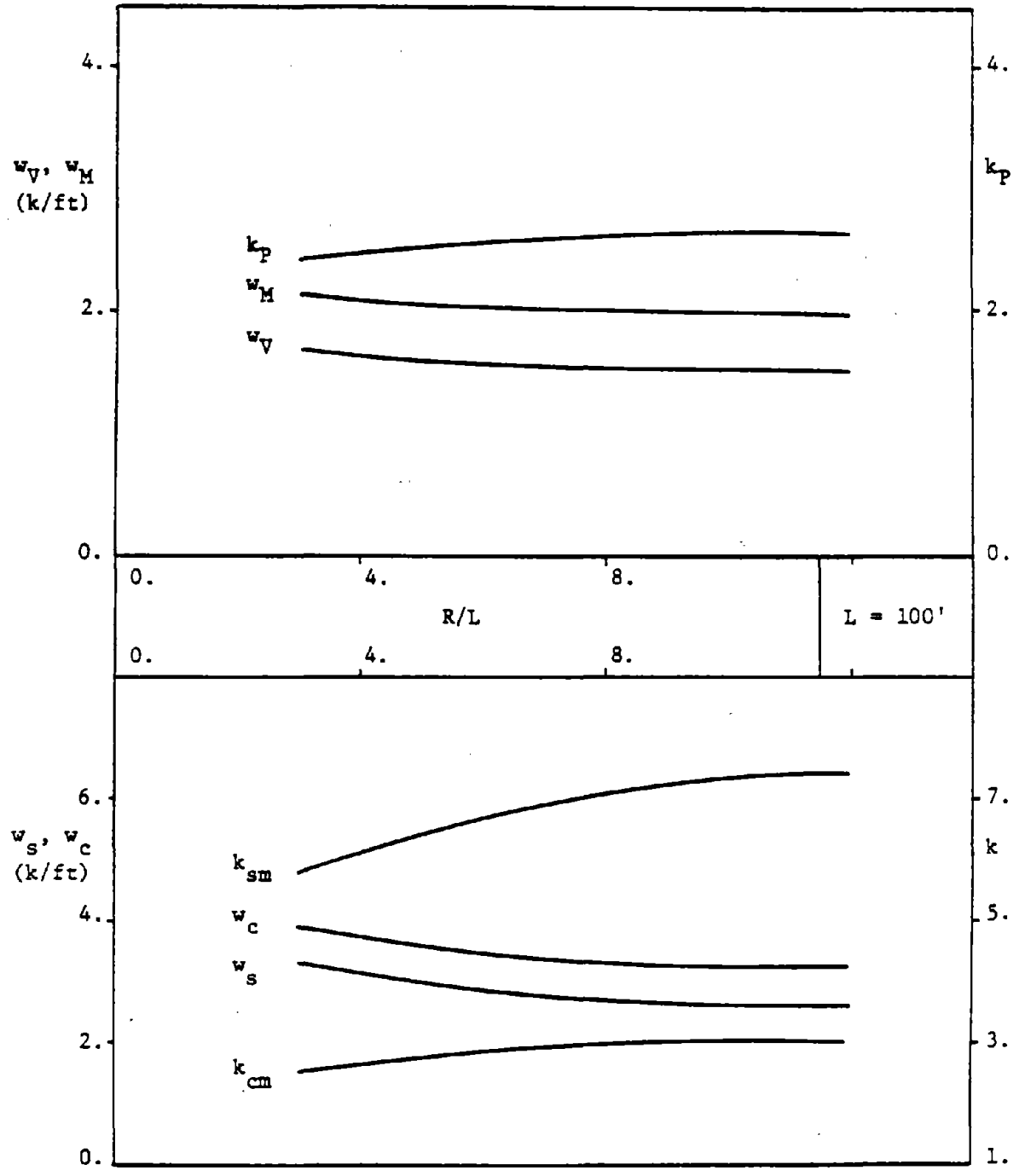


Figure B21.2 Actions at the Attachments and Deck Stresses

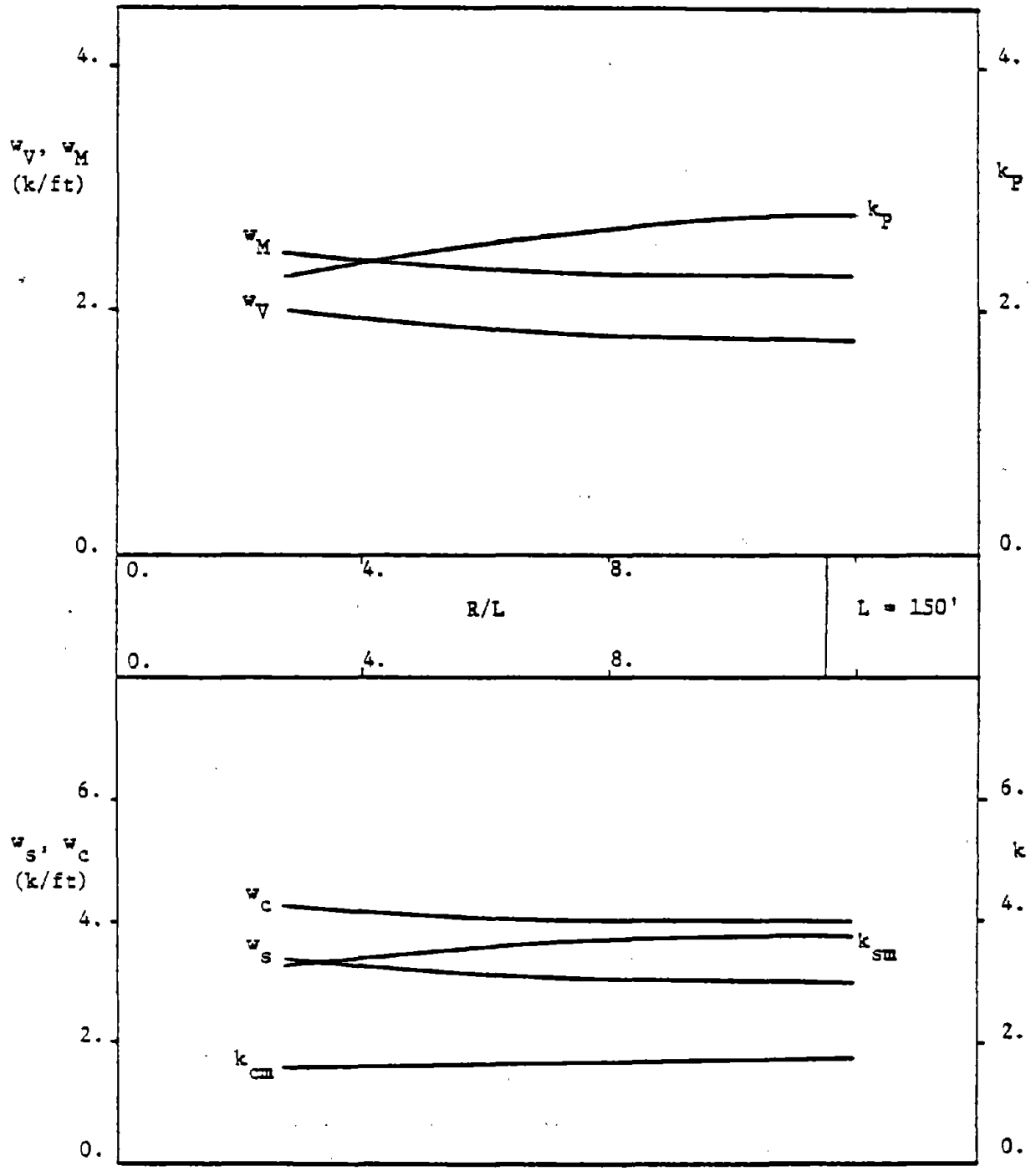


Figure B21.3 Actions at the Attachments and Deck Stresses

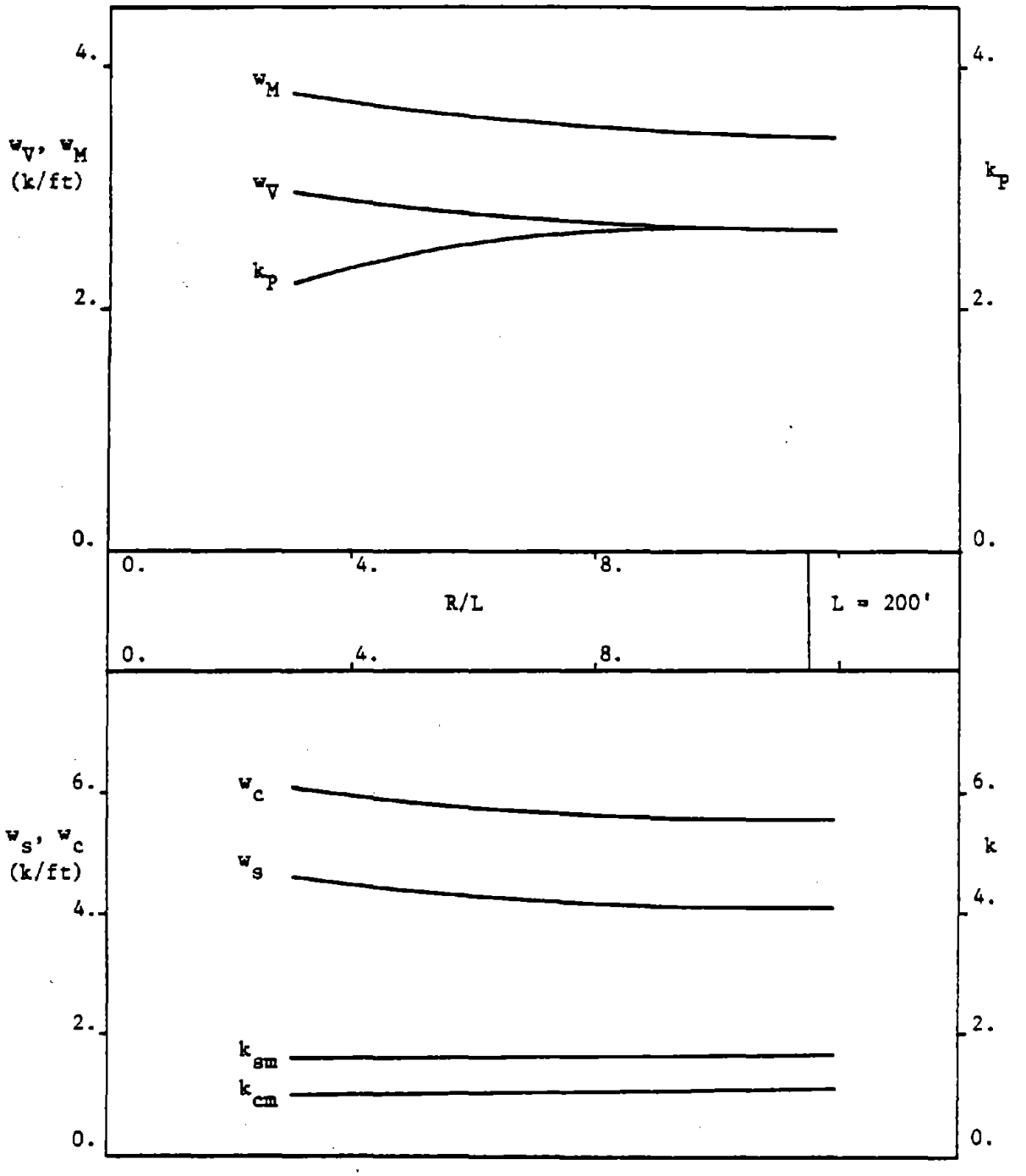


Figure B21.4 Actions at the Attachments and Deck Stresses

## B.2.2 2-Span Bridges

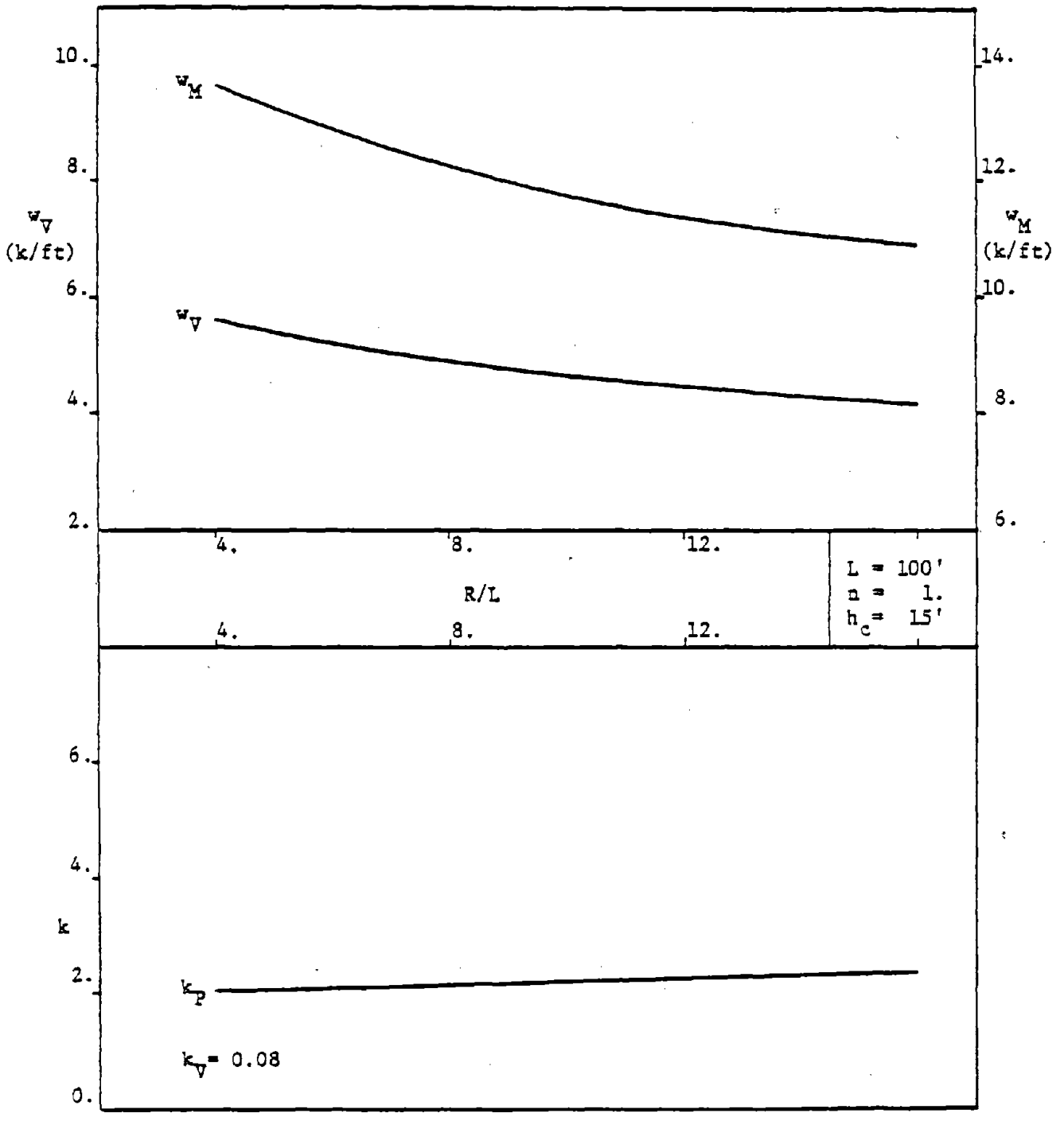


Figure B22.1 Actions at the Attachments

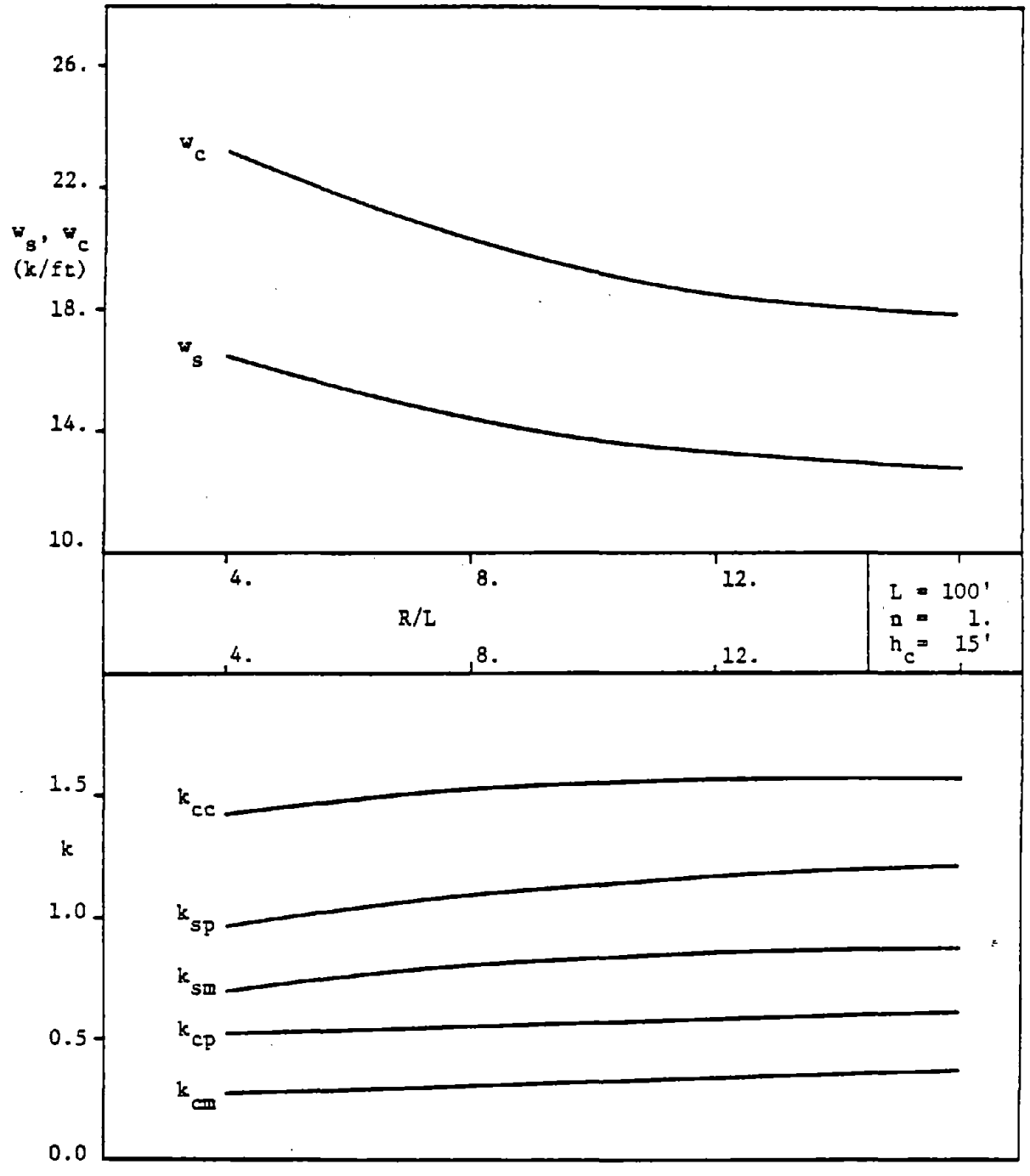


Figure B22.2 Deck and Column Stresses

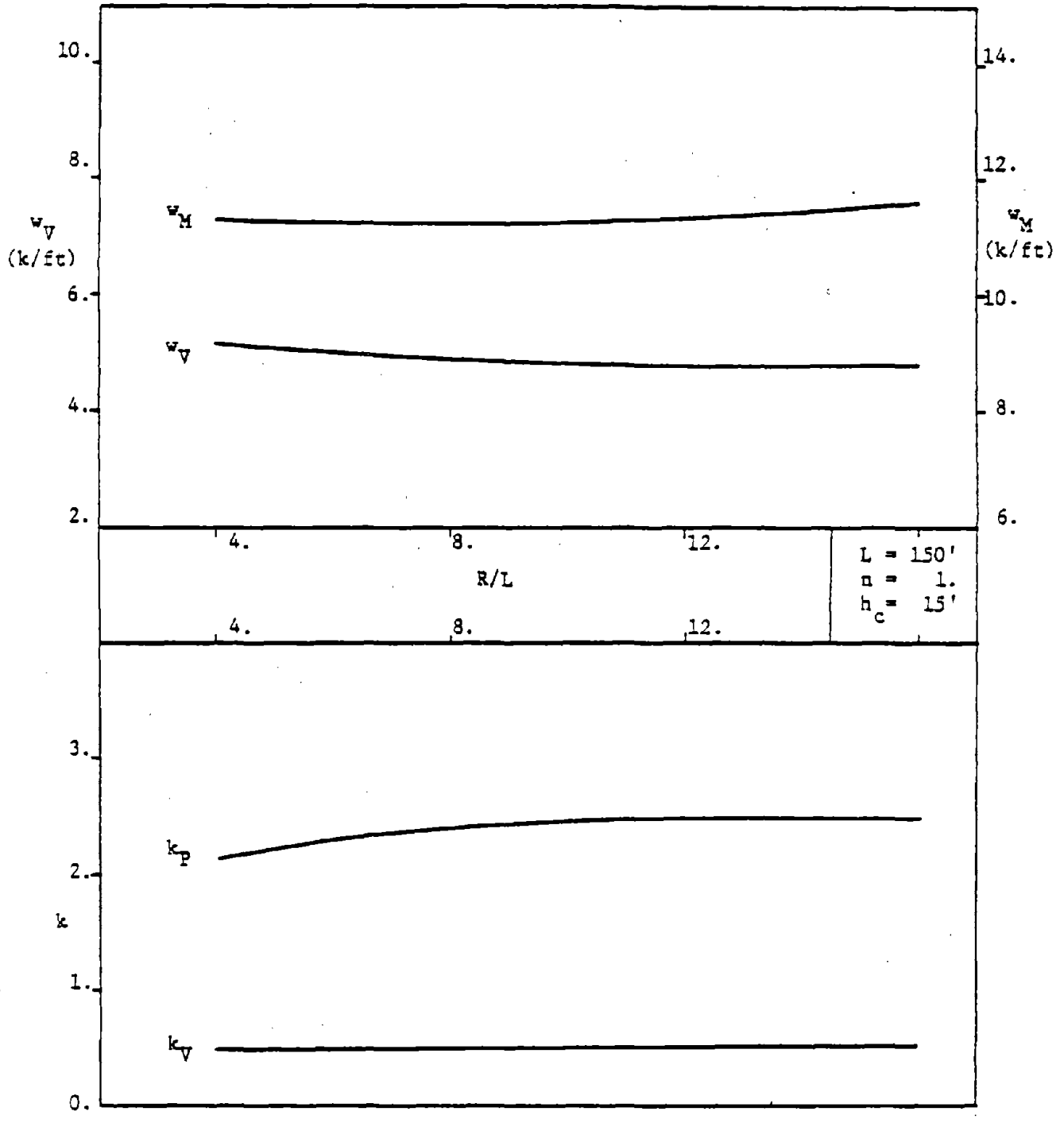


Figure B22.3 Actions at the Attachments

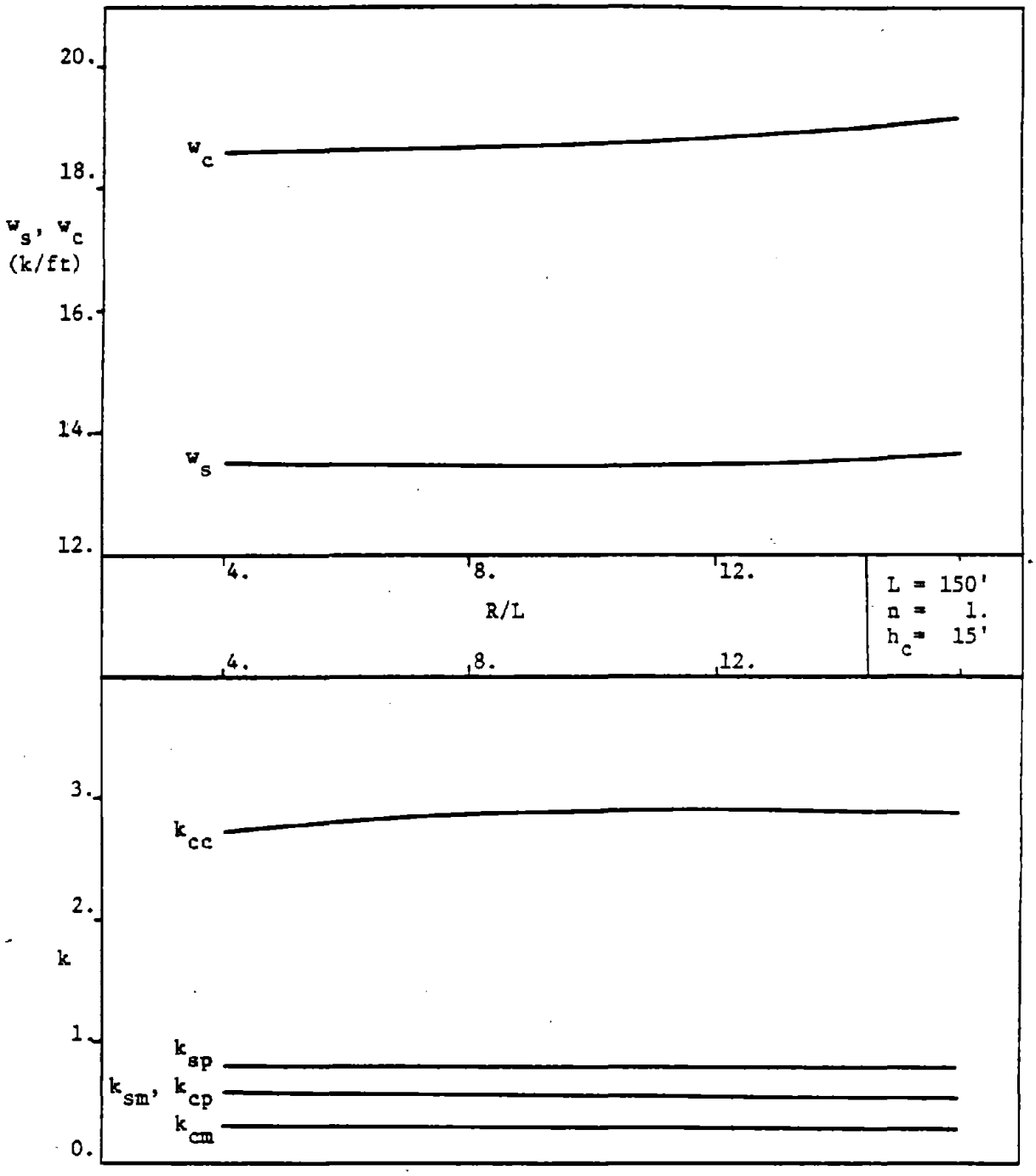


Figure B22.4 Deck and Column Stresses

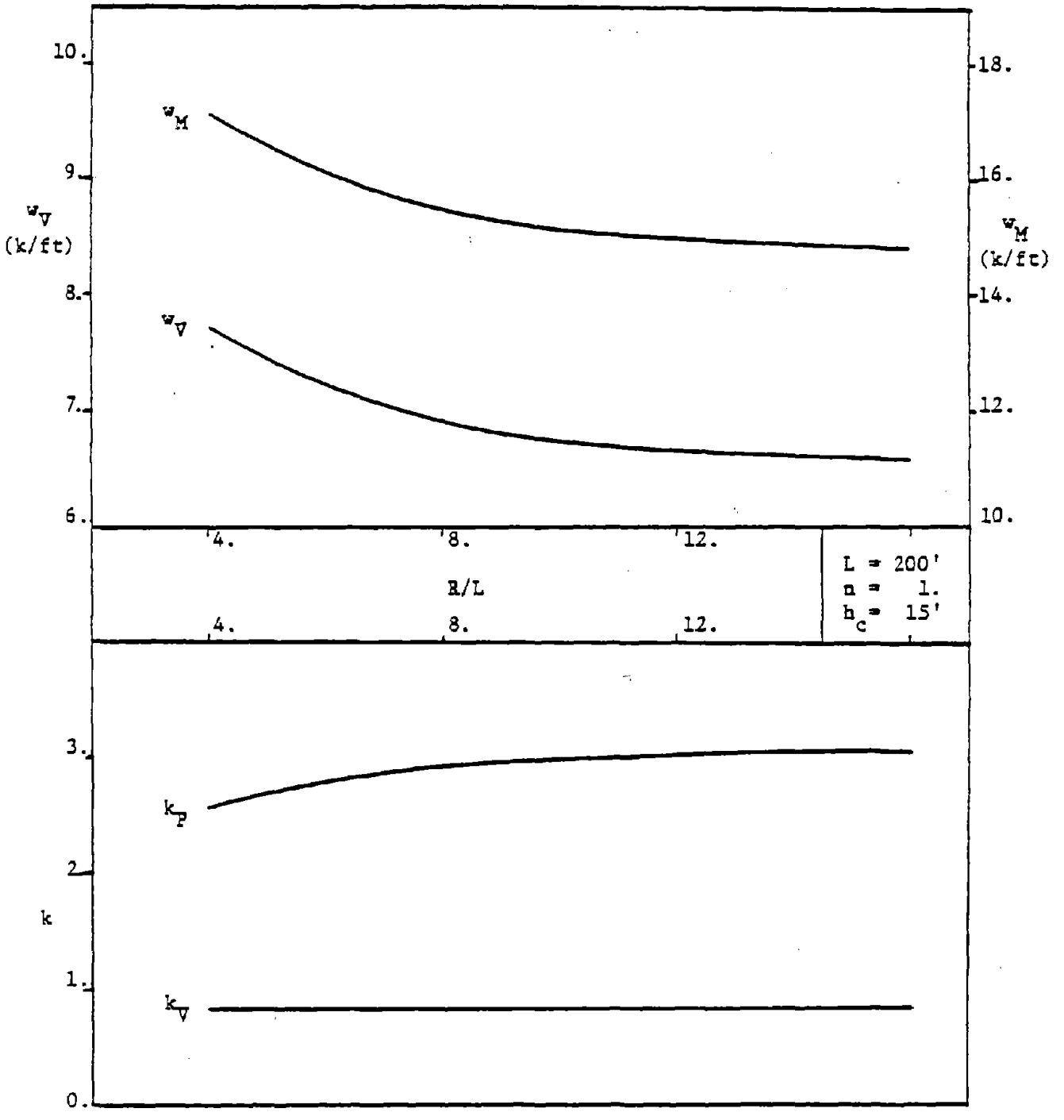


Figure B22.5 Actions at the Attachments

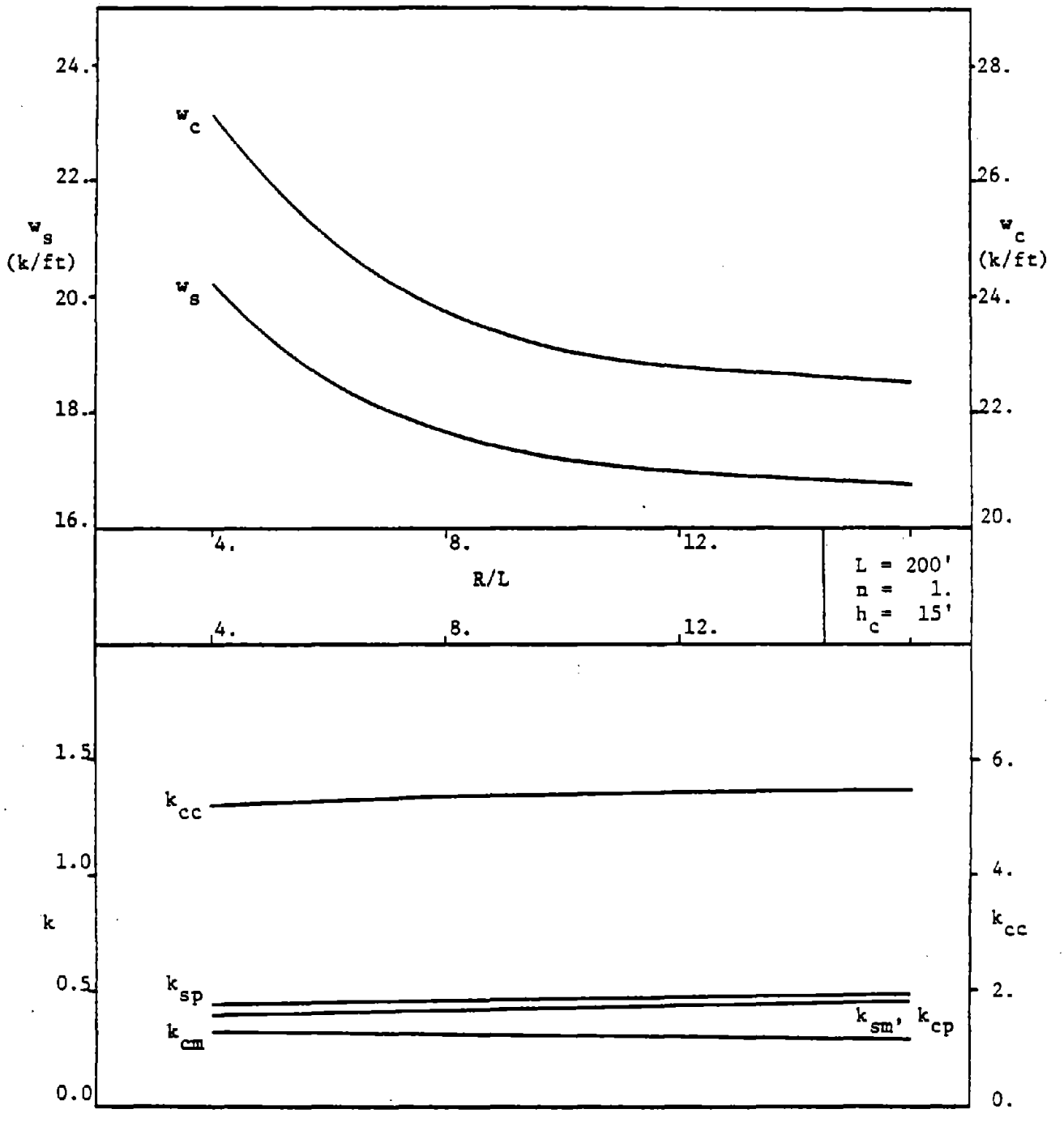


Figure B22.6 Deck and Column Stresses

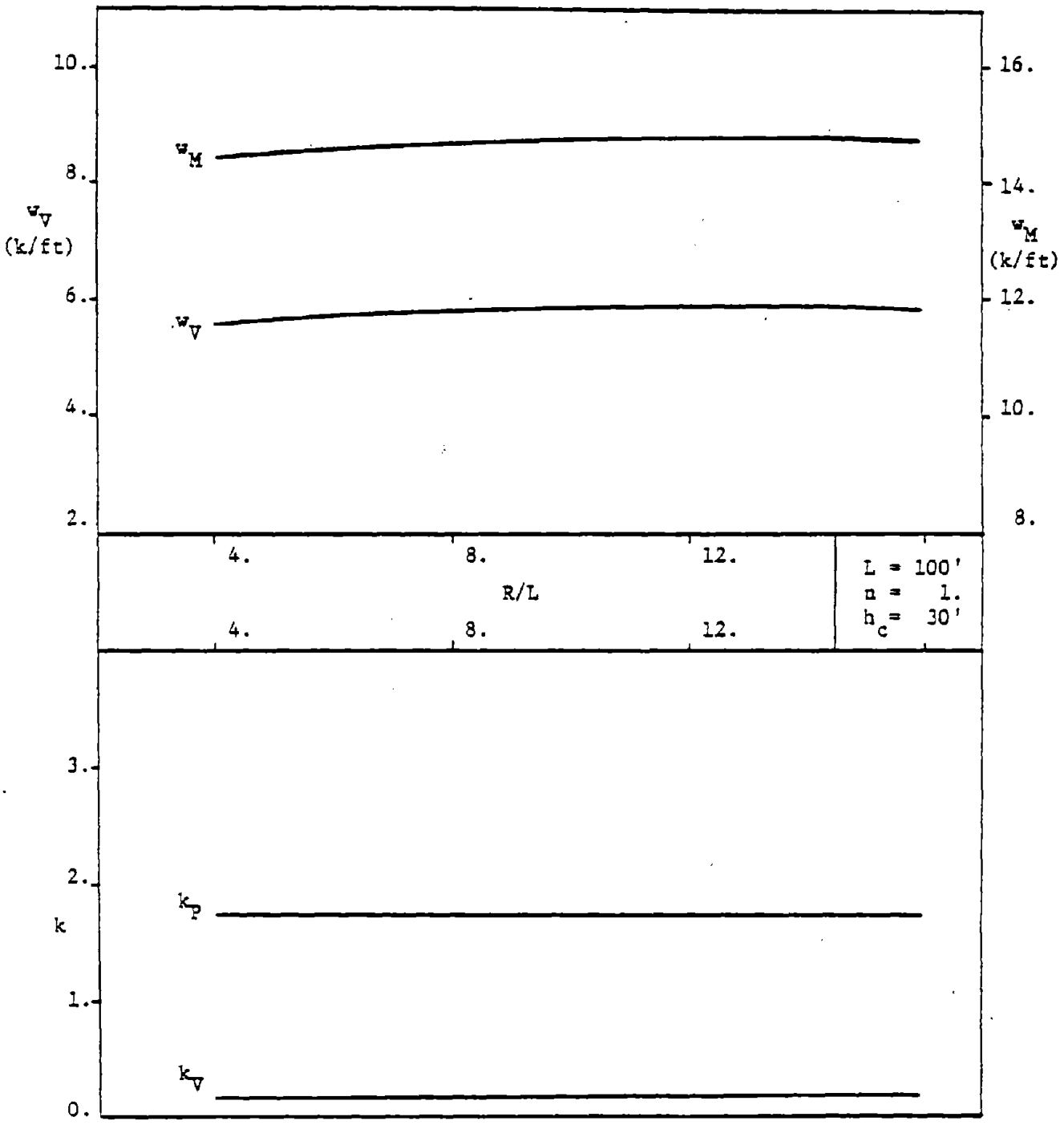


Figure B22.7 Actions at the Attachments

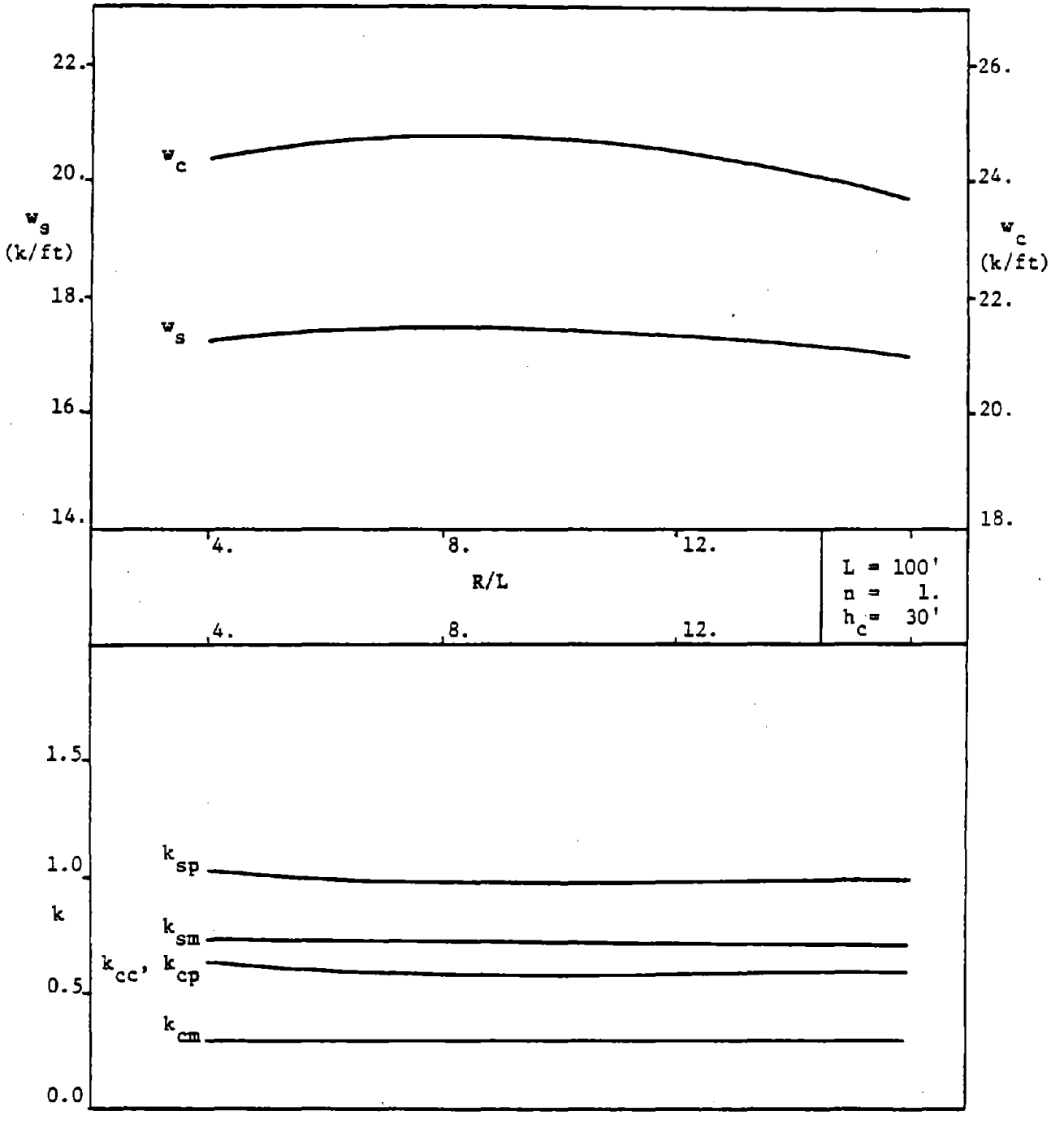


Figure B22.8 Deck and Column Stresses

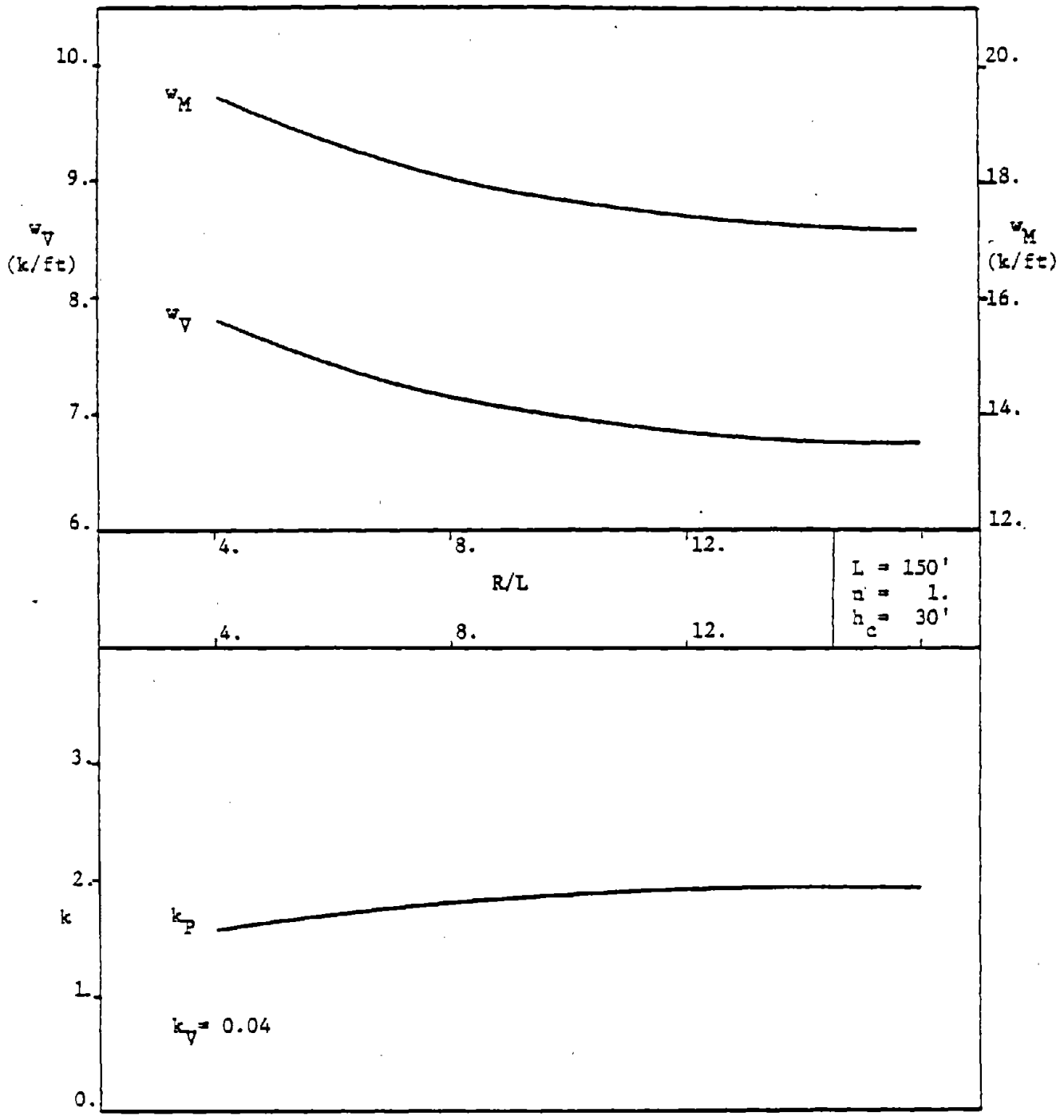


Figure B22.9 Actions at the Attachments

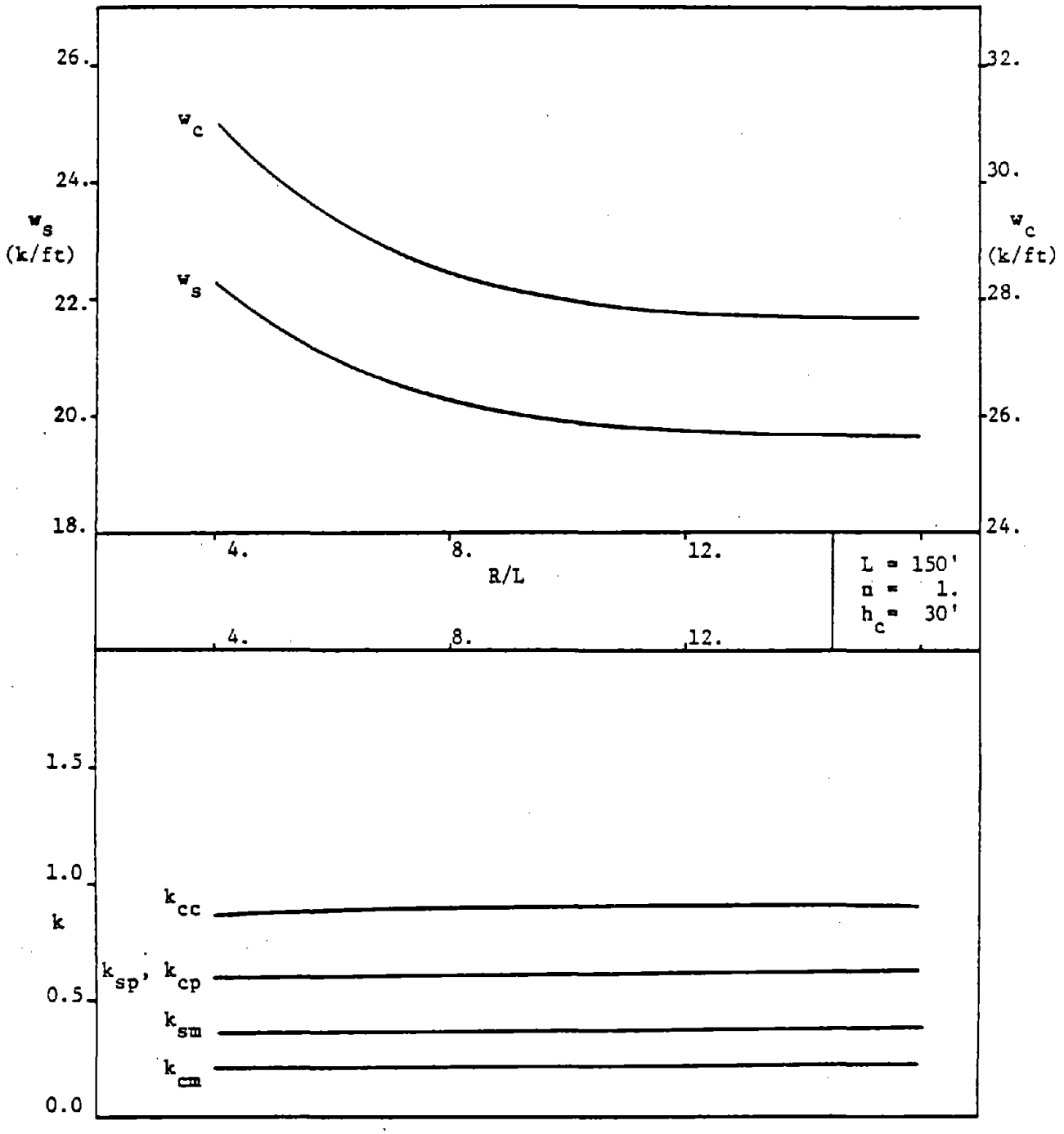


Figure B22.10 Deck and Column Stresses

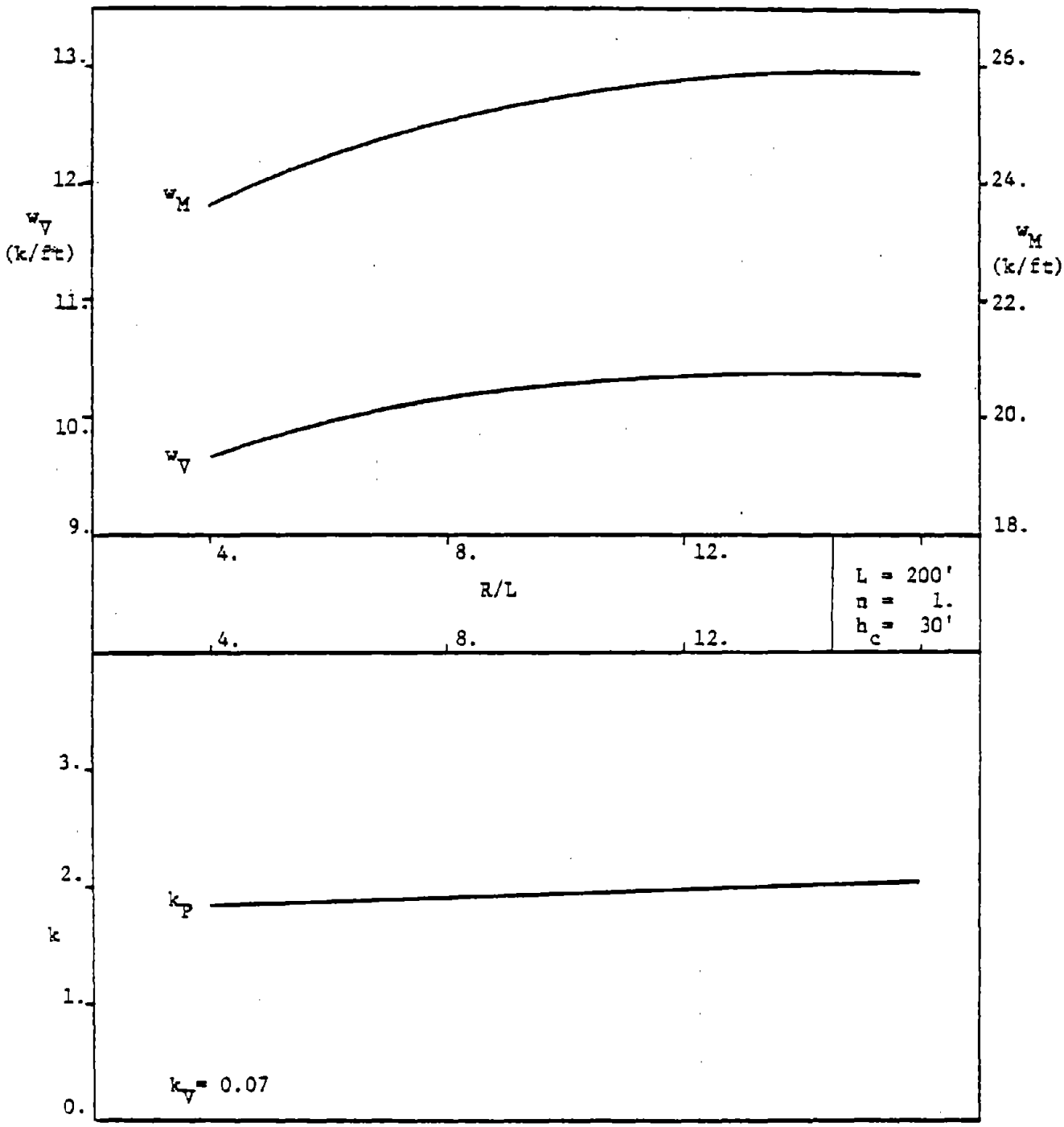


Figure B22.11 Actions at the Attachments

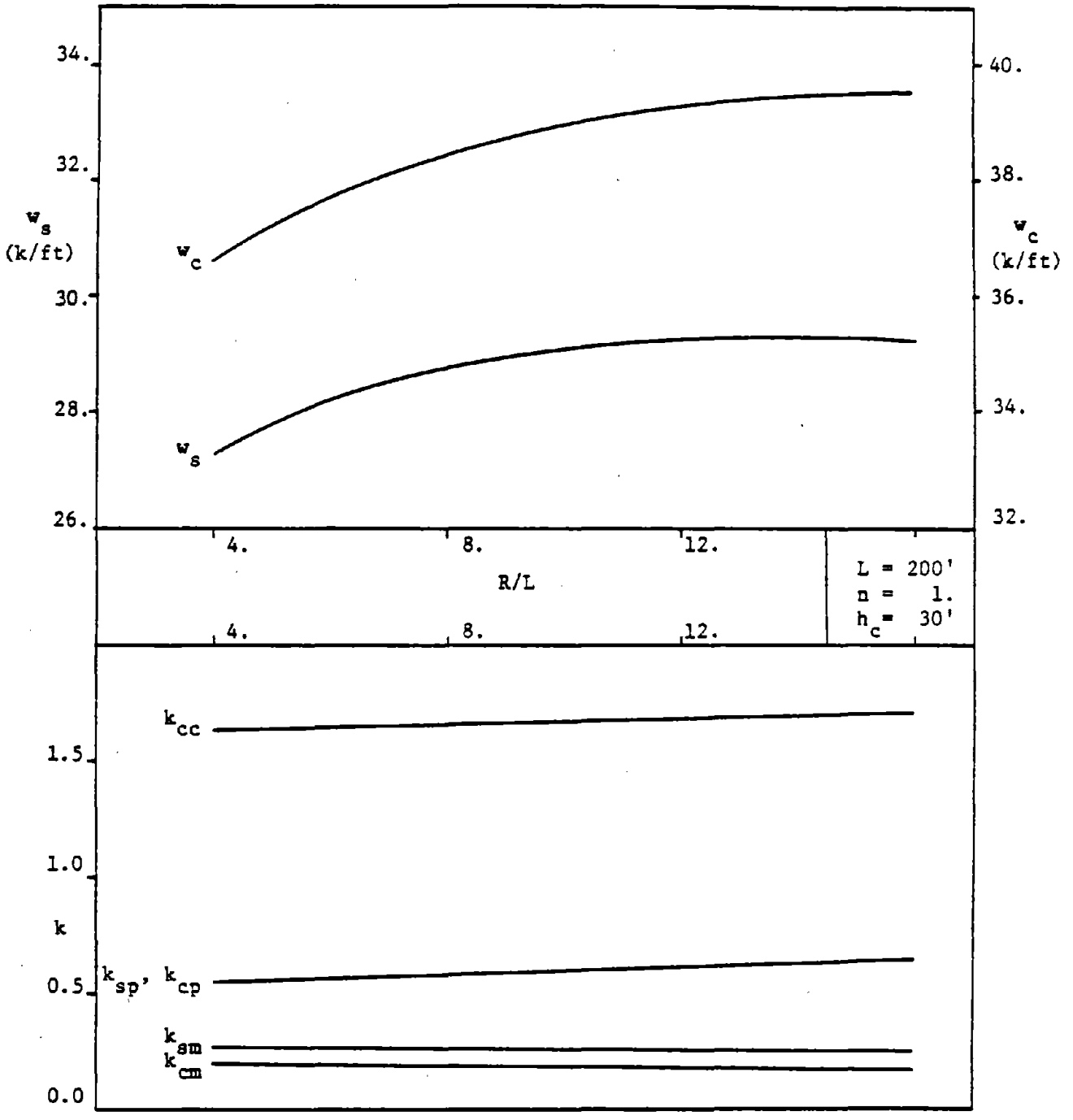


Figure B22.12 Deck and Column Stresses

## B.2.3 3-Span Bridges

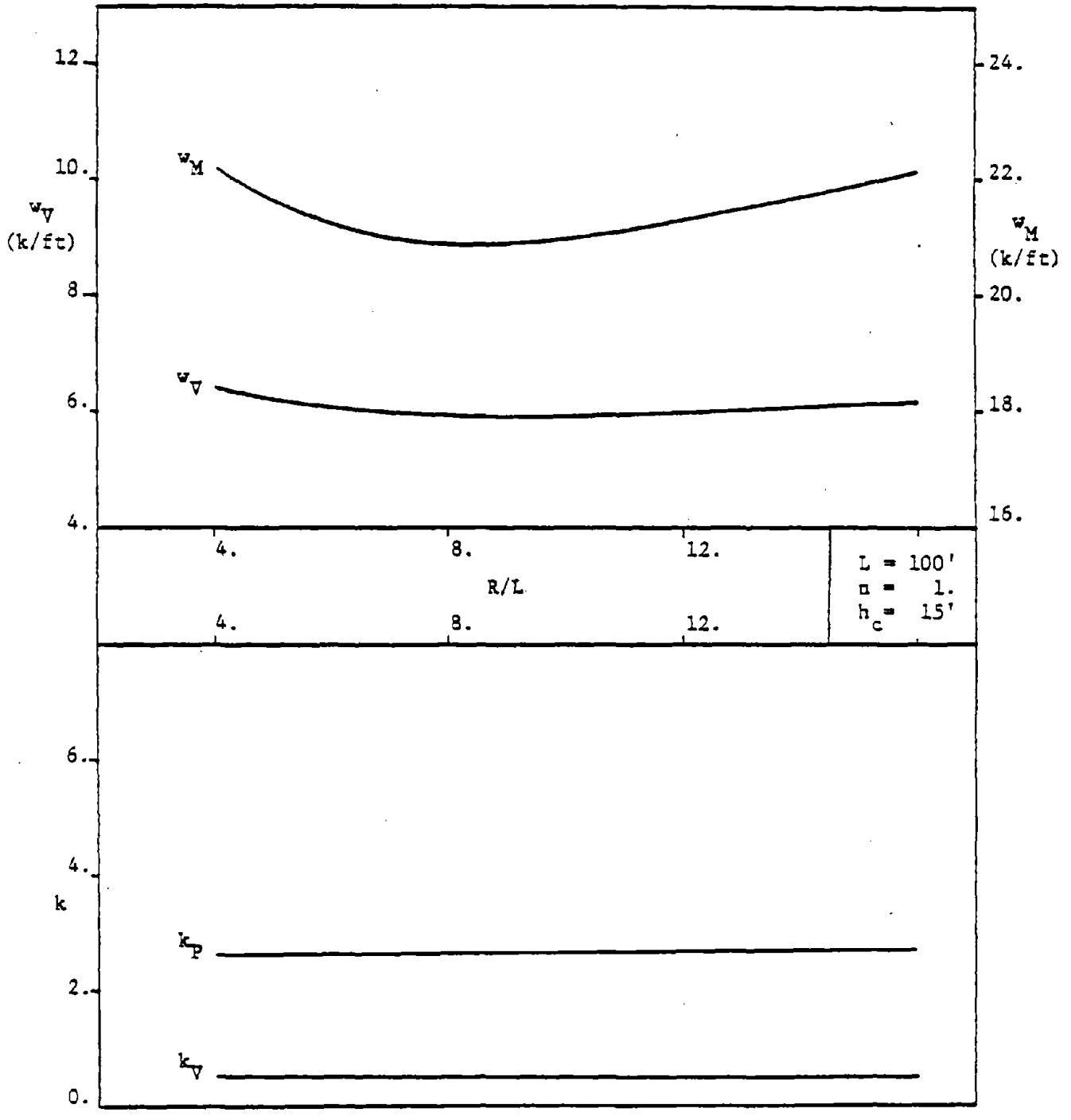


Figure B23.1 Actions at the Attachments

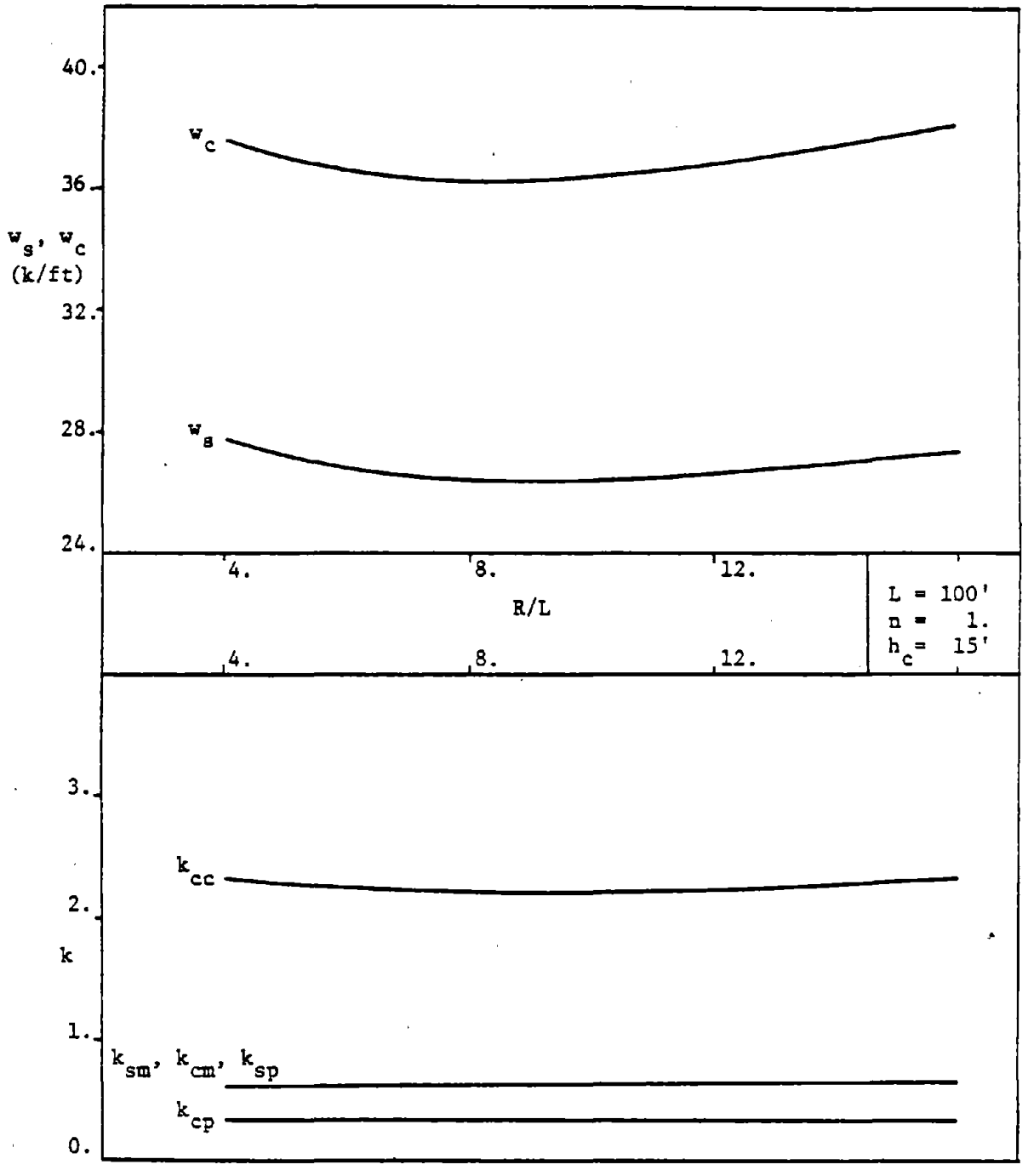


Figure B23.2 Deck and Column Stresses

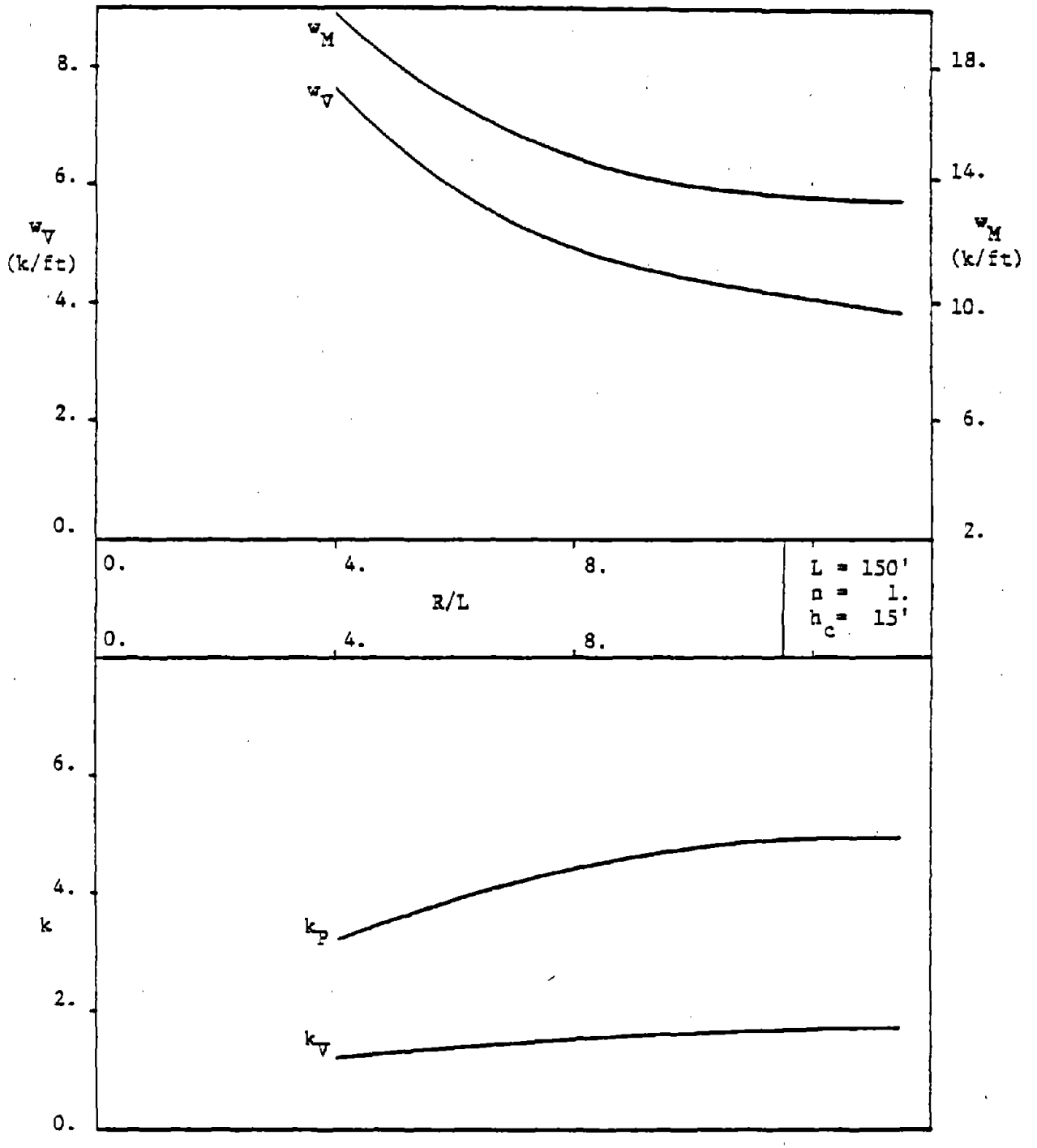


Figure B23.3 Actions at the Attachments

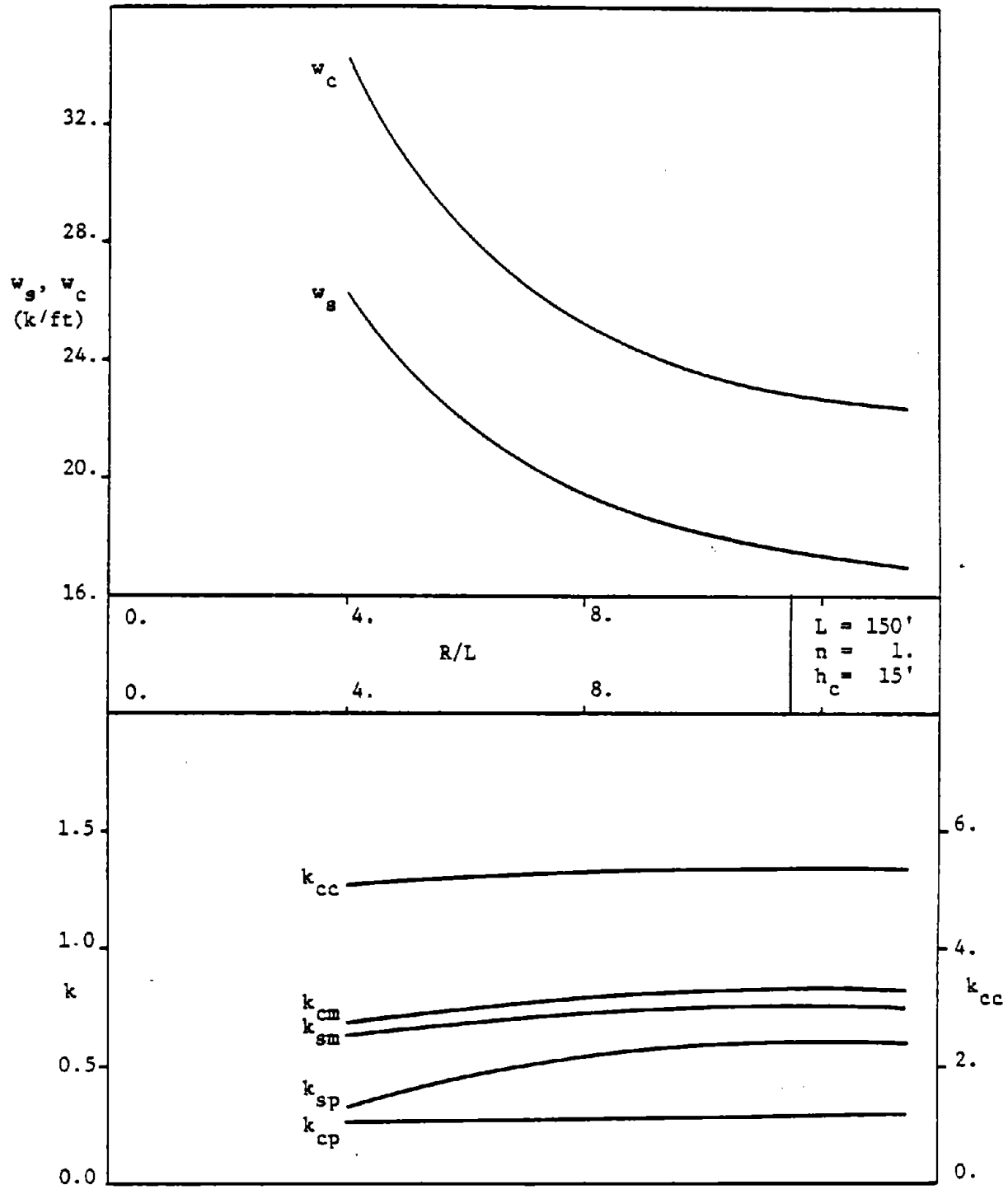


Figure B23.4 Deck and Column Stresses

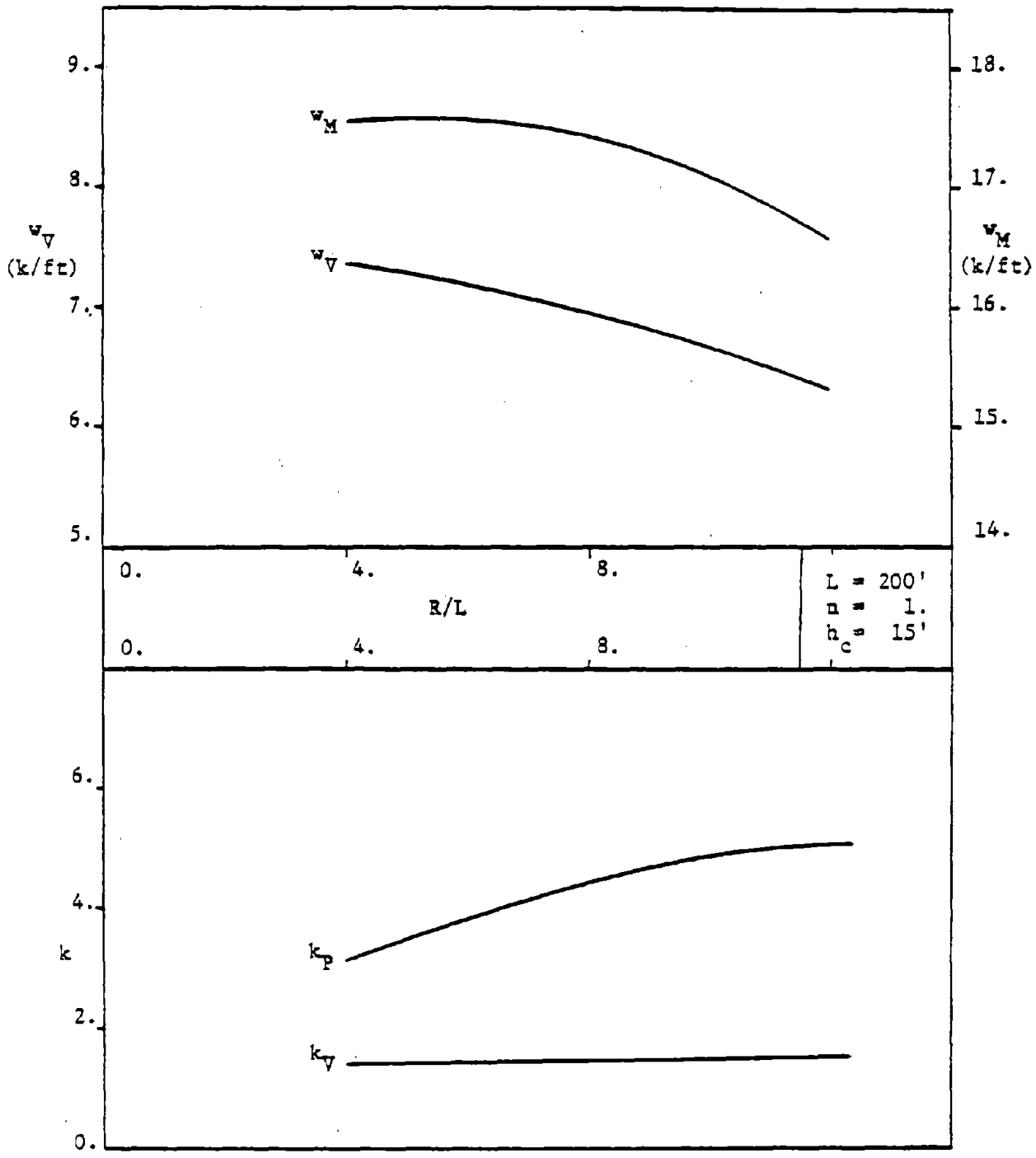


Figure B23.5 Actions at the Attachments

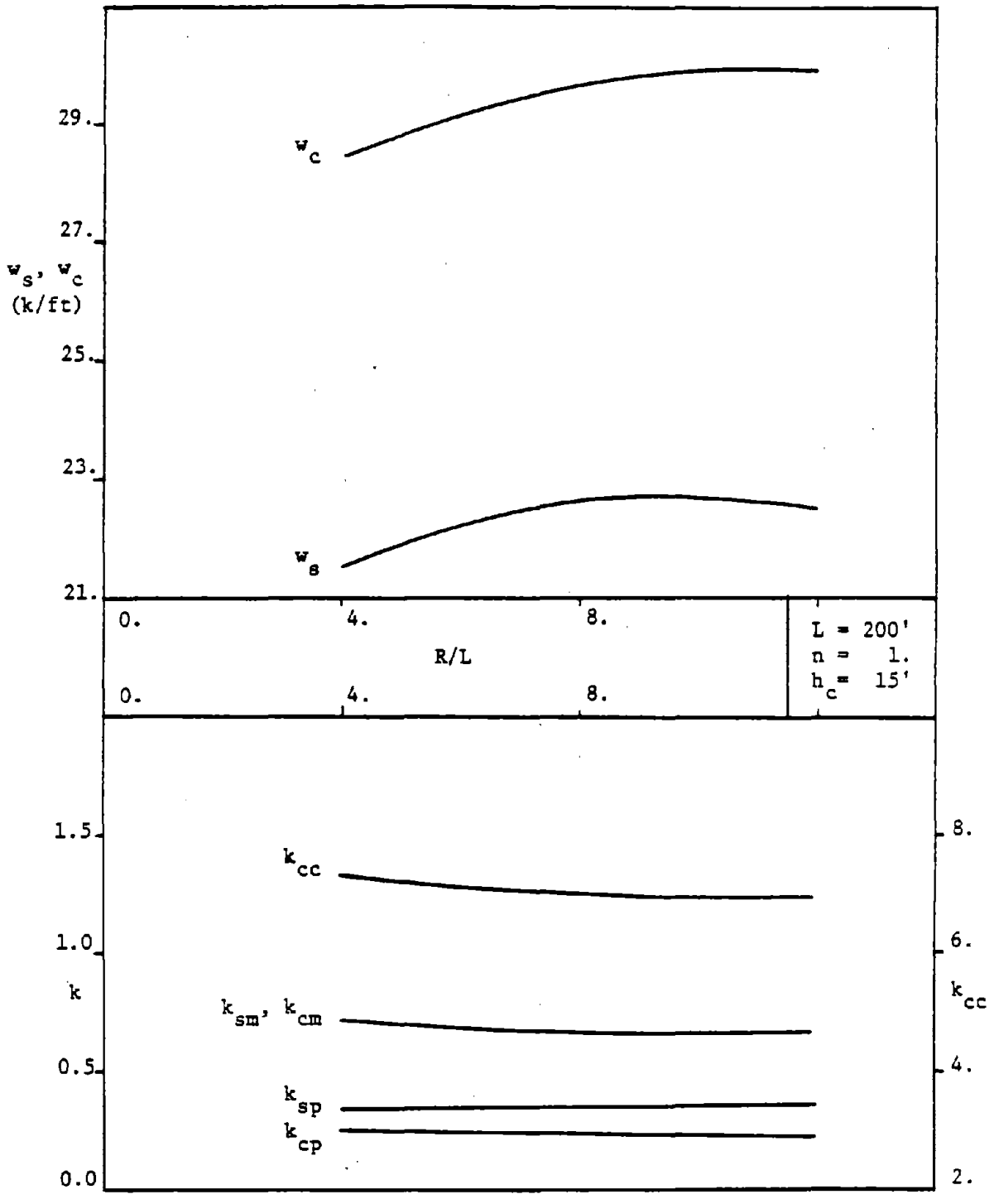


Figure B23.6 Deck and Column Stresses

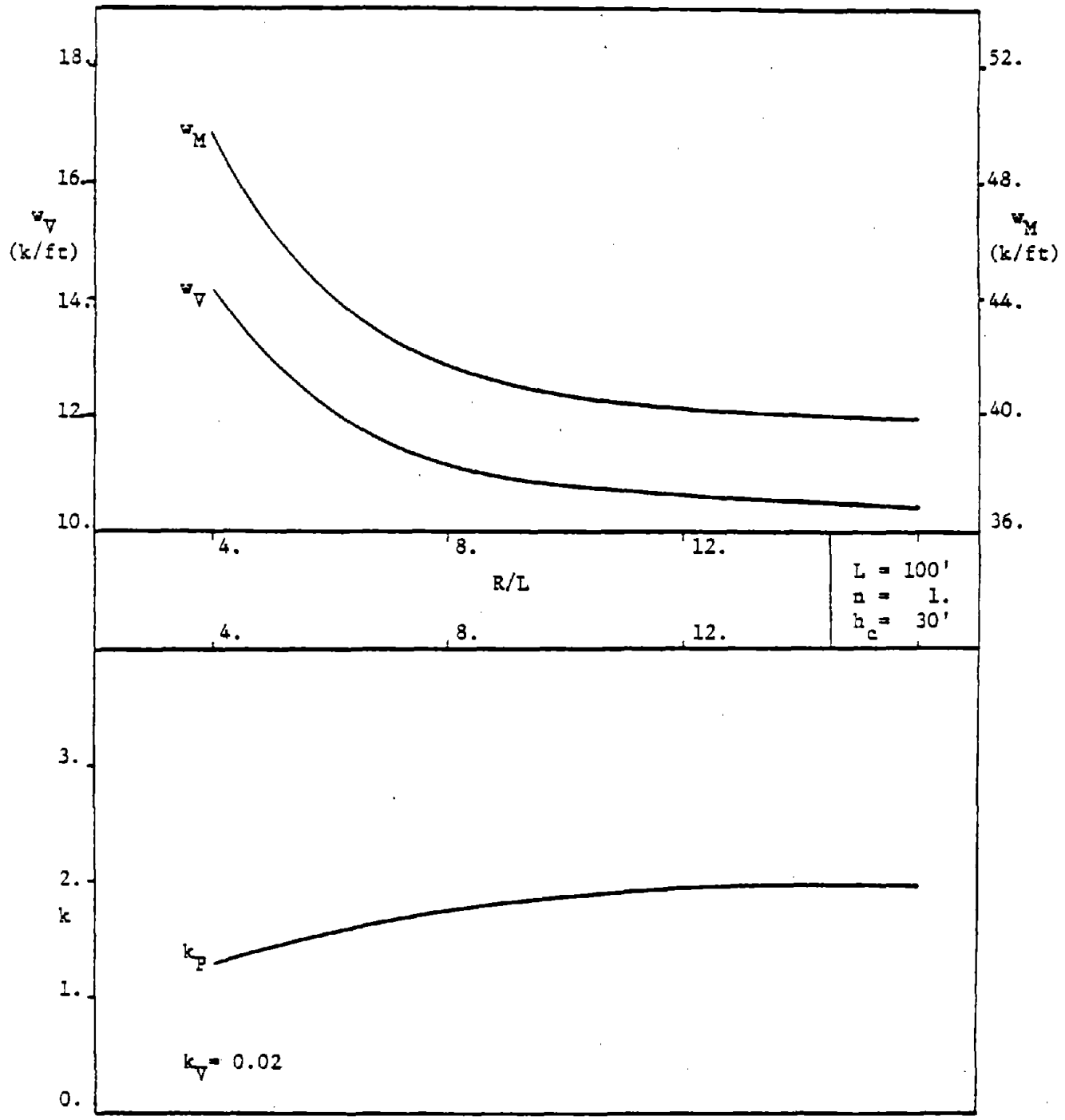


Figure B23.7 Actions at the Attachments

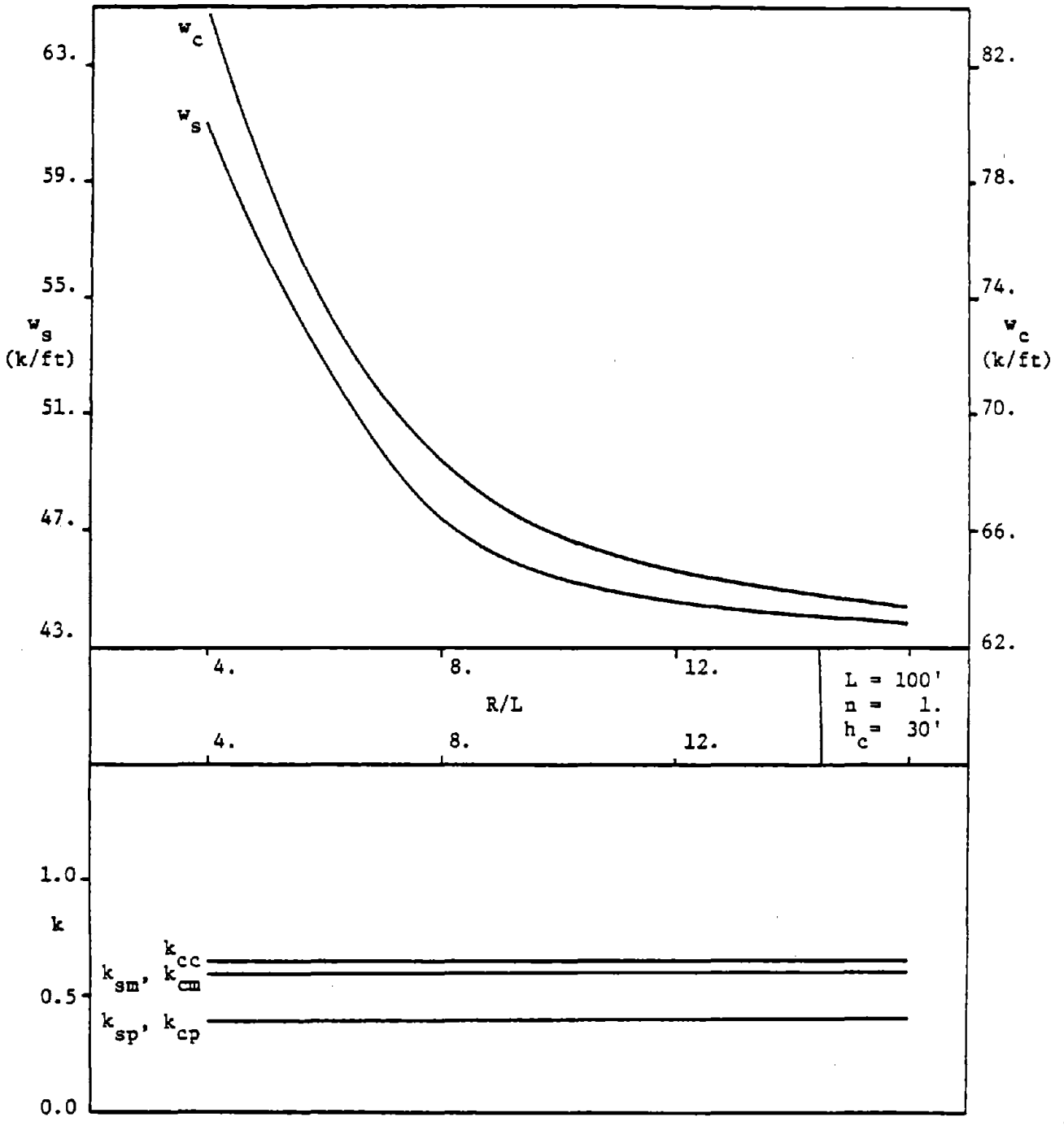


Figure B23.8 Deck and Column Stresses

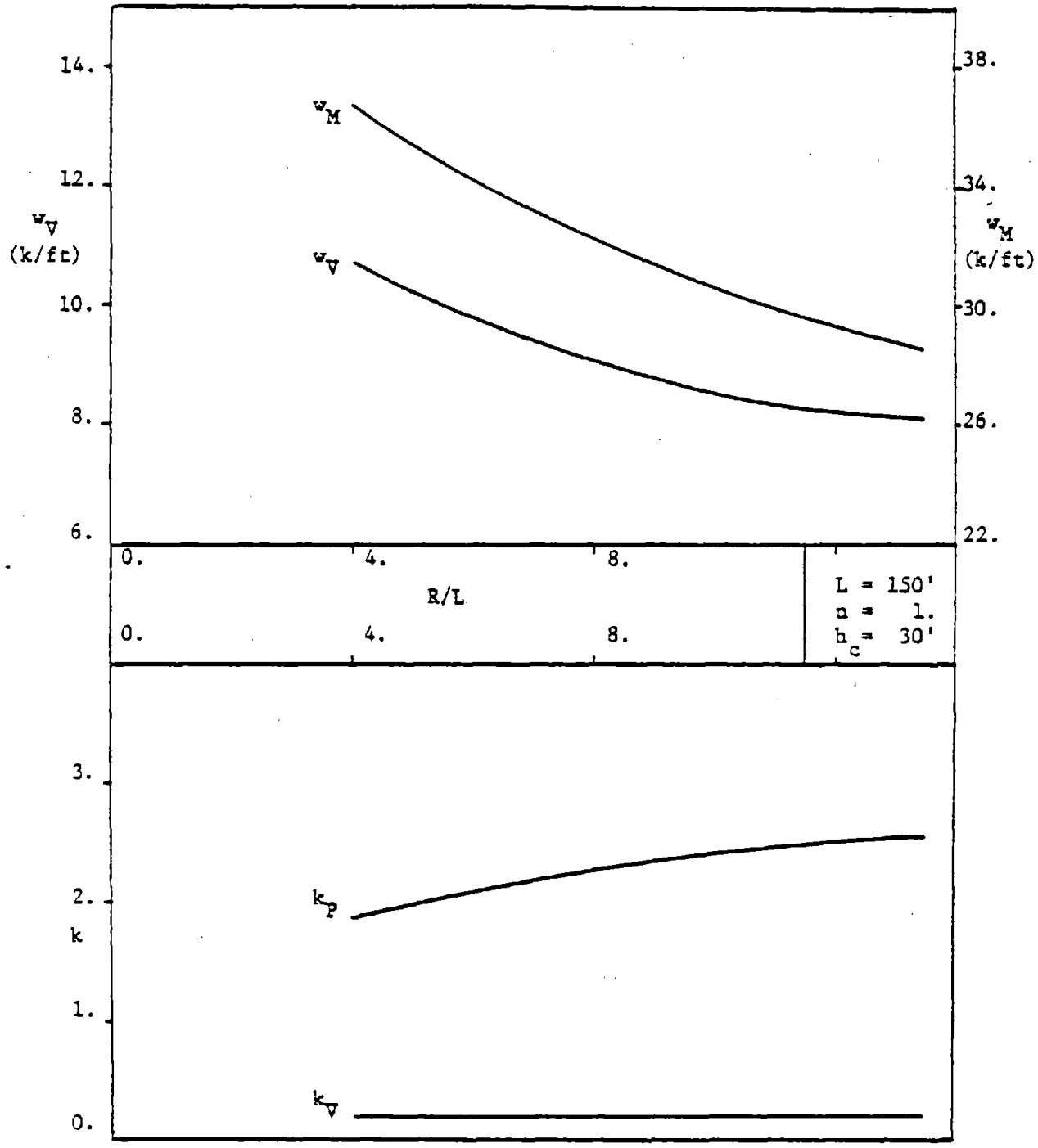


Figure B23.9 Actions at the Attachments

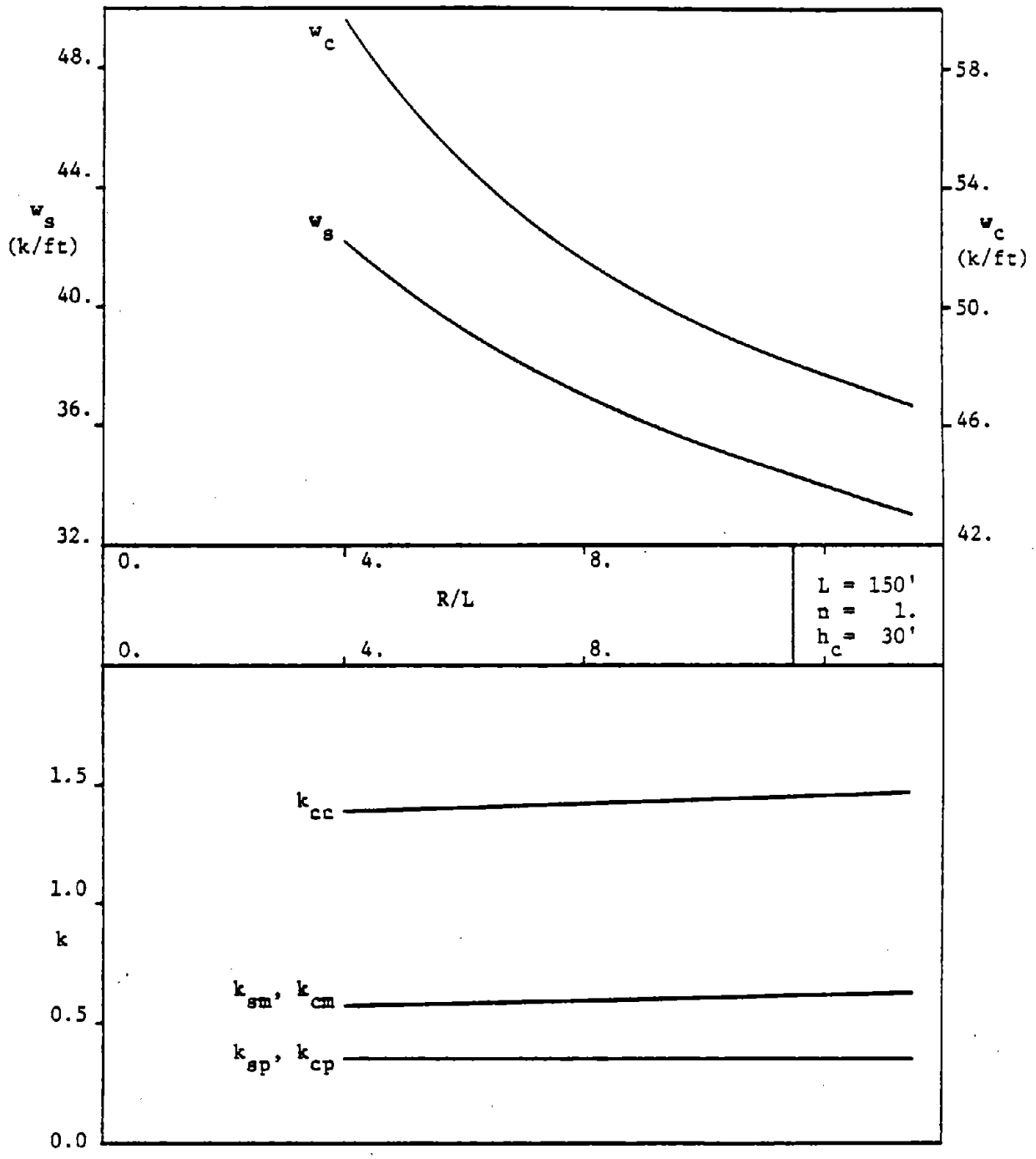


Figure B23.10 Deck and Column Stresses

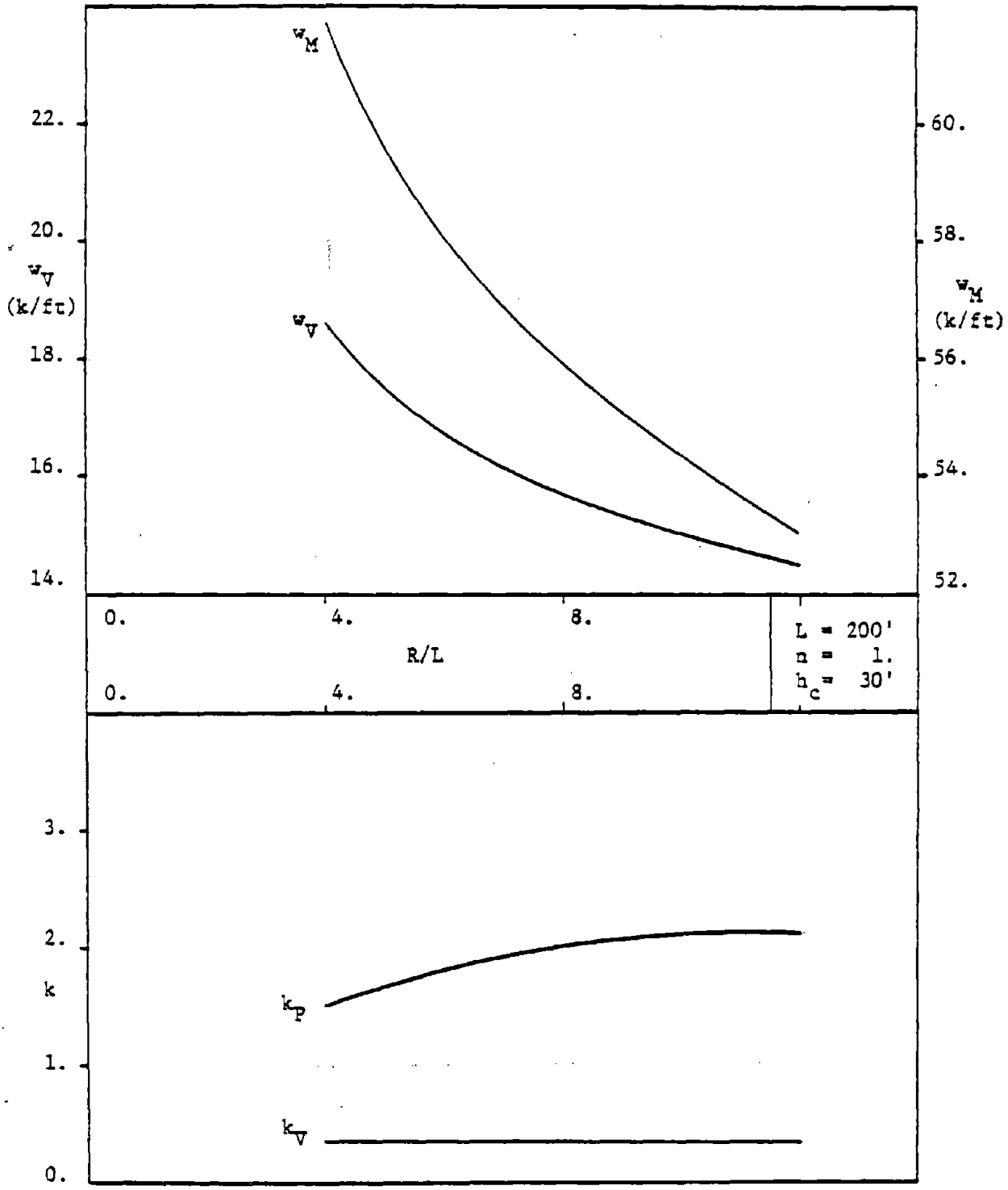


Figure B23.11 Actions at the Attachments

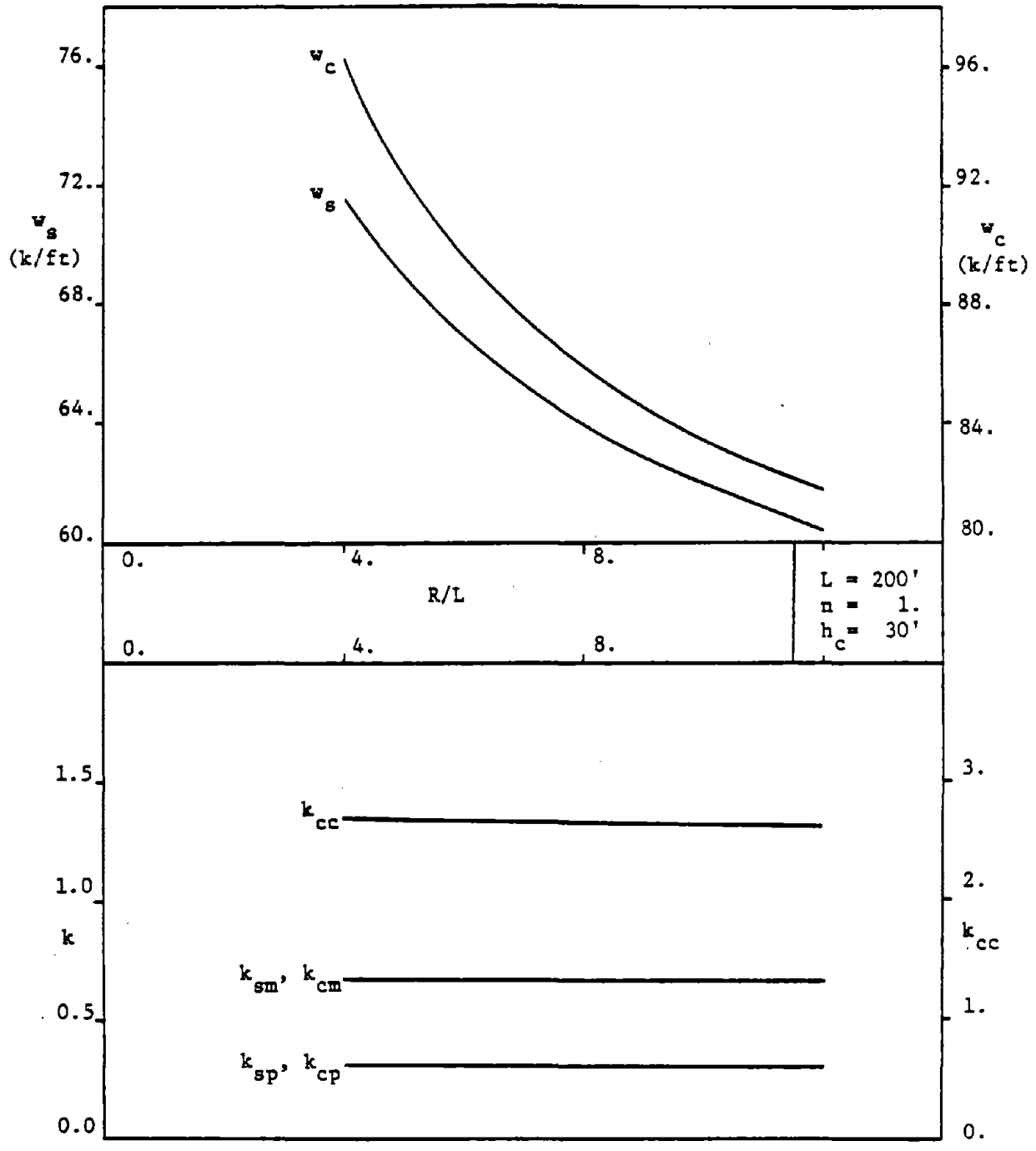


Figure B23.12 Deck and Column Stresses

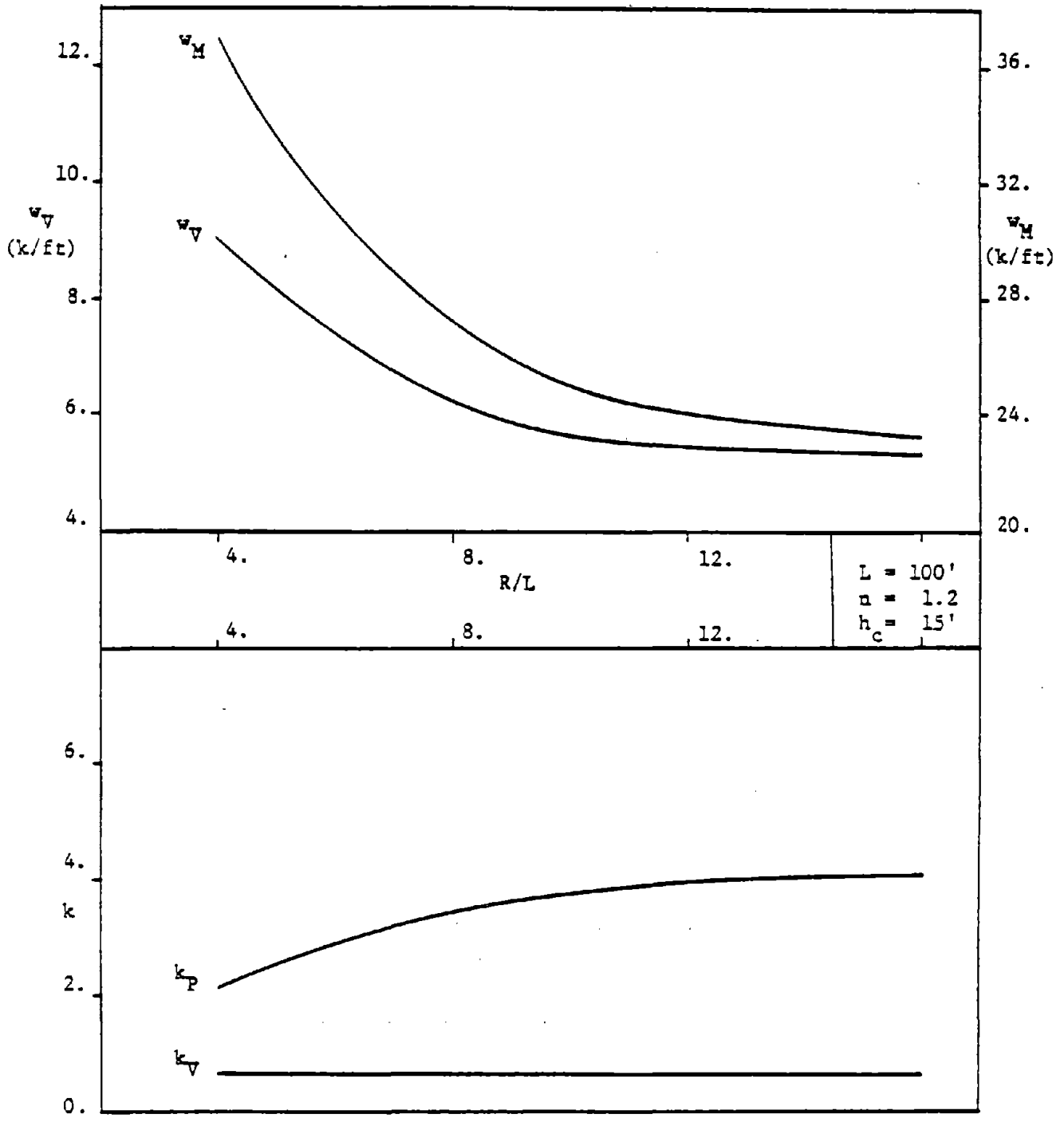


Figure B23.13 Actions at the Attachments

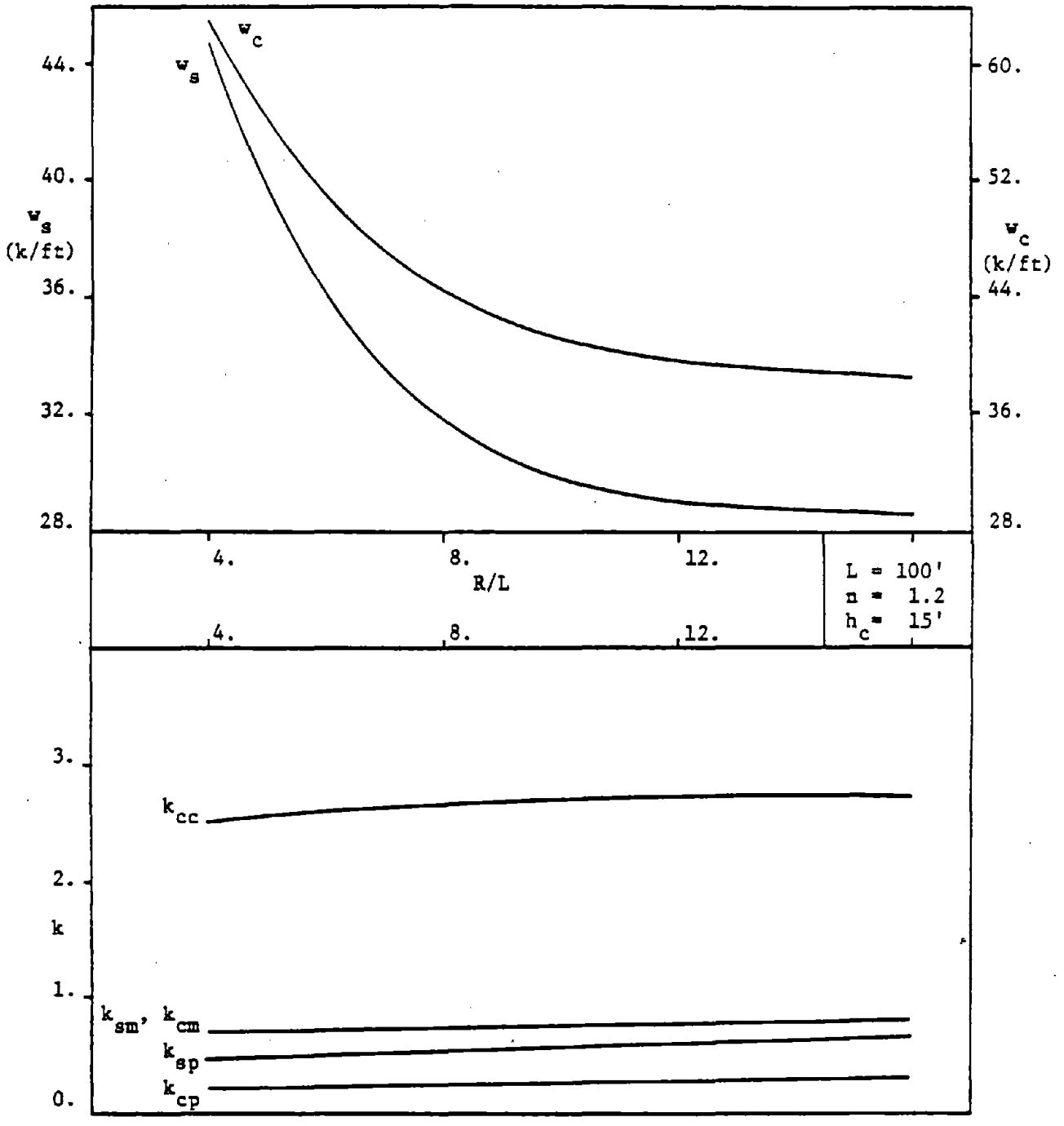


Figure B23.14 Deck and Column Stresses

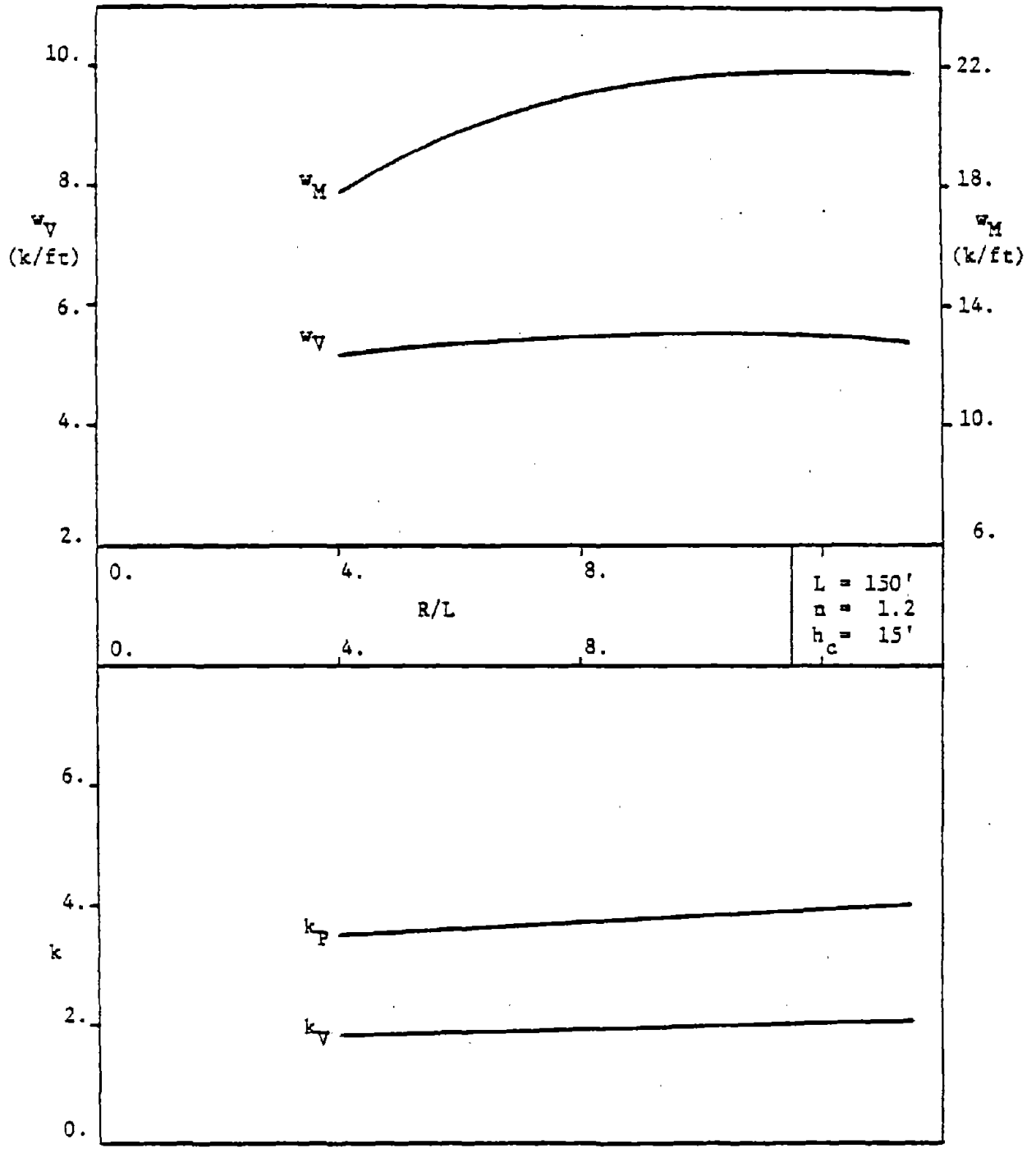


Figure B23.15 Actions at the Attachments

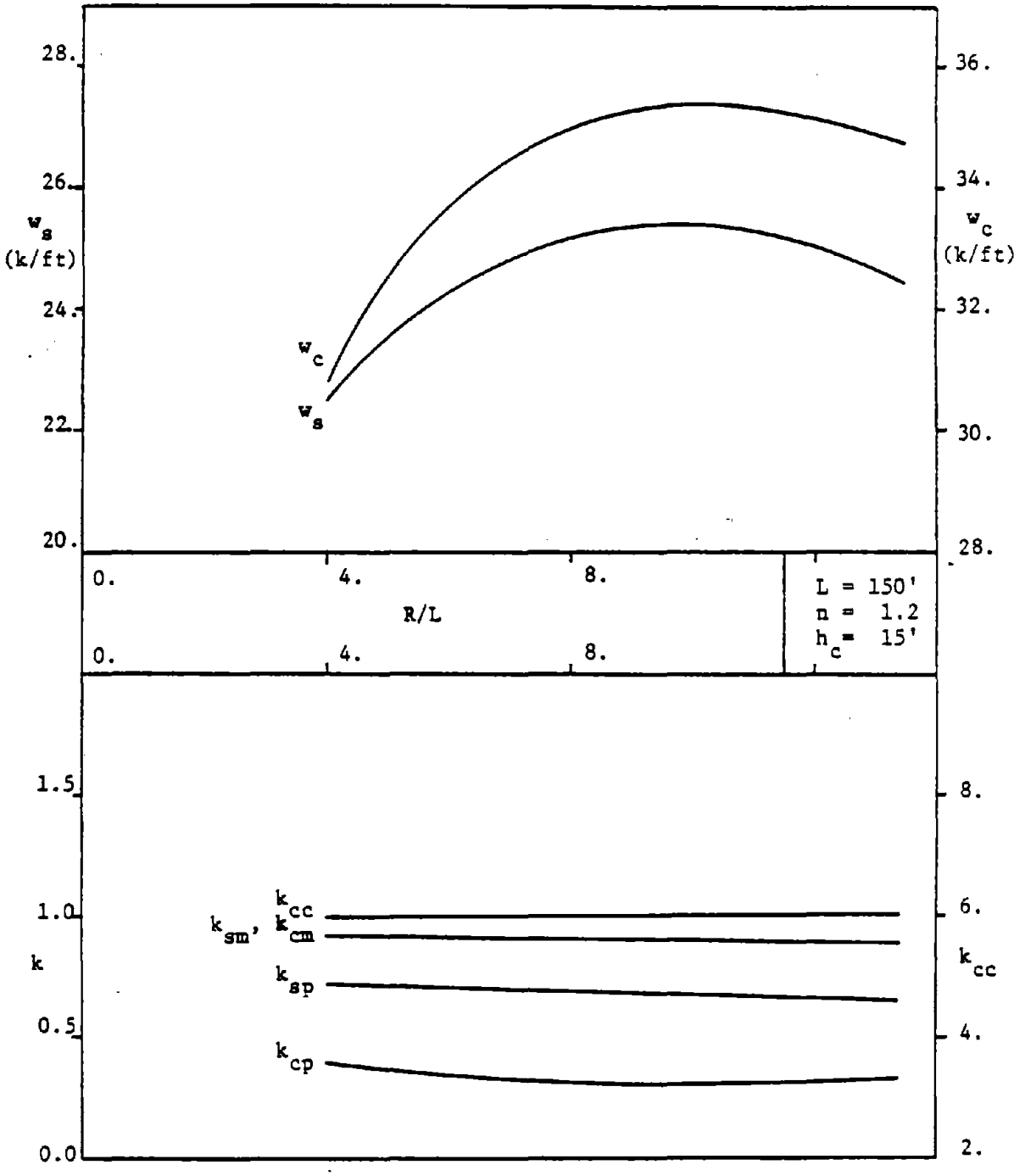


Figure B23.16 Deck and Column Stresses

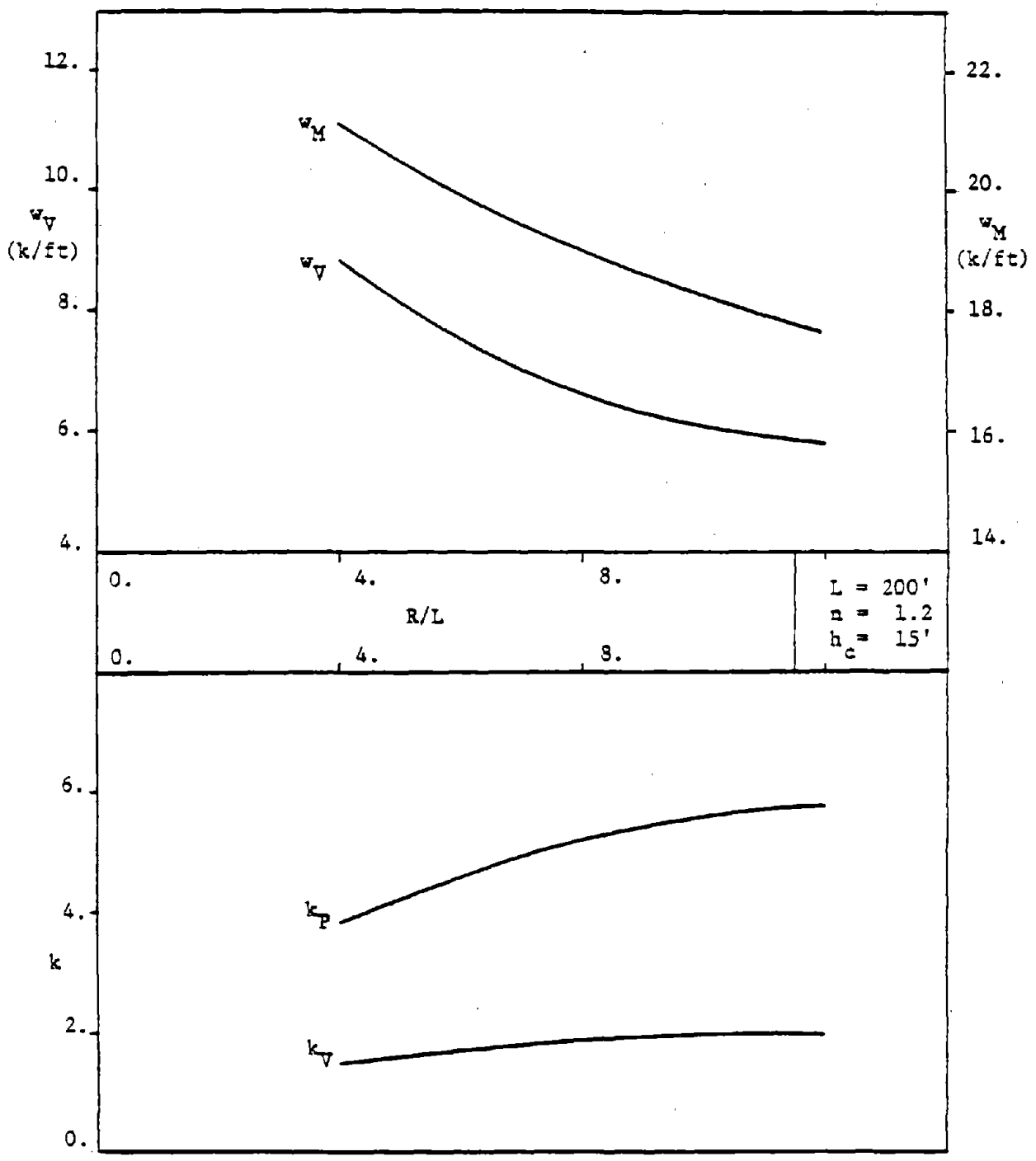


Figure B23.17 Actions at the Attachments

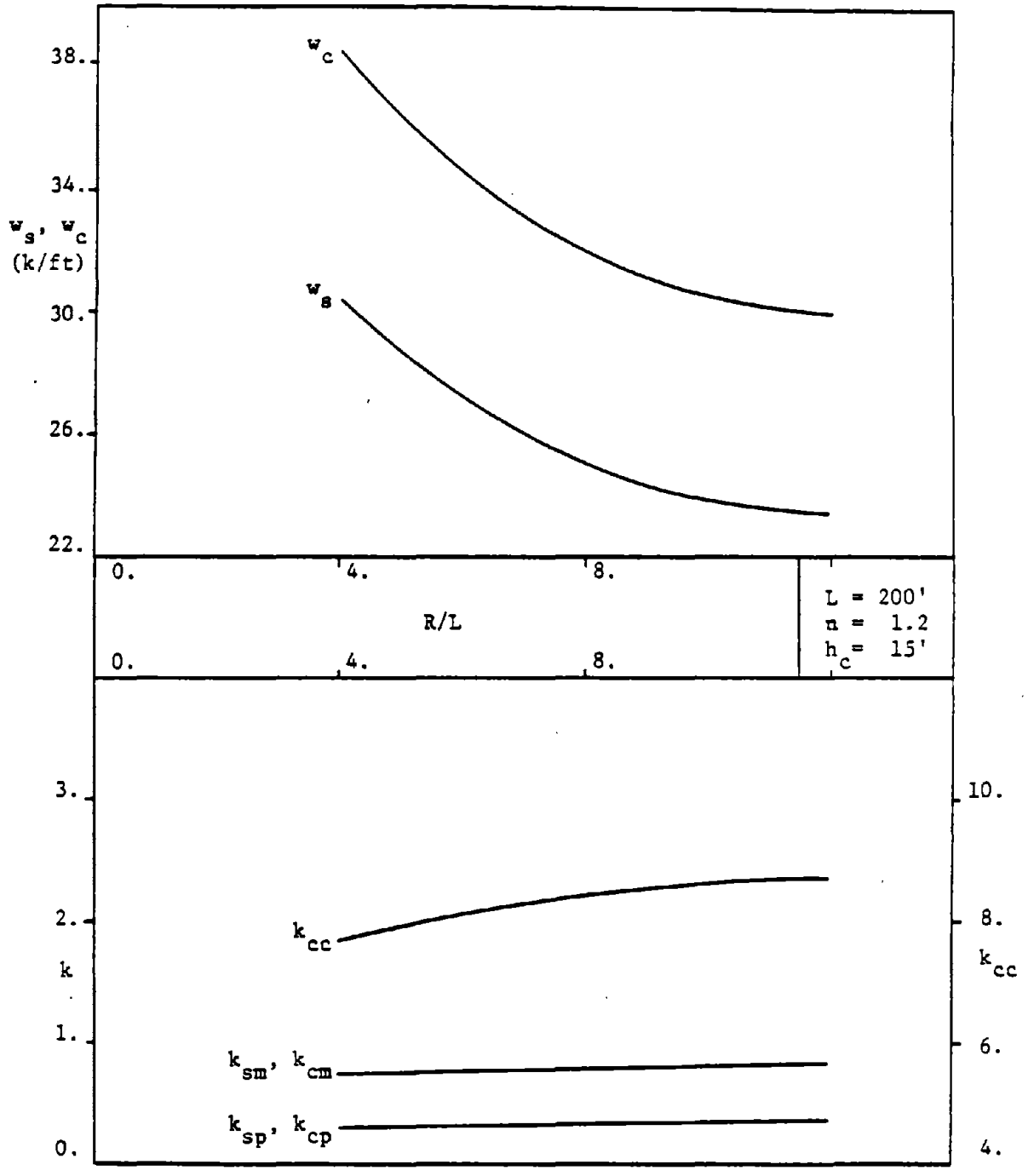


Figure B23.18 Deck and Column Stresses

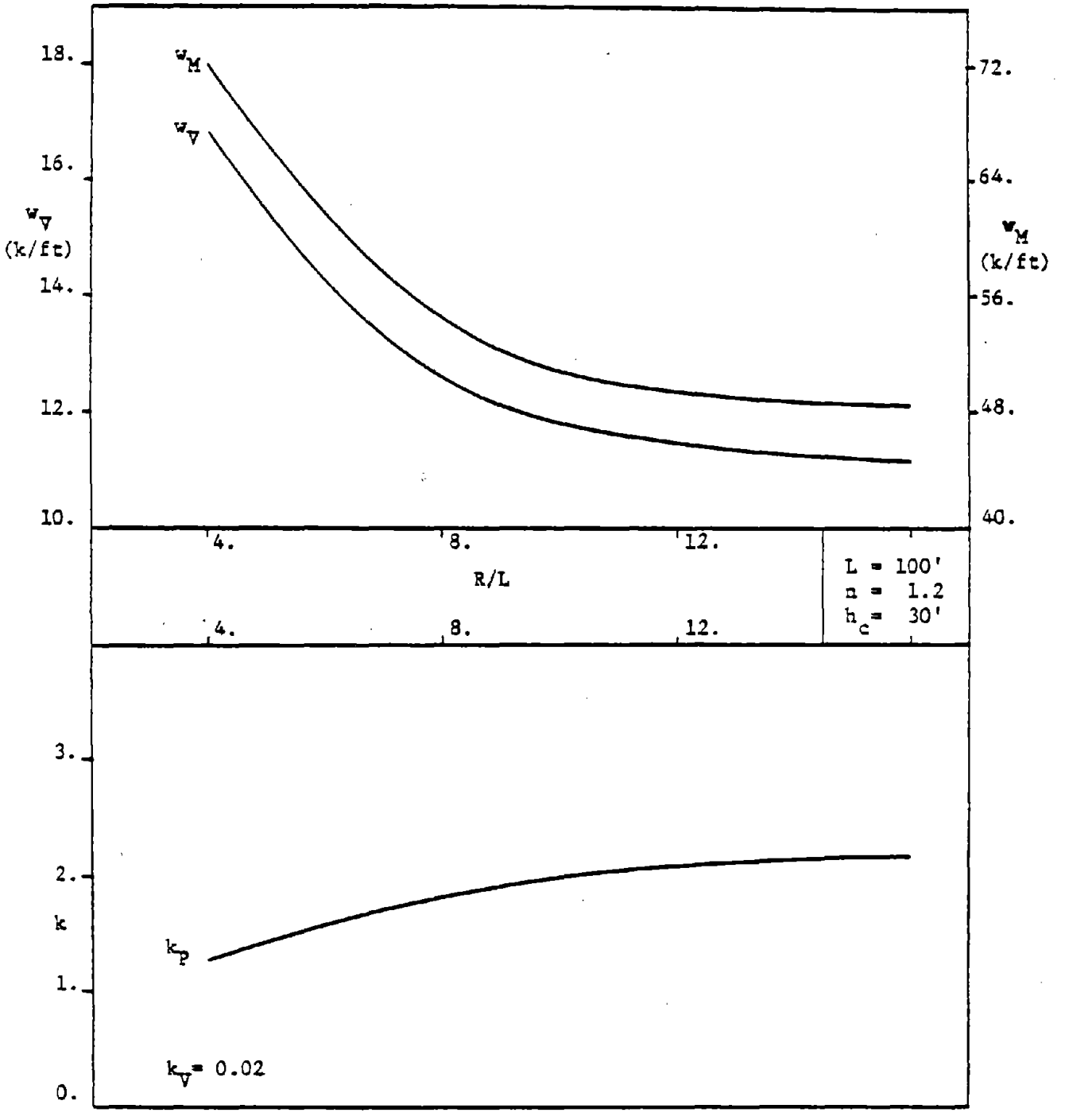


Figure B23.19 Actions at the Attachments

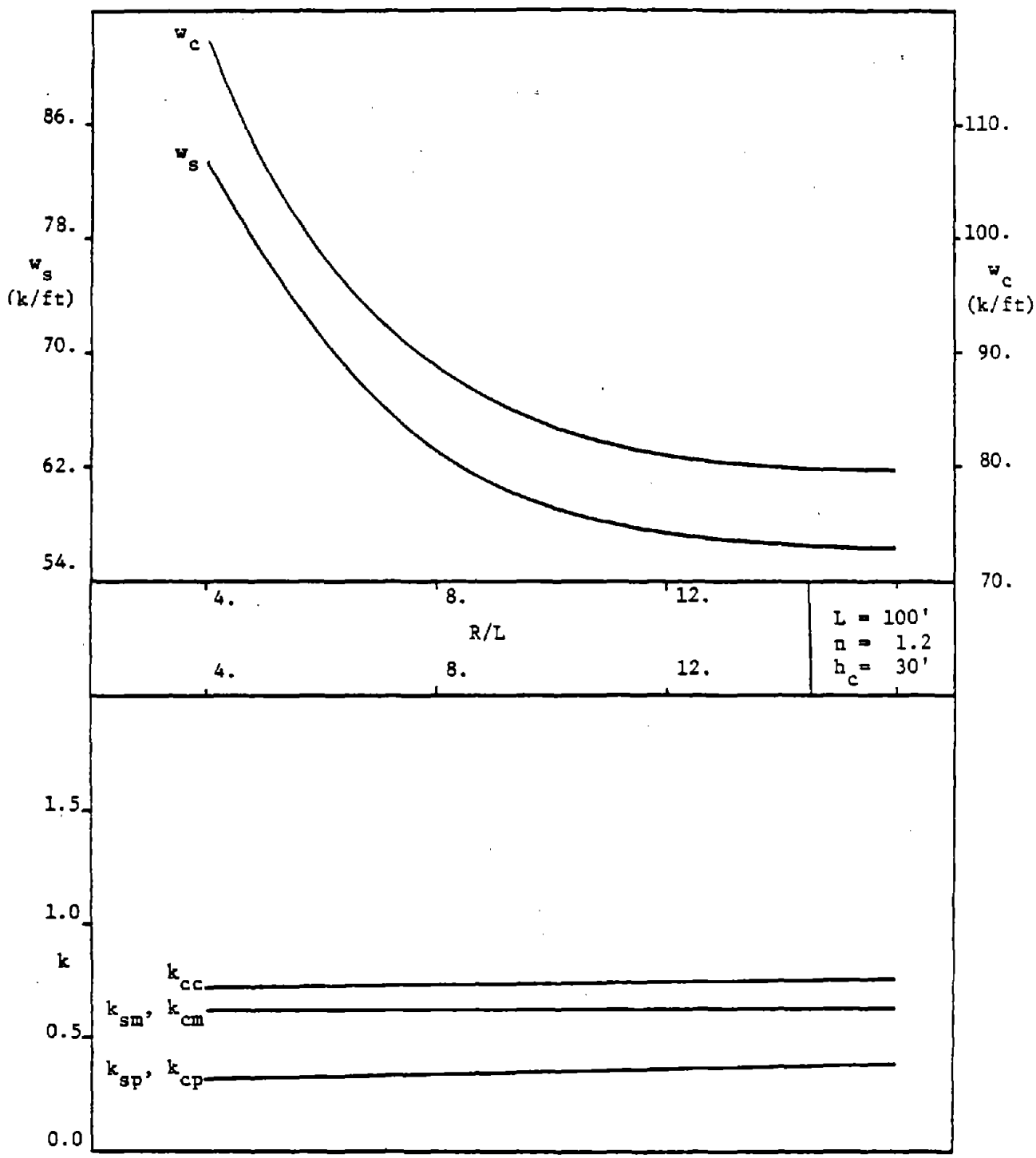


Figure B23.20 Deck and Column Stresses

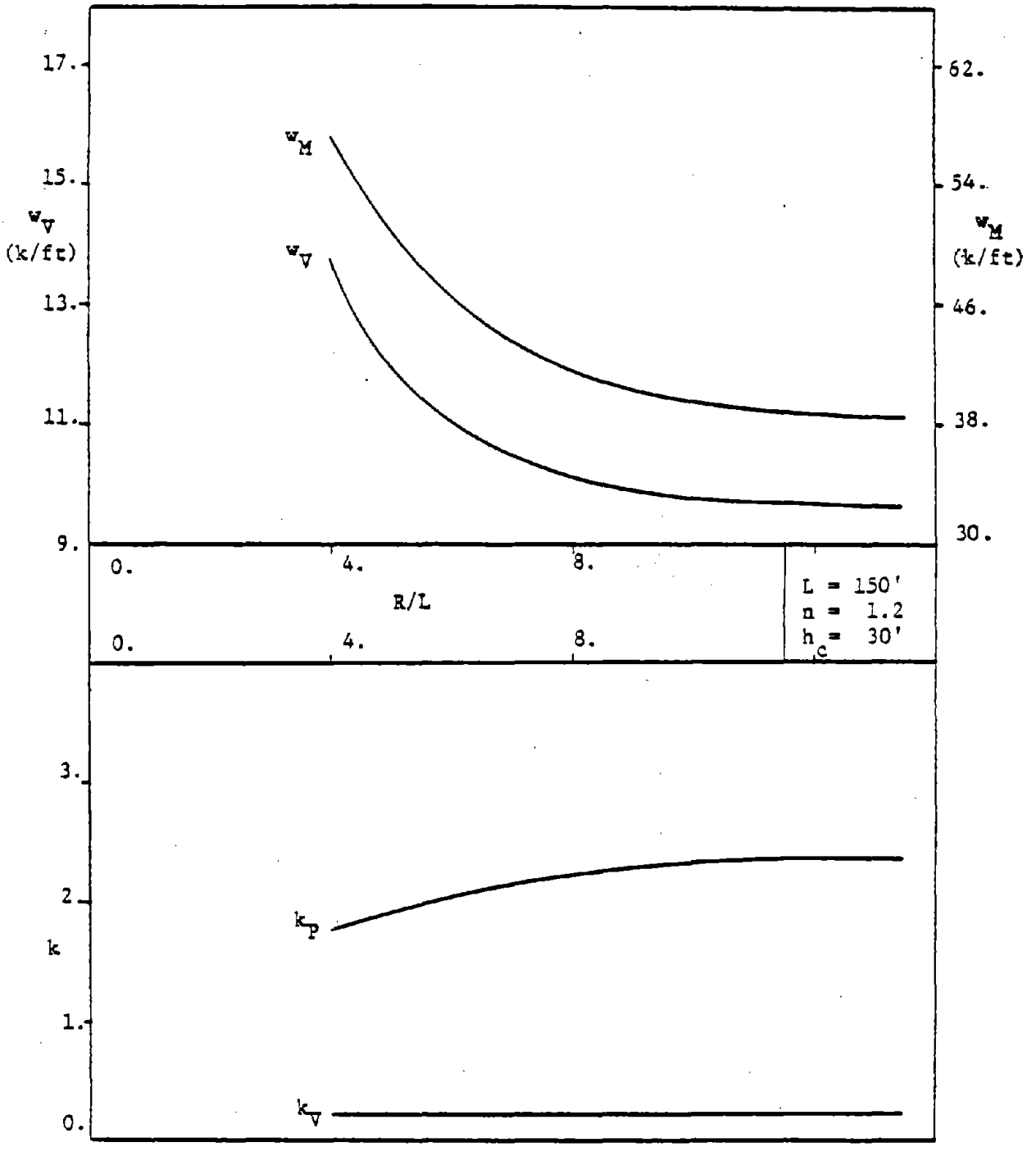


Figure B23.21 Actions at the Attachments

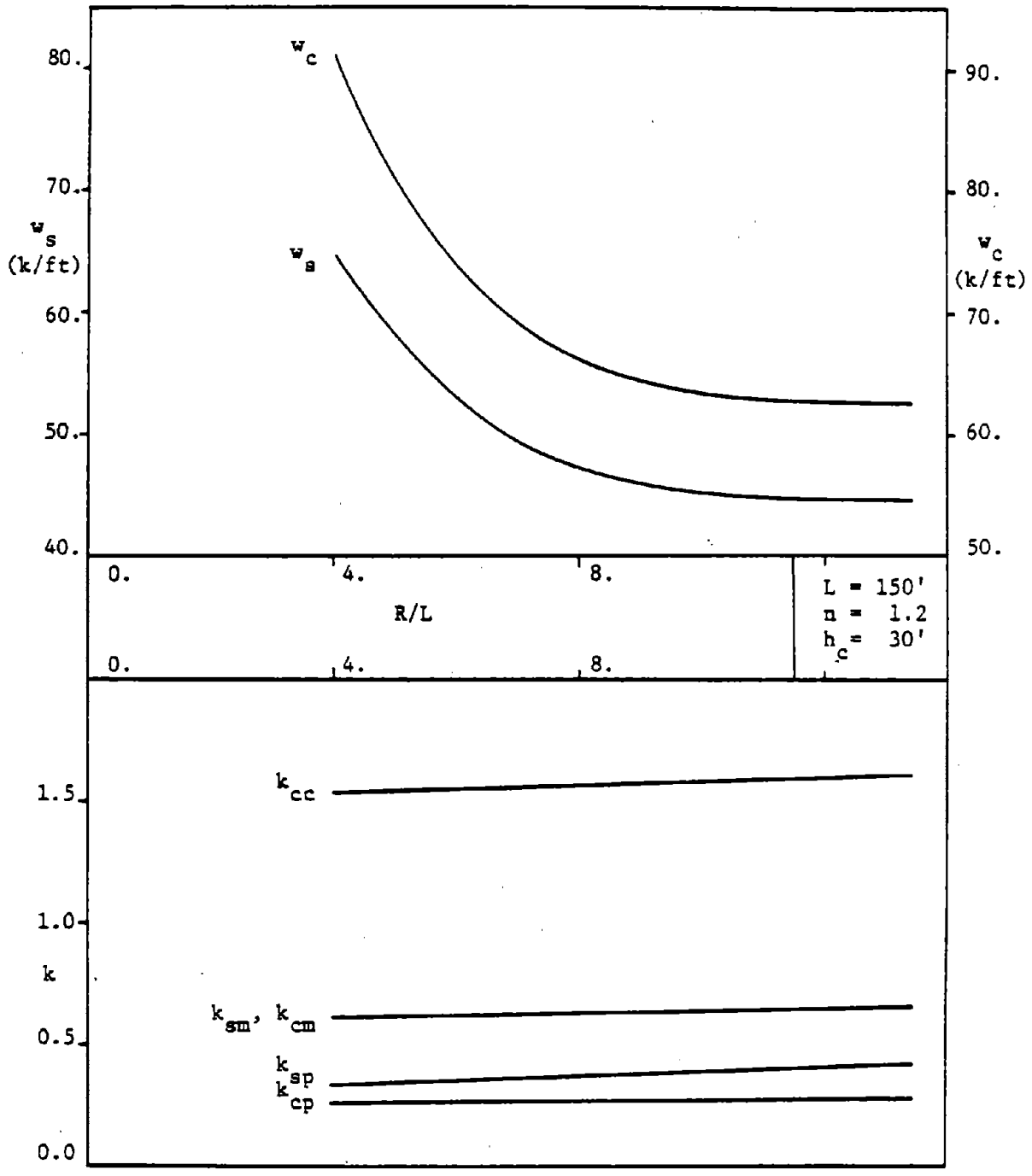


Figure B23.22 Deck and Column Stresses

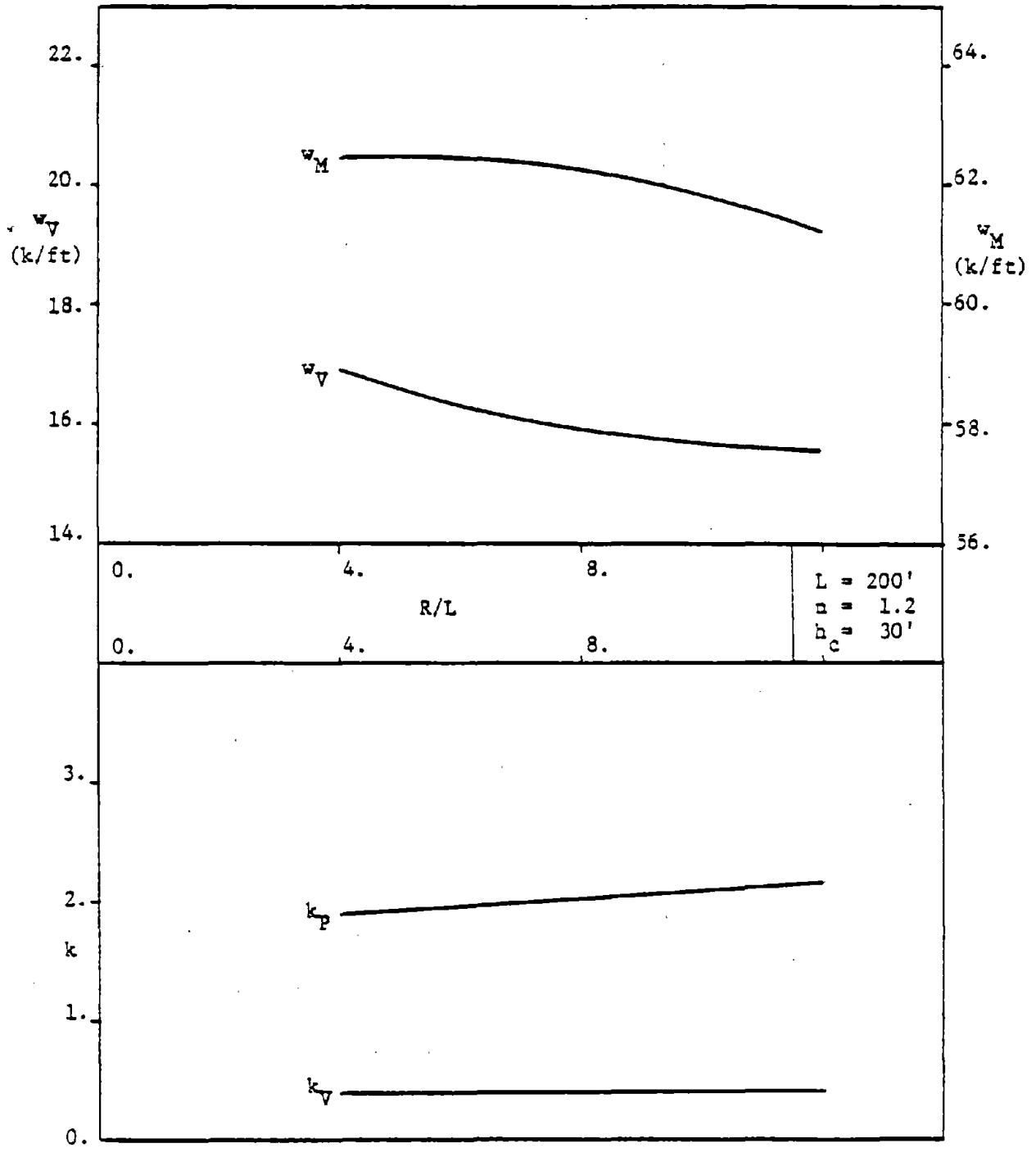


Figure B23.23 Actions at the Attachments

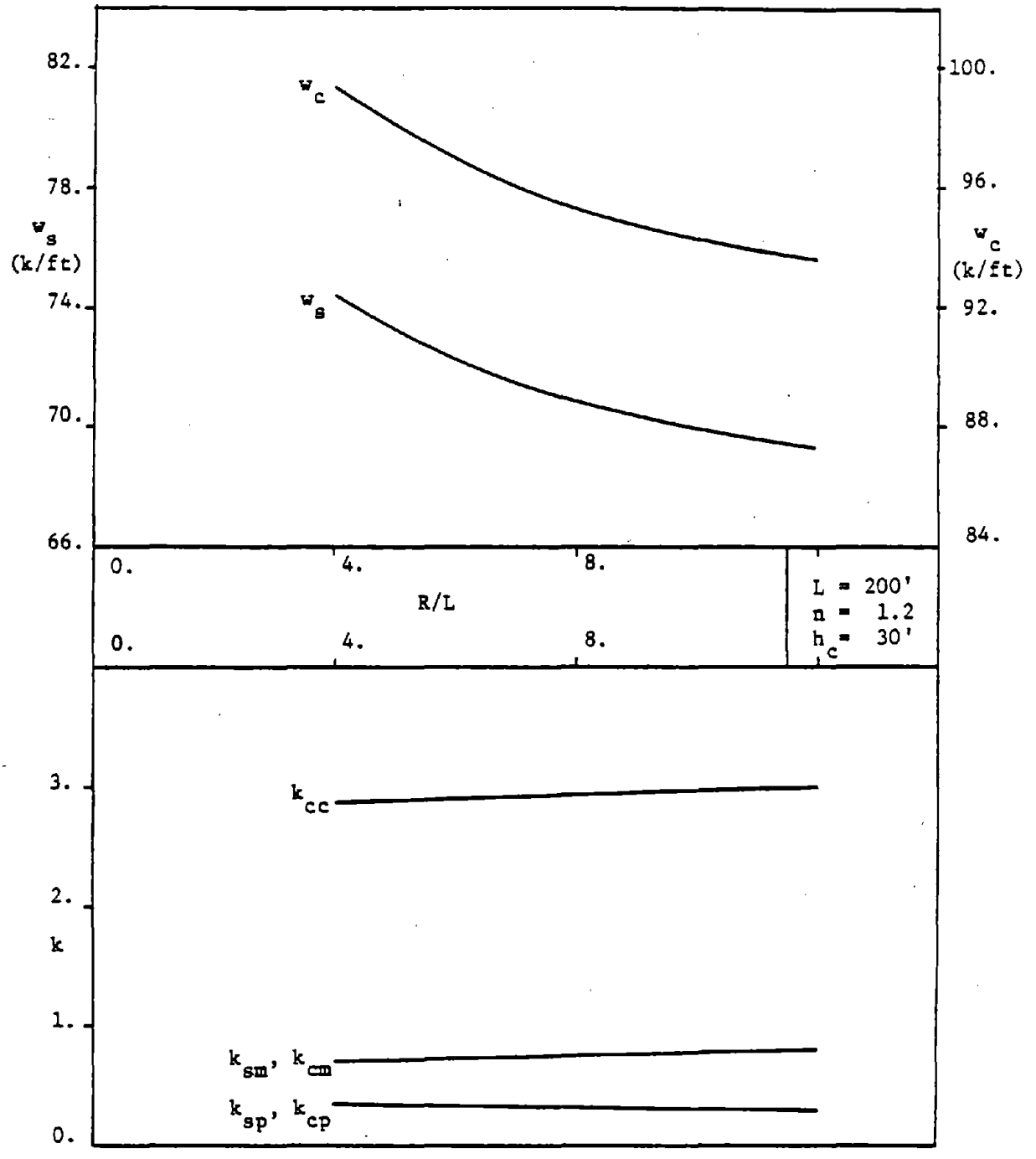


Figure B23.24 Deck and Column Stresses

B.2.4 4-Span Bridges

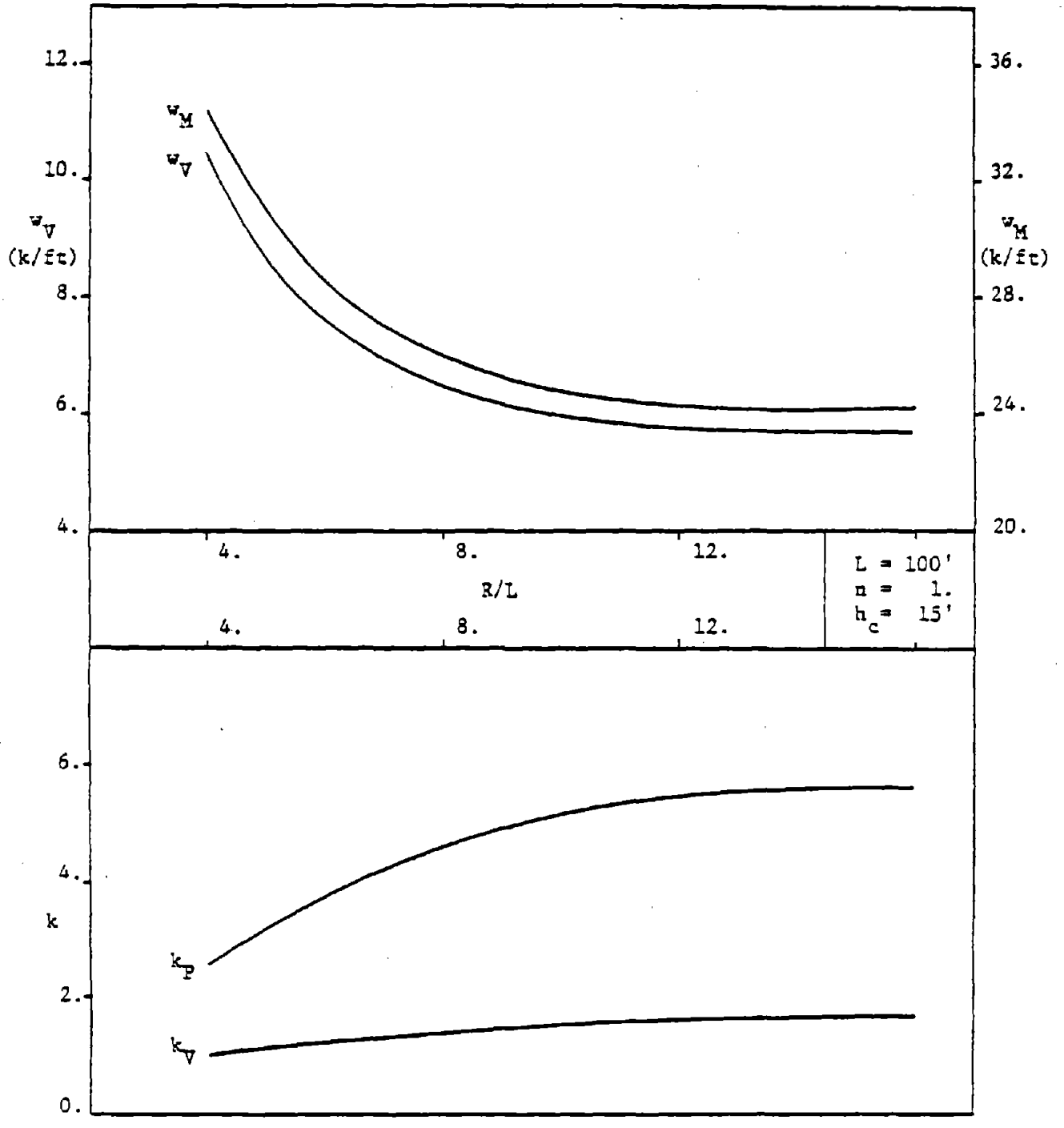


Figure B24.1 Actions at the Attachments

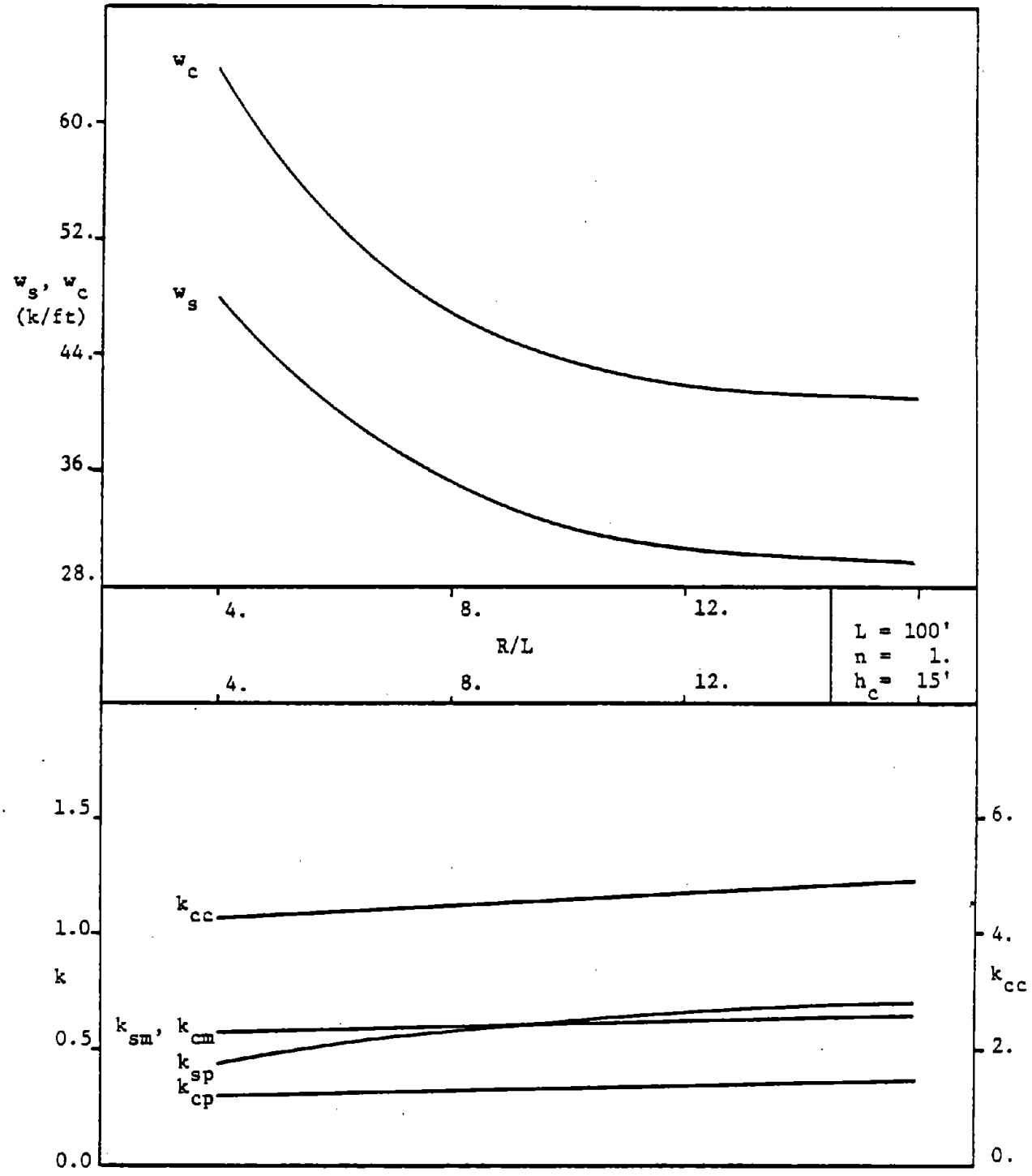


Figure B24.2 Deck and Column Stresses

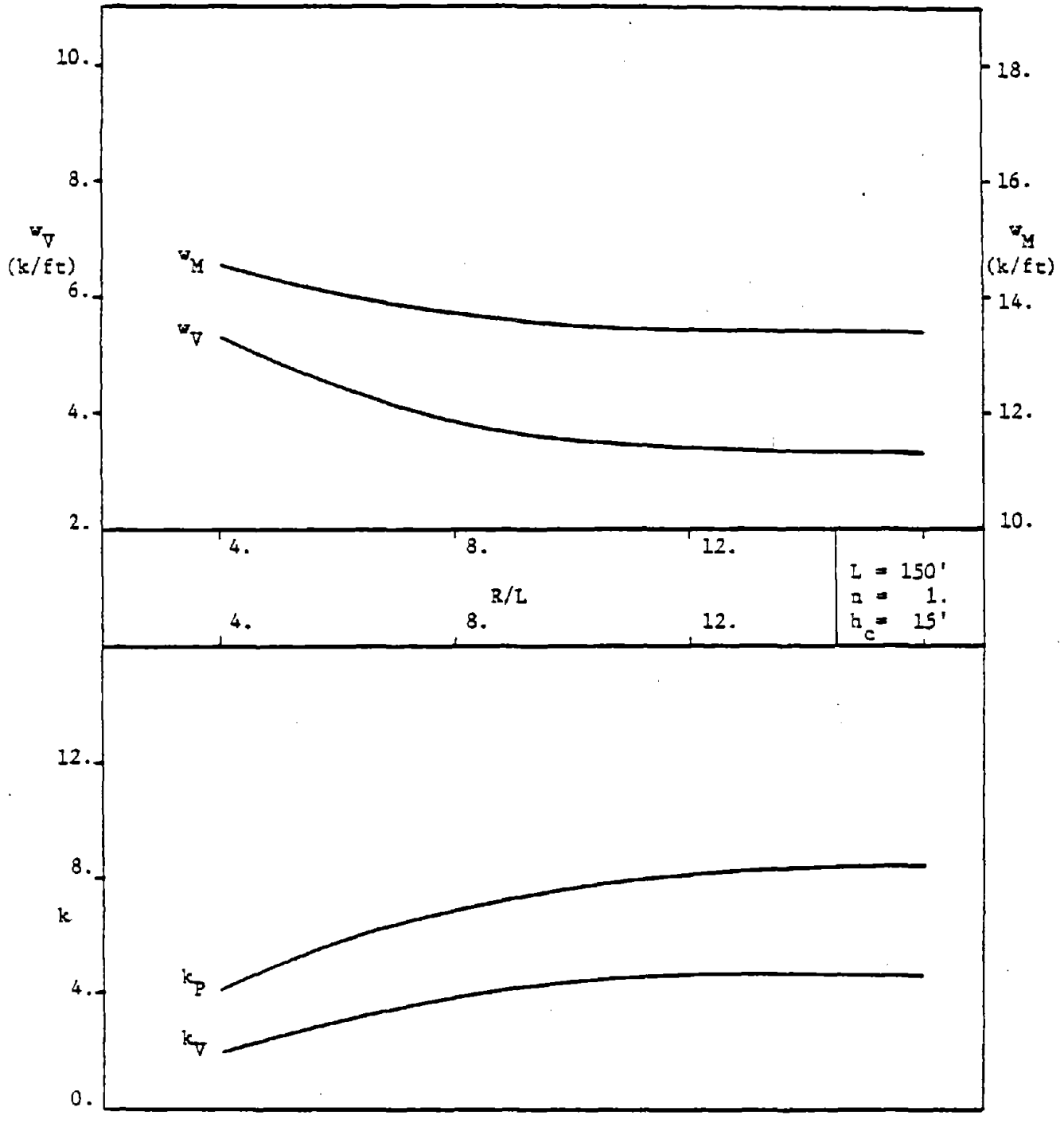


Figure B24.3 Actions at the Attachments

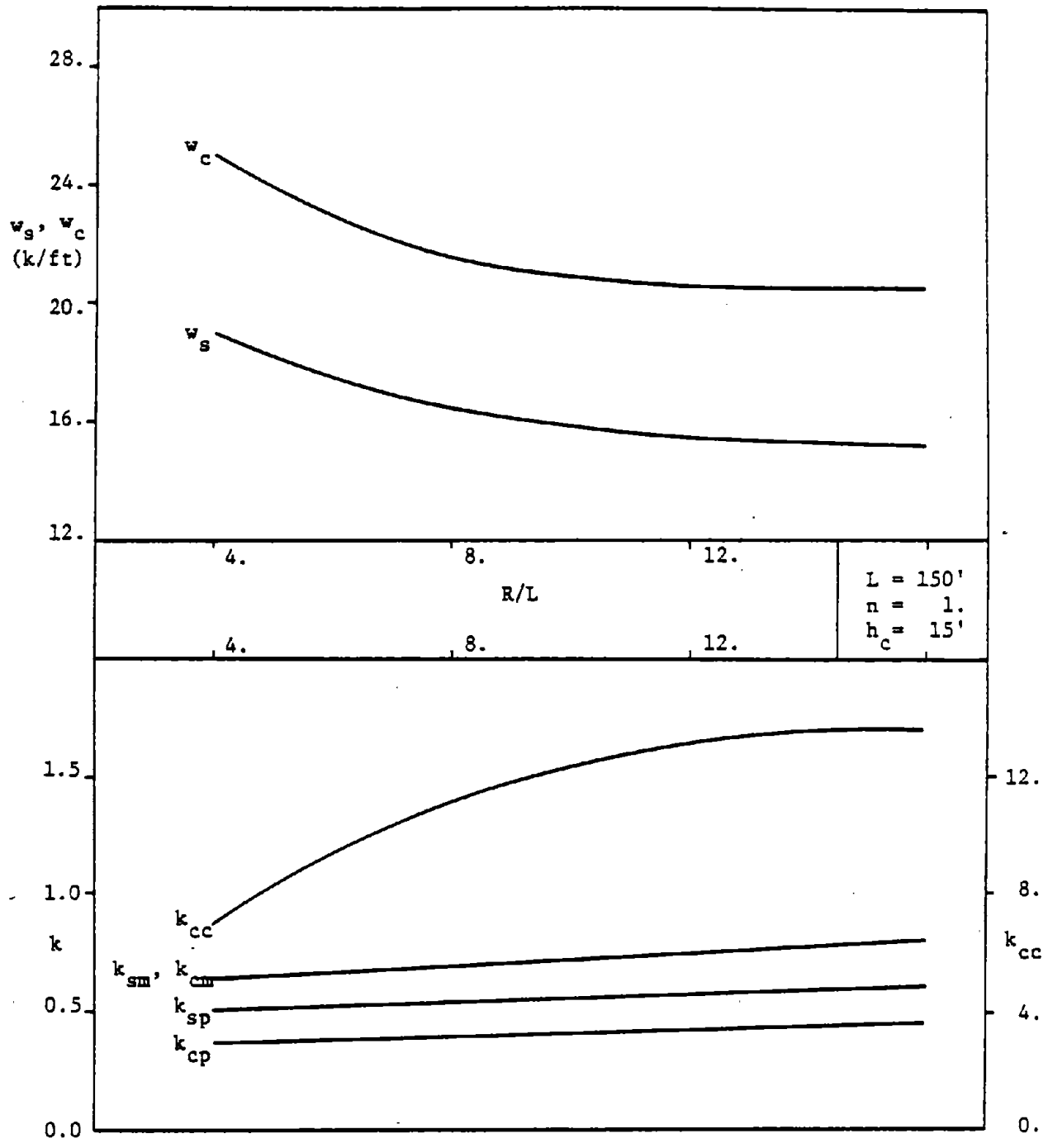


Figure B24.4 Deck and Column Stresses

## B.2.5 5-Span Bridges

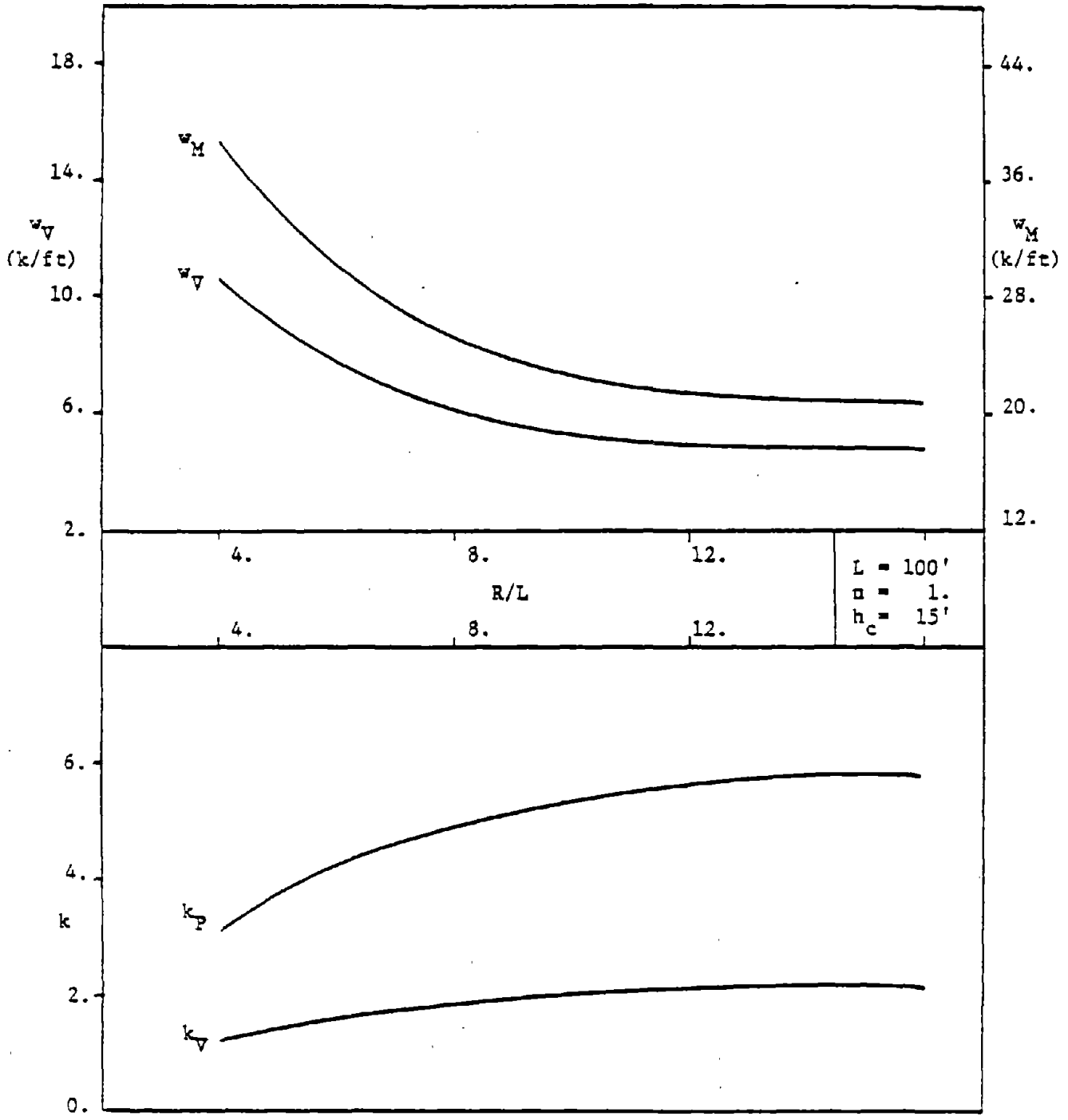


Figure B25.1 Actions at the Attachments

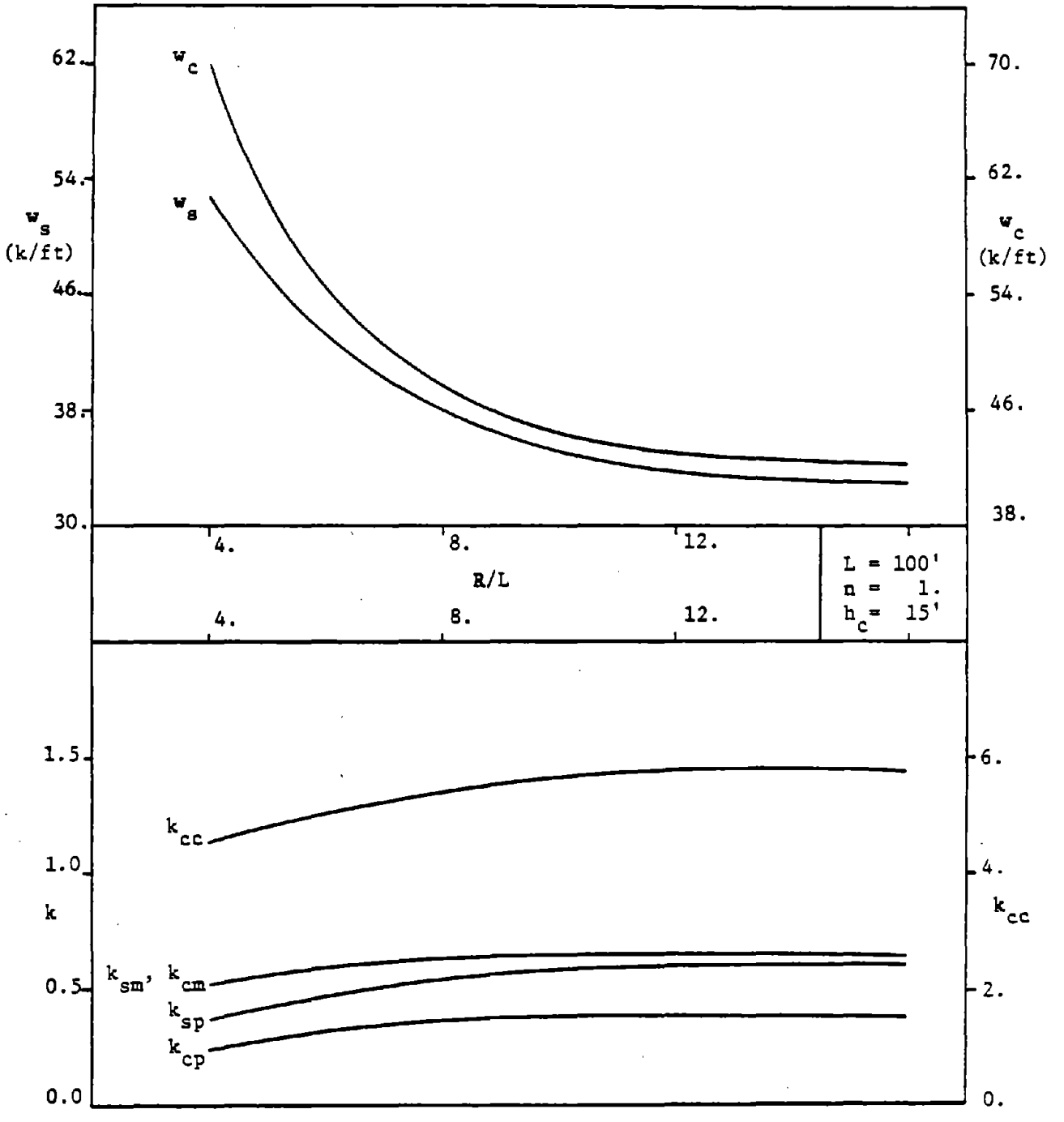


Figure B25.2 Deck and Column Stresses

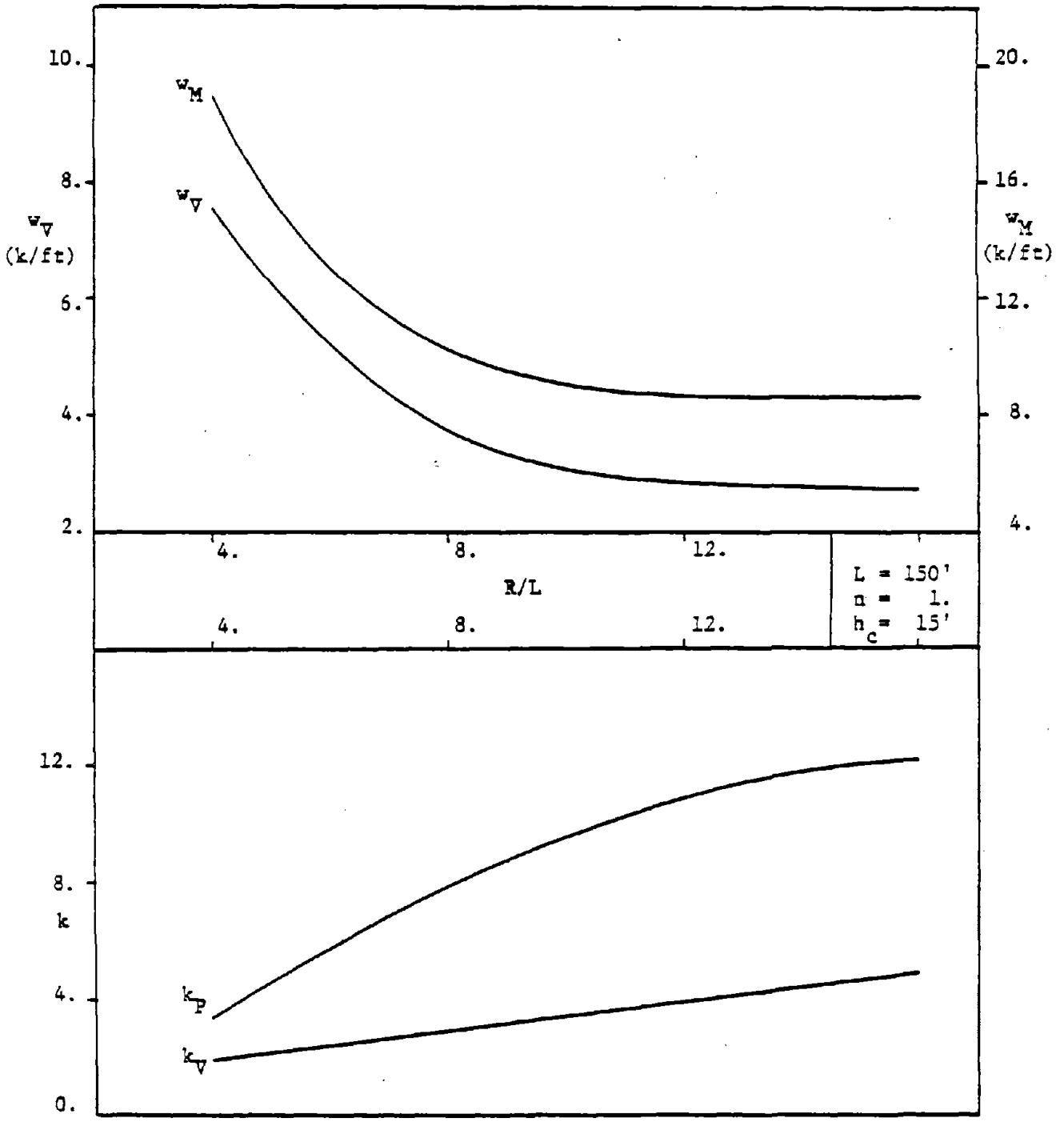


Figure B25.3 Actions at the Attachments

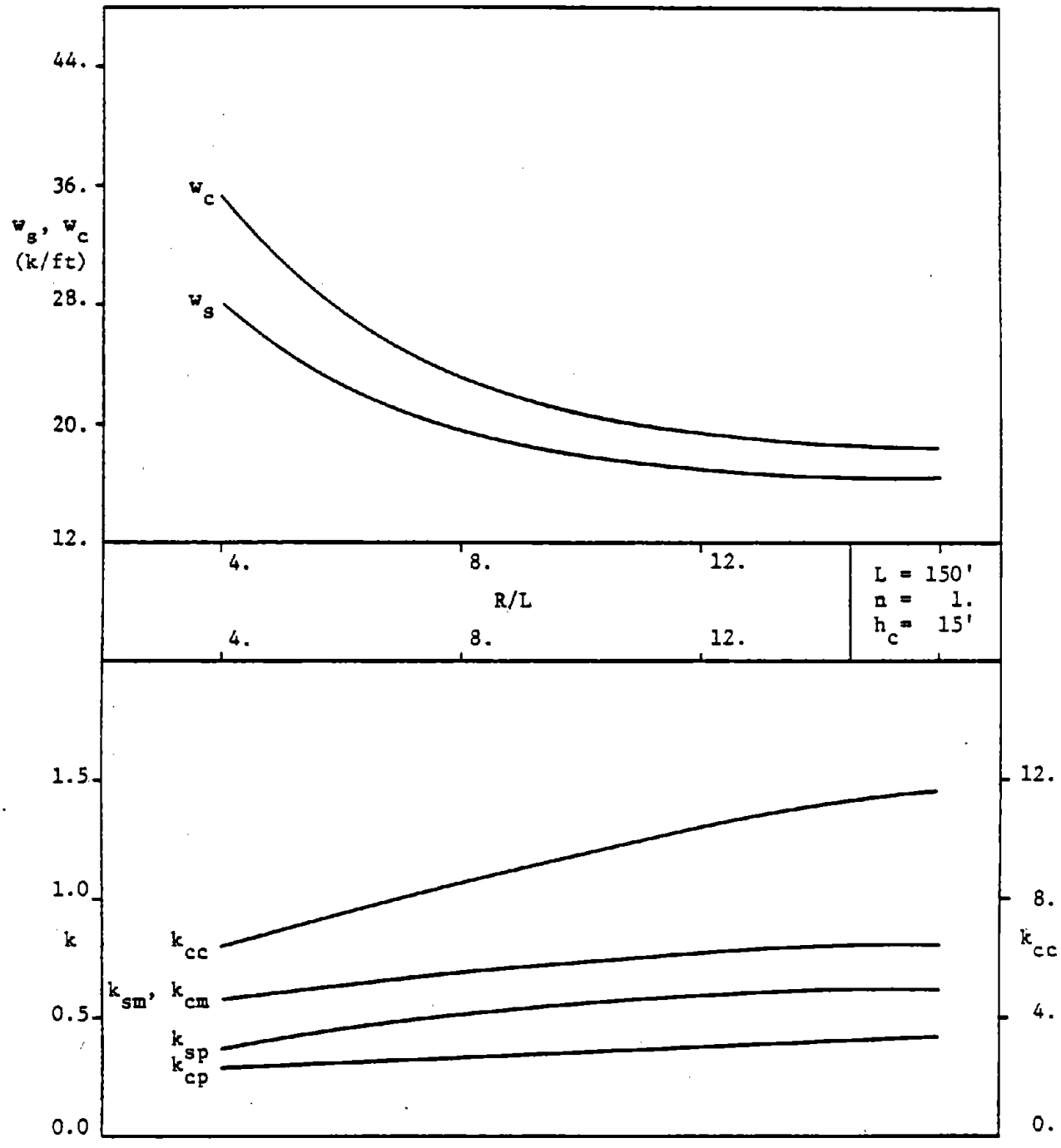


Figure B25.4 Deck and Column Stresses